

TRANSACTIONS OF THE UNIVERSITIES OF KOŠICE



ISSN 1335-2334

3/2008

Anan'ev V., Spirina J.: Band Shapes of the Electronic Spectrum of Anisotropic Center in Uniaxial Crystal	1
Blašková J., Vojteková V., Nováková J.: Ultrasonic Extraction for Evaluation of the Mobility of Fe and Mn Contents in Components of Environment	10
Bova Š., Puliš P., Božok M.: Mass Spectrometry Analysis of Isopropylester Analogues of Methylfluor Phosphoric Acid	16
Bujdoš M., Kubová J., Hagarová I., Matúš P.: Photochemical Vapor Generation in Analytical Atomic Spectrometry – Recent Developments	21
Elsherif K., Kuss H.-M.: Simultaneous Determination of Al, Be, Cr, and V using Multi-Element Graphite Furnace Atomic Absorption Spectrometer (SIMAA 6000)	28
Galusková D., Galusek D., Šajgalík P.: Determination of Si and Al in Corrosion Medium of Sodium Chloride Solution by Inductively Coupled Plasma Atomic Emission Spectrometry	36
Galusková D., Kraxner J., Klement R.: Determination of Si, Al, Ca, Mg and B in Glass Samples by ICP-AES	40
Hagarová I., Matúš P., Bujdoš M., Kubová J.: Separation and Preconcentration of Total Inorganic Antimony by a Nanometer-Sized TiO ₂ and its Determination by Direct TiO ₂ -Slurry Sampling Electrothermal Atomic Absorption Spectrometry	44
Kubová J., Matúš P., Bujdoš M., Hagarová I., Medved' J., Diviš P., Dočekalová H.: Optimized BCR Three-Step Sequential and Dilute HCl Single Extraction Protocols - the Suitable Tools for Soil-Plant Metal Transfer Predictions in Polluted Areas?	50
Laštincová J., Beinrohr E., Pospíšilová L.: Analysis of Cd in Must and Wine	59
Macháčková L., Žemberyová M., Šimonovičová A., Barteková J., Izakovičová L., Janovová L.: Biosorption and Preconcentration of Cd from Aqueous Solution by Fungal Biomass of <i>Aspergillus Niger</i> and Determination Using Flame Atomic Absorption Spectrometry Technique	63

Macharáčková B., Čelechovská O., Vitoulová E.: Content of Arsenic in the Fish Muscle from Intensive Breeding	68
Matějka P., Mrnka L., Procházková S., Člupek M., Tokárová H., Volka K.: FT Raman and Infrared Spectra of Coniferous Needles: What Effects can be Elucidated?	73
Matherny M., Uhrinová K., Ružičková S.: Atmospheric Dustiness of Residential Agglomeration and its Element Analysis	81
Matůš P., Bujdoš M., Kubová J., Hagarová I., Medved' J., Diviš P., Mládková Z.: Comparison of Five Different Methods for the Separation and Determination of Aluminium Phytoavailable and (Phytotoxic) Fractions	86
Matůš P., Čerňanský S., Urík M., Medved' J., Bujdoš M., Kramarová Z., Kališ M., Hagarová I., Kubová J., Ševc J., Diviš P., Brulík L.: Quantification of Biosorption, Bioaccumulation and Biovolatilization of Labile Aluminium and Thallium Species by Fungal Biomass Using the Atomic Spectrometry Techniques	97
Medved' J., Kališ M., Hagarová I., Bujdoš M., Matůš P., Kubová J.: Solid-Phase Extraction and ETAAS Determination of Thallium Species in Water Samples	106
Mohadesi A., Roohparvar R., Taher M.A.: Simultaneous Determination of Trace Amounts of Mercury and Copper by Derivative Spectrophotometric H-Point Standard Addition Method after their Separation and Preconcentration on Modified Natural Clinoptilolite Zeolite	112
Plško E.: Some of our Contributions to the Statistical Valuation of Spectrochemical Results	119
Remeteiová D., Rusnák R., Stolárová S., Dirner V.: Study of Mobility of Chosen Elements in Soils Contaminated by Pollutants of Metallurgical Industry	125
Rusnák R., Fekete I., Halász G., Remeteiová D.: Comparison of Single-Step and BCR Sequential Extraction Procedures of Gravitation Dust Sediment Samples	132
Száková J., Tlustoš P., Frková Z., Najmanová J., Balík J.: Effect of Soil Sample Treatment on Evaluation of Trace Element (Cu, Fe, Mn, Zn) Mobility in Soils	137

Editorial Board „Transactions of the Universities of Košice“

Chairman of the Editorial Board:	Stanislav Kmet' phone: ++421 55 622 2121 e-mail: Stanislav.Kmet@tuke.sk
Honorary Chairman:	Ivan J. Lukáč phone: ++421 55 602 2777 e-mail: Ivan.Lukac@tuke.sk
Executive Director:	Liberios Vokorokos phone: ++421 55 602 4005 e-mail: Liberios.Vokorokos@tuke.sk
Scientific Secretary:	Helena Fialová tel.: ++421 55 602 2318 e-mail: Helena.Fialova@tuke.sk

Editorial Board *(in alphabetical order)*

Michal Cehlár /TU Košice/, Stanislav Fabián /TU Košice/, Karol Flórián /TU Košice/, Helena Fialová /TU Košice/, Jaroslav Jarema /TU Košice/, Stanislav Kmet' /TU Košice/, Dobroslav Kováč /TU Košice/, Ivan J. Lukáč /TU Košice/, Štefan Nižník /TU Košice/, Jozef Považan /TU Košice/, Juraj Smrček /TU Košice/, Vincent Šoltés /TU Košice/, Liberios Vokorokos /TU Košice/

International Advisory Board *(in alphabetical order)*

Adamczak S. /Politechnika Świetokrzyska, Kielce, Poland/, Cigánek J. /Technical University – VŠB, Ostrava, Czech Republic/, Dvořáček J. /Technical University – VŠB, Ostrava, Czech Republic/, Hodolić J. /University of Novy Sad, Novy Sad/, Kuss H.-M. /University of Duisburg, Duisburg, Germany/, Maser S. /BU Wuppertal, Wuppertal, Germany/, Oršula L. /Alcan Děčín Extrusions, Děčín, Czech Republic/, Polách J. /University of T. Baťa, Zlín, Czech Republic/, Rudas I. J. /Polytechnika, Budapest, Hungary/, Záray Gy. /ELTE Budapest, Hungary/

<http://library.upjs.sk>

Foreword

The XIXth Slovak – Czech Spectroscopic Conference was held in Častá-Papiernička, Slovakia on October 12-16, 2008. Since 1993 up to the present time when the Slovak and Czech spectroscopic communities organized separately their conferences, this event is a joint decision to continue in its long-time tradition of common meetings.

The main goal of our Conference is to bring together experts from universities, academia, official centres, various laboratories, and industry on a worldwide scale to summarize the current progress in different areas of spectroscopy and to stimulate contacts and mutual exchange of experience and ideas. The emphasis is put not only on presentations of the latest scientific achievements, new technologies, and instrumentation but also on applications and utilization of spectroscopy in different fields of practical life. The Conference also provides a possibility to get acquainted with new instrumental techniques, spectroscopy equipment, laboratory materials and instruments, reference materials, science literature, etc. which are exhibited by several distribution companies.

This year the Conference offers a 5 day scientific program that consists of 3 honoured and 11 invited lectures, about 42 oral presentations, 62 poster displays, and 15 commercial presentations.

The main Conference topics comprise Theory, Techniques and Trends in Environmental, Geological, Biochemical, Food and Industrial Analysis by Spectroscopy Methods, Speciation Analysis, Sample Preparation and Pretreatment, Chemometrics, Metrology and Quality Assurance.

Full texts of some contributions are presented in this special issue of Transactions of the Universities of Košice.

*Jana Kubová
chair of the organizing committee*

Band Shapes of the Electronic Spectrum of Anisotropic Center in Uniaxial Crystal

Vladimir Anan'ev, Julia Spirina

*Kemerovo State University, Chemistry Faculty, Krasnaya str. 6, Kemerovo, 650043, Russian Federation
e-mail: eprlab@kemsu.ru*

Abstract

The impurity absorption band shape (in UV or visible region) in a uniaxial crystal recorded in non-polarized light has been found to depend on the technique of recording the optical spectrum and the parameters of each component recorded in polarized light. With the optical density increase in the maximum of the impurity absorption band the number of points of inflection can change from two to four. With the impurity concentration increase one can observe the shift of the impurity absorption band maximum. The impurity absorption band calculated as the difference between a total spectrum and host matrix absorption spectrum has one or two maxima.

Key words: *uniaxial crystal, optical spectrum, impurity absorption band*

1. Introduction

Nowadays crystals with anisotropic properties, including uniaxial crystals, attract more and more attention of researchers. It is common knowledge that an optical spectrum of uniaxial crystal, contains an impurity with anisotropic light absorption, must be more easily interpreted if separate investigations are made with light whose electrical field vector \mathbf{E} is polarized parallel or perpendicular to the optical axis \mathbf{L} (director), respectively [1]. This is necessary for separate determination of the tensor component parameters of both the host matrix and/or impurity molar absorptivity. For this purpose crystals must be perfectly cut. Besides, suitable equipment to determine the orientation of \mathbf{L} as to polished crystal faces should be available. It is impossible to be carried out for a great amount of crystals whose growth sides not form 90° with \mathbf{L} in a laboratory whose equipment is not designed for this kind of investigations. Moreover such an approach cannot be optimal as it results in a complication of the experiment and causes errors. Thus, for practical purposes it would be more convenient to use non-polarized light and the crystals with natural faces. However, there are no data on the band shapes of the electronic spectra due to the impurity with anisotropic light absorption in this case.

The goal of the present paper is to analyze the optical spectrum due to an impurity recorded in non-polarized light in a uniaxial crystal. The relationship between the results of optical density measurements in non-polarized light of a uniaxial crystal arbitrarily oriented to the beam, and all tensor components of both host matrix and impurity molar absorptivity has been demonstrated.

2. Theory. Absorption of non-polarized light by a uniaxial crystal

Ordinary and extraordinary waves with equal intensities are linearly polarized perpendicularly to each other when a uniaxial crystal is illuminated with non-polarized light. The former is perpendicular both to \mathbf{L} and to the principal plane, while the latter lies in the principal plane. It is assumed that director \mathbf{L} is directed parallel to the axis \mathbf{z} of a specially fixed coordinate system ($\mathbf{i} = \mathbf{x}, \mathbf{y}, \mathbf{z}$). Then $\mathbf{E}_x \perp \mathbf{L}$ (or \mathbf{z}); $\mathbf{E}_z/\mathbf{E}_y = -\operatorname{tg}\theta$; θ is the angle between \mathbf{L} and the direction of the light beam; \mathbf{E}_i is a projection of an electrical field intensity vector on the \mathbf{i} axis. Light intensity, passing through a transparent uniaxial crystal, \mathbf{I}_0 is the sum of three components – $\mathbf{I}_x, \mathbf{I}_y, \mathbf{I}_z$ connected by the following relations:

$$\mathbf{I}_0 = \mathbf{I}_x + \mathbf{I}_y + \mathbf{I}_z \quad (1)$$

$$\mathbf{I}_0 = 2 \cdot \mathbf{I}_x \quad (2)$$

$$\mathbf{I}_z/\mathbf{I}_y = \operatorname{tg}^2\theta \quad (3)$$

Uniaxial crystal spectrum are believed to be caused by \mathbf{r} band (\mathbf{k} by an anisotropic impurity and \mathbf{n} by the host matrix) $\mathbf{r} = \mathbf{n} + \mathbf{k} \geq 1$. Each transition \mathbf{r} is characterised by eigenvalues of tensor of either molar – $\varepsilon_{\mathbf{k}}^{\mathbf{i}}(\lambda)$ or axial tensor of host matrix absorptivity ($\mathbf{K}^{\perp}, \mathbf{K}^{\parallel}$). Hereinafter, the shape of \mathbf{i} component of \mathbf{r} optical absorption band will be considered Gaussian [2]:

$$p_r(\nu) = p_r \cdot \exp\left\{-5.545 \frac{(\nu - \nu_{0r})^2}{2(2H_{0r})^2}\right\} \quad (4)$$

where p_r is either $\varepsilon_{\mathbf{k}}^{\mathbf{i}}$ (molar absorptivity of impurity) or $\mathbf{K}_{\mathbf{n}}^{\perp} = \mathbf{K}_{\mathbf{n}}^{\mathbf{x}} = \mathbf{K}_{\mathbf{n}}^{\mathbf{y}}, \mathbf{K}_{\mathbf{n}}^{\parallel} = \mathbf{K}_{\mathbf{n}}^{\mathbf{z}}$ (host matrix absorptivity) in the maximum of \mathbf{i} component at ν_{0r} (λ is the wavelength of analysing light, $\lambda = 10^6/\nu$); H_{0r} is half-width (in cm^{-1}).

The change of light intensity on passing through a crystal with thickness l along the axis \mathbf{i} is given in terms of Lambert-Beer law:

$$d\mathbf{I}_i/dl = \left[\sum_n K_n^{\mathbf{i}}(\lambda) + \sum_k \varepsilon_{\mathbf{k}}^{\mathbf{i}}(\lambda) \cdot \mathbf{C} \right] \cdot \mathbf{I}_i \cdot \ln 10 \quad (5)$$

where \mathbf{C} is the impurity concentration. Substituting Eqs.1-3 in Eq.5 for a sample with slight light absorbance the following equation is obtained

$$10^{-\mathbf{A}(\lambda)} = \sum_i \beta_i \cdot 10^{-\left[\sum_n K_n^{\mathbf{i}}(\lambda) + \sum_k \varepsilon_{\mathbf{k}}^{\mathbf{i}}(\lambda) \cdot \mathbf{C} \right] l} \quad (6)$$

where $\mathbf{A}(\lambda)$ is the shape of spectrum in non-polarized light; $\beta_{\mathbf{x}} = 1/2$; $\beta_{\mathbf{y}} = (\alpha - 1/2)$; $\beta_{\mathbf{z}} = (1 - \alpha)$; $\alpha = (\cos^2\theta + 1)/2$. If the light propagates along \mathbf{L} (i.e. $\theta = 0^\circ$) then $\alpha = 1$ and the absorption is isotropic. When the direction of the light is perpendicular to \mathbf{L} (i.e. $\theta = 90^\circ$) the electrical field vector \mathbf{E} is directed along all possible directions with respect to \mathbf{L} , which gives rise to equal amounts of “parallel” and “perpendicular” electrical field directions, on the average, thereby $\alpha = 0.5$. For the other directions of the light beam the α value changes from 0.5 up to 1.

As a rule it is impossible for $\varepsilon_{\mathbf{x}}$ from $\varepsilon_{\mathbf{y}}$ to differ due to the orientation of impurity centres in the \mathbf{xy} plane of a uniaxial crystal. Therefore Eq.6 may be represented as follows

$$10^{-\mathbf{A}(\lambda)} = \alpha \cdot 10^{-\mathbf{A}^{\perp}(\lambda)} + (1 - \alpha) \cdot 10^{-\mathbf{A}^{\parallel}(\lambda)} \quad (7)$$

where $\mathbf{A}^{\perp}(\lambda) = [\sum_k \varepsilon_k^{\perp}(\lambda) \cdot \mathbf{C} + \sum_n K_n^{\perp}(\lambda)] \cdot \mathbf{I}$; $\mathbf{A}^{\parallel}(\lambda) = [\sum_k \varepsilon_k^{\parallel}(\lambda) \cdot \mathbf{C} + \sum_n K_n^{\parallel}(\lambda)] \cdot \mathbf{I}$; $\varepsilon^{\parallel} = \varepsilon_z$; ε^{\perp} is a superposition of ε_x and ε_y . Let us consider the solution of Eq.7 analytically. In the region of high absorbance $\mathbf{A}_{\max}(\lambda)$ two cases are possible:

i) if $[\sum_k \varepsilon_k^{\perp}(\lambda) \cdot \mathbf{C} + \sum_n K_n^{\perp}(\lambda)] \gg [\sum_k \varepsilon_k^{\parallel}(\lambda) \cdot \mathbf{C} + \sum_n K_n^{\parallel}(\lambda)]$ then:

$$\mathbf{A}_{\max}(\lambda) + \lg(1 - \alpha) = [\sum_k \varepsilon_k^{\parallel}(\lambda) \cdot \mathbf{C} + \sum_n K_n^{\parallel}(\lambda)] \cdot \mathbf{I} \quad (8)$$

ii) if $[\sum_k \varepsilon_k^{\perp}(\lambda) \cdot \mathbf{C} + \sum_n K_n^{\perp}(\lambda)] \ll [\sum_k \varepsilon_k^{\parallel}(\lambda) \cdot \mathbf{C} + \sum_n K_n^{\parallel}(\lambda)]$ then:

$$\mathbf{A}_{\max}(\lambda) + \lg \alpha = [\sum_k \varepsilon_k^{\perp}(\lambda) \cdot \mathbf{C} + \sum_n K_n^{\perp}(\lambda)] \cdot \mathbf{I} \quad (9)$$

where the intercept ($\lg(1 - \alpha)$ or $\lg \alpha$) is calculated from linear dependence of absorbance vs. thickness of a sample in the $\mathbf{A}_{\max}(\lambda)$ area.

Let us expand the components in Eq.7 into Taylor series. For low absorbance $\mathbf{A}_{\min}(\lambda)$ all the terms of the series except for the first two can be discarded and

$$\mathbf{A}_{\min}(\lambda) = \alpha' \cdot [\sum_k \varepsilon_k^{\perp}(\lambda) \cdot \mathbf{C} + \sum_n K_n^{\perp}(\lambda)] \cdot \mathbf{I} \quad (10)$$

where $\alpha' = \{\alpha \cdot [\mathbf{m}(\lambda) - 1] + 1\} / \mathbf{m}(\lambda)$. The ratio of optical densities $\mathbf{m}(\lambda) = \mathbf{A}^{\perp}(\lambda) / \mathbf{A}^{\parallel}(\lambda)$ is defined as the degree of absorption polarization. Eqs.8-10 are a modification of Beer's law and may be used to determine the impurity concentration in a uniaxial crystal.

3. Experimental

Alkali nitrate crystals were grown by slow cooling of saturated solutions. The nitrates used were a.r. grade (three times crystallized from redistilled water before use). In every instance the experiments were made on polished crystals (1×0.5 cm and thicknesses l varied from 0.0015 to 0.0130 cm) cut parallel to growth sides of RbNO₃ and CsNO₃ crystals, to the cleavage fracture of NaNO₃ crystals and perpendicular to the crystallographic c -axis of KNO₃ crystals (case 1). Also, a few measurements were carried out with KNO₃ polished crystals cut perpendicular to c -axis (case 2). An analyzing ($\lambda = 253.7$ nm) non-polarized light beam was directed perpendicularly to the polished face of the crystals.

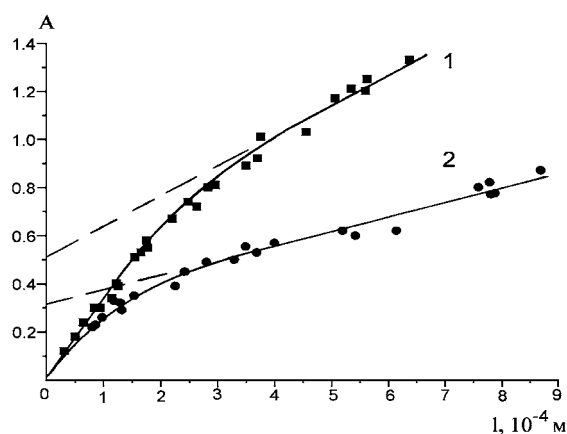
4. Results

For RbNO₃, CsNO₃ and KNO₃ (case 1) crystals, a sufficient degree of accuracy are obtained by considering their light absorption to be isotropic. The values of host matrix absorptivity for these crystals are summarized in Table 1.

Fig. 1 displays the dependence of optical density at 253.7 nm in non-polarized light from thickness of sodium and potassium (case 1) nitrate crystals.

Table 1: The values of host matrix absorptivity and parameter α for alkali nitrate crystals at 300 K

Matrix	$K^{\perp}, \text{cm}^{-1}$	$K^{\parallel}, \text{cm}^{-1}$	α
NaNO ₃	47.2 ± 1.0	14.8 ± 0.3	0.74 ± 0.02
KNO ₃	60.3 ± 1.0 (case 1), 59 ± 2 (case 2)	5.9 ± 0.3	0.51 ± 0.02
RbNO ₃	36 ± 2		1
CsNO ₃	34 ± 2		1

**Fig. 1.** The optical density at 253.7 nm in non-polarized light vs. thickness of sodium and potassium (case 1) nitrate crystals (1 and 2, respectively)

The eigenvalues of axial absorptivity tensor and the value α at 253.7 nm were calculated from experimental data (Fig.1) by means of a solution of the system of equations such as Eq.7 (Table 1). The K^{\perp} values for KNO₃ crystals (cases 1 and 2) are the same. The theoretical α values for KNO₃ (case 1) and NaNO₃ are equal 0.50, and 0.76, respectively, once $\theta = \arccos\{\text{tg}(\varphi/2)/\sqrt{3}\}$; $\varphi = 102^{\circ}40'$ [3] in NaNO₃, and $\theta = 90^{\circ}$ in KNO₃ (case 1). It is known that the type of a light source and the instrumental response of the spectrophotometer influence the polarization of the “natural” light. In most cases, it is partially polarized along the given directions. Therefore the calculated α value slightly differs from its theoretical value. All this is in good agreement with Eq.7.

4. Discussion

4.1. Resolution of overlapping bands in a uniaxial crystal registered in non-polarized light

Analysis of spectra resolution methods shows that they are true only for isotropic light absorption. Let us consider a single absorption band of a host matrix or impurity in a uniaxial crystal. From Eqs.9,10 it follows that

$$m(\lambda) = \{a(\lambda) - (1 - \alpha)\}/\alpha \quad (11)$$

where $a(\lambda)$ is the ratio of optical densities in non-polarized light in the areas $A_{\min}(\lambda)$ and $A_{\max}(\lambda)$ respectively. It follows that there is only one extreme of the $m(\lambda)$ function at $\lambda(\text{ext})$:

$$1/\lambda(\text{ext}) = \{(\mathbf{H}_j^{\perp})^2/\lambda_j^{\parallel}(\mathbf{max}) - (\mathbf{H}_j^{\parallel})^2/\lambda_j^{\perp}(\mathbf{max})\}/[(\mathbf{H}_j^{\perp})^2 - (\mathbf{H}_j^{\parallel})^2] \quad (12)$$

or $m(\lambda)$ is constant if $\lambda^{\perp}(\mathbf{max}) = \lambda^{\parallel}(\mathbf{max})$ and $\mathbf{H}^{\perp}(\mathbf{max}) = \mathbf{H}^{\parallel}(\mathbf{max})$.

If the optical spectrum is caused by two or more bands then a few extrema of the $m(\lambda)$ function are usually observed. Thus the number of $m(\lambda)$ extrema depend on the number of bands and $m(\lambda)$ function is both qualitative and quantitative characteristics of a uniaxial crystal absorption spectrum.

4.2. The shape of an impurity single absorption band recorded in non-polarized light

Let us determine the number of maxima and their positions for the single band due to the impurity with anisotropic light absorption in a uniaxial crystal. The first derivative for the function described by Eq.(7) is:

$$\frac{dA(v)}{dv} = 10^{A(v)} \cdot [\alpha \cdot 10^{-\varepsilon^\perp(v) \cdot C \cdot l} \cdot \frac{d\varepsilon^\perp(v)}{dv} + (1-\alpha) \cdot 10^{-\varepsilon^\parallel(v) \cdot C \cdot l} \cdot \frac{d\varepsilon^\parallel(v)}{dv}] \cdot C \cdot l \quad (13)$$

where

$$\frac{d\varepsilon(v)}{dv} = -\varepsilon \cdot \exp[-5.545 \cdot \frac{(v-v_0)^2}{8H_0^2}] \cdot 5.545 \cdot \frac{(v-v_0)}{4H_0^2} \quad (14)$$

For most cases it is $|v_0^\perp - v_0^\parallel| < H_0^\perp$ and H_0^\parallel . Let us consider the case when $\varepsilon^\perp > \varepsilon^\parallel$. The obtained results can be easily extended to $\varepsilon^\perp < \varepsilon^\parallel$. When $A_{\max} < -\lg(1-\alpha)$ (A_{\max} is the optical density in the maximum of the band), the first derivative is equal to zero in the only one point whose position can be calculated when solving the following equation

$$\alpha \cdot 10^{-\varepsilon^\perp(v) \cdot C \cdot l} \cdot \frac{d\varepsilon^\perp(v)}{dv} = -(1-\alpha) \cdot 10^{-\varepsilon^\parallel(v) \cdot C \cdot l} \cdot \frac{d\varepsilon^\parallel(v)}{dv} \quad (15)$$

Thus, the optical band due to the impurity has only one maximum located between v_0^\perp and v_0^\parallel .

When $A_{\max} \gg -\lg(1-\alpha)$ both terms in Eq. (15) are equal to zero when $v = v_0^\parallel$ because the value $-\varepsilon^\perp(v_0^\parallel) \cdot C \cdot l \rightarrow 0$. Thus, when increasing the concentration of the impurity C or thickness of a crystal l the band maximum recorded in non-polarized light is shifted to v_0^\parallel .

Let us determine the number of points of inflection for the function describing an impurity band shape. The second derivative for the function described by Eq.(7) is

$$\begin{aligned} \frac{d^2 A(v)}{dv^2} = & \ln 10 \cdot \left[\frac{dA(v)}{dv} \right]^2 - 10^{-A(v)} \cdot \ln 10 \times \{ \alpha \cdot 10^{-\varepsilon^\perp(v) \cdot C \cdot l} \cdot \left[\left(\frac{d\varepsilon^\perp(v)}{dv} \right)^2 \cdot C \cdot l + \right. \\ & \left. + \frac{d^2 \varepsilon^\perp(v)}{dv^2} \right] + (1-\alpha) \cdot 10^{-\varepsilon^\parallel(v) \cdot C \cdot l} \cdot \left[\left(\frac{d\varepsilon^\parallel(v)}{dv} \right)^2 \cdot C \cdot l + \frac{d^2 \varepsilon^\parallel(v)}{dv^2} \right] \} \end{aligned} \quad (16)$$

where

$$\frac{d^2 \varepsilon(v)}{dv^2} = -\varepsilon \cdot \exp[-5.545 \cdot \frac{(v-v_0)^2}{8H_0^2}] \cdot \frac{5.545}{4H_0^2} \cdot [5.545 \cdot \frac{(v-v_0)^2}{4H_0^2} - 1] \quad (17)$$

When $A_{\max} < -\lg(1-\alpha)$ from Eqs.(16,17) it follows that the second derivative is equal to zero only in two points whose values are calculated when solving a quadratic equation and, hence, their positions depend on the parameters of each component of the impurity band.

When $A_{\max} \gg -\lg(1-\alpha)$ the second derivative in the general expression can be equal to zero in four points, two of them are located in the region of wavelengths for which $A \gg -\lg(1-\alpha)$ because all

the terms with the co-factor $10^{-\varepsilon^\perp(\mathbf{v}_0^\parallel) \cdot \mathbf{C} \cdot l} \rightarrow 0$ and whose values are calculated when solving a quadratic equation and the positions of the other two depend on the parameters of each component of the impurity band and are located in the region of the wavelengths for which $\mathbf{A} < -\lg(1-\alpha)$. But 2-4 points of inflection can be observed when the parameters of the components possess certain values.

4.3. Difference optical spectrum of the impurity in a uniaxial crystal

A common procedure of determining the number of impurity bands and their parameters is to analyze a difference spectrum $-\Delta\mathbf{A}(\mathbf{v})$ which is the difference between the optical spectra of a doped crystal $-\mathbf{A}_{\text{doped}}(\mathbf{v})$ and a pure crystal $-\mathbf{A}_{\text{pure}}(\mathbf{v})$. Let us assume that there is the single impurity band, whose component parameters are described above, which overlaps the single absorption band of a pure uniaxial crystal with the following parameters $\mathbf{v}_{0\text{pure}}^\perp$, $\mathbf{H}_{\text{pure}}^\perp$, \mathbf{K}^\perp and $\mathbf{v}_{0\text{pure}}^\parallel$, $\mathbf{H}_{\text{pure}}^\parallel$, \mathbf{K}^\parallel . The difference spectrum is described by:

$$\begin{aligned} \Delta A(\nu) &= A_{\text{doped}}(\nu) - A_{\text{pure}}(\nu) = -\lg 10^{-A_{\text{doped}}(\nu)} + \lg 10^{-A_{\text{pure}}(\nu)} = \\ &= -\lg \frac{\alpha \cdot 10^{-[K^\perp(\nu) + \varepsilon^\perp(\nu) \cdot \mathbf{C}] \cdot l} + (1-\alpha) \cdot 10^{-[K^\parallel(\nu) + \varepsilon^\parallel(\nu) \cdot \mathbf{C}] \cdot l}}{\alpha \cdot 10^{-K^\perp(\nu) \cdot l} + (1-\alpha) \cdot 10^{-K^\parallel(\nu) \cdot l}} \end{aligned} \quad (18)$$

The first derivatives of the function $\Delta\mathbf{A}(\mathbf{v})$ is

$$\frac{d\Delta A(\nu)}{d\nu} = \frac{1}{A_{\text{doped}}(\nu)} \cdot \frac{dA_{\text{doped}}(\nu)}{d\nu} - \frac{1}{A_{\text{pure}}(\nu)} \cdot \frac{dA_{\text{pure}}(\nu)}{d\nu}, \quad (19)$$

where $d\mathbf{A}(\mathbf{v})/d\mathbf{v}$ is described by Eq.(13).

If the optical density of the doped crystal spectrum recorded in its maximum is $\mathbf{A}_{\text{max}} < -\lg(1-\alpha)$ the first derivative is equal to zero only in one point whose position is due to the parameters of the impurity band components and is in the $\mathbf{v}_0^\perp < \mathbf{v} < \mathbf{v}_0^\parallel$ region.

When $\Delta\mathbf{A}(\mathbf{v}) \gg -\lg(1-\alpha)$ in the $\mathbf{v}_0' < \mathbf{v} < \mathbf{v}_0''$ region (\mathbf{v}_0' and \mathbf{v}_0'' are minimum and maximum values from \mathbf{v}_0 , respectively), the general expression converges. When in Eq.(19) the value of co-factor $10^{-[K^\perp(\mathbf{v}_0^\parallel) + \varepsilon^\perp(\mathbf{v}_0^\parallel) \cdot \mathbf{C}] \cdot l} \rightarrow 0$ and the value of co-factor $10^{-[K^\parallel(\mathbf{v}_0^\parallel) + \varepsilon^\parallel(\mathbf{v}_0^\parallel) \cdot \mathbf{C}] \cdot l} = 0$ the first derivative is equal to zero only in one point ($\mathbf{v} = \mathbf{v}_0^\parallel$), the spectrum has one maximum. In some other cases the first derivative is equal to zero in two points. It can be observed if spectra of the impurity and the host matrix are polarized differently; hence, the difference spectrum has two maxima.

5. Calculations

It is evident that from the theoretical point of view the case, when an analyzing non-polarized light beam directed perpendicularly to \mathbf{L} , is of greatest interest. The theoretical optical spectra were calculated for $\alpha = 0.5$ in terms of Eqs. (4,7) with the program written by the author. The values of the components' parameters are selected so that to confirm the theoretical conclusions made in the previous chapter, moreover they have been observed.

Figs. 2-4 display a selection of the theoretical absorption spectra for the cases with absorption of non-polarized light in uniaxial crystals with dissimilar optical properties of the impurities. These figures show that the function describing the impurity band shape has only one maximum and 2-4 points of inflection whose positions depend on the parameters of each component of the impurity band and on the optical density value corresponding to the maximum of the band. All this is in good agreement with the above deductions.

From curves 4 and 5 presented in each figure it follows that the shape of the impurity absorption band recorded in non-polarized light at $A_{\max} > -\lg(1-\alpha)$ differs from “parallel and perpendicular” optical band of the impurity and, as a rule, cannot be described by any shape used in spectroscopy. When changing the angle θ from 90° to 0° the above peculiarities of the impurity optical band disappear and when $\theta = 0^\circ$ the impurity band shape is Gaussian and corresponds to the band when $\mathbf{E} \perp \mathbf{L}$.

Fig. 5 a displays the theoretical absorption spectrum in polarized light of uniaxial crystal with impurity and their analysis and Fig. 5 b displays a theoretical difference spectrum of doped uniaxial crystal in non-polarized light.

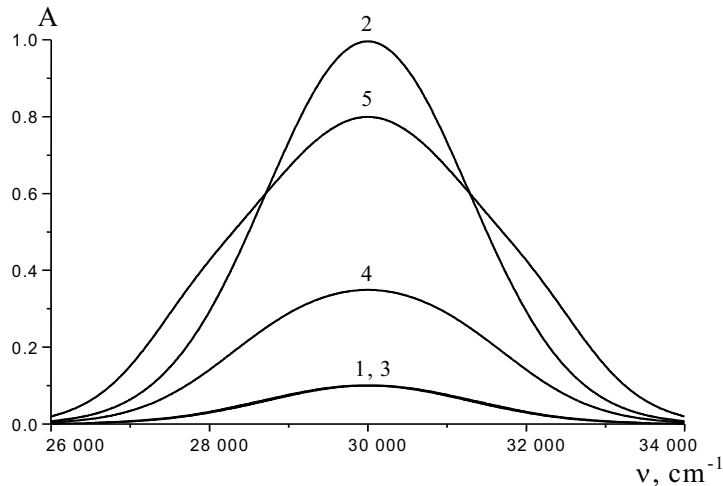


Fig. 2. Theoretical impurity spectra in a uniaxial crystal for polarized (1 – $\mathbf{E} \parallel \mathbf{L}$, 2 – $\mathbf{E} \perp \mathbf{L}$) and non-polarized light (3-5). $\varepsilon^\perp/\varepsilon^\parallel = 10.0$; $\mathbf{H}^\perp = \mathbf{H}^\parallel = 3\,000\text{ cm}^{-1}$, $\mathbf{v}_0^\perp = \mathbf{v}_0^\parallel = 30\,000\text{ cm}^{-1}$. $\varepsilon^\perp \cdot C \cdot l$ is equal to 0.2, 1.0, and 5.0 (3, 4, and 5, respectively)

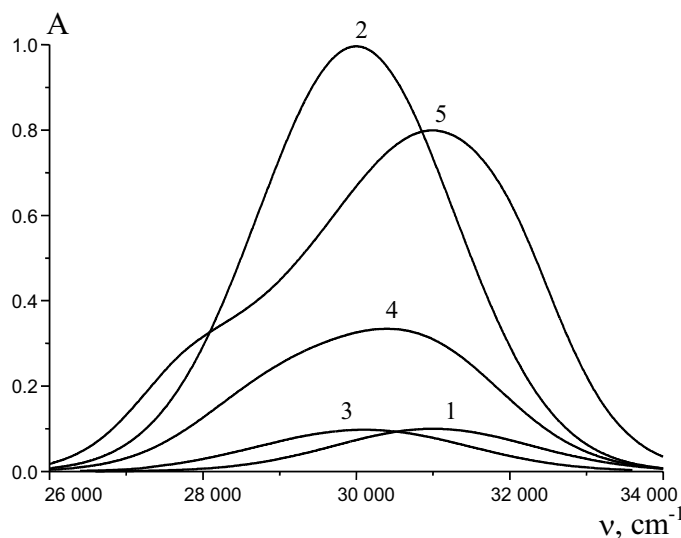


Fig. 3. Theoretical impurity spectra in a uniaxial crystal for polarized (1 – $\mathbf{E} \parallel \mathbf{L}$, 2 – $\mathbf{E} \perp \mathbf{L}$) and non-polarized light (3-5). $\varepsilon^\perp/\varepsilon^\parallel = 10.0$; $\mathbf{H}^\perp = \mathbf{H}^\parallel = 3\,000\text{ cm}^{-1}$, $\mathbf{v}_0^\perp = 30\,000\text{ cm}^{-1}$, $\mathbf{v}_0^\parallel = 31\,000\text{ cm}^{-1}$. $\varepsilon^\perp \cdot C \cdot l$ is equal to 0.2, 1.0, and 5.0 (3, 4, and 5, respectively)

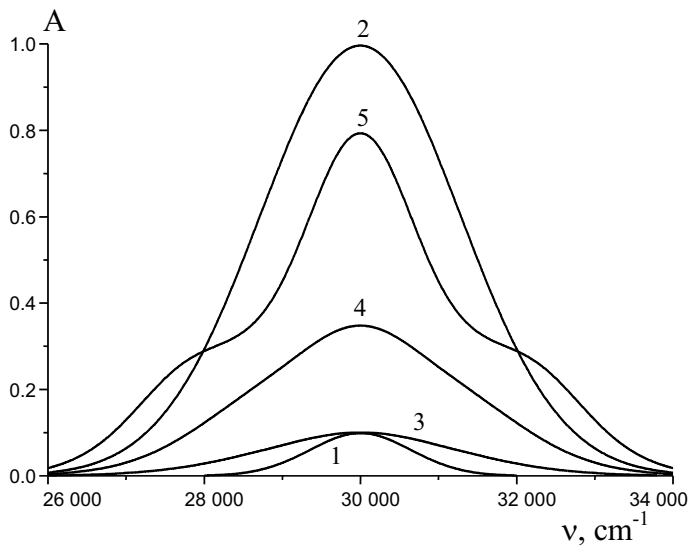


Fig. 4. Theoretical impurity spectra in a uniaxial crystal for polarized (1 - $\mathbf{E}\parallel\mathbf{L}$, 2 - $\mathbf{E}\perp\mathbf{L}$) and non-polarized light (3-5). $\epsilon^{\perp}/\epsilon^{\parallel}=10.0$; $\mathbf{H}^{\perp} = 3\,000\text{ cm}^{-1}$, $\mathbf{H}^{\parallel} = 1\,500\text{ cm}^{-1}$, $\mathbf{v}_0^{\perp} = \mathbf{v}_0^{\parallel} = 30\,000\text{ cm}^{-1}$. $\epsilon^{\perp}\cdot C\cdot l$ is equal to 0.2, 1.0, and 5.0 (3, 4, and 5, respectively)

Thus, when increasing the impurity concentration and/or the thickness of uniaxial crystal the position of the maximum of the difference spectrum in non-polarized light changes or the second maximum may be observed. It testifies to the fact that the spectrum is due to the single impurity band whose components have their own degrees of polarization of light rather than by two isotropic bands.

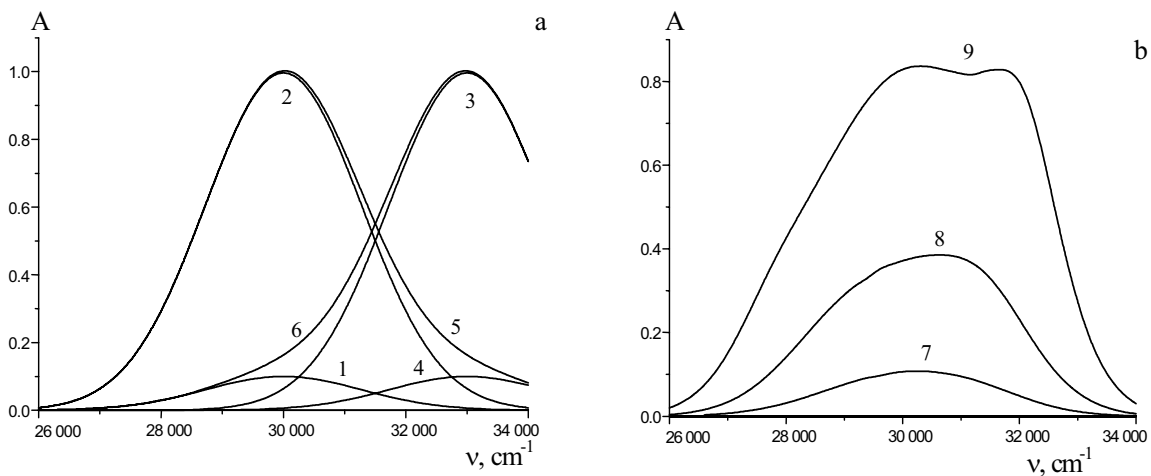


Fig. 5. Theoretical absorption spectra (1, 2 - impurity absorption spectra ($\mathbf{H}^{\perp} = \mathbf{H}^{\parallel} = 3\,000\text{ cm}^{-1}$, $\mathbf{v}_0^{\perp} = \mathbf{v}_0^{\parallel} = 30\,000\text{ cm}^{-1}$, $\epsilon^{\perp}/\epsilon^{\parallel} = 0.1$); 3, 4 - host matrix absorption spectra ($\mathbf{H}^{\perp} = \mathbf{H}^{\parallel} = 3\,000\text{ cm}^{-1}$, $\mathbf{v}_0^{\perp} = \mathbf{v}_0^{\parallel} = 33\,000\text{ cm}^{-1}$, $\mathbf{K}^{\perp}/\mathbf{K}^{\parallel} = 10.0$); 5, 6 - doped uniaxial crystal absorption spectra; 1, 3, 5 - $\mathbf{E}\perp\mathbf{L}$, 2, 4, 6 - $\mathbf{E}\parallel\mathbf{L}$) in polarized light (a) and theoretical absorption difference spectra in non-polarized light (b); $\epsilon^{\perp}/\epsilon^{\parallel} = 10.0$; $\epsilon^{\parallel}\cdot C\cdot l = 0.2, 1.0$ and 5.0 for curves 7, 8 and 9, respectively

6. Conclusion

On the basis of the analysis of light absorption in uniaxial crystal it can be concluded that the impurity band shape registered in non-polarized light substantially differs from the one registered in

polarized light. In spite of the fact that the analysis was made assuming the components' band shape to be Gaussian, the above results can be easily obtained for other band shapes.

Based on the above theoretical data the following procedure to estimate the number of impurity bands in a uniaxial crystal can be proposed. First, it is necessary to register the absorption spectrum of a single crystal when $A_{\max} < -\lg(1-\alpha)$. Second, to register the absorption spectrum of a few packed crystals when directions of the optical axis of all the crystals coincide and when total optical density $A_{\max} \gg -\lg(1-\alpha)$. The coincidence of the positions of the impurity absorption band maximum in the first and the second cases and/or the stability of the impurity band shape prove that the impurity absorption spectrum is due to a few isotropic absorption bands.

References

- [1] Born M., Wolf E.: Principles of Optics. 4^{ed}. Pergamon Press, Oxford, London, Edinburg, N.Y., Paris, Frankfurt, 1968
- [2] Sharaf M.A., Illman D.L., Kowalski B.R.: Chemometrics. Willey-Interscience Pub., N.Y., 1986
- [3] Wyckoff R.V.G.: Crystal structures. V.2. John Wiley & Sons, N.Y., London, 1964

Ultrasonic Extraction for Evaluation of the Mobility of Fe and Mn Contents in Components of Environment

Jana Blašková¹, Viera Vojteková¹, Jarmila Nováková²

¹University of P.J. Šafárik, Institute of Chemical Science, Department of Analytical Chemistry, Moyzesova 11, SK-041 67 Košice, Slovakia, e-mail: jana.blaskova@upjs.sk, viera.vojtekova@upjs.sk

²State Geological Institute of Dionýz Štúr, Geoanalytical Laboratories, Markušovská cesta 1, SK-052 40 Spišská Nová Ves, Slovakia, e-mail: mackovych@gsrscsnv.sk

Abstract

The application of a strong chelating agent for the screening test of element mobility in sedimentary systems was investigated. Ultrasonic extraction into ethylenediaminetetraacetic acid (EDTA) was used for the evaluation of iron and manganese mobility in the polluted sediments and compared with the conventional mechanical EDTA extraction. This work presents the description of sample preparation, the optimization of the iron and manganese ultrasonic sediment extractions, the comparison of the optimized ultrasonic extraction with the conventional 6 hour extraction into EDTA, with the optimized IRMM (Institute for Reference Materials and Measurements) recommended sequential extraction procedure and with the values of total element contents analysed by method XRF.

Key words: *Fe, Mn extractability, element mobility, sediments, conventional and ultrasonic extractions optical emission spectrometry, total element content analysis XRF*

Introduction

Quantification of extractable forms of Fe and Mn, and trace metals in contaminated sediments and soils provides the basis for element mobility studies in the environment [1,2]. Extraction into strong complexing agents could be used for evaluation of the nonresidual elemental content of sediments and soils. Assessment of the extractability of iron and manganese oxides provide information about majority of elements associated with this environmentally important phase. Changes of iron release into a water solution induce the trace element mobility changes, transport of elements through the environment components and a change in the water's potential to affect the aquatic life [3,4,5]. The extraction and determination of iron and manganese using ethylenediaminetetraacetic acid serves as a fast additive screening for actual contamination and mobility changes in a sedimentary system [6]. Ultrasonic extraction into a strong chelating agent like Na₂EDTA is able to release mobile and potentially mobile extractable forms of Fe, Mn associated with specific phases of sediments and soils. The application of ultrasonic single-step extraction procedure is interesting both from economical and from time-saving point of view [7]. This method offers to shorten the extraction time more than ten times because an optimised Na₂EDTA sediment extraction takes six hours while the

modified IRMM extraction requires 64 hours in total [8]. Thus, Na₂EDTA extraction of Fe and Mn can serve as an economical, time-saving supplementary test for the IRMM procedure.

Experimental

Topographical localization of the selected sampling region and the list of sampling sites are given in Fig. 1 and Table 1. Conventional and ultrasonic single-step extraction procedures were applied to sediment samples collected from an industrially polluted region of Eastern Slovakia. Original samples comprised of sand, silt and clay fractions. The sediments were dried at 40 °C and passed through a 0.125 mm stainless steel sieve. A fraction with the particle size smaller than 0.125 mm was milled on an agate planetary treadmill to grain size under 0.09 mm. 0.5 g portions of homogenized samples were weighted for the determination of the content of extractable Fe and Mn [9]. The ultrasonic extraction into disodium EDTA salt was developed for this study and compared with the conventional six hour Na₂EDTA extraction [7] and the modified BCR (Community Bureau of Reference) sequential extraction protocol (see Table 3) [12,13]. There were compared the summary Fe and Mn contents, which were extracted in the first three steps (original norm) [11], modified five steps [12,13] sequential extraction and the Fe, Mn contents extracted into EDTA solutions.

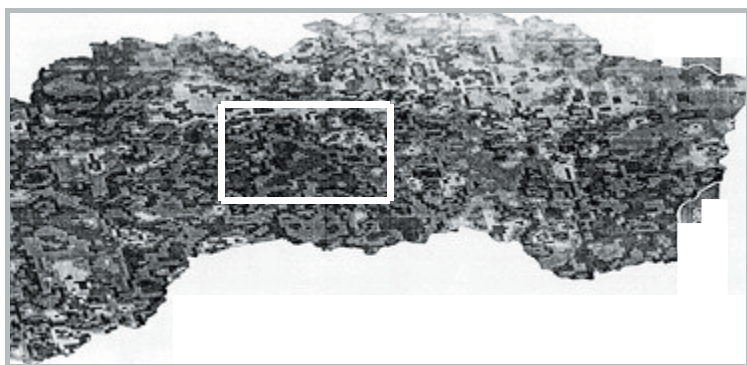


Fig. 1. Topographical location of the sampling area in Slovakia

Table 1. Sampling places of the chosen region

	Place of the sampling	Sediment	River / Stream
1	Rudňany – Markušovce	Sediment 1	Hornád
2	Slovinky	Sediment 2	Poráčsky jarok
3	Richnava	Sediment 3	Hornád
4	Jaklovce	Sediment 4	Hnilec

Chemicals and reagents. All standards and chemicals were obtained from the Sigma-Aldrich group and Merck (Darmstadt, Germany) and it was used Na₂EDTA for analysis. Distilled water was cleaned by reverse osmosis and by an ion exchanger. Deionised water was used in all experiments.

The preparation of extractant solutions. For the single-step extraction procedure 0.05 mol dm⁻³ Na₂EDTA solution (pH – changed within 3 and 7, adjusted with HCl, NH₄OH, alternatively) was prepared. The pH of untreated 0.05 mol dm⁻³ Na₂EDTA solution was 4.7.

The ultrasonic extraction procedure: 0.05 mol dm⁻³ solution of Na₂EDTA was prepared and solution had a pH = 4.7. It is analogical, the same when using the single-step extraction procedure.

For sequential extraction procedure, the solutions of 0.11 mol dm⁻³ acetic acid (CH₃-COOH); 0.1 mol dm⁻³ hydroxylammonium hydrochloride (HO-NH₂.HCl); hydrogen peroxide (H₂O₂): concentrated H₂O₂ was acidified with diluted nitric acid (1:1) to a pH value between 2 and 3, and 1 mol dm⁻³ ammonium acetate (CH₃-COONH₄) were used.

Single-step extraction with $0.05 \text{ mol dm}^{-3} \text{ Na}_2\text{EDTA}$: The standard soil extraction procedure with $0.05 \text{ mol dm}^{-3} (\text{NH}_4)_2\text{EDTA}$ [10] was modified for the sediments. Modified $0.05 \text{ mol dm}^{-3} \text{ Na}_2\text{EDTA}$ solution was prepared and extraction of soils was optimized for sediments from the studied area. The original and modified conditions of the extraction procedure are given in the Table 2. The optimized time was 6 hours, the optimized solid sediment/solution - extraction ratio (w/v ratio) was 1:150 (it was weighed 0.5 g of the sediment sample and added 75 cm^3 of the Na_2EDTA solution). The pH of used extraction medium was 4.7.

Table 2. Standard and modified procedure for single and ultrasonic extraction into $0.05 \text{ mol dm}^{-3} \text{ EDTA}$ -salt

	Standard procedure	Modification of standard procedure	Ultrasonic extraction
extraction agent	$(\text{NH}_4)_2\text{EDTA}$	Na_2EDTA	Na_2EDTA
time of extraction	1 hour	6 hours, without pH modification, pH = 4.7 1 hour during optimization of pH	5 – 15 minutes
temperature	$20 \pm 2 \text{ }^\circ\text{C}$	$20 \pm 2 \text{ }^\circ\text{C}$	$20 \pm 2 \text{ }^\circ\text{C}$
solid sample/solution extraction ratio (w/v ratio)	1:10	1:150	1:150
acidity of extraction agent	pH = 7 (modified with NH_4OH)	3-7	pH = 6.7
Extraction vessel	250 cm^3 PE (washed by H_2O , $4 \text{ mol dm}^{-3} \text{ HNO}_3$ and $0.05 \text{ mol dm}^{-3} \text{ EDTA}$ -salt)		
Filtration	„paper with blue stripe“ $\varnothing = 18.5 \text{ cm}$		

Ultrasonic extraction procedure: It was weighted 0.5 g of the sediment sample and added 75 cm^3 of the Na_2EDTA solution. The w/v ratio was 1:150. The extract was strained through filtration paper with blue stripe and the zinc content in filtrate was determined by using atomic emission spectrometry.

BCR sequential extraction: The method of sequential extraction used in this work was slightly modified with respect to the regional geological conditions. Apart from the usual three steps of the IRMM procedure [11], the first step (for elements extractable into the water phase) and the fifth step (digestion of the sediment residue) were added [12,13]. The standard and modified IRMM procedure for sequential extraction is listed in Table 3. All results were obtained as the average values of 5 repeated extractions.

Table 3. Standard and modified IRMM procedure for sequential extraction

Step	Extracted fraction	Standard IRMM procedure	Modified IRMM procedure
1	Water-soluble	-	deionised water, pH \approx 6.7
2	Acid extractable	$0.11 \text{ mol dm}^{-3} \text{ CH}_3\text{COOH}$, pH=3	$0.11 \text{ mol dm}^{-3} \text{ CH}_3\text{COOH}$, pH=3
3	Reducible	$0.1 \text{ mol dm}^{-3} \text{ HONH}_2\cdot\text{HCl}$, pH=2	$0.1 \text{ mol dm}^{-3} \text{ HONH}_2\cdot\text{HCl}$, pH=2
4	Oxidizable	$8.8 \text{ mol dm}^{-3} \text{ H}_2\text{O}_2$, $1 \text{ mol dm}^{-3} \text{ CH}_3\text{COONH}_4$ pH=2	$8.8 \text{ mol dm}^{-3} \text{ H}_2\text{O}_2$, $1 \text{ mol dm}^{-3} \text{ CH}_3\text{COONH}_4$ pH=2
5	Residual	-	HNO_3 , HF, HClO_4

Analytical apparatus: The conventional extraction was performed on a mechanical shaking machine, model T22. The ultrasonic extraction was performed on an ultrasound disintegrator UZD 500. The power of disintegrator was 90 % and the maximal power of disintegrator was 500 watt. The range of the optimized time was from 5 to 15 minutes. Atomic emission spectrometry with inductively coupled plasma was used for the determination of iron and manganese in extracted fractions. The measurements were carried out on a Vista MPX spectrometer. Experimental conditions of ICP OES measurements for iron and manganese are listed in Table 4.

Table 4. Experimental conditions for ICP – OES measurements

Element	Wavelength	Correction	LOD (mg dm ⁻³)
Fe	238.204	dynamic	< 3
Mn	257.610	dynamic	< 3

Results and discussion

The results of extractability of Fe and Mn in four sediment samples could be discussed as follows:

The investigation of the accuracy of 6 hours conventional EDTA extraction and ultrasonic EDTA extraction brought acceptable results. The comparison of the extracted iron and manganese contents with and without ultrasound is given in Fig. 2. The time of the ultrasonic extraction was optimized and the results of the optimized ultrasonic EDTA extraction (see the 3rd column on the Fig. 2) were compared with the results of the conventional „six hour EDTA extraction“ (see the 1st column on the Fig. 2), 5-step sequential extraction (see the 5th column on the Fig. 2) and with total element content analysis by the roentgen-fluorescent spectrometry (see the 6th column on the Fig. 2). The results of the sequential extraction procedure and the total elemental content analysis of Fe and Mn obtained by the XRF method are in good agreement with those determined using ultrasonic Na₂EDTA extraction. Detailed description the values of sequential extraction procedure and the total element contents of studied sediment samples analysed by method XRF bring references [7,14].

The optimal time of the Mn and Fe ultrasonic extraction was 15 minutes for all sediment samples. On the diagram in Fig. 2 see the comparison of the Fe and Mn contents obtained by optimized ultrasonic (the 3rd column) and conventional EDTA extraction (the 1st column) with the summary Fe and Mn contents of first, second and third steps (the 4th column) of the five-step sequential extraction. The extracted Fe and Mn contents during the optimized ultrasonic extraction (15 minutes) achieve the contents of the 6 hours conventional EDTA extraction, evenly much higher with that of USG extraction (see Fig. 3). The time of extraction could be considered as the sufficient for extraction of the mobile and mobilizable Fe and Mn portions.

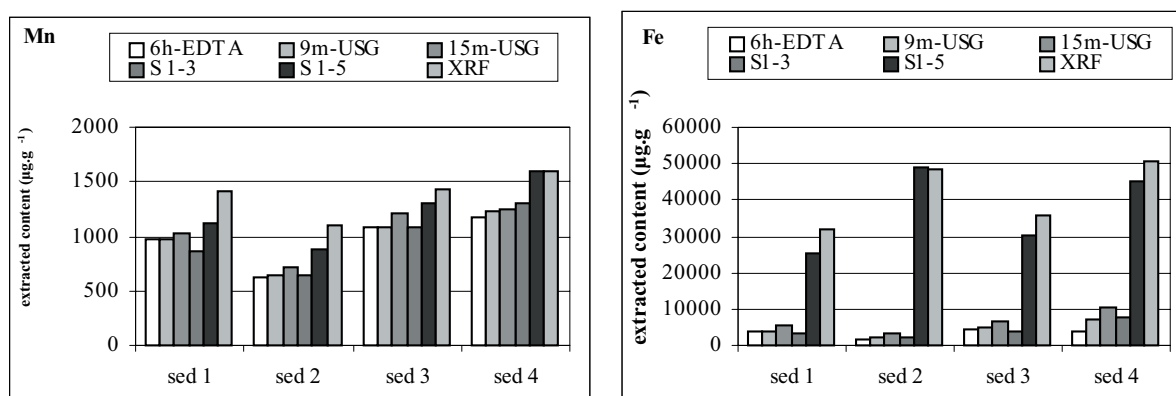


Fig. 2. Comparison of single-step (6hours), USG (9,15 min.), SEP (S 1-3, S 1-5) and XRF analysis of Fe and Mn
 6-h EDTA – six hours extraction into 0.05 mol dm⁻³ Na₂EDTA
 9-min. USG – nine minutes ultrasonic extraction into 0.05 mol dm⁻³ Na₂EDTA
 15-min. USG – ten minutes ultrasonic extraction into 0.05 mol dm⁻³ Na₂EDTA
 S 1-3 – the sum of the 1st, 2nd and 3rd step of the five-step SEP
 S 1-5 – the sum of the 1st, 2nd, 3rd, 4th, 5th step of the five-step SEP
 XRF – total element content analysis obtained by XRF

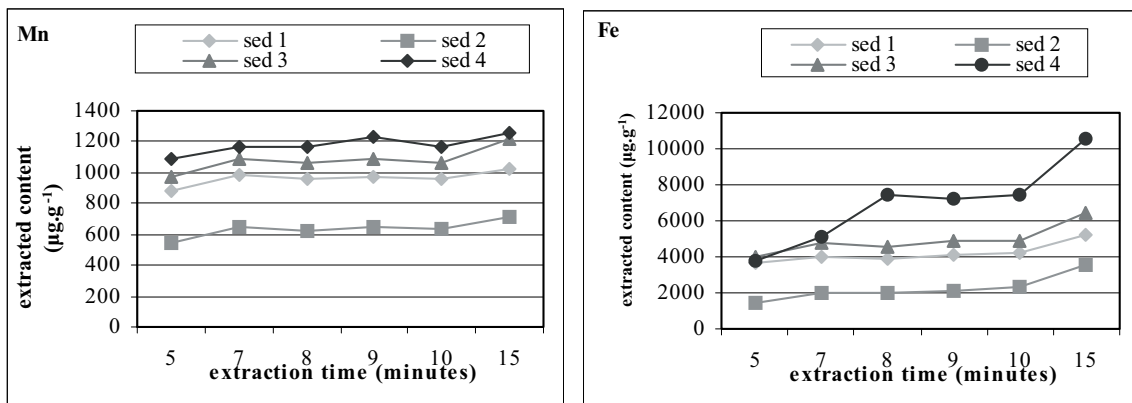


Fig. 3. Optimization of the extraction time, determination of Mn and Fe extracted portions in the sediments (USG extraction)

Fig. 4 documented RSD values during the optimization of time. On the base of diagram running (see Fig. 4) could be concluded the next: The RSD values achieve the highest values in sediment 2 and 3. The fluctuations of the RSDs by other sediment samples are not so significant and obviously do not exceed 10 %, except sediment 3 by 15 minutes extraction for Mn. The running of the RSD diagram shows the necessity of time extension and the next experimental optimization.

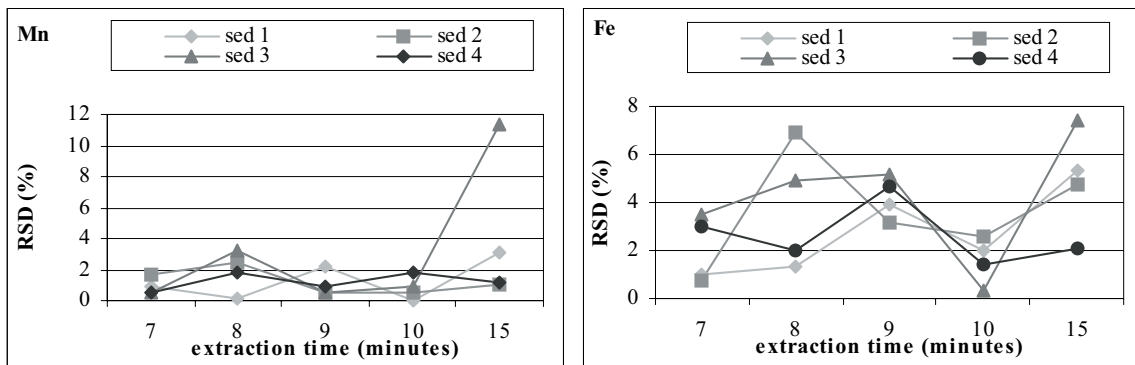


Fig. 4. The RSDs (%) by time optimisation of Mn and Fe in the sediment samples from extraction time (USG)

Conclusion

With respect to the running of presented experiments it is possible to state that an ultrasonic extraction into the Na_2EDTA is able to release mobile and potentially mobile metal forms and Na_2EDTA can therefore be considered capable to extract the majority of elements associated with the reducible sedimentary phase – bound to Fe and Mn oxides in the regional geological conditions of the monitored region. The contents of elements extracted by Na_2EDTA by the conventional (6-hours) and ultrasonic (15 minutes) extraction bring comparable results. The extraction efficiency of the single-step procedure was compared with that of SEP and results were in good agreement with the sum of the first three steps of SEP for Fe and Mn. The observed fluctuations of the RSD values still require the next supplementary experiments.

Thus, ultrasonic extraction is the innovative time saving supplementary test to the IRMM procedure for the element mobility evaluation.

Acknowledgement

This work was financially supported by Scientific Grant Agency of the Ministry of Education of Slovak Republic (the grants No. VEGA 1/4450/07 and VVGS PF 19/2008/CH). The authors would like to express their gratitude for this support.

References

- [1] Batley G.E.: Trace Element Speciation: Analytical Methods and Problems (2nd Ed.). CRC Press, Inc. Boca Raton, 1990
- [2] Slaveykova V.I., Wilkinson K.J.: Predicting the bioavailability of metals and metal complexes: Critical review of the biotic ligand model. *Environmental Chemistry* 2, 9-24, 2005
- [3] Ussher S.J., Achterberg E.P., Worsfold P.J.: Marine biogeochemistry of iron. *Environmental Chemistry* 1, 67-80, 2004
- [4] Laan R.G., Verburg T., Wolterbeek H.T., de Goeij J.J.M.: Photodegradation of iron (III)-EDTA: Iron speciation and domino effects on cobalt availability, *Environmental Chemistry* 1, 107-115, 2004
- [5] Howitt J.A., Baldwin D.S., Rees G.N., Hart B.T.: Facilitated heterogeneous photodegradation of dissolved organic matter by particulate iron, *Environmental Chemistry* 1, 197-205, 2004
- [6] Vojteková V., Krakovská E., Mackových D., Nováková J., Šoltýsová H.: Determination of removable portion of some elements in stream sediments of Spišsko-gemerské rudohorie Mountains. *Slovak Geol. Mag.*, 2003, 9 (2-3), 133-136
- [7] Vojteková V., Nováková J., Mackových D., Blašková J.: A new method of evaluation of element pollutant mobility in sediments. *Chem. Pap.*, 2008, 62(2), 160-167
- [8] Vojteková V., Krakovská E.: Fractionation analysis of the sediments – limitations in the selectivity of the extractants. *Chem. Pap.*, 2006, 100, 1096-1104
- [9] Vojteková V., Nováková J., Mackových D.: Fast monitoring of the element mobility changes in environmental pollution. *Transaction of the Universities of Košice*, 2006, 2-3, 136–142
- [10] Ure A.M., Davidson C.M., Thomas R.P.: Single and sequential extraction schemes for trace metal speciation in soils and sediments. In P. Quevauviller, E.A. Maier, B. Griepink (Eds.), *Quality Assurance for Environmental Analysis*. Amsterdam: Elsevier, 1995, 505-523
- [11] Fiedler H.D., López-Sánchez J.F., Rubio R., Rauret G., Quevauviller P., Ure A.M., Muntau H.: Study of the stability of extractable trace-metal contents in a river sediment using sequential extraction. *Analyst* 119, 1109-1114, 1994
- [12] Mackových D.: *Geological Survey of the Slovak Republic. Subproject 2, (GAL/ŠVL/ČS/3-2000)*, 2000
- [13] Tessier A., Campbell P.G.C.: Comments on the testing of the accuracy of an extraction procedure for determining the partitioning of trace metals in sediments. *Analytical Chemistry* 60, 1475-1476, 1988
- [14] Vojteková V., Flórián K., Krakovská E., Mackových D.: Fractionation analysis of typical river sediments and comparison with direct XRF and DC-OES spectrometry analysis of total element contents in chosen samples. *Transaction of the Universities of Košice* (2), 47-52, 2004

Mass Spectrometry Analysis of Isopropylester Analogues of Methylfluor Phosphoric Acid

Štefan Bova¹⁾, Pavel Pulíš²⁾, Milan Božok¹⁾

¹⁾ Military base 7945, Šafárikova 109, 048 01 Rožňava, Slovakia

²⁾ Academy of Armed Forces of general M.R. Štefánik, Demänová 393, 031 01 Liptovský Mikuláš, Slovakia

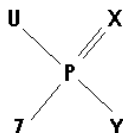
Abstract

Identification of isopropylester of methylfluor phosphoric acid and dimethyl, N,N – phosphoramidates next to toxic organic compounds, like sarin or VX agent, allows observation of procedure probably used for preparing this toxic chemical agent. Standard procedures prefer use of more time consuming derivation techniques followed by gas chromatography and mass spectrometry, mainly with V agents analysis. Direct measurements coupled with minimalization procedures necessary for sample preparation, are preferred for quick analysis and laboratory control analysis in mobile equipment. Methods for identification performance were optimized within mobile laboratory by gas chromatography and EI (Electron Impact) mass spectrometry, which allow quick analysis directly in extract of samples with acceptable result for purpose of quick decision-making process. Interpretation of analysis result by simple comparison with databases appears to be available and effective answer, which we confirmed from the point of reproducibility and identification reliability. Identification reliability was proved by mass spectrum comparison with database, also by structure fragmentation prediction of observed agents and by comparison of possible fragments mass with measurement.

Key words: *phosphoramidates, EIMS, sarin, GB*

Introduction

Isopropylester of methylfluor phosphoric acid, designed as SARIN, GB or TRILON 46, eventually T144 was prepared in 1938 by IG-Farben laboratories, headed by G. Schrader, looks like perspective chemical toxic agent for chemical weapons. It was a success of systematic research in new area of esters, amides and halogenids of phosphoric acids with general formula,

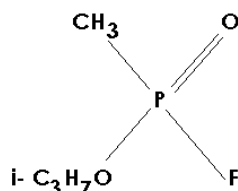


where constitutes X: = O, =S, Y: -F, -Cl, -OR, -O-PO(OR)₂, Z: -OR, -N(R)₂ a U: -R, -N(R)₂. Toxic effects of its less-effective down homologue methylester of methylfluor phosphoric acid had been known at that time. Category of toxic chemical agents was formed during World War Two, which regarding to its extreme toxicity, rapid penetration to organism by all sites of entrance and low-time

latency constitutes the group of most important toxic chemical agents in armament of several armies up to nowadays. Tempestuous expansion of chemistry in 30's and 40's showed by discovery of new very toxic compound of phosphorus in connection with searching for effective vegetable protection agents and a great deal of compounds has been prepared up to this day, including widespread spectrum of toxic chemical agents designed for military purposes, for example agents GA, GD, GF, GP, GE, or agents derived from cholin, as VX, VM, VG. These agents represent very significant risk, for example misuse by terrorists, and in the case of using analogues and homologues of such compounds in industry and agriculture.

Experimental

Agent sarin was prepared in laboratory designed by OPCW, as 10 % solution in toluene by "rearrangement mode", without cleaning from residua of precursors and contained high fraction of O,O-diisopropyl methyl phosphanate. The sample for analysis was prepared by applying 1 ml of technical sarin native solution on the surface 100 cm², containing 1 kg silica sand with 12,7 % water and after 10 minutes was taken surface sample from 10 cm² with 2 cm depth of sampling. Sample was quartered and the first fraction was extracted with n-hexane in mechanical homogenizator with total volume 100 ml of solvent. After separation the filtrate was analyzed GC/MSEI. The GC/MS analyses were performed in EI mode (70 eV) with EM 640 BRUKER, equipped with quadrupole selective detector. DB-5 capillary column with 20-m length was used with the following temperature program: 50 °C (2 minute) – 280 °C (5 minute). Nitrogen was used as a carrier gas. The samples were analyzed in splitless mode at an injection temperature of 250 °C, EI source temperature of 230 °C and quadrupole analyzer temperature of 180 °C. From chromatograph report was after deconvolution by AMDIS software isolated peak for DIMP with RI = 1071,8 iu and peak for sarin with RI = 823,8 iu. Observed peak DIMP was in accordance mass spectrum (MSEI), which was compared with database NIST. In mass spectrum of the sample were observed important fragments 139, 123, 121, 97, 80, 79 a 45 m/z. Other typically fragments 27, 41 and 43 m/z were not present, because they occurred out of device measuring range, that is 45 to 680 m/z. Typical fragments 141, 125, 99, 98, 47 for sarin were observed. Other typical fragments 43, 39, 42, 27, 41 for sarin were not report, thanks to same reasons. Therefore their express identification preformed after detection of contamination has crucial importance. In this group sarin represents still extremely important agent that is being produced by the two basic processes. First one is based on „salt“ technology and originates on phosphoric chloride that with methylalcohol yields dimethylphosphite. This one after transformation to sodium salt, by Arbuzov rearrangement in presence of methylchloride is transformed to dimethylester of methylphosphoric acid. The product is then chlorinated and consequently undergoes its synchronous fluoration and esterification to final product. The second process marked as „rearrangement“ is similar to the first stage. But further the dimethylphosphide is isomerated by the thermal rearrangement and the produced methylester is chlorinated and consequently fluorized to mixture of difluoride and dichloride of methylphosphoric acid that is transformed by esterification to sarin.



The final product is usually stabilized by adding diethylaniline. Also different methods are used. Final products hydrolysis speed is in ordinary environment relatively high. Water with pH = 7 breaks down a half of sarin volume in 100 minutes. Hydrolysis is catalysed by hydroxyl and hydrogen ions, thus observed reaction speed constant factor of first order reaction at constant pH, besides direct reaction with water molecules will contain also factors describing reaction speeds of second reaction

order, dependant from hydrogen and hydroxyl ions concentration. It means that in the case of samples identification, suspected from sarin presence is necessary to count with presence of all mentioned compounds. The present analogues will be mainly represented by the reaction interproduct O,O-diisopropyl methyl phosphonate (DIMP) with molecular weight 180. This interproduct we analysed detaily. However from the point of urgent analysis identification of presence of sarin, detection of precursors, interproducts and decay products is of decisive importance and in later stage can yield information on the production procedure and the time of contamination outbreak, what can support solution of the crisis situation.

For performing the DIMP identification we chose gas chromatography method with mass spectrometry utilizing ionization by electron impact. After compounds separation by the GC method peaks the deconvolution by AMDIS software with the use of mass spectrum was performed. Consequently peak mass spectrum corresponding with DIMP agent was evaluated, compared with NIST database and analogue spectra. Based on the data we suggested probable ways of analyte of interest fragmentation to facilitate the DIMP identification process, supposing the contemporary presence of sarin and similar agents in sample, including DIMP.

Results and discussion

Comparing of mass specters of O,O-diisopropylmethyl phosphanate (DIMP), gained by measuring in gass chromatograph with mass spectrometer (GC/MSEI) EM-640 BRUKER with reference mass spectrum NIST and OPCW a total match of important peaks in specific range has been found out. For identification the match over 90 % is sufficient, therefore we can consider the DIMP identified. Its identification in the mixture with sarin, as a major and dominant product, other reactional products and precursors in term of data interpretation gained by GC/MSEI appears to be without problems after optimization of experiment condition on selected instrument.

Dimethyl N,N-dialkylphosphoramidates, which are analogues of another important toxic chemical agents, VX, have been examined with similar method. Also in this case we have discovered similar results. In contrast to G agent it is necessary to use different condition for gas chromatography analysis. Dialkylphosphoramidate dichloride (0,01 mmol/ml in propanol) have been used for the experiment and then analysed directly by the GC/MS. Dimethyl N,N-dialkylphosphoramidates produced a fragmentation ion $[\text{CH}_3\text{OP}(\text{O})\text{OCH}_3]^+$ at m/z 109, which is presumable formed via loss dialkylamino radical from the molecular ion. The cation could further disintegrate by elimination HCHO and typically produced the fragmentation ion at m/z 79 $[\text{CH}_3\text{OPOH}]^+$. Rearranged dialkylaminocation was also characteristically observed. This particular ion is of diagnostic value as it revealed the kind of dialkylamino group present in given phosphoramidate.

Conclusion

In analysis of toxic chemical agents G and V, is after gas chromatography conditions optimalization possible direct identification of isopropylester analogues of methylfluor phosphoric acid and dimethyl, N,N-phosphoramidates, without derivatization. The results are well-interpretable by accessible reference databases NIST. Reliability of analysis is confirmed by analysation of presumable fragmentation scheme. The methodic is very available for implementation in mobile laboratories, equipped with appropriate devices and software.

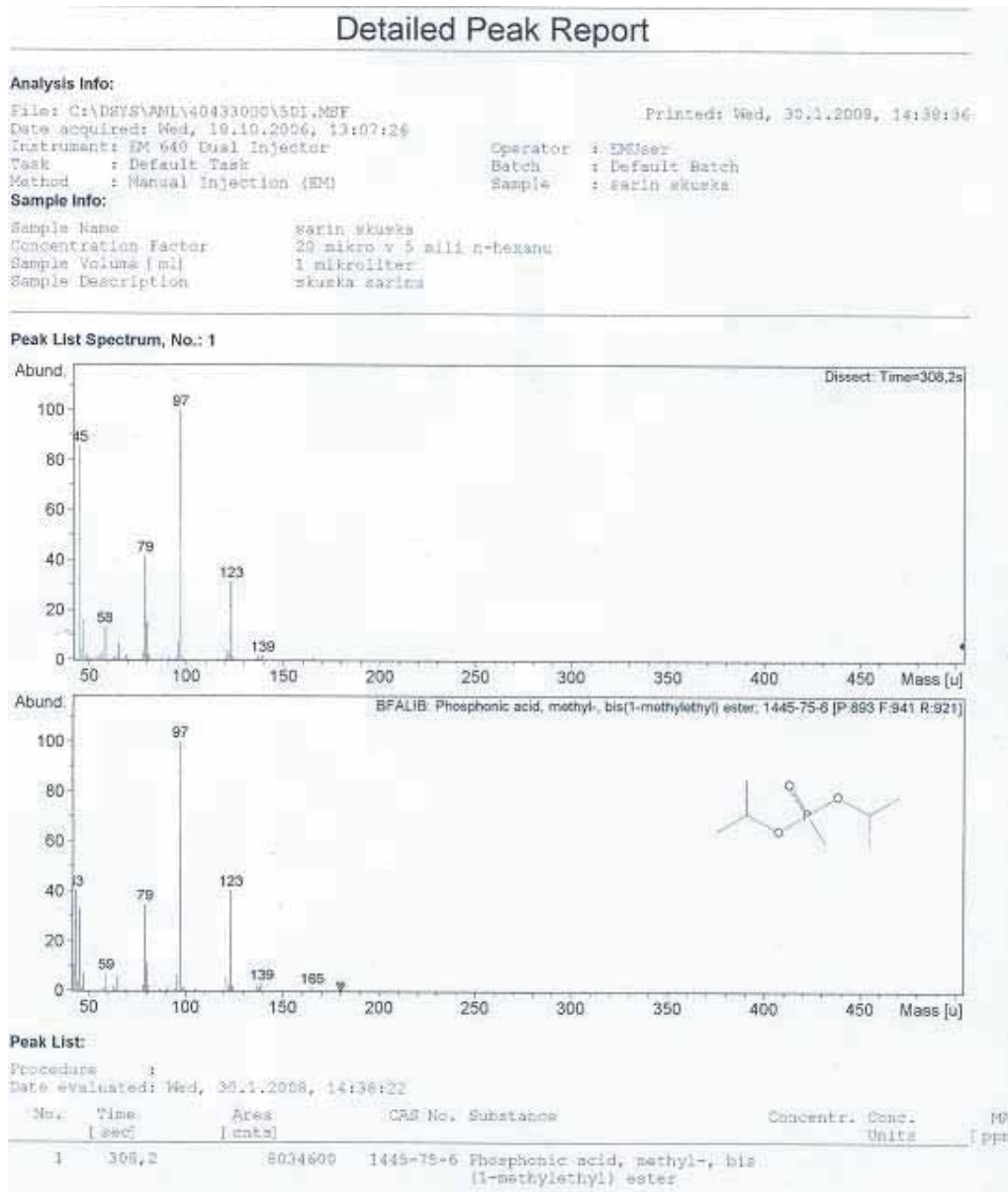


Fig. 1. DIMP mass spectrum report compared with NIST DIMP database mass spectrum

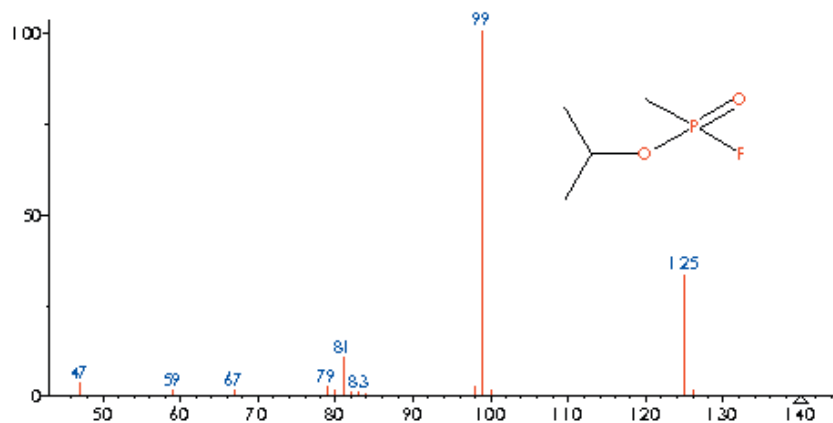


Fig. 2. Sarin mass spectrum

References

- [1] Príručka NATO pre odber vzoriek a identifikáciu bojových biologických a otravných látok AEP-10, Vol. 1., 5. ed., 2000
- [2] Puliš P., Bova Š. et al.: Požiadavky na mobilnú analýzu u jednotiek RCHBO, *Zborník príspevkov 7. medzinárodnej vedeckej konferencie*, TU Košice, 2006
- [3] Bova Š., Božok M.: Skúsenosti z nasadenia síl RCHBO v rámci vojenskej asistencie orgánom IZS. *Zborník príspevkov z konferencie „Terorizmus – hrozba súčasnosti“*, AOS Liptovský Mikuláš, 2006
- [4] Puliš P., Bova Š.: Prístupy pre riešenie otázok mobilnej analýzy chemickej kontaminácie prostredia v krízových situáciách. *Zborník príspevkov z 26. vedeckej konferencie*, Piešťany, 2006
- [5] EPA Method 8080B, *Test methods for Evaluating Solid Waste*, SW 846, November 1990
- [6] Wagner J., Kotas P.: *Guide to Environmental Analytical Methods*, Second Ed., Genium, Schenectady, New York, 1994
- [7] Kanu A.B., Haigh P.E., Hill H.H.: Surface detection of chemical warfare agent simulants and degradation products, *Analytica Chimica Acta* 2005, **553**, 148-159
- [8] U.S. EPA Contact Laboratory Program, Statement of Work for Organic Analysis, OL MOB-1, August 1994
- [9] IX. letná škola plynovej chromatografie, Kapilárna plynová chromatografia a jej spojenie s hmotnostnou spektrometriou, STU Bratislava, september 2003
- [10] Klouda P.: *Moderní analytické metody*, Ostrava, 2003
- [11] Garaj J., Hladký Z., Labuda J.: *Analytická chemie I*. STU Bratislava, 1996
- [12] Němcová I., Čermáková L., Rychlovský P.: *Spektrometrické analytické metody I*. Učebný text Univerzity Karlovy v Prahe, 2004

Photochemical Vapor Generation in Analytical Atomic Spectrometry – Recent Developments

Marek Bujdoš, Jana Kubová, Ingrid Hagarová, Peter Matúš

Comenius University in Bratislava, Faculty of Natural Sciences, Geological Institute, Mlynská dolina G, 842 15 Bratislava, Slovakia, e-mail: bujdos@fns.uniba.sk

Abstract

Photochemical vapor generation is a new method for sample introduction in analytical atomic spectrometry. Nonvolatile analyte species are converted to volatile species and transferred to gas phase by means of radiation instead of the chemical reductants. The advantages of efficient matrix separation, high analyte transport efficiency, high selectivity and simple instrumentation which are connected with conventional chemical vapor generation (CVG) systems are extended by advantages of lower blanks and avoiding of hazardous chemicals. A development of new and promising vapor generation techniques for determination of mercury, selenium and other analytes using photochemical vapor generation are described in this brief review.

Key words: *photochemical vapor generation – hydride – cold vapor – atomic spectrometry*

1. Introduction

The determination of the trace elements at very low concentration levels is still an actual analytical problem. Atomic absorption spectrometry (AAS) with different methods of atomization are very powerful methods of analytical chemistry. One of the most sensitive methods of AAS is electrothermal atomic absorption spectrometry (ETAAS), however it has high cost of equipment and operational costs as well. Other powerful sample introduction method to AAS is the vapor generation AAS (VGAAS). This technique usually outperforms ETAAS, however, the number of elements forming volatile species is limited (e.g. As, Bi, Ge, Hg, In, Pb, Sb, Se, Sn, Te, Tl). Fortunately, in recent years, determination of other elements becomes feasible [1]. Hydride generation AAS (HGAAS) is still the most utilised vapor generation approach, using chemical reduction employing sodium (or potassium) tetrahydroborate from strongly acidic media of strong mineral acid [2-5]. In case of typical hydride-forming elements this method is well evolved and it is used as routine analytical technique. The problem common to all chemical vapor generation approaches is interferences that usually decrease sensitivity and reproducibility. Typically, these occur during the generation step, due to the coproduction of the active metals that catalytically decompose NaBH_4 . In addition, the efficiency of vapor generation may depend strongly on the chemical form of the analyte in the sample. Furthermore, NaBH_4 , as well as other derivatization reagents, is expensive and a potential source of contamination. The efforts to develop new vapor generation systems that may replace or reduce the use of chemical reagents remain an important research area in VGAAS.

It is well known that reactive free radicals can be generated by the application of ultraviolet (UV) light. In waste water treatment a photocatalytic process based on UV/VIS irradiation provided

for oxidation of dissolved organic matter is widely used. Irradiation of semiconductor-electrolyte interfaces with photons of energy greater than the semiconductor band gap generates electron-hole pairs (e^-h^+) in the conduction/valence bands of the material, and these charge carriers transfer to the surface where they are capable of both reducing or oxidizing those species in solution which have suitable redox potentials [6,7]. Metal ions can be reduced on the surface of particles of semiconductor. The most used semiconductor (acting as catalyst) for this purpose is nano-TiO₂. The rapid recombination of the photogenerated electrons and holes affects the photoreaction rate, therefore the addition of hole or electron scavenger is necessary. Low molecular weight (LMW) organic acids or aliphatic alcohols are the most widely used hole scavengers (electron donors). Subsequently were found also conditions for the photochemical vapor generation in the absence of semiconductor catalysts [8].

Fig. 1 shows the laboratory-made photochemical VG device with flow-through photochemical reactor. The reactor coil is made from quartz capillary with total length of 2.0 m.

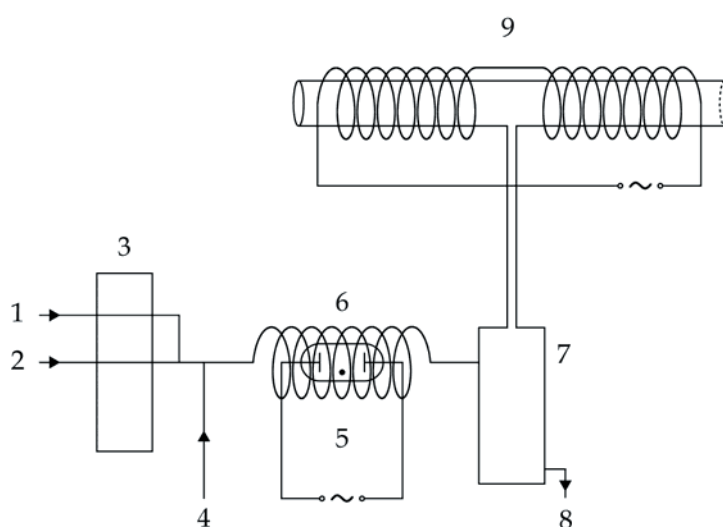


Fig. 1. Scheme of the laboratory-made photochemical vapor generation device with flow-through photochemical reactor. 1 – acid solution, 2 – sample solution, 3 – peristaltic pump, 4 – argon input, 5 – high-pressure mercury discharge lamp (254 nm) with power supply, 6 – quartz photochemical reactor, 7 – gas-liquid separator, 8 – waste, 9 – electrically heated quartz tube atomizer

2. Photochemical generation of mercury cold vapor

The most commonly used technique for the determination of mercury is cold vapor generation-atomic absorption spectrometry or atomic fluorescence spectrometry (CVG-AAS / AFS) due to their excellent detectability [8]. Reduction of Hg^{2+} to Hg^0 is often accomplished in aqueous solution using various reducing agents. The most frequently used reductants are sodium (or potassium) tetrahydroborate ($NaBH_4$ or KBH_4). The chemical generation process is accompanied with disadvantages as chemical interferences from transition metals, the reductant solution is unstable and it is a potential source of contamination. Fortunately in the recent years the photochemical generation of mercury cold vapor was introduced. Khalil et al. [6] used TiO₂ as photocatalyst and UV light for the removal of Hg(II) salts from waters. The authors determined that mercury was converted to Hg(0) and the efficiency of process was increased up to 100% by addition of methanol (hole scavenger) to the solution. The first analytical application of the photochemical vapor generation for mercury was introduced by Zheng et al. [8]. The procedure used formic acid to react with Hg^{2+} or MeHg in aqueous solution, under room natural light (VIS) or ultraviolet irradiation (UV), for the generation of cold mercury vapor, which was subsequently detected by AFS. In the presence of the UV, both Hg^{2+} and MeHg were converted to Hg^0 for the determination of total mercury; and only Hg^{2+} was reduced to

Hg^0 with the VIS, thus determining Hg^{2+} only. Then, the concentration of MeHg was calculated by subtracting the Hg^{2+} concentration from the total mercury concentration. No photocatalyst was used, a 125W high-pressure mercury vapor lamp was used as a source of UV radiation. No significant interference was observed from $100 \text{ mg L}^{-1} \text{ Co}^{2+}$ or Ni^{2+} , and $50 \text{ mg L}^{-1} \text{ Cu}^{2+}$ for the determination of $5 \text{ mg L}^{-1} \text{ Hg}^{2+}$. The limit of detection was 0.003 or 0.2 mg L^{-1} for total mercury with the UV or Hg^{2+} with the VIS, respectively. Bendl et al. [9] investigated the generation of mercury vapor by the reduction of mercury species in an acetic acid solution using UV radiation. They studied the interferences of metal ion species to a 1 mg L^{-1} solution of Hg. Significant interferences they observed for transition metals Cr(VI), Fe(III), Cu(II), and Pb(II). Little effect was observed for Zn(II), Mn(II), and Mg(II), while an enhancement effect was observed for Ni(II) and Co(II). These results were consistent with previously reported interference effects for chemical vapor generation [10], suggesting that the mechanism of interference is independent of the generation method (chemical or photoreduction). An optimized system was found to provide a detection limit (3σ of the blank) of $2.1 \mu\text{g L}^{-1}$ with a precision of 2.9% RSD ($n = 8$) for a $500 \mu\text{g L}^{-1}$ Hg standard. Li et al. [12] proposed a new photo-induced mercury cold/chemical vapor generation (PI-CVG), which directly used sample matrix as a reductant for atomic fluorescence spectrometric detection of trace mercury in wine or liquor samples. With UV radiation, the ethanol (naturally present in sample matrix) reduced mercury compounds or ions to atomic mercury vapor which was subsequently swept (by argon carrier gas) into an AFS for the measurements. The addition of nano-TiO₂ to samples was tested and increased the method sensitivity by factor of 2 (the optimized nano-TiO₂ concentration was 3 g L^{-1}). The limits of detection were 20 and 70 ng L^{-1} with and without catalyst addition, respectively. Han et al. [12] converted Hg^{2+} into Hg^0 cold vapor by LMW alcohols, aldehydes, and carboxylic acids, e.g., methanol, formaldehyde, acetaldehyde, glycol, 1,2-propanediol, glycerol, acetic acid, oxalic acid, and malonic acid. It was found that the presence of nano-TiO₂ more or less improved the efficiency of the PI-CVG with most of the organic reductants. The instrumental limits of detection (3σ of the blank) were around $0.02 - 0.04 \mu\text{g L}^{-1}$. Real sample analysis revealed that this method is promising for water and geological analysis of ultralow levels of mercury. A photochemical vapor generation system for Hg species based on the irradiation of mercaptoethanol (ME) with UV was developed for AFS by Yin et al. [13]. The limits of determination for inorganic divalence mercury and methyl mercury were 60 and 50 ng L^{-1} , respectively. The method was applied for the determination of total and methyl Hg in environmental and biological samples. Vieira et al. [14] determined methylmercury and total mercury in biological samples using CVAAS based on photochemical reduction. The authors utilised two approaches: (a) tissues were digested in either formic acid or tetramethylammonium hydroxide (TMAH), and total mercury was determined following reduction of both species by exposure of the solution to UV irradiation; (b) tissues were solubilized in TMAH, diluted to a final concentration of 0.125% m/v TMAH by addition of 10% v/v acetic acid and CH_3Hg^+ was selectively quantitated, or the initial digests were diluted to 0.125% m/v TMAH by addition of deionized water, adjusted to pH 0.3 by addition of HCl and CH_3Hg^+ was selectively quantitated. The photochemical reduction efficiency was estimated to be 95% by comparing the response with traditional chemical reduction. Limits of detection of 6 ng g^{-1} for total mercury using formic acid, 8 ng g^{-1} for total mercury and 10 ng g^{-1} for methylmercury using TMAH were obtained. Su et al. [15] proposed a method based on ultrasonic slurry sampling atomic absorption spectrometry (AAS) for the determination of trace mercury in geological samples by use of mercury cold vapor generation using formic acid under UV irradiation. Interference study showed no significant interference of up to 1000-fold excess of Cu(II), Co(II), Ni(II), Cr(VI), Mn(II), Fe(III), and Zn(II) with the determination of 50 mg L^{-1} Hg. The detection limit was $0.6 \mu\text{g L}^{-1}$.

3. Photochemical prereduction and vapor generation of selenium

It is known that the selenium hydride can be efficiently generated only from selenium present in Se(IV) valence state. The classical approach uses different reduction media and sample pretreatment to achieve the prereduction of Se(VI) species. It was found that the photochemistry can be used to

efficient prereduction of Se(VI) to Se(IV) and subsequently for the generation of SeH₂, too. The pioneer work was done by Kikuchi and Sakamoto [15]. They studied the system with formic acid and TiO₂ under UV irradiation in a batch mode. They found that Se(VI) is reduced to Se(IV) and further to SeH₂, but they didn't utilize their finding in analytical application. Guo et al. explored the analytical potential of the photochemical reduction of selenium in a series of papers [16–19]. In the first one [16] authors described a vapor generation technique utilizing UV irradiation coupled with atomic absorption for the determination of selenium in aqueous solutions in the presence of LMW organic acids. A flow-through photoreactor, consisting of a 5-m length PTFE tubing wrapped around either of 3 or 15 W low-pressure Hg vapor UV lamps was constructed. Identification of the volatile products using cryotrapping GC/MS analysis revealed that inorganic Se(IV) is converted to volatile selenium hydride, selenium carbonyl, dimethyl selenide, and diethyl selenide in the presence of formic, acetic, propionic, and malonic acids, respectively. The highest generation efficiency $50 \pm 10\%$ was achieved in the acetic acid solution. No interference from Ni²⁺ and Co²⁺ at concentrations of 500 and 100 mg L⁻¹, respectively, was observed. A detection limit of 2.5 µg L⁻¹ and a relative sensitivity of 1.2 µg L⁻¹ (1% absorption) with a precision of 1.2% (RSD, n = 11) at 50 µg L⁻¹ were obtained. In paper [17] authors documented that in the presence of LMW organic acids (formic, acetic, propionic and malonic), inorganic Se(IV) is converted by UV irradiation to volatile selenium carbonyl, dimethylselenide and diethylselenide, depending on the acid used. In 0.7 mol L⁻¹ formic acid solution, approximately 60–70% (v/v) SeH₂ and 30–40% (v/v) SeCO were formed. The efficiency of SeH₂ and SeCO formation was greatly affected by the presence of the NO₃⁻ ions in the solution which increase threefold the formation of SeCO while completely suppress the formation of SeH₂. In the next work [18] the method was utilized for Se(IV) removal from contaminated agricultural drainage waters using a batch photoreactor system. Sun [20] developed an UV/nano-TiO₂ vapor generation device, which coupled a chromatographic column and an ICP mass spectrometer. The method was used for speciation of Se(IV) and Se(VI) without the need to use conventional chemical VG techniques. The photochemical reactor consisted of a 2m PTFE tube wrapped around a 14W low-pressure mercury vapor lamp. Authors optimized a number of the operating parameters, including the acidity, the amounts of TiO₂ and formic acid, and the length of the reaction coil, with respect to their effects on the reduction efficiency of the analyte species. The generation efficiency was without TiO₂ addition 100% from Se(IV) form and negligible from Se(VI). By addition of TiO₂ at an optimal concentration of 0.1 g L⁻¹ the generation efficiency was 80–90%, similar for both forms. The detection limits for the determination of Se(IV) and Se(VI) in aqueous samples were 0.06 and 0.03 µg L⁻¹, respectively. García et al. [21] implemented a flow-through UV reactor, and used it for on-line generation of Se volatile derivatives prior to detection by QTAAS. They used LMW organic acid (formic or acetic) in the carrier without need of the photocatalyst. The flow-through photoreactor consisted of 12 m PTFE tubing wrapped around a 78W low-pressure mercury lamp. The effect of concomitants in the online generation of Se vapours was investigated. Tolerance of typical hydride-forming elements such as As and Sn was much higher with UV vapour generation as compared to chemical hydride generation. The presence of Cu(II) caused interference effects from 0.05 mg L⁻¹, but tolerance of Ni(II) was greater with UV vapour generation. The detection limit was achieved 0.5 µg L⁻¹ Se.

On-line Se(VI) prereduction on a UV/TiO₂ photocatalysis reduction device was studied by Wang et al. [22]. The media of HCOOH was used for prereduction. The reduction to SeH₂ was achieved in a conventional KBH₄-HCl VG system and AFS was used for the detection. The vapor generation efficiency for the Se(VI) after the UV/TiO₂ prereduction (compared to the SeH₂ generation from Se(IV) without need of the prereduction) was 53%. The same UV/TiO₂ photocatalysis reduction device was subsequently utilized in [23] where the authors after photo-prereduction used electrochemical vapor generation. Figueroa et al. [24] developed a headspace single-drop microextraction (SDME) method in a combination with ETAAS for determination of total inorganic Se and Se(IV). Selenium volatile compounds were generated and trapped onto a Pd(II)-aqueous solution containing drop at the needle tip of a chromatographic syringe. Several organic acids (formic, oxalic, acetic, citric and ethylenediaminetetraacetic) have been tried for photoreduction of Se(IV) into volatile Se compounds under UV irradiation using 500W high-pressure mercury vapor lamp. Formic and acetic provided optimal photogeneration of volatile Se species at a 0.6 mol L⁻¹ concentration.

Citric and ethylenediaminetetraacetic acid allowed to use a concentration as low as 1 mmol L^{-1} , but extraction times were longer than for formic and acetic acids. Photogeneration of $(\text{CH}_3)_2\text{Se}$ from Se(IV) in the presence of acetic acid provided a detection limit of 20 ng L^{-1} , a preconcentration factor was nearly 285. Zheng et al. [25] proposed a method based on UV photochemical vapor generation for the speciation analysis of Se(IV) and Se(VI). They used different reaction conditions for selective generation of volatile species from Se(VI) and Se(IV) prior the determination using AFS or ICP-MS. At low temperature, only Se(IV) was photochemically converted to volatile species; however, by using boiling water bath together with nano-TiO₂ as a catalyst, both Se(IV) and Se(VI) can be photochemically converted to volatile species, thus determining the total of Se(IV) and Se(VI). The limits of detection ranged from 0.02 to $0.1 \text{ } \mu\text{g L}^{-1}$, depending on the kind of organic acid and the detector.

4. Photochemical vapor generation of other analytes

The photochemical generation of volatile species was recently investigated for the conventional hydride-forming elements (As, Bi, Sb, Se, Sn, Pb, Cd, Te), Hg, transition metals (Ni, Co, Cu, Fe), noble metals (Ag, Au, Rh, Pd, Pt), and nonmetals (I, S)[19]. The aqueous solutions of analytes with addition of LMW carboxylic acids (formic, acetic, propionic) were irradiated using UV light (UVC pen lamp). The volatile species were analyzed using ICP-MS spectrometer. Authors yield volatile species for all examined analytes with various efficacies, the calculated signal-to-background ratios were >1500 for 5 ng/mL As, Sb, Bi, Se, and Te; 20 for 10 ng/mL Sn, Cu, Rh, Au, Pd, Pt, and Cd; 2400 for 1 ng/mL Hg; and 1000 for Co. In the case of Ni and Se, the tetracarbonyl and alkylated selenium compounds have been identified, respectively. Photochemical alkylation of arsenic by UV irradiation of aqueous solutions of arsenite in LMW carboxylic acid media (formic, acetic, propionic and butyric) was studied by Guo et al. [26,27]. The MS studies revealed that inorganic arsenite was alkylated to yield AsH₃ in the presence of formic acid, trimethylarsine in acetic acid, triethylarsine in propionic acid and tripropylarsine in butyric acid solutions. Mixed ligand arsenic species such as methylarsine, dimethylarsine, dimethylethylarsine and diethylmethylarsine were also formed when a mixture of acids was used. The methylation efficiency of approximately 75% was achieved in 3.1 mol L^{-1} acetic acid using 0.05 mg L^{-1} As(III) test solution. The water-soluble species formed during photochemical vapor generation in the sample solution were studied using multidimensional liquid chromatography and electrospray mass spectrometry. 13 organoarsenic species were identified, 6 of which are previously unreported organoarsenic species. Recently Grinberg et al. [28] studied the volatile cobalt carbonyl formation in LMW carboxylic acid solutions after UV irradiation. The volatile species were cryogenically trapped and analysed using ICP-MS. The efficiency of cobalt transformation to volatile species tentatively identified as a carbonylated cobalt species, was about 0.3-0.4 %.

5. Conclusions

The photochemical vapor generation is a useful new alternative to the commonly employed chemical and electrochemical hydride generation techniques. It brings new unique features as lower blanks, less interferences, higher number of detectable elements. However more work remain to be done to prove the benefits of this new vapor generation technique.

Acknowledgement

The work was supported by Science and Technology Assistance Agency under the contract No. LPP-0188-06, LPP-0038-06, SK-CZ-0044-07 and Scientific Grant Agency of the Ministry of Education of Slovak Republic and the Slovak Academy of Sciences under the contracts Nos. VEGA 1/4463/07, VEGA 1/4464/07 and 1/0272/08.

References

- [1] H. Matusiewicz, M. Kopras, R.E. Sturgeon, Determination of cadmium in environmental samples by hydride generation with in situ concentration and atomic absorption detection, *Analyst* 122 (1997) 331–336
- [2] A. D'Ulivo, M. Onor, E. Pitzalis, Role of hydroboron intermediates in the mechanism of chemical vapor generation in strongly acidic media, *Anal. Chem.* 76 (2004) 6342–6352
- [3] A. D'Ulivo, C. Baiocchi, E. Pitzalis, M. Onor, R. Zamboni, Chemical vapour generation for atomic spectrometry. A contribution to the comprehension of reaction mechanisms in the generation of volatile hydrides using borane complexes, *Spectrochim. Acta Part B* 59 (2004) 471–486
- [4] A.A. D'Ulivo, Chemical vapor generation by tetrahydroborate(III) and borane-complexes in aqueous media. A critical discussion of fundamental processes and mechanisms involved in reagent decomposition and hydride formation, *Spectrochim. Acta Part B* 59 (2004) 793–825
- [5] R.E. Sturgeon, Z. Mester, Analytical applications of volatile metal derivatives, *Appl. Spectrosc.* 56 (2002) 202–213
- [6] L.B. Khalil, W.E. Mourad, M.W. Rophael, Photocatalytic reduction of environmental pollutant Cr(VI) over some semiconductors under UV/visible light illumination. *Appl. Catal. B* 17 (1998) 267–273
- [7] Y. He, X. Hou, C. Zheng, R.E. Sturgeon, Critical evaluation of the application of photochemical vapor generation in analytical atomic spectrometry. *Anal. Bioanal. Chem.* 388 (2007) 769–774
- [8] C.B. Zheng, Y. Li, Y.H. He, Q. Ma, and X.D. Hou, Photo-induced chemical vapor generation with formic acid for ultrasensitive atomic fluorescence spectrometric determination of mercury: potential application to mercury speciation in water. *J. Anal. At. Spectrom.* 20 (2005) 746–750
- [9] R.F. Bendl, J.T. Madden, A.L. Regan, N. Fitzgerald, Mercury determination by cold vapor atomic absorption spectrometry utilizing UV photoreduction. *Talanta* 68 (2006) 1366–1370
- [10] C. Vargas-Razo, J.F. Tyson, Determination of cadmium by flow injection-chemical vapor generation-atomic absorption spectrometry. *Fresenius J. Anal. Chem.* 366 (2000) 182–190
- [11] Y. Li, C.B. Zheng, Q. Ma, L. Wu, C.W. Hu, X.D. Hou, Sample matrix-assisted photo-induced chemical vapor generation: a reagent free green analytical method for ultrasensitive detection of mercury in wine or liquor samples. *J. Anal. At. Spectrom.* 21 (2006) 82–85
- [12] C.F. Han, C.B. Zheng, J. Wang, G.L. Cheng, Y. Lv, X.D. Hou, Photo-induced cold vapor generation with low molecular weight alcohol, aldehyde, or carboxylic acid for atomic fluorescence spectrometric determination of mercury. *Anal. Bioanal. Chem.* 388 (2007) 825–830
- [13] Y.M. Yin, J.H. Qiu, L.M. Yang, Q.Q. Wang, A new vapor generation system for mercury species based on the UV irradiation of mercaptoethanol used in the determination of total and methyl mercury in environmental and biological samples by atomic fluorescence spectrometry. *Anal. Bioanal. Chem.* 388 (2007) 831–836
- [14] M.A. Vieira, A.S. Ribeiro, A.J. Curtius, R.E. Sturgeon, Determination of total mercury and methylmercury in biological samples by photochemical vapor generation. *Anal. Bioanal. Chem.* 388 (2007) 837–847
- [15] E. Kikuchi, H. Sakamoto, Kinetics of the reduction reaction of selenate ions by TiO₂ photocatalyst. *J. Electrochem. Soc.* 147 (2000) 4589–4593
- [16] X. Guo, R.E. Sturgeon, Z. Mester, G.J. Gardner, UV vapor generation for determination of selenium by heated quartz tube atomic absorption spectrometry. *Anal. Chem.* 75 (2003) 2092–2099
- [17] X. Guo, R.E. Sturgeon, Z. Mester, G.J. Gardner, UV light-mediated alkylation of inorganic selenium. *Appl. Organomet. Chem.* 17 (2003) 575–579
- [18] X. Guo, R.E. Sturgeon, Z. Mester, G.J. Gardner, Photochemical alkylation of inorganic selenium in the presence of low molecular weight organic acids. *Environ. Sci. Technol.* 37 (2003) 5645–5650
- [19] X. Guo, R.E. Sturgeon, Z. Mester, G.J. Gardner, Vapor generation by UV irradiation for sample introduction with atomic spectrometry. *Anal. Chem.* 76 (2004) 2401–2405

- [20] Y.C. Sun, Y.C. Chang, C.K. Su, On-line HPLC-UV/Nano-TiO₂-ICPMS system for the determination of inorganic selenium species. *Anal. Chem.* 78 (2006) 2640–2645
- [21] M. García, R. Figueroa, I. Lavilla, C. Bendicho, On-line photoassisted vapour generation implemented in an automated flow-injection/stopped-flow manifold coupled to an atomic detector for determination of selenium. *J. Anal. At. Spectrom.* 21 (2006) 582–587
- [22] Q.Q. Wang, J. Liang, J.H. Qiu, B.L. Huang, Online pre-reduction of selenium(VI) with a newly designed UV/ TiO₂ photocatalysis reduction device. *J. Anal. At. Spectrom.* 19 (2004) 715–716
- [23] J. Liang, Q.Q. Wang, B.L. Huang, Electrochemical vapor generation of selenium species after online photolysis and reduction by UV-irradiation under nano TiO₂ photocatalysis and its application to selenium speciation by HPLC coupled with atomic fluorescence spectrometry. *Anal. Bioanal. Chem.* 381 (2005) 366–372
- [24] R. Figueroa, M. García, I. Lavilla, C. Bendicho, Photoassisted vapor generation in the presence of organic acids for ultrasensitive determination of Se by electrothermal-atomic absorption spectrometry following headspace single-drop microextraction. *Spectrochim. Acta Part B* 60 (2005) 1556–1563
- [25] C.B. Zheng, L. Wu, Q. Ma, Y. Lv, X.D. Hou, Temperature and nano-TiO₂ controlled photochemical vapor generation for inorganic selenium speciation analysis by AFS or ICP-MS without chromatographic separation. *J. Anal. At. Spectrom.* 23 (2008) 514–520
- [26] X.M. Guo, R.E. Sturgeon, Z. Mester, G.J. Gardner, Photochemical alkylation of inorganic arsenic. Part 1. Identification of volatile arsenic species. *J. Anal. At. Spectrom.* 20 (2005) 702–708
- [27] S. McSheehy, X.M. Guo, R.E. Sturgeon, Z. Mester, Photochemical alkylation of inorganic arsenic. Part 2. Identification of aqueous phase organoarsenic species using multidimensional liquid chromatography and electrospray mass spectrometry. *J. Anal. At. Spectrom.* 20 (2005) 709–716
- [28] P. Grinberg, Z. Mester, R.E. Sturgeon, A. Ferretti, Generation of volatile cobalt species by UV photoreduction and their tentative identification. *J. Anal. At. Spectrom.* 23 (2008) 583–587

Simultaneous Determination of Al, Be, Cr, and V using Multi-element Graphite Furnace Atomic Absorption Spectrometer (SIMAA 6000)

Khaled Elsherif and Heinz-Martin Kuss

*University of Duisburg-Essen, Department of Instrumental Analytical Chemistry, Lotharstr. 1, 47057 Duisburg, Germany,
e-mail: elsherif@lims.uni-duisburg.de*

Abstract

Simultaneous multi-element graphite furnace atomic absorption spectrometer (SIMAA 6000) has been used for developing multi-element determinations methodology for Al, Be, Cr, and V in the presence of $\text{Mg}(\text{NO}_3)_2$ as a modifier and using end-capped tubes. The setting of the compromised conditions, the characteristic mass and detection limits for each element in the simultaneous multi-element determination have been determined and compared with the single mode. To study the effect of the matrix, urine standard sample (Seronom-LOT 0511545) has been used. The accuracy of the method has been confirmed by analysis of different biological reference materials. The analyzed values in the simultaneous multi-element determinations were in good agreement with the certified values. Simultaneous multi-element GF-AAS provides a rapid, low cost and sensitive method for routine analysis of trace elements.

Keywords: *simultaneous multi-element Graphite Furnace - AAS*

Introduction

Among the instrumental techniques available for trace and ultra-trace element determinations, Graphite Furnace Atomic Absorption Spectrometry (GFAAS) occupies an outstanding position due to its high specificity, selectivity and sensitivity, low spectral interference, ease of operation, low sample volume and low cost. The major challenge facing the future of GFAAS stems from an increased competition from other modern spectroscopic techniques, e.g. ICP-MS. But in comparison with other techniques, GFAAS offers several features, especially for routine analysis. However, GFAAS suffers from the very beginning from the fact that it has developed as a single-element technique, which implies a multiplied analysis time, when more than one element has to be measured.

Among the most recent requirements in analytical atomic spectrometry is the capability for simultaneous multi-element determinations in small size samples with a variety of matrices. This capability is particularly important in such fields as clinical and biochemical fields where a large sample size is difficult to obtain. Many different multi-element instruments have been used for the simultaneous multi-element determination of trace metals, such as Inductively Coupled Plasma-Atomic Emission Spectrometry (ICP-AES) [1], Inductively Coupled Plasma-Mass Spectrometry (ICP-MS) [2], X-ray Fluorescence Spectrometry [3.], Cathodic Stripping Voltammetry (CCV) [4], and Multi-element Graphite Furnace Atomic Absorption Spectrometry [5-11]. Among of them, the ICP-

based instruments are the most commercially available. The applicability of ICP-based instruments has been somewhat limited by difficulty in dealing with high salt concentrations and the need for relatively large sample volumes. Consequently, separation or pre-concentration of analyte from matrix prior to measurement is necessary. Although ICP-MS has emerged as a method with high detection power, the MS detector is rather complex and expensive, which limited the widespread use of ICP-MS for routine analytical works [11].

Multi-element Atomic Absorption researches have aroused interest since the first AAS stage in order to conceive a spectrometer able to determine several elements simultaneously [12,13]. At the end of the 1980s, the analytical society has been faced with the first commercial systems. Hitachi (1988), Thermo Jarrell Ash (1990), Leeman Labs (1993) and Perkin-Elmer (1994) introduced more or less successful multi-element AAS instruments on the market. At the present, the most updated commercial instrumentation is a line source simultaneous spectrometer, equipped with transversely heated graphite atomizer, THGA with integrated platform, Zeeman Effect background corrector and solid-state detector, making possible the operation under Stabilized Temperature Platform Furnace (STPF) conditions [14-16]. This instrument allows simultaneous determinations up to six elements, improved the analytical frequency of ETAAS, reducing costs related to instrument maintenance, sample and high purity reagent consumption. In spite of saving time and costs, multi-element determinations carried out by SIMAAS (Simultaneous Multi-element Atomic Absorption Spectrometry) require the adoption of compromised conditions, which can cause loss of sensitivity and damage the precision of analytical results. Therefore, the optimization of pyrolysis and atomization temperatures and chemical modifier selection are critical to evaluate a reliable method. They must be carefully chosen while taking into account all analytes to be determined simultaneously.

The aim of this study is to develop simultaneous multi-element graphite furnace atomic absorption methodology for the analysis of Al, Be, Cr, and V with $\text{Mg}(\text{NO}_3)_2$ as a modifier in biological samples.

Instrumentation

Measurements were carried out by using a SIMAA 6000 electrothermal atomic absorption spectrometer with a longitudinal Zeeman-effect background correction system, Echelle optical arrangement, Solid-state detector and end-capped THGA tube with pyrolytic coated integrated platform (Perkin-Elmer GmbH, Bodenseewerk). The rate of flow of the normal gas (Ar) was $250 \text{ ml}\cdot\text{min}^{-1}$. Stopped flow during the atomization was used. The lamps used were hollow cathode lamps (HCL). They were from Perkin-Elmer and the wavelengths used were: Al 309.3 nm, Be 234.9 nm, Cr 357.9 nm and V 318.4 nm. The sample injection volume was $20 \mu\text{l}$ and $5 \mu\text{g}$ $\text{Mg}(\text{NO}_3)_2$ was injected as a modifier. The integrated absorbance of the atomic absorption signal was used for the determination.

Reagents and Samples

High purity water ($18 \text{ M}\Omega \text{ cm}$) was prepared with de-ionized water system (Milli-Q, Millipore Corp.). Analytical reagent-grade nitric acid (KMF) was purified by sub-boiling distillation. AAS-Standard reference solutions of Al, Be, and V (Brend Kraft GmbH) and Cr (Charleston SC 29423) were used to prepare the reference analytical solutions. The chemical modifier solution (AAS-Standard Magnesium) was from Bernd Kraft GmbH.

The accuracy of the method was confirmed by the determination of Al, Be, Cr and V in biological samples. Each sample has been diluted according to the concentration of the elements in the sample. Some elements have been added because not certified for them. The samples prepared as follows:

Trace Elements Urine Sample (LOT 0511545): Exactly 5 ml de-ionized water was added to the sample and let it stand for 30 min, and then transfer it to a plastic tube. The sample was then kept in a refrigerator at -20°C for later use. Before use, the sample was diluted 1:4 with 0.2 % HNO₃.

Lyphocheck Urine Metals Control Level 1 (LOT 69061): The same procedure was applied as Seronorm sample except that, 25 ml de-ionized water was added and the sample was diluted 1:1 before use.

Bovine Liver (NIST-SRM 1577b), and Pork Liver (GBW 08551): The samples were digested as described by Ronald Treble [17]. Firstly, the samples were dried at 80 °C for 4 hrs and stored in desiccators before use. 0.5069 g (GBW 08551) and 0.5129 g (NIST-SRM 1577b) dried samples were allowed to digest in 5 ml concentrated distilled HNO₃ for a period of 72 hrs at room temperature. The digested/acidified samples were transferred into 50 ml volumetric flask and diluted to the mark with de-ionized water. Before use, each sample was diluted as required.

All sample containers, auto-sampler cups, etc. were acid washed with 10 % v/v nitric acid for 24 hrs and then rinsed several times with de-ionized water before use. The analytical reference solutions were prepared daily by diluting with 0.2 % nitric acid.

Results and Discussion

Single-element mode optimization

When ETAAS is used for single-element determination, all experimental and instrumental parameters are optimized for only one analyte. Consequently, the best optimized pyrolysis and atomization temperatures are used in the heating program, minimizing condensed and gas-phase interference. The best pyrolysis and atomization temperatures were determined according to the pyrolysis and atomization curves and the absorbance peak for each element. The heating program was summarized in Table 1. The heating program for each element was used to determine the detection limits and the characteristic mass for each element and they were summarized in Table 2.

Table 1. Temperature program for single-element determination of Al, Be, Cr, and V with Mg modifier

Step	Temperature [°C]	Ramp time [s]	Hold time [s]	Gas Flow [ml min ⁻¹]
Drying 1	110	1	30	250
Drying 2	130	15	30	250
Pyrolysis	Various ^a	10	20	250
Atomization	Various ^b	0	5	0
Clean-out	2550	1	5	250

^a 1500, 1600, 1700 °C for Cr, Bi, (Al and V) and 1500 °C for the multi-determination

^b 2300, 2500 °C for (Al, Be, and Cr) and V and 2500 °C for the multi-determination

Table 2. The characteristic mass and detection limits for the single-element and multi-element determinations

Element	Detection limit [µg dm ⁻³]		Characteristic mass [pg]	
	Single-element	Multi-element	Single-element	Multi-element
Al	0.18	0.62	25.9	30.4
Be	0.013	0.021	1.9	2.0
Cr	0.032	0.081	4.7	4.7
V	0.47	0.83	46.3	48.9

Multi-element mode optimization

In this case, the experimental and instrumental parameters are optimized for all elements in the multi-element mode. The heating program temperature and the chemical modifier must be carefully selected to achieve the best atomization efficiency for all the analytes. In general, the most volatile analyte determines the pyrolysis temperature while the least volatile one determines the atomization temperature.

The $\text{Mg}(\text{NO}_3)_2$ modifier has been recommended for the stabilization of Al, Be [18-20], and Cr [21-23]. Therefore, this modifier has been used in this work. The heating program temperature was summarized in Table 1. Fig. 1 shows the pyrolysis and atomization curves for each element, the best pyrolysis temperatures for the multi-element determinations was 1500°C because the absorption signal for Be and Cr decreased above 1500°C . The atomic signal for Al and V was almost constant until 1700°C and then gradually decreased. From the atomization curves, Al, Be, and Cr atomic absorption signals increased with increasing the atomization temperature until 2300°C and then start to decrease. However, for V, the absorption signal continued to increase after 2300°C . Generally, atomization temperature more than 2600°C can not be used with SIMAA 6000 and with that temperature the lifetime of the tube will be decreased, for that reason we have decided to choose 2500°C as the optimum atomization temperature. The pyrolysis and atomization curves were made using the following concentrations: 30 ppb Al, 4 ppb Be, 10 ppb Cr, and 100 ppb V in 0.2% HNO_3 .

The detection limits and the characteristic mass for each element were determined and summarized in Table 2. The values of the characteristic mass are comparable with those of the single-element determinations. The higher detection limits for multi-element mode in comparison with single-element mode, can be related to the compromised conditions adopted for the simultaneous determination.

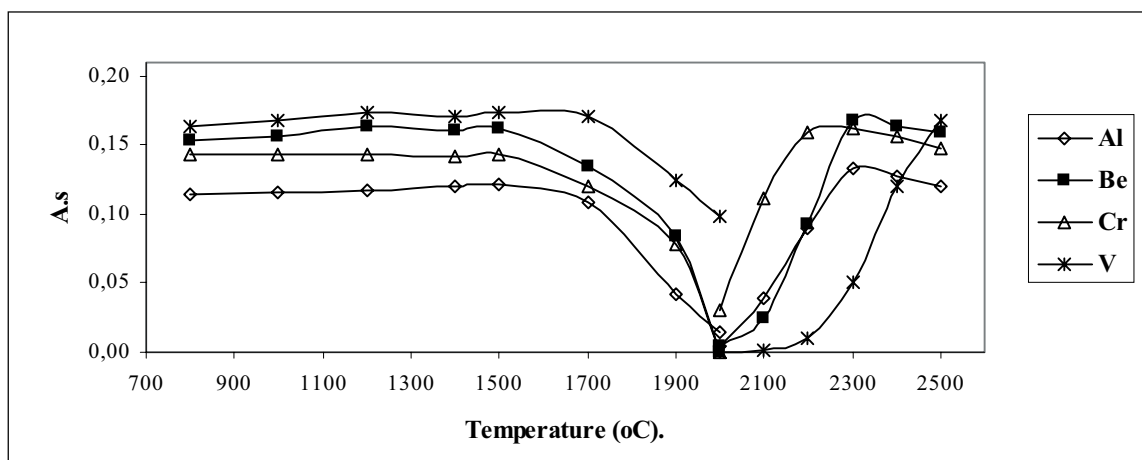


Fig. 1. Pyrolysis and atomization curves of multi-element determination of Al, Be, Cr and V in aqueous solution with Mg modifier

Study the effect of the matrix

The diluted reference material (1:4) has been spiked with 10 ppb Al, 2 ppb Be, 6 ppb Cr, and 80 ppb V and injected ($20\ \mu\text{l}$) with $5\ \mu\text{g}\ \text{Mg}(\text{NO}_3)_2$ as a modifier into the atomizer each time during this study. From the pyrolysis curves, Fig. 2, the absorption signals were studied at an atomization temperature of 2500°C . The absorption signals remained approximately constant as the pyrolysis varied from $800\text{-}1500^\circ\text{C}$ for Be and Cr, from $800\text{-}1600^\circ\text{C}$ for Al, and from $800\text{-}1700^\circ\text{C}$ for V. When the temperature increased above 1500°C , the absorption signal randomly decreased for Be and Cr due

to the volatilization of these elements. 1500 °C was chosen as an optimum pyrolysis temperature. The effects of atomization temperature were studied at a pyrolysis temperature of 1500 °C. For Al, Be, and Cr, the atomic absorption signal increased with increasing atomization temperature and has its maximum at 2300 °C. However, for V, the absorption signal increased with increasing atomization temperature until 2500 °C. 2500 °C was as an optimum atomization temperature for the multi-element determination of this group. The absorption peaks at the optimum pyrolysis and atomization temperatures are shown in Fig. 3.

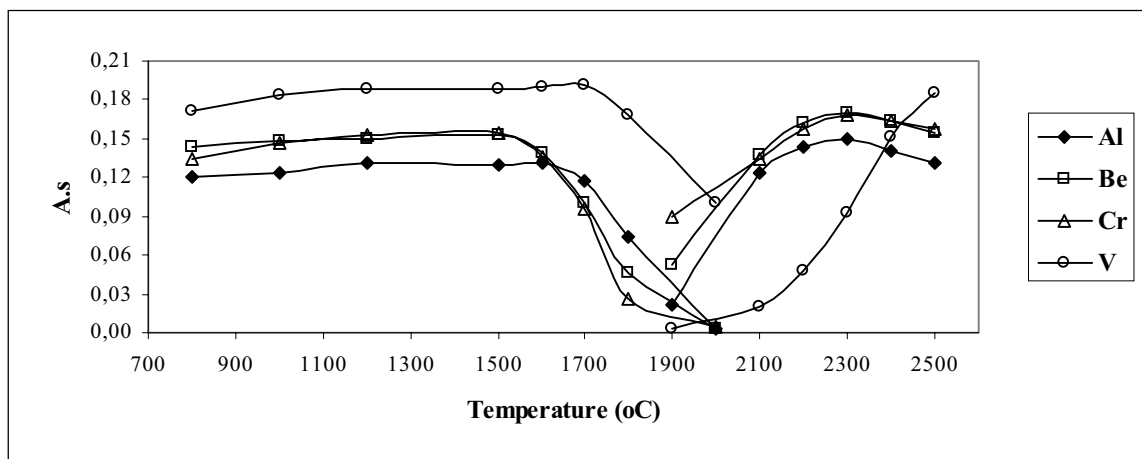


Fig. 2. Pyrolysis and atomization curves of Al, Be, Cr and V in diluted urine sample (1:4) with Mg modifier

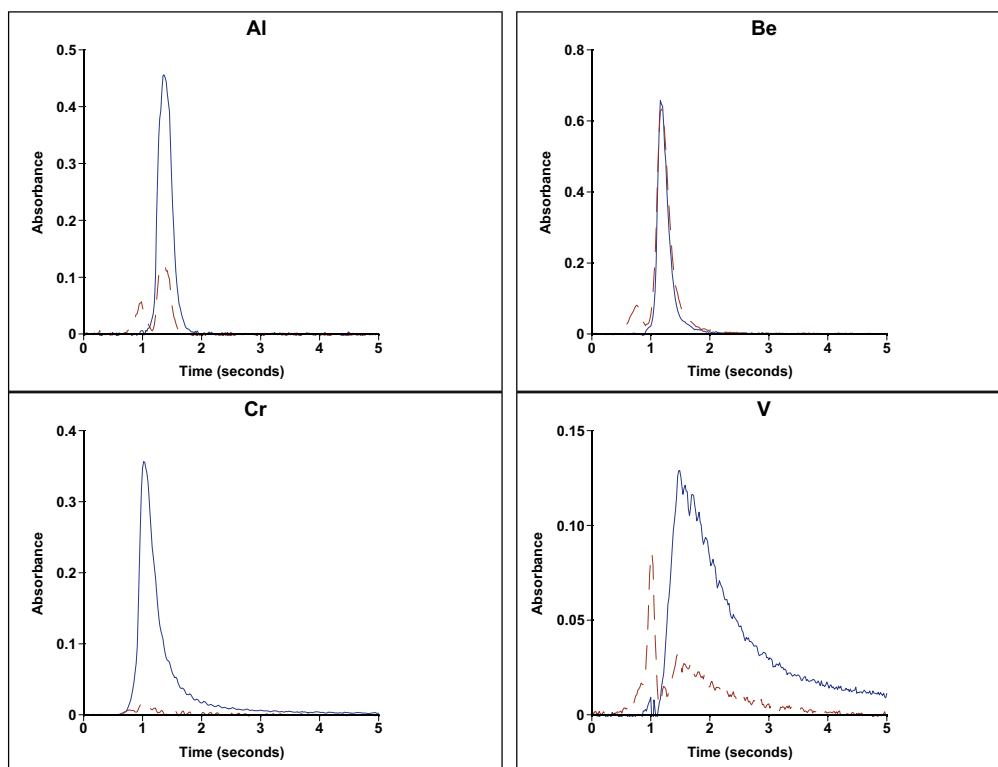


Fig. 3. Peak signals for multi-element determination in diluted urine sample

Analysis of certified reference materials

Trace Element Urine Sample from Seronorm (0511545):

The sample was diluted (1:4, v/v) with 0.2 % HNO₃. For each measurement, 20 µl of the diluted sample and 5 µl of 1.00 g.dm⁻³ Mg(NO₂)₃ modifier solution were injected into the graphite tube at 20 °C. The standard addition curves with good linearity ($R^2 = 0.9991, 0.999, 0.9994, \text{ and } 0.9994$ for Al, Be, Cr, and V, respectively) were used to determine the concentration of the elements in the sample. The results are summarized and compared with the certified concentrations in Table 3. The analyzed values were in the range of 96.3, 98.0, 101.0, and 96.8 % for Al, Be, Cr, and V, respectively. Detection limits were calculated as three times the standard deviation of ten replicate measurements of the blank. The detection limits (LOD) and the characteristic mass (CM) were determined and given in Table 3.

Lyphochek Urine Metals Control Level 1 from BIO-RAD (69061):

The sample was diluted (1:1, v/v) with 0.2 % HNO₃. For each measurement, 20 µl of the diluted sample and 5 µl of 1.00 g.dm⁻³ Mg(NO₂)₃ modifier solution were injected into the graphite tube at 20 °C. There were no certified values for beryllium and vanadium, therefore, the sample has been spiked with them before the dilution. The standard addition curves with good linearity ($R^2 = 0.9996, 0.9998, 0.9999, \text{ and } 0.9997$ for Al, Be, Cr, and V, respectively) were used to evaluate the concentration of the elements in the sample. The results are summarized and compared with the certified concentrations in Table 3. The analyzed values were in the range of 111.3, 91.7, 95.0, and 100.0 % for Al, Be, Cr, and V, respectively. Detection limits and characteristic mass were determined and given in Table 3.

Bovine Liver from National Institute of Standards and Technology (NIST-SRM 1577b):

Since there were no certified values for beryllium and chromium and the concentration of vanadium is too low for the determination, the sample has been spiked with the elements before the dilution. The sample was diluted (1:9, v/v) with 0.2 % HNO₃. The standard addition curves with good linearity ($R^2 = 0.9999, 0.9998, 0.9999, \text{ and } 0.9999$ for Al, Be, Cr, and V, respectively) were used to determine the concentration of the elements in the sample. The results are summarized and compared with the certified concentrations in Table 3. The analyzed values were in the range of 99.4, 102.0, 96.5, and 100.0 % for Al, Be, Cr, and V, respectively. Detection limits and characteristic mass were determined and given in Table 3.

Table 3. The results of simultaneous determination of Al, Be, Cr, and V in different certified reference materials

Sample		Al	Be	Cr	V
Seronorm	Con. found (µg dm ⁻³)	96.3	4.8	19.9	24.4
	Con. Certified (µg dm ⁻³)	100	4.9	19.7	25.2
	LOD (µg dm ⁻³)	0.96	0.022	0.11	0.83
	CM (pg)	31.4	1.6	4.5	48.9
Bio-Rad	Con. found (µg dm ⁻³)	33.4	1.1	1.9	20
	Con. Certified (µg dm ⁻³)	30	1.2*	2.0	20*
	LOD (µg dm ⁻³)	0.68	0.027	0.081	0.86
	CM (pg)	28.4	2.0	5.9	62.9
Bovine Liver	Con. found (µg dm ⁻³)	1.54	0.150	0.250	5.00
	Con. Certified (µg dm ⁻³)	1.55	0.147*	0.259*	5.00*
	LOD (µg dm ⁻³)	0.62	0.034	0.088	1.5
	CM (pg)	30.3	2.5	6.4	73.3
Pork Liver	Con. found (µg dm ⁻³)	1.17	0.048	0.101	2.00
	Con. Certified (µg dm ⁻³)	1.00*	0.050*	0.101	2.00*
	LOD (µg dm ⁻³)	0.62	0.031	0.082	0.86
	CM (pg)	30.3	2.3	6.0	62.9

* added

Pork Liver from National Research Centre for Certified Reference Materials (GBW 08551):

No certified values for aluminium, beryllium, and vanadium; therefore the sample has been spiked with the elements before the dilution. The sample was diluted (1:3, v/v) with 0.2 % HNO₃. The standard addition curves with good linearity ($R^2 = 0.9995, 0.9999, 0.9998, \text{ and } 0.9999$ for Al, Be, Cr, and V, respectively) were used to determine the concentration of the elements in the sample. The results are summarized and compared with the certified concentrations in Table 3. The experimentally determined concentrations were in good agreement with the certified values. The analyzed values were in the range of 117.0, 96.0, 100.0, and 100.0 % for Al, Be, Cr, and V, respectively. Detection limits and characteristic mass were determined and given in Table 3.

Conclusion

Simultaneous multi-element determination for a set of elements can be carried out using Simultaneous Multi-element GFAA Spectrometer (SIMAA 6000) under compromised conditions. These include pyrolysis and atomization temperature and the use of a suitable modifier. The sensitivity and the accuracy of this technique are comparable to those of the single-element determination. The detection limits were higher because of the set of the compromised conditions. Different combinations of elements can be directly determined by SIMAA 6000 if the compromised conditions have been carefully chosen.

References

- [1] Akagi T., Fuwa K., Harguchi H., Simultaneous Multi-element Determination of Trace Metals in Sea Water by Inductively-coupled Plasma Atomic Emission Spectrometry after Coprecipitation with Gallium, *Analytica Chimica Acta*, 1985, 177, 139-151
- [2] Chapple G., Byrne J.P., Direct Determination of Trace Metals in Sea-water using Electrothermal Vaporization Inductively Coupled Plasma Mass Spectrometry, *Journal of Analytical Atomic Spectrometry*, 1996, 11, 549-553
- [3] Prange A., Knöchel A., Michaelis W., Multi-element Determination of Dissolved Heavy Metal Traces in Sea Water by Total-reflection X-ray Fluorescence Spectrometry, *Analytica Chimica Acta*, 1985, 172, 79-100
- [4] Colombo C., van den Berg C.M.G., Simultaneous Determination of Several Trace Metals in Seawater using Cathodic Stripping Voltammetry with Mixed Ligands, *Analytica Chimica Acta*, 1997, 337, 29-40
- [5] Berglund M., Frech W., Baxter D.C., Radzink B., A Critical Evaluation of a Multielement ETAAS System using Line Sources and a Transversely Heated Graphite Atomizer with Zeeman effect Background Correction, *Spectrochimica Acta*, 1993, 48B, 1381-1392
- [6] Sen Gupta J.G., Bouvier J.L., Direct Determination of Traces of Ag, Cd, Pb, Bi, Cr, Mn, Co, Ni, Li, Be, Cu and Sb in Environmental Waters and Geological Materials by Simultaneous Multi-element Graphite Furnace Atomic Absorption Spectrometry with Zeeman-effect Background Correction, *Talanta*, 1995, 42, 269-281
- [7] Edel H., Quick L., Cammann K., Simultaneous Multielement Determination in Complex Matrices using Frequency-modulated Electrothermal Atomic Absorption Spectrometry, *Analytica Chimica Acta*, 1995, 310, 181-187
- [8] Iversen B.S., Panayi A., Cambor J.P., Sabbioni E., Simultaneous Determination of Cobalt and Manganese in Urine by Electrothermal Atomic Absorption Spectrometry. Method Development using a Simplex Optimization Approach, *Journal of Analytical Atomic Spectrometry*, 1996, 11, 591-594
- [9] Lee Y.I., Smith M.V., Indurthy S., Deval A., Sneddon J., An Improved Impaction-Graphite Furnace System for the Direct and Near Real-time Determination of Cadmium, Chromium, Lead

- and Manganese in Aerosols and Cigarette Smoke by Simultaneous Multielement Atomic Absorption Spectrometry, *Spectrochimica Acta*, 1996, 51B, 109-116
- [10] Gottelet V., Henrion G., Kalahne R., Stoyke M., Simultanbestimmungsmethoden für die Elemente Kupfer, Zink, Eisen und Mangan sowie Natrium, Kalium, Calcium und Magnesium mittels Flammen-Atomabsorptionsspektrometrie (F-AAS), *Nahrung Food*, 1996, 40, 313-318
- [11] Pi-guey Su, Shang-da Huang, Direct and Simultaneous Determination of Copper and Manganese in Seawater with a Multielement Graphite Furnace Atomic Absorption Spectrometer, *Spectrochimica Acta*, 1998, 53B, 699-708
- [12] Lewis S.A., O'Haver T.C., Determination of metals at the microgram-per-liter level in blood serum by simultaneous multielement atomic absorption spectrometry with graphite furnace atomization, *Analytical Chemistry*, 1985, 57, 2-5
- [13] Lewis S.A., O'Haver T. C., Simultaneous multielement analysis of microliter quantities of serum for copper, iron and zinc by graphite furnace atomic absorption spectrometry, *Analytical Chemistry*, 1984, 56, 1651-1654
- [14] Feuerstein M., Schlemmer G., The simultaneous determination of Pb, Cd, Cr, Cu and Ni in potable and surface waters by GFAAS according to international regulations, *Atomic Spectroscopy*, 1999, 20, 149-154
- [15] Amorim Filho V.R., Polito W.L., Oliveira S.R., Freschi G.P.G., Gomes Neto J.A., Simultaneous determination of Cd and Pb in antibiotics used in sugar-cane fermentation process by GFAAS, *Ecl. Quím., São Paulo*, 2006, 31, 7-12
- [16] Kitagawa K., Shimazaki Y., A simultaneous multielement atomic absorption spectrometer with an inverse polychromator and fast Fourier transformation, *Analytical Sciences*, 1993, 9, 663-669
- [17] Treble R.G., Thompson T.S., H.R. Lynch H.R., Determination of Copper, Manganese and Zinc in Human Liver, *BioMetals*, 1998, 11, 49-53
- [18] Manning D.C., Slavin W., Carnrick G.R., Investigation of Aluminum Interferences Using the Stabilized Temperature Platform Furnace, *Spectrochimica Acta*, 1982, 37B, 331-341
- [19] Slavin W., Carnrick G.R., Manning D.C., Pruszkowska E., Recent Experiences with The Stabilized Temperature Platform Furnace and Zeeman Background Correction, *Atomic Spectroscopy*, 1983, 4, 69-86
- [20] Styris D. L. and Redfield D. A., Mechanisms Controlling Graphite Atomization and Stabilization of Beryllium, *Analytical Chemistry*, 1987, 59, 2897-2903
- [21] Thomaidis N.S., Piperaki E.A., Polydorou C.K., Efstathiou C.E., Determination of Chromium by Electrothermal Atomic Absorption Spectrometry with Various Chemical Modifiers, *Journal of Analytical Atomic Spectrometry*, 1996, 11, 31-36
- [22] Burguera J.L., Burguera M., Rondon C., Rodriguez L., Carrero P., Petit de Pena Y., Burguera E., Determination of Chromium in Urine by Electrothermal Atomic Absorption Spectrometry Using Different Chemical Modifiers, *Journal of Analytical Atomic Spectrometry*, 1999, 14, 821-825
- [23] Quinaia S.P., Nobrega J.A., A Critical Evaluation of The Graphite Furnace Conditions for The Direct Determination of Chromium in Urine, *Fresenius Journal of Analytical Chemistry*, 1999, 364, 333-337

Determination of Si and Al in Corrosion Medium of Sodium Chloride Solution by Inductively Coupled Plasma Atomic Emission Spectrometry

Dagmar Galusková¹, Dušan Galusek², Pavol Šajgalík²

¹*Vitrum Laugaricio – Joint Glass Centre of the Institute of Inorganic Chemistry, Slovak Academy of Sciences, Alexander Dubček University of Trenčín, and RONA, j.s.c., Študentská 2, 911 50 Trenčín, Slovak Republic, e-mail: galuskova@tmuni.sk*

²*Institute of Inorganic Chemistry, Slovak Academy of Sciences, Bratislava, Slovak Republic*

Abstract

Inductively coupled plasma atomic emission spectroscopy was used for determination of Si and Al originated from the corrosion of widely used structural ceramic, alumina, in an aqueous solution containing 0.5 mol/l NaCl at temperatures of 150 and 200 °C. The internal standardisation (IS) was used as a correction technique for matrix effects and compared with simple matrix matching technique. The IS method was shown to be sensitive with acceptable limits of detection: Al (308.215 nm) 0.095, Si (251.611 nm) 0.099 (all in mg.L⁻¹) and exhibited satisfactory precision (relative standard deviation 1 – 5 %) with high analytical recoveries varying between 95 and 100 %.

Key words: *Atomic emission spectrometry, inductively coupled plasma, effect of Na*

Introduction

In the past automotive exhaust systems were only expected to last for a few years at best. In today's vehicles lifetime expectancies are higher, and therefore many parts are made of some stainless steel alloy. Despite of this, they still show low resistance against salt corrosion due to winter road maintenance.

As high-performance structural materials, advanced ceramics can find various applications including their use in such destructive environments. To evaluate the corrosion resistance of the mentioned materials, such as alumina and silicon nitride, a set of corrosion experiments in aqueous sodium chloride solution needs to be carried out. After contact with corrosive solution the morphology changes in materials are studied, and the solution itself needs to be analysed by common techniques as are AAS, ICP OES or ICP MS in order to understand the mechanisms of corrosion process. However, depending on ceramic material and conditions of the corrosion experiment the amounts of elements transferred from material to solution can be rather low.

Regarding common spectral and non-spectral interferences caused by matrix, determination of low concentration of metals in salts using mentioned techniques is possible only in strongly diluted salt solutions [1]. On line separation and pre-concentration was used prior to analysis of the trace elements in urine [2] or sea water [3]. However, these techniques are time-consuming, labour-

intensive and costly, and pose the risk of contamination. In addition dilution of the sample negatively influences the detection limits.

ICP OES is an efficient technique for rapid multi-element analysis of a wide scale of various sample types. The presence of easily ionized elements in ICP OES may result either in an enhancement or a depression in the analyte signal intensity, accompanied by a shift of the spatial distribution. Mermet [4] and Romero [5] reported that the effects seem to be strongly dependent on the operating conditions, particularly on the power and the carrier gas flow rate, and observation height in case of radial plasma viewing. One of simple procedures, which help to eliminate such influences, is matrix matching: the practical composition of the sample matrix is modelled in calibration standards. Another possibility is internal standardisation: a simple internal standardization technique has been utilised by Krejčová [6,7] for multi-element analysis in solutions of analytically pure hydroxides and salts by ICP OES.

With regard of the corrosion mechanisms of studied ceramic materials, silicon and aluminium are the most relevant elements. The present study reports on the results of determination of both elements in aqueous solution containing 0.5 mol L^{-1} NaCl. Specifically, the objective of this study is to verify the applicability of internal standardization technique [6,7] for analysis of the content of aluminium in the samples originated from the corrosion experiments and to extend the applicability of the methodology to determination of silicon. This technique is then compared with simple matrix matching procedure.

Experimental

Measurements were carried out with the sequential, radially viewed ICP atomic emission spectrometer Vista MPX (VARIAN), equipped with V-groove nebulizer and the spray chamber MK11.

NaCl "ACS" purity ISO, Reag. Ph Eur produced by MERCK KGaA (Darmstadt, Germany) and distilled water prepared by reverse osmosis purification system (CHEZAR, Bratislava, Slovak Republic) were used to prepare aqueous sodium chloride solution.

Single component standards of Si, Al, Be, Y were used ($1000 \pm 2 \mu\text{g mL}^{-1}$) (ANALYTIKA, Praha, Czech Republic).

Calibration standards

Multi-element standard was prepared containing (i) Al, Si (100 mg L^{-1}), (ii) the same elements with half of the concentrations as in (i), (iii) the same elements in five and ten-fold dilution of (ii). All standards as well samples were stabilized with 0.25 mL of $65\% \text{ w/v HNO}_3/100\text{mL}$ of solution to keep pH of the solution below 2. To the solutions described above, internal standards were also added. Calibration solutions without the addition of internal standards were prepared in 0.5 mol L^{-1} NaCl.

Internal standardization

Internal standards Be (0.1 mg L^{-1}), Be (1 mg L^{-1}), and Y (1 mg L^{-1}) were used.

Samples

Two samples were selected from the corrosion experiments performed in 0.5 mol L^{-1} NaCl. The first, polycrystalline alumina ceramics (purity 99.995 %) sintered without additives, being in contact with a 0.5 mol L^{-1} NaCl solution for 4 days at $200 \text{ }^\circ\text{C}$. The second, polycrystalline alumina prepared in the presence of sintering additives (5 wt. % $\text{CaO} \cdot 5\text{SiO}_2$) in contact with a 0.5 mol L^{-1} NaCl solution for 2 days at 150°C . The accuracy of measurement was verified by the analysis of a certified reference material (CRM) CENTMIX 4, containing Al, Si in concentrations of $10 \text{ mg} \cdot \text{L}^{-1}$ (ANALYTIKA, Praha, Czech Republic).

The ICP OES method

The measurement conditions were optimised on the basis of the signal-to-background ratio of the least concentrated elements (Al). The measurement conditions are listed in Tables 1. All detection limits were calculated from the standard deviations (SD) of the measurements of 10 blank replicates measured for each element. The detection limit was set equal to the average of the standard deviations multiplied by three.

Table 1: Operating conditions of the ICP OES analysis

Rf power	1.15 kW	Nebulizer pressure	160 kPa
Viewing height	8 mm	Background correction	Fixed point correction
Plasma gas	15.0 L min ⁻¹	Number of replicates	3
Auxiliary gas	1.5 L min ⁻¹		
Gas	Argon 99.998 %		

Results and discussion

The results of determination of Si and Al in solution from corrosion experiments are summarized in the Table 2 and 3, respectively, and evaluated with regard to the certified reference material. The samples containing 3 % of NaCl were analysed for Si and Al using the internal standardisation (IS) with Be of various concentrations. Yttrium was also used as an internal standard, but only to evaluate matrix effect for determination of Al.

Table 2: Concentrations of Si in mg.L⁻¹ measured in the certified reference material and in solution obtained from corrosion experiments

Oxide	Analytical results (mg.L ⁻¹)							
	Si [251.611 nm]							
	Be (0.1ppm)	RSD (%)	Be (1ppm)	RSD (%)	no IS	RSD (%)	Y(1 ppm)	RSD (%)
CRM	9.64	0.40	9.29	2.71	7.01	4.61	-	-
AH	9.71	0.61	9.11	3.20	8.42	4.74	-	-
A	9.02	1.04	8.92	1.90	7.97	10.9	-	-

* no IS – results obtained from matrix matching technique

Table 3: Concentrations of Al in mg.L⁻¹ measured in the certified reference material and in solution obtained from corrosion experiments

Oxide	Analytical results (mg.L ⁻¹)							
	Al [308.215 nm]							
	Be (0.1ppm)	RSD (%)	Be (1ppm)	RSD (%)	no IS	RSD (%)	Y (1ppm)	RSD (%)
CRM	10.63	1.01	10.00	3.06	11.99	1.31		
AH	1.49	2.84	1.45	2.66	1.57	4.52	1.45	2.09
A	0.81	5.31	0.92	9.56	0.97	13.6	0.90	10.5

* no IS – results obtained from matrix matching technique

The measured concentrations of Si and Al in the presence of internal standards are comparable, and achieve satisfactory precision. The relative standard deviations (RSD in %) vary in the interval from 1 to 5 %. With the use of matrix matching technique enhancement or suppression of the analytical intensity signal was observed. The effect of sodium ions in solution on the intensities of ionic lines in ICP OES has been studied by Romero and Mermet [5]. The effect was assigned both to a change in the excitation and ionization processes in the plasma and to a change in the aerosol

formation and transport. Determination of the selected elements with the use of the matrix matching technique did not provide satisfactory results due to low recoveries varying from 60 to 95 % depending on the analysed element.

Conclusions

From previously published work [6,7] a proposed analytical method was utilised for elemental analysis of Al in aqueous sodium chloride solution and the applicability of the method was extended to the analysis of Si in 3 % water solution of analytically pure NaCl. The simple internal standardisation technique was shown to be sensitive with satisfactory limits of detection: Al (308.215 nm) 0.095, Si (251.611 nm) 0.099 (all in mg.L⁻¹). Various concentrations of internal standard Be do not have any significant effect on accuracy of determination. The method exhibited satisfactory precision (relative standard deviation 1 – 5 %) and high analytical recoveries ranged between 95 and 100 %. Simple matrix matching technique was shown to be not sufficient for elimination of non-spectral interferences that in case of Si led to suppression of the analytical signal intensity. In the contrary, slight enhancement of the analytical signal was observed in the analysis of Al. Determination of the selected elements with the use of the matrix matching technique did not provide satisfactory results due to low recoveries varying from 60 to 95 % depending on the analysed element.

Acknowledgement: The financial support of this work by the grant APVV 0171-06 and by VEGA 2/6181.26 is gratefully acknowledged.

References

- [1] Montaser A., Golightly D.W. (1992): Inductively coupled plasmas in analytical atomic spectrometry, 3rd ed., VCH Publishers, Inc. New York
- [2] Dressler V.L., Pozebon D., Curtius A.J.: *Spectrochim Acta*, 1998, 53B, 1527
- [3] Batterham G.J., Munksgaard N.C., Parry D.L.: *J Anal Atom Spectrom*, 1997, 12, 1277
- [4] Mermet J.M.: *J Anal At Spectrom*, 1998, 13, 419
- [5] Romero X., Poussel E., Mermet J.M.: *Spectrochim Acta*, 1997, 52B, 495
- [6] Krejčová A., Černohorský T., Pouzar M.: *Microchim Acta*, 2007, 156, 271-275
- [7] Krejčová A., Černohorský T., Pouzar M.: *Anal Chim Acta*, 2007, 582, 208-213

Determination of Si, Al, Ca, Mg and B in Glass Samples by ICP-AES

Dagmar Galusková, Jozef Kraxner, Róbert Klement

Vitrum Laugaricio – Joint Glass Center of the Institute of Inorganic Chemistry, Slovak Academy of Sciences, Alexander Dubček University of Trenčín, and RONA, j.s.c., Študentská 2, 911 50 Trenčín, Slovak Republic; e-mail: klement@tmuni.sk, galuskova@tmuni.sk, kraxner@tmuni.sk

Abstract

A comparative study of several decomposition techniques of E-glass like samples has been carried out. The glass samples were dissolved by fusion with lithium tetraborate, by alkaline fusion with sodium peroxide and acidic decomposition with hydrofluoric and perchloric acids. Accuracy of analytical results was confirmed by analyzing the certified reference material of borosilicate glass (NCS DC61104). The contents of particular elements were determined by inductively coupled plasma-atomic emission spectrometry (ICP-AES). The obtained results and achieved precision showed that each of considered techniques is adequate for determination of particular elements. On the basis of the analytical results more than one decomposition technique need to be applied in order to determine overall chemical composition of E-glass like samples.

Key words: *glass analysis, ICP-AES, wet-acid decomposition, alkaline fusion, lithium tetraborate*

Introduction

The rapid preparation of silicate samples for analysis is very important for automatic and routine analysis of a large number of samples. A number of destructive and non-destructive instrumental multi-element techniques are available for the analysis of glasses, ceramics and other silicate matrices. Inductively coupled plasma atomic emission spectrometry (ICP-AES) is a widely used technique for the above samples as it is sensitive, accurate and with low detection limits [1,2]. Due to the fact that ICP-AES uses mainly liquid samples, fast, effective and convenient decomposition and/or dissolution methods are usually necessary. Two approaches are commonly applied to this problem [3,4]: (i) wet-acid decomposition with mixtures of hydrofluoric acids and various mineral acids; (ii) fusion with one of, or various combinations of boric acid, alkali metal carbonates, alkali metal borates, sodium hydroxide, sodium peroxide and potassium superoxide. In a lot of cases (depending on elements determined) more than one decomposition method is usually needed for analysis of multi-element glass samples.

In the present work, we report a comparative study of several decomposition techniques applied on the certified standard reference borosilicate glass (NCS DC61104) and E-glass like samples. The composition of the reference glass is close to composition of studied E-glass like samples. E-glass is commercially produced glass for production of glass fibres used as insulators.

Experimental

All chemical reagents (Merck, Sigma-Aldrich) of analytical grade were used. The certified standard reference material NCS DC61104 (China National Analysis Centre for Iron and Steel) of borosilicate glass with composition close to studied glass samples was used. All glass samples, standard and calibration solutions were prepared using deionized water (Milli-Q™, Millipore Corp., Bedford, MA).

Instrumentation:

A Varian Vista-MPX atomic emission spectrometer with inductively coupled plasma (ICP-AES) was used throughout, according to the following operating conditions: 1. For acid decomposition: RF power, 1.7 kW, plasma gas flow rate, 15 L/min, auxiliary flow rate, 1.5 L/min, nebuliser pressure, 140 kPa, gas, Ar-99.998 %, viewing height, 7 mm, background correction, fixed point correction, number of replicates, 2. For fusions: power, 1.6 kW, plasma gas flow rate, 15 L/min, auxiliary flow rate, 1.5 L/min, nebuliser pressure, 120 kPa, gas, Ar-99.998 %, viewing height, 7 mm, background correction, fixed point correction, number of replicates, 3. The analytical wavelengths were set at the following spectral lines: Si: 251.611 nm, B: 249.678 nm, Al: 308.215 nm, Ca: 422.673 nm, Mg: 280.270 nm.

Calibration methods and standard solutions:

Working multi-element standard solutions of the analytes were prepared by appropriate stepwise dissolutions of stock standard solutions of 1000 mg L⁻¹ (Analytica, Prague, Czech Republic) in blank solutions resulted from decomposition procedures (see below) carried out without the glass samples. The final working standards were made at the following concentrations: For acid decomposition: 10, 50 and 100 mg L⁻¹ for Al, Ca and 5, 20 and 50 mg L⁻¹ for Mg. For alkaline fusion: 20, 50 and 100 mg L⁻¹ for Si, Al, Ca and 5, 10 and 20 mg L⁻¹ for Mg, B.

Decomposition of samples:

Wet-acid decomposition: Amount of 0.1 g of dried glass samples (powdered in agate mortar and sieved to fraction < 45 μm) in platinum dish was soaked with two drops of distilled water and 0.5 ml of 32 % HF and 10 ml of concentrated HClO₄ were added. The platinum dish was left at RT for 30 min. The mixture was heated in platinum dish on sunbath at 130 °C until a practically clear solution was formed, then the temperature was raised to 160 °C and the mixture was evaporated until wet solid product was obtained. This step with addition of 3 ml of concentrated HClO₄ was repeated three times. Finally, the wet solid product was dissolved in 4 % HNO₃ with addition of hydrogen peroxide to avoid the precipitation (8 ml of 35 % of H₂O₂ was added to 1 litre of 4 % HNO₃) and solution was quantitatively transferred to volumetric flask and made up to 100 ml with pure water.

Decomposition by alkaline fusion: A dried sample of 0.1 g (particle size < 45 μm) was well mixed with 2.0 g of sodium peroxide in zirconium crucible. The crucible covered with a lid was heated in an electric furnace at 700 °C for 10 min under Ar-atmosphere. After cooling, the solid melt was dissolved in 0.1M HNO₃ and solution was quantitatively transferred to volumetric flask and made up to 250 ml with 0.1M HNO₃.

Decomposition by fusion with lithium tetraborate: A dried sample of 0.1 g (particle size < 45 μm) was well mixed with 2.0 g of lithium tetraborate in graphite crucible. The mixture was heated in an electric furnace at 1250 °C for 10 min in a first step and then at 1350 °C for 10 min under N₂-atmosphere. The hot melt drop was poured into 0.1M HNO₃, and after dissolution the solution was quantitatively transferred to volumetric flask and made up to 100 ml with 0.1M HNO₃.

Results and Discussion

The results of analysis for certified standard reference material NCS DC61104 and selected analysed glass sample decomposed by various decomposition techniques are summarized in Tab. 1

and Tab.2. The total oxide contents of five elements determined, according to certificate is 98.29 %, because the standard reference contain also other, although minor oxides, e.g. $\text{Fe}_2\text{O}_3 - 0.34 \pm 0.01$ %; $\text{TiO}_2 - 0.19 \pm 0.02$ %; $\text{K}_2\text{O} - 0.59 \pm 0.04$ %; $\text{Na}_2\text{O} - 0.096 \pm 0.011$ %; $\text{F} - 0.54 \pm 0.04$ %.

Table 1: Analytical results for the certified standard reference material NCS DC61104

Oxide	Certified value (wt %)	Analytical results (wt.%)			Analytical results (wt.%)			Analytical results (wt.%)		
		Acid decomposition			Alkaline fusion			Tetraborate fusion		
		Av. $\pm \sigma$	RSD (%)	Deviation (%)	Av. $\pm \sigma$	RSD (%)	Deviation (%)	Av. $\pm \sigma$	RSD (%)	Deviation (%)
SiO_2	53.98 \pm 0.14	–	–	–	54.16 \pm 3.96	7.3	+0.3	54.34 \pm 0.15	0.3	+0.7
Al_2O_3	14.50 \pm 0.12	14.32 \pm 0.18	1.3	-1.2	14.41 \pm 1.84	12.8	-0.6	14.75 \pm 0.05	0.3	+1.7
B_2O_3	8.87 \pm 0.11	–	–	–	8.49 \pm 0.55	6.5	-4.3	–	–	–
CaO	16.54 \pm 0.09	16.02 \pm 0.17	1.1	-3.1	16.71 \pm 0.87	5.2	+1.0	17.62 \pm 0.22	1.2	+6.5
MgO	4.40 \pm 0.12	4.24 \pm 0.05	1.2	-3.6	4.22 \pm 0.34	8.1	-4.1	6.75 \pm 0.09	1.3	+53.4

Note: "Av.", " σ ", and "RSD" represent the average, standard deviation, and relative standard deviation. "Deviation" represents the deviation of average value from the certified value for the glass standard NCS DC61104.

Table 2: Analytical results for the studied glass

Oxide	Expected value (wt %)	XPS (wt %)	Analytical results (wt.%)		Analytical results (wt.%)	
			Acid decomposition		Alkaline fusion	
			Av. $\pm \sigma$	RSD (%)	Av. $\pm \sigma$	RSD (%)
SiO_2	54.17	54.03	–	–	53.11 \pm 0.26	0.5
Al_2O_3	14.32	13.33	12.11 \pm 0.36	1.3	14.17 \pm 0.18	1.3
B_2O_3	5.01	–	–	–	5.00 \pm 0.29	5.8
CaO	23.28	22.95	22.05 \pm 0.70	1.1	25.37 \pm 1.03	4.1
MgO	3.23	3.37	3.09 \pm 0.10	1.2	3.25 \pm 0.19	5.8

Note: "Av.", " σ ", and "RSD" represent the average, standard deviation, and relative standard deviation.

For wet-acid decomposition, silica is not determined due to its transformation to volatile SiF_4 ; the resulting solution is almost free from the bulk concentration of Si. For the decomposition by fusion with lithium tetraborate, the boron is not determined, because the high concentration of boron in the solution. Only in the case of alkaline fusion with sodium peroxide, it was possible to determine all five elements in ICP analysed solution. As it is clearly seen from Table 1, the analytical results of reference material decomposed by wet-acid decomposition and alkaline fusion agree quite well with its certified values. In case of lithium tetraborate decomposition, reasonable results are obtained for SiO_2 and Al_2O_3 content, however higher values for CaO and MgO were found, which is not clear yet. Also the analytical results for studied glass sample from the system $\text{CaO-MgO-SiO}_2\text{-B}_2\text{O}_3\text{-Al}_2\text{O}_3$, show (see Table 2), that for the wet-acid decomposition and alkaline fusion, results agrees reasonably well with expected values; for acid decomposition the values are a bit lower than in the case of alkaline fusion.

Conclusion

The wet-acid decomposition technique is suitable especially for determination of alkaline in the glass samples. On the other hand, the alkaline fusion with sodium peroxide is also suitable technique for glass sample decomposition and compared to wet-acid chemistry much faster. In order to determine the content of all elements in glass samples by ICP-AES, however, more than one decomposition technique is needed.

Acknowledgement

This work was supported by Slovak Research and Development Agency under the contract No. APVV-20-P06405 and by university grant No. 19/20007.

References

- [1] Papadopoulos D.N., Zachariadis G.A., Anthemidis A.N., Tsirliganis N.C., Stratis J.A., *Anal. Chim. Acta*, 2004, 505, 173
- [2] Bruno P., Caselli M., Curri M.L., Genga A., Striccoli R., Traini A., *Anal. Chim. Acta*, 2000, 410, 193
- [3] Sulcek Z., Povondra P.: *Methods of Decomposition in Inorganic Analysis*, CRC Press, Boca Raton, FL, 1989
- [4] Yoshikuni N., *Talanta*, 1996, 43, 1949, and references cited therein

Separation and Preconcentration of Total Inorganic Antimony by a Nanometer-Sized TiO₂ and its Determination by Direct TiO₂-Slurry Sampling Electrothermal Atomic Absorption Spectrometry

Ingrid Hagarová, Peter Matúš, Marek Bujdoš, Jana Kubová

Comenius University, Faculty of Natural Sciences, Geological Institute, Mlynská dolina G, 842 15 Bratislava, Slovakia,
e-mail: hagarova@fns.uniba.sk

Abstract

In this work, nanometer sized TiO₂ was used for separation/preconcentration of total inorganic antimony followed by the direct TiO₂-slurry sampling into a graphite tube. The optimal conditions for separation/preconcentration of antimony (pH, mass of TiO₂, extraction time), effect of its different valence and effect of coexisting ions on the extraction recovery were investigated in detail. The optimization of furnace conditions for antimony determination in liquid and slurry solutions by electrothermal atomic absorption spectrometry was also performed. The accuracy of the optimized extraction method was checked by certified reference material for trace elements in riverine water SLRS-4.

Key words: antimony, preconcentration, titanium dioxide, slurry sampling, electrothermal atomic absorption spectrometry

1. Introduction

Although electrothermal atomic absorption spectrometry (ETAAS) offers excellent detection limit for trace determination of antimony, ultratrace determination is impossible without using a suitable separation/preconcentration procedure. Solid phase extraction (SPE) is frequently used for this purpose. Different inorganic metal oxides can be applied as solid sorbents. Among them, TiO₂ offers a high surface area/body weight ratio and high adsorption capacity. Generally, TiO₂ is used to adsorb metal ions as a sorbent in a column system. In this case, the elution is necessary before determination of these ions. However, the elution is time-consuming and sometimes results in a loss of analyte. Slurry sampling of the used sorbent is an effective mode to solve this problem.

In this work, nanometer sized TiO₂ was used for separation and preconcentration of total inorganic antimony. Then, adsorbed antimony was directly detected by TiO₂-slurry sampling ETAAS.

2. Experimental

2.1 Apparatus

All measurements were carried out with a Perkin-Elmer 3030 atomic absorption spectrometer (Norwalk, CT, USA) equipped with HGA 600 graphite furnace. The spectrometer was provided with a Zeeman-based background corrector. All the measurements were performed in the peak area mode. Pyrolytic graphite tubes (Perkin-Elmer) were exclusively used. Argon was used as the purge gas. Electrodeless discharge lamp for Sb (Perkin-Elmer) was operated at 8 W with a spectral band width of 0.7 nm. The selected wavelength was 217.6 nm. Injection of a slurry solution (20 μ l) was followed by modifier solution (10 μ l of palladium nitrate). Temperature programme is shown in Table 1.

Ionometer MS-31 (Praque, Czech republic) equipped with a glass-combination electrode, analytical balance Sartorius 1702 (Göttingen, Germany), mechanical shaker LT2 (Kavalier, Sazava, Czech republic), and centrifuge MPW-360 (Mechanika precyzyjna, Warsaw, Poland) were used for extraction procedure and slurry sample preparation.

Table 1. Temperature programme

Stage	Temperature (°C)	Ramp time (s)	Hold time (s)	Ar flow rate (ml/min)
Drying	110	10	20	250
Pyrolysis	1200	10	20	250
Atomization	2500	0	3	0
Cleaning	2550	1	1	250

2.2 Reagents and solutions

All used reagents were of analytical grade and all solutions were prepared in doubly deionized water (DDW). Titanium dioxide (anatase form, nanopowder, < 25 nm, 99.7 %; Sigma-Aldrich, Steinheim, Germany) was used as a sorbent. Stock standard antimony(III) and antimony(V) solutions (1000 mg/l) were prepared by dissolving appropriate amounts of potassium antimony tartrate (Sigma-Aldrich) and potassium hexahydroxyantimonate (Sigma-Aldrich) in DDW, respectively. Working antimony standard solutions were prepared by stepwise dilution of the stock solutions in DDW just before use. Nitric acid (Merck, Darmstadt, Germany) and sodium hydroxide (Merck) were employed to adjust the final pH of the standard and model solutions. All stock solutions were stored in polyethylene bottles in a refrigerator held at 4 °C. All glassware was kept in 10 % (v/v) nitric acid (Lachema, Brno, Czech republic) for at least 24 hrs and washed three times with DDW before use. A chemical modifier solution was prepared by diluting palladium nitrate stock solution (10 g/l of Pd) (Merck) in DDW. Solutions with studied concentrations of potentially interfering elements were prepared by stepwise dilution of their stock solutions (1000 mg/l) (Merck) in DDW just before use. Certified reference material for trace elements in riverine water SLRS-4 (National Research Council of Canada, Ottawa, Canada) was used for checking the accuracy of the optimized method for the total antimony determination.

2.3 Analytical procedure

Sample solution was transferred into a 600 ml glass beaker. Then, the pH was adjusted to 2.0 with 2 M HNO₃. The sample solution was placed into a 100 ml HNO₃-washed high-density polyethylene (HDPE) bottle containing 100 mg of nanometer sized TiO₂. The sample solution was shaken by a mechanical shaker for 10 min. Then, the mixture was centrifuged at 4000 rpm for 10 min and the bulk aqueous phase was easily decanted by simply inverting the bottle. Finally 5 ml of DDW was added to prepare a slurry sample. The described procedure was repeated four times for every sample solution. The slurry sample was agitated for 1 min and transferred into an autosampler cup (immediately before injection into a graphite tube). Antimony in the slurry samples was determined according to the furnace conditions listed in Table 1.

3. Results and discussion

3.1 Optimization of the furnace conditions

To establish a suitable temperature programme for antimony determination in liquid and slurry solutions, pyrolysis and atomization curves were obtained in the presence of palladium nitrate (1 g/l of Pd). The pyrolysis and atomization temperatures were investigated in the range of 300–1800 °C and 1500–2500 °C, respectively (see Fig. 1). The analysis of the TiO₂-slurry sample resulted in a maximum loss-free pyrolysis temperature of 1300 °C; the analysis of the liquid standard solution resulted in a maximum loss-free pyrolysis temperature of 1200 °C. The absorbance reached the maximum increasing the atomization temperature to 2400 °C in the both cases.

Based on the observations described above, the pyrolysis temperature of 1200 °C and atomization temperature of 2500 °C were selected and used in the following experiments (see Tab. 1).

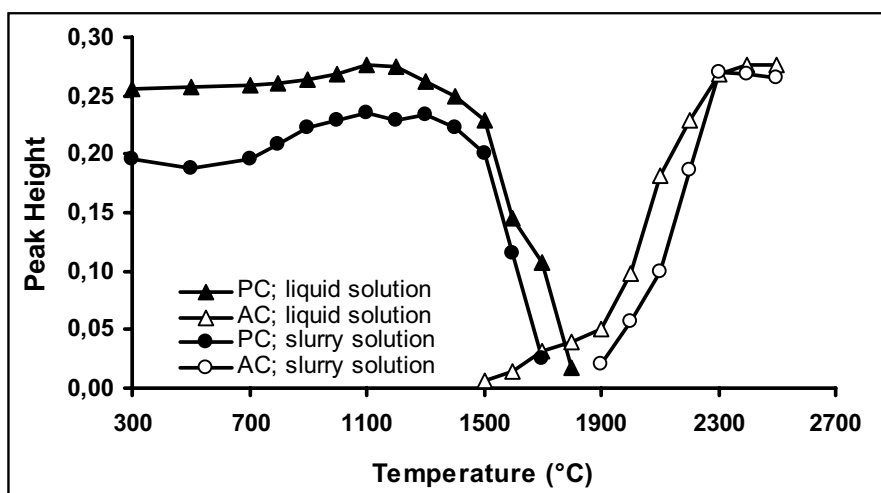


Fig. 1. Pyrolysis and atomization curves for antimony in the presence of palladium
PC – pyrolysis curve; AC – atomization curve

3.2 Optimization of the analytical procedure

3.2.1 Effect of pH

Titanium dioxide can adsorb anions when the pH of a solution is lower than 6.2 (isoelectric point) [1], so the pH values of model solutions prior to adsorption were changed from 1.0 to 6.0. The recoveries around 96.5 ± 3.0 % were found in the studied range (see Fig. 2). Another factor, which can be affected by the pH of the media is the stability of TiO₂ slurry [2]. When the pH of the solution is lower than the pH of the isoelectric point, the spontaneous adsorption of H⁺ on titania results in a positive charge on the anatase surface [1]. The action among these ions with the same positive charge can keep the slurry stable. In our experiments, relative standard deviation (RSD) less than 5 % was achieved at the pH below 3.0 and the TiO₂ slurry remained stable at least 10 min. At higher values of the pH, RSD was measurably increased. Finally, the pH 2.0 was chosen and used for subsequent experiments.

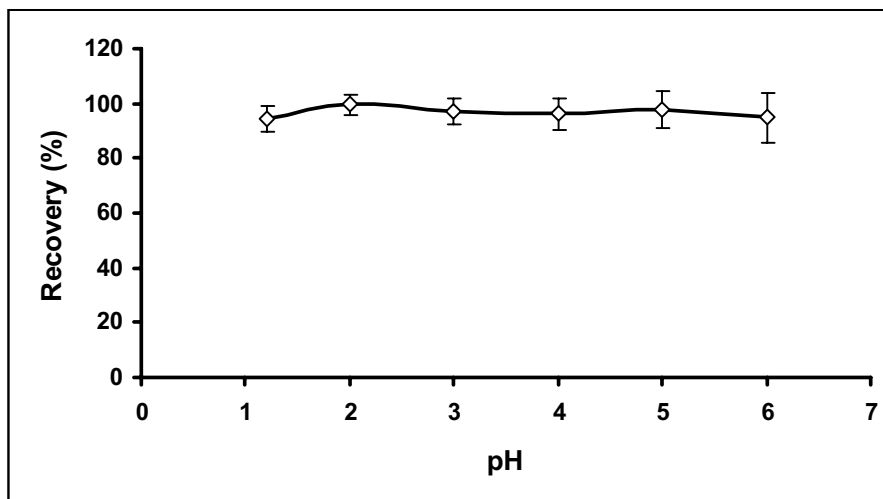


Fig. 2. Effect of pH on the extraction recovery of antimony

3.2.2 Effect of TiO_2 mass

In these experiments, the range of TiO_2 mass was varied from 5.0 mg to 200.0 mg. While mass of TiO_2 was up to 40.0 mg, the recoveries of antimony were over 95 %, after that, the recoveries were basically kept at equality (see Fig. 3). Finally, 100.0 mg of TiO_2 was chosen as a sorbent mass and used in the optimized procedure.

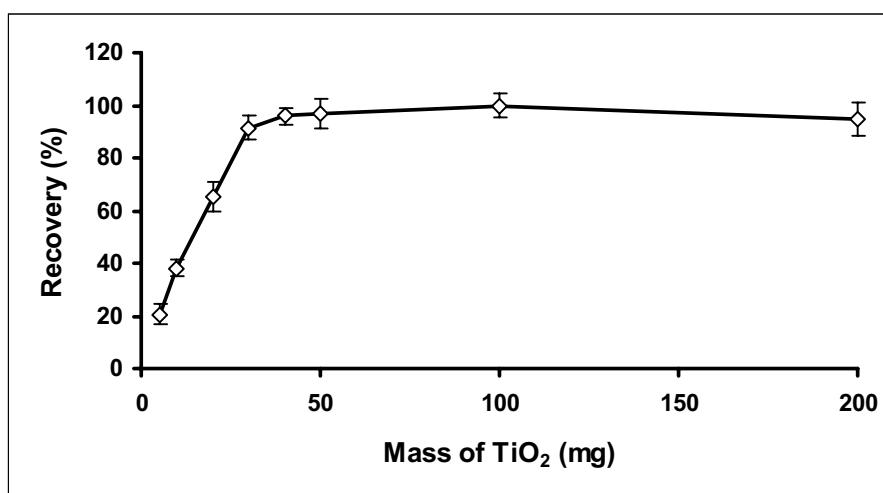


Fig. 3. Effect of TiO_2 mass on the extraction recovery of antimony

3.2.3 Effect of extraction time

The effect of extraction time on the recovery of antimony was investigated in the range of 2–20 min under the optimal adsorption conditions. The results (see Fig. 4) show excellent recoveries for all the studied range but RSD less than 5 % was achieved when stirring time was up to 10 min. Finally, the extraction time of 10 min was chosen as optimal and used in all experiments.

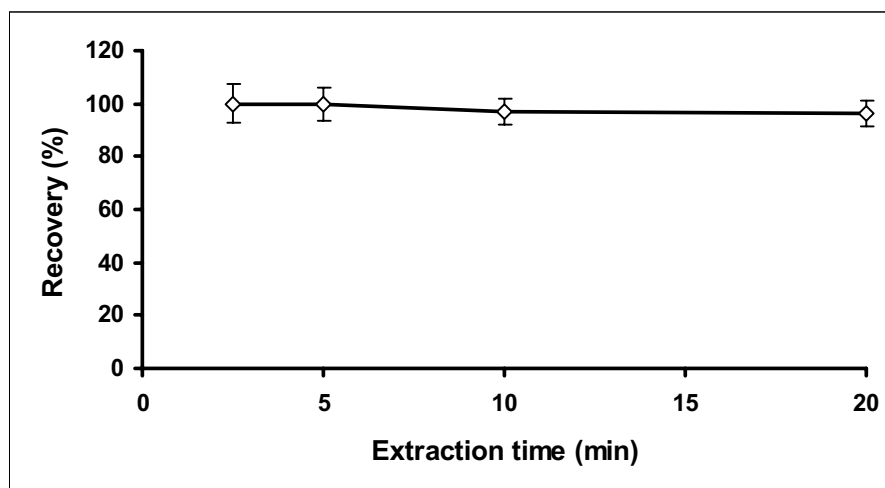


Fig. 4. Effect of extraction time on the extraction recovery of antimony

3.2.4 Effect of valence of antimony

In this investigation, model solutions containing Sb(III), Sb(V), and mixed solutions containing different ratios of Sb(III) + Sb(V) were used. The achieved results showed similar behaviour of Sb(III) and Sb(V) under conditions described above. Thus, the selected experimental conditions are appropriate for the both valences of antimony and the total inorganic antimony can be separated and preconcentrated by the optimized extraction procedure.

3.2.5 Effect of coexisting ions

The effect of coexisting ions on the determination of antimony was investigated under the optimal extraction conditions. Model solutions of 1.0 µg/l Sb(V) containing a foreign ion were separately pretreated according to the analytical procedure. The coexisting ions and their maximal studied concentrations are listed in Table 2. The obtained results suggest that the presence of the ions at the studied concentrations has no obvious influence on the determination of antimony under the selected conditions.

Table 2. Extraction recovery of antimony achieved in the presence of coexisting ions

Ion	Concentration (mg/l)	Recovery (%)	Ion	Concentration (µg/l)	Recovery (%)
Na ⁺	1000	102	Cu ²⁺	100	103
K ⁺	100	99	Co ²⁺	100	105
Ca ²⁺	100	94	Ni ²⁺	100	99
Mg ²⁺	100	100	Zn ²⁺	100	96
SO ₄ ²⁻	100	95	Pb ²⁺	100	91
PO ₄ ³⁻	100	92	Fe ³⁺	1000	94
Cl ⁻	1000	94	Al ³⁺	1000	96

3.3 Analytical figures of merit

The figures of merit for the optimized procedure were as follows. The enrichment ratio of 20 was used in all the study (the ratio between the first sample volume and 5.0 ml of the slurry prepared according to the described procedure). The RSD obtained for 10 samples of 1.0 µg/l Sb(V) subjected to the procedure was 3.8 %. The detection limit, calculated according to $3s_0/s$, where s_0 was obtained from the standard deviation for 10 replicates of a blank solution, and s is the slope of the calibration

graph obtained after the procedure, was 0.04 µg/l. A certified reference material for trace elements in riverine water SLRS-4 was used for checking the accuracy of the optimized method for the total inorganic antimony determination. The mean determined value ± SD was 0.22 ± 0.03 µg/l (n = 10), while the certified value ± SD was 0.23 ± 0.04 µg/l.

4. Conclusion

In the present work, a relatively simple and rapid method for the determination of ultratrace amounts of total inorganic antimony was optimized. The enrichment ratio of 20 was used in all the experiments. At this condition, the quantification limit of 0.11 µg/l was achieved. The obtained result showed that the presented procedure could effectively improve the analyte sensitivity and allow determining ultratrace amounts of antimony. Using larger initial volumes of samples, higher enrichment ratios and better quantification limit can be achieved.

Acknowledgement

The work was supported by Scientific Grant Agency of the Ministry of Education of Slovak Republic and the Slovak Academy of Sciences under the contracts No. VEGA 1/4464/07, VEGA 1/4463/07, VEGA 1/3561/06, and VEGA 1/0272/08 and by Slovak Research and Development Agency under the contracts No. LPP-0038-06, LPP-0188-06, and SK-CZ-044-07 and Grant No. MEB 080813.

References

- [1] Zhang L., Morita Y., Yoshikawa K., Isozaki A.: Direct simultaneous determination of ultratrace As, Se and Sb in river water with graphite furnace atomic absorption spectrometry by TiO₂-slurry sampling. *Anal. Sci.*, 2007, 23, 365-369
- [2] Dong H.M., Krivan V., Welz B., Schlemmer G.: Determination of trace impurities in titanium dioxide by slurry sampling electrothermal atomic absorption spectrometry. *Spectrochim. Acta, Part B*, 1997, 52, 1747-1762

Optimized BCR Three-Step Sequential and Dilute HCl Single Extraction Protocols – the Suitable Tools for Soil-Plant Metal Transfer Predictions in Polluted Areas?

¹Jana Kubová, ¹Peter Matúš, ¹Marek Bujdoš, ¹Ingrid Hagarová, ¹Ján Medved',
²Pavel Diviš, ²Hana Dočekalová

¹Comenius University in Bratislava, Faculty of Natural Sciences, Mlynská dolina 1, 842 15 Bratislava 4, Slovakia, e-mail: kubova@fns.uniba.sk

²Brno University of Technology, Faculty of Chemistry, Purkyňova 118, 61200 Brno, Czech Republic

Abstract

In this work, the fractions of selected risk metals (Al, As, Cd, Cu, Fe, Mn, Ni, Pb, Zn) that can be taken up by various plants were obtained by optimized BCR (Community Bureau of Reference) three-step sequential extraction procedure (SEP) and by single 0.5 mol l⁻¹ HCl extraction. These procedures were validated using five soil and sediment reference materials (SRM 2710, SRM 2711, CRM 483, CRM 701, SRM RTH 912) and applied to significantly different acidified soils for the fractionation of studied metals. The new indicative values of Al, Cd, Cu, Fe, Mn, P, Pb and Zn fractional concentrations for these reference materials were obtained by the dilute HCl single extraction. The influence of various soil genesis, content of essential elements (Ca, Mg, K, P) and different anthropogenic sources of acidification on extraction yields of individual risk metal fractions was investigated also. The concentrations of studied elements were determined by atomic spectrometry methods (F AAS, GF AAS, HG AAS, ICP OES). It can be concluded that the data of extraction yields from first BCR SEP acid extractable step and soil-plant transfer coefficients can be applied to the prediction of qualitative mobility of selected risk metals in different soil systems.

Key words: *optimized BCR three-step sequential extraction, dilute HCl single extraction, soils and plants, prediction of phytoavailability, F AAS, GF AAS, HG AAS, ICP OES*

Introduction

The soil-plant transfer of risk metals is a part of chemical element cycling in the nature. It is a very complex process governed by several factors, both natural and affected by man. Soil is the main source of the elements for the plants both as nutrients and pollutants and its conditions plays a crucial role in environmentally significant metal behaviour. In natural environments the surface soil layer elements concentrations are a function of litter inputs and the parent material. The dry and wet depositions, which enrich the canopies of the trees and surface soils, cause high elements concentrations in the overground plant parts and in the soils. The heavy metal pollution of the ecosystems due to anthropogenic activities like smelting or mining as well as atmospheric deposition

has the serious consequences. If the soils contain high contents of heavy metals and suffer from serious acid deposition, it can obviously wonder about the impacts on the ecosystem. The bioavailability, mobility and activity of heavy metals in the soils with a certain deposit of them, mostly due to cation exchange with H^+ , Ca^{2+} , Mg^{2+} , K^+ and NH_4^+ , are coming from acid deposition. Acid deposition has become one of the most important factors resulting in environment acidification. Predicting the impact of a contamination event on the environment requires information about the pollutant mobility pattern. The soil properties, metal speciation and plant species, especially soil-plant interactions, determine the bioavailability of soil metals.

The prediction of soil metal phytoavailability using the chemical extractions is a conventional approach routinely used in soil testing [1-5]. The adequacy of such soil tests for this purpose is commonly assessed through a comparison of extraction results with metal contents in relevant plants.

The aim of the present study was to evaluate the adequacy of optimized BCR SEP and single extraction with dilute HCl for the prediction of the soil pollutants effects affected by different anthropogenic sources of the acidification in a terrestrial ecosystems. These procedures were used after their validation to obtain the distribution of both the major (Al, Fe, Mn) and trace (As, Cd, Cu, Ni, Pb, Zn) risk metals in the soils with various levels and types of the contamination. The element contents in individual soil fractions and in the plants growing on studied localities were determined by atomic spectrometry methods (flame, graphite furnace and hydride generation atomic absorption spectrometry and inductively coupled plasma optical emission spectrometry).

Experimental

Soil and plant sample sites description

The acid soil and plant samples were collected from different locations of Slovakia reflecting the various chemical and physical soil characteristics as well as different types of atmospheric deposition.

Locality A: The first sampling site was situated near open quartzite mine Šobov (Banská Štiavnica, central Slovakia) where a large amount of pyrophyllite-pyrite gangue rock was excavated and deposited on the dump. Intensive pyrite oxidation in the mining dump produces extremely acid water which attacks minerals and causes a higher migration rate of various risk elements and the degradation of the soil and the meadow vegetation.

Locality B: The second sampling site was situated in the part of National park of the Low Fatra called Lúčanská Fatra. The studied acid soil profile was collected from the higher level of the Veľká Lúka locality. The source of its acidity is the podzolization process, which is connected with great rainfall, percolating regime and acid vegetation (e.g. dwarf pine, blueberry, grass) where their decomposition products are acidifying the whole soil profile.

Locality C: The third sampling site was situated in the region of Pezinok, which is famous for its important ore deposits in the Malé Karpaty Mts. The soil samples were collected from the dumpsite of Sb ore deposit situated on the south-eastern side of the mountains above the city of Pezinok. Mining and dressing of Sb deposits have significantly contributed to Sb and As contamination of soils, sediments and waters.

Soil samples

Some of important soil characteristics, listed by individual sampling locality, are shown in the Table 1 Before the analysis the soil samples were air-dried, sieved through a 2 mm sieve and milled in an agate pot to the fine powder, which was used for the chemical analysis.

Table 1. Some characteristics of studied soil samples (pH, TOC, EC and sulfate concentration values from three replicates)

Locality	Soil depth (cm)	pH (H ₂ O)	pH (KCl)	TOC (%)	EC (μS cm ⁻¹)	Sulfate (g kg ⁻¹)	Soil type
A	0-20	2.99	2.81	4.66	902	9.29	Acid sulphatic earth
B	0-20	3.40	2.84	35.9	117	6.25	Histo-humic Podzol
C	0-20	3.51	3.13	5.37	200	16.6	Fluvi-eutric Gleysol

Plant samples

Plant samples were collected together with the soil sampling. They included dominant or typical species, which had grown in the sampling area. Before the analysis the plant root, stem, leaf and fruit samples were separated, carefully rinsed in redistilled water, air-dried and cutted on the small pieces.

Locality A (Šobov) – grass *Festuca Rubra* (root and stem) with higher natural resistance to unfavourable conditions of the environment.

Locality B (Veľká Lúka) – blueberry *Vaccinium Myrtillus L.* (root, stem, leaf and fruit), long wearing plant included to semi-bush with dual creeper twigs which have root forming possibility.

Locality C (Pezinok) – blackberry *Rubus fruticosus* (root, stem, leaf), deciduous semi-bush. It occurs on the light forest localities and it requires the humus soils with soft humidity.

Reference materials

Four soils, one sediment and two plant reference materials listed in Table 2 were used for the validation of decomposition procedures applied to the samples for the determination of total soil and plant concentrations of studied elements. Listed soils RMs were used also for the validation of sequential and single extractions applied to soil samples for the fractionation of studied metals.

Table 2. The reference materials used in this study (NIST, National Institute of Standards and Technology, USA; BCR, Institute for Reference Materials and Measurements or Standards, Measurements and Testing Programme, EU; WEPAL, Wageningen Evaluating Programs for Analytical Laboratories, Netherlands; NRCCRM, National Research Centre for Certified Reference Materials, China)

Reference material	Description
SRM 2710 (NIST)	Highly contaminated soil collected from the top of pasture land in Montana area
SRM 2711 (NIST)	Moderately contaminated agricultural soil collected in Montana area
CRM 483 (BCR)	Sewage sludge amended soil collected from Great Billings Sewage farm, Northampton
CRM 701 (BCR)	Freshwater sediment collected from lake Orta, Piemonte
SRM RTH 912 (WEPAL)	Loess soil from a forest in Switzerland
CRM GBW 07603 (NRCCRM)	Bush branches and leaves collected from an arid area, Qinghai province
CRM GBW 07604 (NRCCRM)	Leaves of poplar collected from Beijing

Determination of total content

Total concentrations of studied elements (Al, As, Ca, Cd, Cu, Fe, K, Mg, Mn, Ni, P, Pb, Zn) in soil samples were determined after their decomposition by acid mixture of HF+HNO₃+HClO₄+H₂O₂ in open system at 200 °C. Total concentrations of studied elements in plant samples were determined after their decomposition by acid mixture of HF+HNO₃ in an autoclave at 160 °C. For As determination the soil and plant samples were decomposed with HNO₃ in an autoclave at 160 °C.

Sequential extraction

The optimized BCR three-step sequential extraction procedure (BCR SEP); first acid extractable step: extraction with 0.11 mol l⁻¹ acetic acid (v/w ratio = 40/1, 16 h extraction time), second reducible step: extraction with 0.5 mol l⁻¹ NH₂OH·HCl in 0.05 mol l⁻¹ HNO₃ (v/w ratio = 40/1, 16 h extraction

time), third oxidizable step: digestion with conc. H_2O_2 at 85 °C followed by extraction with 1 mol l^{-1} ammonium acetate adjusted to pH 2.0 by conc. HNO_3 (v/w ratio = 50/1, 16 h extraction time) was applied to soil samples. The soil samples were consecutively shaken with these agents at given conditions and obtained suspensions were centrifuged (2500 g) for 20 min.

Single extraction

The soil samples were shaken with 0.5 mol l^{-1} HCl (v/w ratio = 20/1) for 1 h and obtained suspensions were centrifuged (2500 g) for 20 min.

Instrumentation

Flame atomic absorption spectrometry (FAAS) was used for determination of Ca, Cd, Cu, Fe, K, Mg, Mn, Ni, Pb and Zn using a PerkinElmer Model 1100 spectrometer (USA) with air-acetylene flame. Graphite furnace atomic absorption spectrometry (GF AAS) was used for determination of Cd, Ni and Pb at low concentration levels using a PerkinElmer Model 3030 Zeeman (USA). Inductively coupled plasma optical emission spectrometry (ICP OES) was used for determination of Al, P and some other elements using a Kontron Model Plasmakon S 35 sequential spectrometer (Germany). The concentration of Al was measured also by FAAS using a PerkinElmer Model 5000 spectrometer (USA) with nitrous oxide-acetylene flame. The concentration of As was measured by hydride generation atomic absorption spectrometry (HG AAS) using a PerkinElmer Model 1100 spectrometer (USA) equipped with an HG-2 continuous-flow hydride generator (Czech Republic) and an electrically heated quartz tube.

Results and discussion

Total concentrations of the elements

The determined total contents of macronutrients and studied risk metals concentrations in the investigated samples of topsoils and plants are given in Table 3 and Table 4. The low Ca and Mg soil contents on locality A are related with the main mineral composition of soil samples and type of the anthropogenic activity. The primary reason of low soil pH on this locality is an acid sulphatic weathering and low humus content which cause not only the degradation of these soils but the lost of meadow vegetation as well. The low pH values indirectly influence accessibility of Ca^{2+} , Mg^{2+} and K^+ ions because in exchangeable positions they are replaced by Al^{3+} ions. In case of phosphorus it can be fixed on Fe and Al in acid medium. Chemical data, which indicate important losses of exchangeable Ca, Mg and K are associated with low soil pH and increase of exchangeable Al. At soil pH < 4.5 aluminium is accumulated to root system as well as to overgrown parts and it reduces root accretion and evolution what is reflected in inhibition of the synthesis of some substances important for plant growth. In plant tissues the aluminium is bounded in organic macromolecules (proteins, polynucleotides) and it can cause the changes in polypeptides states which have the important function of plant tolerance on metal impact by so-called stress polypeptide production. The negative impact of liberated aluminium is manifested by high concentration of phytoavailable aluminium, which strongly affects the meadow ecosystem at examined study site. Original dominant grassland on this locality was replaced by grass *Festuca Rubra*, which is very resistant to extreme unfavourable properties of the environment. The total contents of Cu and Pb are slightly higher than the A limit maximum allowable concentration (MAC) values for Slovakian agricultural soils. The Dutch limits A, B and C based on background values were adopted in the definition of MAC values. The higher concentrations of Cu and Pb are connected with the occurrence of polymetallic ores in this locality. These metals and Cd, Ni, Zn as well are affecting the plant root growth and they cause the changes in plant photosynthetic apparatus namely in pigments. In the central tissues they are not localized excessively.

The low contents of Ca, K and P were determined in the soils from locality B (Table 3), which can be classified as Histo-Humic Podzol on granitic and metamorphic rocks. These naturally acid soils can contain also larger amounts of free Al, Fe and Mn. The source of this acidity originates from the process of soil podzolization, which is connected with high rainfalls, water system on this locality and acid vegetation, which decomposition products acidify whole soil profile and long-haul acid deposit

transfers as well. According to Ulrich theory the specific neutralization reactions run all in the soils are depending on ion occurrence in soil solution. By this theory it can be distinguished the buffering system of carbonates, silicates, exchangeable cations, aluminium/iron and iron. If the soil loading by acid deposits exceeds the specific buffering capacity of given system, the soil is acidified and degraded to other buffering system. In the extremely acidified stadium ($\text{pH} < 3.8$) the neutralization reactions of aluminium proceed sharing the iron hydroxides and organic complexes formation. By subsequent decrease of pH value below 3.2 the buffering reactions are shifting to the phase of neutralization reactions for iron only. The action of acids presented or incoming to the system is attenuated by the dissolving of iron oxides and releasing of Fe cations migrating in the profile. Thus the clay fraction can be destroyed, the soil life is drastically restricted and the organic matter is accumulated on the soil surface as raw humus. The organic matter fraction is represented by the living and dying off plants and animal organisms, which produce the different acid types. The important components of soil humus are the acids too. Hydrogen of their functional groups is capable of the exchangeable reactions with basic cations and thus loose hydrogen acidifies the soil solution. On the other hand the humic and fulvic acids can prevent the acidification, e.g. they generate the water insoluble Ca and Mg humates and fulvates, which keep from floating and losses of these ions from the soils. They can also create aluminium complexes and the increased content of organic matter in the soil decreases not only the exchangeable Al concentration at given pH but it decreases the total acidity as well. Metal concentrations in the upper soil horizon on locality B exceed the A limit MAC levels for Slovakian agricultural soils by 7 times for As, 28 times for Cu, 11 times for Pb, 1.3 times for Zn, the B limit MAC levels by 6 times for As, 10 times for Cu, 6 times for Pb and the C limit MAC levels by 4 times for As, 2 times for Cu and 1.5 times for Pb, respectively (Table 4). Iron exceeds the statistical value of anomalous concentration in top horizons of Slovakian soils by 1.3 times. The high accumulation of these metals in soil surface can be derived not only from natural processes but also from heavy atmospheric contamination with industrial smelting activity as well. The evidence for atmospheric pollution arises from the fact that the concentration of these metals in individual deeper soil horizons are much more lower (10-100 times).

Table 3. Selected chemical data of soil and plant samples – macronutrients content values from three replicates (mean \pm standard deviation)

Locality	Sample	Ca (mg kg^{-1})	Mg (mg kg^{-1})	K (mg kg^{-1})	P (mg kg^{-1})
A	Soil	1180 \pm 23	4020 \pm 60	19900 \pm 300	1050 \pm 32
	Grass root	919 \pm 19	632 \pm 10	1590 \pm 30	1000 \pm 31
	Grass stem	1280 \pm 15	882 \pm 12	25260 \pm 400	2403 \pm 75
B	Soil	1980 \pm 25	7300 \pm 109	2300 \pm 40	817 \pm 35
	Blueberry root	1405 \pm 22	438 \pm 8	1890 \pm 30	263 \pm 10
	Blueberry twig	8283 \pm 125	1180 \pm 10	3970 \pm 40	715 \pm 30
	Blueberry leaf	7826 \pm 120	2218 \pm 32	11070 \pm 220	964 \pm 32
	Blueberry fruit	2465 \pm 38	1240 \pm 10	11800 \pm 200	1570 \pm 62
C	Soil	20180 \pm 220	25600 \pm 400	11860 \pm 220	930 \pm 42
	Blackberry root	4590 \pm 70	1250 \pm 30	3110 \pm 50	736 \pm 38
	Blackberry twig	5900 \pm 60	1370 \pm 30	10590 \pm 220	965 \pm 35
	Blackberry leaf	12600 \pm 200	4710 \pm 60	16470 \pm 300	1395 \pm 42

Mining and dressing of the ore deposits characterized by antimonite, pyrite-pyrrhotite and arsenopyrite mineralization have significantly contributed to As, Cu, Ni, Zn and Pb soil contamination in the locality C. Concentrations of these metals exceed the A limit MAC values for Slovakian agricultural soils (6 times for As, 1.1 times for Cd, 2 times for Cu and Ni and 1.5 times for Zn) and B and C limit MAC values (6 and 3.7 times for As) but also recommended limits of contamination in this area (1.5 times for Fe). In the immediate vicinity of pyrite pile the intensive acidification is arising, however, it has only the local range. In the short distance from pile the concentration of Ca and Mg increases but the phosphorus content remains low due to high Fe content presence. The

increased concentrations of risk metals (Table 4) in the soils occurred on the locality C are the significant hazard for soil utilization by agricultural activity and close urban agglomeration as well.

Table 4. Selected chemical data of soil and plant samples – risk metals concentration values from three replicates (mean±standard deviation); ^a Maximum allowable concentration (MAC) with limits A, B and C for risk elements in top horizons of agricultural soils of Slovakia (Declaration No. 531/1994-540); data in square brackets are statistical values of anomalous concentration of elements in top horizons of Slovakian soils

Locality	Sample	Al (mg kg ⁻¹)	As (mg kg ⁻¹)	Cd (mg kg ⁻¹)	Cu (mg kg ⁻¹)	Fe (mg kg ⁻¹)
A	Soil	58950±1470	18.9±0.8	0.30±0.02	37±0.8	32730±980
	Grass root	2870±100	1.73±0.08	0.4±0.035	21.7±0.5	10740±250
	Grass stem	990±40	0.66±0.03	< 0.05	4.7±0.3	513±11
B	Soil	23430±380	195±6	0.618±0.04	1004±25	74800±1500
	Blueberry root	550±22	1.08±0.05	0.215±0.022	94.3±2.2	614±15
	Blueberry twig	200±18	1.03±0.04	0.3±0.02	12.7±0.8	146±7
	Blueberry leaf	275±22	0.91±0.04	0.242±0.025	9.73±0.8	169±5
	Blueberry fruit	51.5±3	< 0.005	< 0.05	16.1±1.1	63.7±2.3
C	Soil	52980±1500	186±4	0.854±0.05	72.3±2	87710±1580
	Blackberry root	904±36	2.47±0.12	0.844±0.055	9.2±0.7	2199±47
	Blackberry twig	411±20	1.82±0.08	0.482±0.038	5.69±0.42	463±12
	Blackberry leaf	903±42	3.74±0.11	0.4±0.035	8.1±0.66	977±20
MAC A ^a			29	0.8	36	
MAC B ^a	[103800]		30	5	100	[56200]
MAC C ^a			50	20	500	
Locality	Sample	Mn (mg kg ⁻¹)	Ni (mg kg ⁻¹)	Pb (mg kg ⁻¹)	Zn (mg kg ⁻¹)	
A	Soil	163±1.3	5.3±0.25	99.4±2.5	92.5±2.2	
	Grass root	62.9±1.1	1.7±0.07	9.6±0.62	64.5±1.6	
	Grass stem	458±5	2.45±0.08	< 2.5	29.5±0.8	
B	Soil	346±2	6.9±0.22	890±18	176±4	
	Blueberry root	303±1	0.65±0.04	125.3±3.5	64.5±2	
	Blueberry twig	1342±16	0.7±0.04	7.2±0.6	94±1.8	
	Blueberry leaf	1084±14	0.63±0.05	3.2±0.25	15.8±0.5	
C	Soil	524±16	72±2.2	48.7±1.8	210±4	
	Blackberry root	134±1	10.1±0.2	4.59±0.36	82.5±2.5	
	Blackberry twig	197±3	4.05±0.28	< 2.5	95.2±2.2	
	Blackberry leaf	807±11	7.05±0.35	< 2.5	77.5±1.6	
MAC A ^a			35	85	140	
MAC B ^a	[2230]		100	150	500	
MAC C ^a			500	600	3000	

Soil-plant metal transfer study

The soil-plant transfer coefficients were calculated from ratio of the metal total plant concentration to metal total concentration in corresponding top soil horizon where plant had grown to establish a relative sequence of analyzed metals mobility on the examined localities. The results listed in Fig. 1. are in accord with contemporary knowledge and they affirm the plant roots ability to intake the risk metals presented in exchangeable forms in soil solutions. These metals enter to the plants not only through the plant root system but also their bioaccessibility from atmospheric deposition through the overground parts, mainly plant leaves, are relatively significant. The absorption through the plant leaves is composed of two fundamental phases. The first one is nonmetabolic cuticular penetration,

which is regarded as the important way of risk metals input to the plants. The second phase is responsible for ions transport through the plasmatic membranes inwards to protoplasmic cells. Like the metals intake by root system also the metals absorption by leaves they can be transferred to another plant tissues where their excess is stored. The rate of risk metal transport among the individual tissues mostly depends on plant bodies, their age and given metal properties.

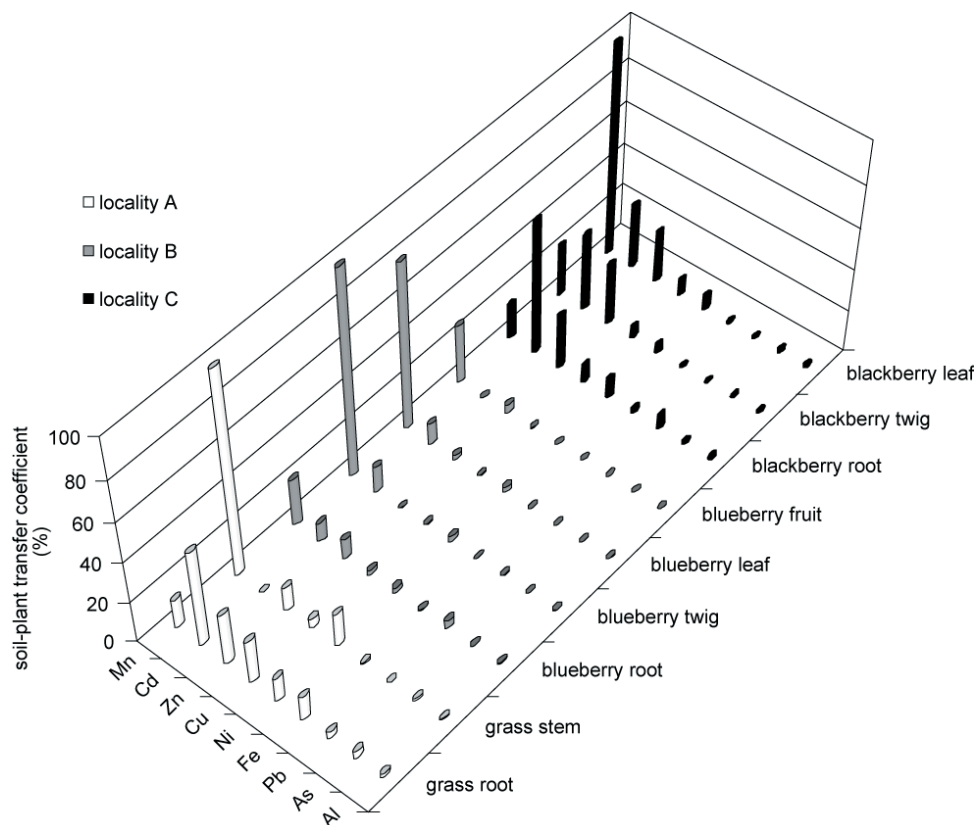


Fig. 1. Distribution of the soil-plant transfer coefficients normalized separately for each one from three sampling localities regardless of the plant part

The soil-plant transfer coefficient data normalized separately for each one from three sampling localities regardless of the plant part allow to assess the plant intake intensity, phytoavailability and phytoaccumulation of studied metals for each examined site (A, B and C) individually. The results show that Mn, Cd and Zn are the most phytoavailable from all nine studied metals in all three ecosystems. These metals are significantly absorbed and accumulated by almost all given plants and their individual parts. Manganese is characterized by the highest soil-plant transfer coefficients (normalized for 100 %) and the highest phytoaccumulation (the Mn soil-plant transfer coefficients range from 25 to 388 %) from all studied metals for all examined ecosystems. In contrast to this fact Al, As, Pb and Fe are mostly inert to the plant ability to take up these metals at given pH value in spite of the finding that both As and Pb occur in the soils on sampling sites at very high concentration levels which exceed all three limit MAC values (A, B and C) for Slovakian agricultural soils.

The extractions yield data in Fig. 2 with the first three BCR SEP steps sum and HCl extraction yields normalized separately for each one from three sampling localities regardless of the metal and the extraction procedure allow to assess the soil distribution and mobility of studied metals for each examined site (A, B and C) individually. Sums of the results obtained from first three BCR SEP steps represent so-called mobilizable fractions of given metals. These data for all studied metals except As are related to the results from dilute HCl single extraction. On the basis of extraction yields from both used procedures it can be concluded that Cd and Cu are the most mobile metal from all nine studied metals in all three ecosystems. Cadmium is characterized by the highest extraction yields of BCR SEP

mobilizable fractions (normalized for 100 %) from all studied metals for all examined ecosystems. In contrast to this fact As is mostly inert to the leaching by both used extraction methods.

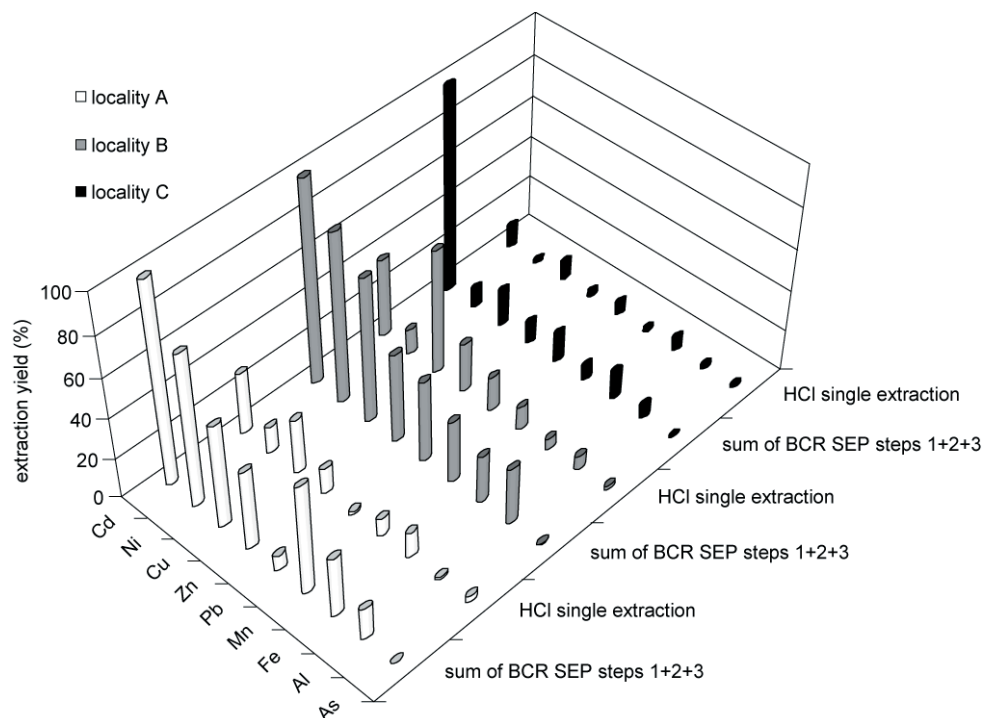


Fig. 2. Distribution of the extraction yields normalized separately for each one from three sampling localities regardless of the metal and the extraction procedure

From previous findings it is obvious that from all studied metals only cadmium has the attributes of high phytoavailability and phytoaccumulation and it simultaneously disposes of considerable soil mobility in the ecosystem as well. Since Cd is very toxic the environmental risk assessment of this metal on all three examined localities is needed under such conditions. For the other studied metals with the actual contents above the A limit MAC values (e.g. Pb in A and B localities, Zn in B and C, Ni in C and Cu in all localities, see Table 4.) the calculated transfer coefficients are lower than Cd. This fact can be explained by the lower phytoavailability and phytoaccumulation of these metals.

In certain conditions the studied plants can be remark as the bioanalytical tools for in-situ separation of phytoavailable metals species directly in the ecosystem and the calculated soil-plant transfer coefficients represent the yields of such bioseparations. They express the ratio of partial soil metal concentration separated by the plants (represented by total plant metal concentration) to total soil metal content. In this case the studied plants can be considered for the long-term extraction medium. Also the analyte phytoaccumulation can play the important role in such phytoseparations what it is reflected by the soil-plant transfer coefficients higher than 100 %. Therefore the calculated soil-plant transfer coefficients can be compared with the extraction yield data of all steps and their sums of optimized BCR SEP and single extraction by dilute HCl applied to soil samples.

In our previous work [3] the high correlation between dilute HCl extractable amounts of some metals (Al, Cu, Fe, Mn, Pb, Zn) in the soils and their amounts obtained using the sum of all three steps of BCR SEP was found. Thus the dilute HCl single extraction can supersede more labour BCR SEP. This approach can be utilized as a simple, rapid and cost-effective tool for the monitoring of contaminated areas. The presented results confirm the fitness of this procedure only for standard fractionation of these metals in soil samples but this technique is not suitable for the study of soil-plant mobility. The first BCR SEP acid extractable step is much suitable for this purpose. This fact is also

indicated by the correlation between first BCR SEP step extraction yields and soil-plant root transfer coefficients for all studied metals and the localities A and C ($R=0.7701$ and $R=0.8539$, respectively).

Conclusion

The partitioning of major and trace risk metals in acid soils contaminated by different sources by optimized BCR three-step SEP allowed to predict the relative mobility of these metals in examined ecosystems. Moreover the results from this study can be utilized for qualitative transfer metal mobility prediction in soil-plant systems on examined localities as well. The relative mobility of the considered metals can be well predicted in general when comparing the yields of the first step of BCR SEP with calculated soil-plant transfer coefficients. Based on these results it could be classified the relative mobility of studied metals in different soil systems. However for quantitative and more reliable estimation of the metal phytoavailability this approach requires to complete this study by other soil parameters.

Acknowledgements

The work was supported by Science and Technology Assistance Agency under the contracts No. APVT-20-042002, APVT-20-010204, LPP-0038-06, LPP-0188-06 and SK-CZ-0044-07, by Scientific Grant Agency of Ministry of Education of Slovak Republic and the Slovak Academy of Sciences under the contracts No. VEGA 1/3561/06, VEGA 1/4463/07 and VEGA 1/0272/08 and by Ministry of Education, Youth and Sports of Czech Republic under the contract No. MEB 080813.

References

- [1] Kubová J.: Utilization of selective extraction techniques for element speciation in soils and sediments – Critical evaluation of the contemporary state: *Slovak Geol. Mag.* 6 (2000) 43-52
- [2] Medved' J., Streško V., Kubová J., Chmielewská E.: Evaluation of atomic spectrometry methods for determination of some heavy metals in soils, soil extracts, plants and biota, *Chem. Pap.* 57 (2003) 169-171
- [3] Kubová J., Streško V., Bujdoš M., Matúš P., Medved' J.: Fractionation of various elements in CRMs and in polluted soils, *Anal. Bioanal. Chem.* 379 (2004) 108-114
- [4] Kubová J., Matúš P., Bujdoš M., Hagarová I., Medved' J.: Utilization of optimized BCR three-step sequential and dilute HCl single extraction procedures for soil-plant metal transfer predictions in contaminated lands, *Talanta* 75 (2008) 1110-1122
- [5] Bujdoš M., Diviš P., Dočekalová H., Fišera M., Hagarová I., Kubová J., Machát J., Matúš P., Medved' J., Remeteiová D., Vitoulová E.: Špeciácia, špeciálna analýza a frakcionácia chemických prvkov v životnom prostredí, Univerzita Komenského v Bratislave, Bratislava, 2008

Analysis of Cd in Must and Wine

J. Laštincová,²E. Beinrohr and ³L. Pospíšilová

Central Controlling and Testing Institute in Agriculture, Matúškova 21, 833 16 Bratislava, SK, e-mail: lastincovaj@uksup.sk

²*Slovak Technical University, Faculty of Chemical and food Technology, Radlinského 9, 812 37 Bratislava, SK*

³*Mendel University of Agriculture and Forestry, Faculty of Agronomy, Zemědělská 1, 613 00 Brno, CZ*

Abstract

Cadmium is a well-known toxic and persistent element, therefore it is very important to determine it in must and viti-vinicultural products. The must is a copy of heavy metals in soil. We were achieved that there is 21-50% of metals in grapes stem, 23-32% in the skin, 7-7.7% in seeds and 18-38% in the pulp of grape. Slovakian wines according to affiliation to vineyard regions are different from imported wines, therefore some heavy metals /Cd, Cu, Cr, Sr, Ba, Ca, Mg, Rb and V/ could be the markers of origin of the wine. Concentrations of cadmium are often determined by atomic absorption spectrophotometry (AAS), but also stripping chronopotentiometry gives good results. Chronopotentiometry is based on Faraday's law. The Cd(II) ions are electrochemically deposited from the flowing sample solution in the porous working electrode. The deposition is performed by applying a suitable potential. In the next step, the deposit is stripped Galvanostatically, whereas the stripping chronopotentiogram is recorded and evaluated. AAS determination of Cd was performed by atomic absorption spectrometer UNICAM 939/959 and calibration curve was achieved from 8 points. In this work we determined Cd in must and wine and compared results using both techniques.

Key words: *chronopotentiometry, AAS, cadmium determination*

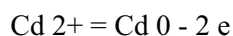
Introduction

Cadmium is a well-known toxic and persistent element, therefore it is very important to determine it in must and vitivinicultural products. There is 21-50% of heavy metals in grapes stem, 23-32 % in the skin, 7-7.7 % in seeds and 18-38 % in the pulp of grape [1-3]. It means the must contain more heavy metals than wine.

Materials and methods

Principle of stripping chronopotentiometry determination:

The Cd(II) ions are electrochemically deposited from the flowing sample solution in the porous working electrode:



The deposition is performed by applying a suitable potential. In the next step, the deposit is stripped galvanostatically, whereas the stripping chronopotentiogram is recorded and evaluated (Fig. 1).

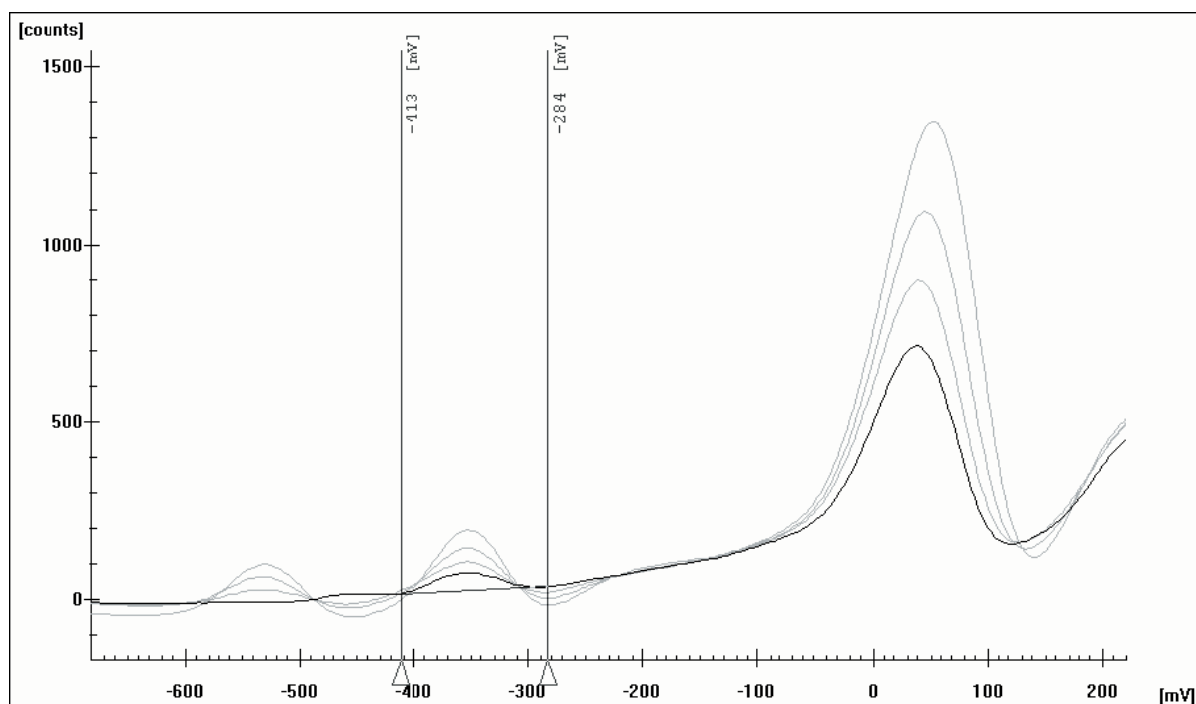


Fig. 1. Chronopotentiogram of the sample measured by making use of additions of a standard. The signals from left to the right: Cd, Pb, Cu (Grey lines are standard additions)

The potential-time dependence gives the duration of the dissolution (chronopotentiometric stripping time), which, according to Faraday's laws of electrolysis, is proportional to the analyte concentration. The compact flow system operates fully automatically, it contains computer controlled electromagnetic valves for switching either to the sample or electrolyte solution or to a standard solutions. The solutions are driven by a peristaltic pump. The heart of the system is the patented compact electrochemical cell with porous flow-through working electrode.

Solutions: R-013: Carrier electrolyte (0.1 mol/dm³ HCl) and Certified reference material: 1000 µg/dm³ Cd(II) (from Slovak Institute of Metrology).

Preparation

Add 45 ml of the electrolyte solution R-013 to 5 ml of the must sample. Heat the solution to 80-95 °C for 5-10 min and on cooling down analyse the resulting solution.

Blank solution: R-013 electrolyte solution.

ECAflow GLP 150 (ISTRAN, Bratislava)

Electrode **E56 L**

Experimental parameters:

Starting potential: -5 mA

End potential: 150 mV

Stripping current: 200 μA
Quiescence time: 10 s
Sample volume: 1 ml
Flow rate: 3 ml/min

AAS Determination

The atomic absorption spectrophotometer UNICAM 939/959 was used.

Flame: acetylen-air

Lamp: Cd

Flow rate: 1 ml/min

Cal. curve: Normal quadratic fit

Y axis: Signal high absorbance

X axis: conc. in mg/l

Equation: $y = (-3.650\text{E-}002) x^2 + (2.261\text{E-}001) x + (1.336\text{E-}003)$

X intercept: $-5.901 \text{E-}003 \text{ mg/l}$

Coef. of determination: $1.000 \text{E} + 000$

The calibration curve was achieved from 8 points and is shown in Fig. 2.

The sample was measured without dilution or special preparation only HNO_3 was added.

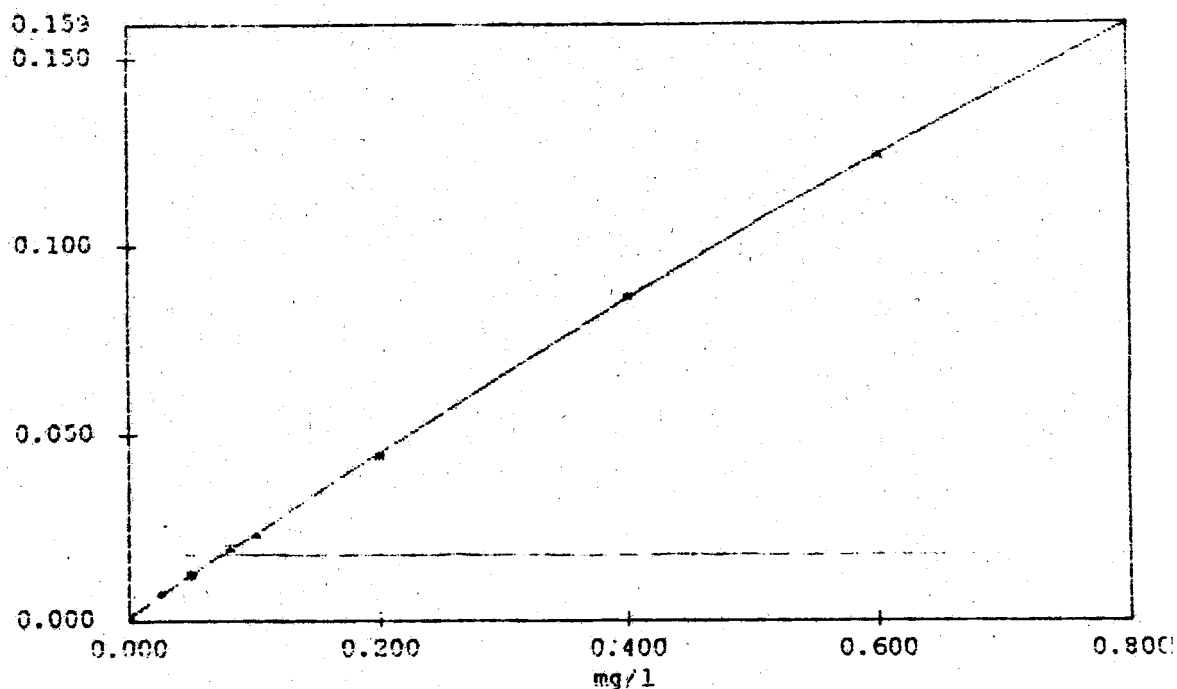


Fig. 2. The calibration curve from 8 points

Results and discussion

From this study it is evident, that in a must which is without alcohol (0.05 %vol.), has pH about 5 and has high sugar (200 g/l) could be determined Cd by both methods with good results [4]. The

objective of this study was to develop a fast and accurate procedure based on stripping chronopotentiometry to determine Cd in must and compare results with AAS technique.

The results are shown in Table 1.

Table 1. Results from determination of Cd by AAS and stripping method

must	alc%	sugar	tartaric acid	Cd-AAS	Cd-strip
1	0.07	196 g/l	5.5 g/l	0.273 mg/l	0.280 mg/l
2	0.00	204 g/l	5.6 g/l	0.305 mg/l	-
3	0.05	228 g/l	4.8 g/l	0.068 mg/l	0.058 mg/l
4	0.04	208 g/l	5.9 g/l	0.046 mg/l	0.033 mg/l
wine					
1	12.6	1.8 g/l	5.3 g/l	1.59 ug/l	1.44 ug/l
2	12.8	2.8 g/l	4.1 g/l	1.89 ug/l	1.76 ug/l
3	12.0	1.8 g/l	6.0 g/l	2.06 ug/l	1.79 ug/l
4	12.9	1.8 g/l	5.8 g/l	20.60 ug/l	20.45 ug/l

Must and wine were delivered by firm BCS Slovakia s.r.o., which is watching the heavy metals in ecosystem. Must 1, 2 and wine 1, 2 were from white grapes variety Rizling vlašský. Must 3, 4 and wine 3, 4 were from red grapes variety Frankovka modrá.

The results shows, that stripping chronopotentiometry is very useful method and concentration of cadmium in must and wine could be determine very quickly.

References

- [1] Ribéreau-Gayon P., Glories Y., Maujean A., Dubourdiou D.: Handbook of enology, Vol. 2, The Chemistry of Wine Stabilization and Treatment, 2001
- [2] Doboš A.: Štúdia optimalizácie kvality, rozšírenia a uplatnenia hrozna a jeho výrobkov vo výžive. Výskumný ústav vinohradnícky a vinársky, Matúškova 25, Bratislava, 1995
- [3] Korenovska M., Suhaj M.: Application of metals analysis on tracing the geographical origin of food. In: Book of abstracts XVIIIth Slovak spectroscopic conference, October 15-18, 2006, Spišská Nová Ves, Slovakia
- [4] Lastincova J. at al: Stripping chronopotentiometry-suitable method for determination of heavy metals in wine. In: Book of summaries XXX. world congress of vine and wine, June 10-16, 2007, Budapest, Hungaria

Biosorption and Preconcentration of Cd from Aqueous Solution by Fungal Biomass of *Aspergillus Niger* and Determination Using Flame Atomic Absorption Spectrometry Technique

¹Lenka Macháčková, ¹Mária Žemberyová, ²Alexandra Šimonovičová, ¹Jana Barteková, ¹Lenka Izakovičová, ²Lubica Janovová

¹Comenius University in Bratislava, Faculty of Natural Sciences, Department of Analytical Chemistry, Mlynská dolina CH-2, 842 15 Bratislava, Slovakia, e-mail: zemberyova@fns.uniba.sk

²Comenius University in Bratislava, Faculty of Natural Sciences, Department of Soil Science, Mlynská dolina B-2, 842 15 Bratislava, Slovakia

Abstract

Preconcentration procedures for metal quantification at low concentration levels despite recent advances in analytical instrumentation are often necessary before the determination step. Solid-liquid extraction comprises metallic species retention on an adequate sorbent with a posterior desorption by using an inorganic or organic solvent. The preconcentration procedures employing solid materials as sorbents and applied to atomic spectrometry present some advantageous characteristics, such as simplicity and higher preconcentration factors. The synthetic exchangers/ adsorbers and biological substrates are classified as the most important materials for solid-liquid extraction. In the present work the preconcentration of cadmium from aqueous solutions under laboratory conditions by fungal biomass of two strains of *Aspergillus niger* was investigated.

Key words: cadmium, biosorption, *Aspergillus Niger*, flame atomic absorption spectrometry

Introduction

In environmental sciences there is a need to develop technologies that can help by removal of toxic heavy metals found in natural waters and waste waters.

Bioadsorption is a process that utilizes inexpensive biomass to sequester toxic heavy metals and is particularly useful for removal of contaminants from industrial effluents [1,2].

In comparison with conventional methods for removing toxic metals from industrial effluents, the biosorption process offers the advantages of low operating cost and minimization of the volume of chemicals. These advantages have served as the primary incentives for developing full-scale biosorption process to clean up heavy-metal pollution. Living and dead cells of fungi are able to remove heavy metal ions from aqueous solutions. Uptake of heavy metal ions by fungal microorganisms may offer an alternative method for their removal from wastewater. Fungal biomass could serve as an economical means for removal/recovery of metal ions from aqueous solution. Fungi

as potential biomass for the removal of heavy metals from aqueous solutions have already been studied [3,4], but little is known on the removal of cadmium from aqueous solutions using the fungal *Aspergillus niger*, which are applied in a variety of industrial fermentation processes, such as citric acid production. Cadmium pollution is considered a serious health hazard.

In the present work the removal of cadmium from aqueous solutions under laboratory conditions by fungal biomass of two strains of *Aspergillus niger* was investigated. Various parameters such as pH of the solutions, different initial cadmium concentrations, time of accumulation have been studied. Some experiments were performed for comparison of batch and dynamic equilibrium studies for accumulation of cadmium from waters.

Experimental

Two strains of genus *Aspergillus niger* were studied. Strain AN1 (control strain) was isolated from Eutric Fluvisols FMm (pH H₂O/KCl 7.7/7.4) in the region of Gabčíkovo. Strain AN3 was isolated from the stream sediment of river Blatina (pH H₂O/KCl 5.27/4.8) in the region of Pezinok-Kolársky hill with very intensive mine activities. Both strains were cultivated during 14 days on solid Sabouraud Maltose Agar medium (HiMedia, Bombay). After 14 days cultivation conidia-spores in volume of 5 ml of both strains AN1 and AN3 were added to 45 ml liquid Sabouraud media (glucose 40 g, mycological peptone 10 g, H₂O 1000 ml). Mycelia were grown 14 days by T = 25 °C. Fungi mycelia in the sporulation phase of the growth were filtered off and pre-washed with H₂O (Water Pro LS, Labconco, USA). Subsequently they were put in 50 ml of water solution with Cd (citrate buffer solution with Cd, citric acid solution with Cd). Treatment was done by T = 25 °C.

The dried mycelium after accumulation of Cd was decomposed by HNO₃ and H₂O₂ using microwave oven and filled up to the appropriate volume with deionized water. The concentration of Cd was measured by flame atomic absorption spectrometry (FAAS).

A Perkin-Elmer flame atomic absorption spectrometer 1100B with air-acetylene flame (acetylene flow rate of 2.5 l/min, air flow rate of 8.0 l/min) was used to determine cadmium content in mycelium and SAB medium. Hollow cathode lamp for cadmium (lamp current 4 mA), spectral band pass of 0.7 nm was selected to isolate the 228.7 nm line.

Results and discussion

Solid – liquid extraction by biological substrates

Biological substrates such as bacteria, algae and fungus are materials able to accumulate metals from aqueous solutions through the biosorption process. The utilization of microbial cells with combination of sensitive and selective atomic spectrometry techniques used for metal determination is very important from the environmental analytical chemistry point of view for metal preconcentration purposes [5].

When this process takes place on the cellular membrane, it can mainly be considered as adsorptive, because no biological activity is present. Otherwise, when live cells are used, the metallic species are firstly adsorbed on a cellular membrane and after passing through this membrane, they are absorbed into the structure. There are evidences that some phenomena such as absorption, cationic exchange, chelating take place in cellular membranes of microorganisms. The groups responsible for the adsorption processes are found from biomolecules, which contain sulphates, carboxylates and phosphates [6] in their structure.

Fungal biosorption largely depends on parameters such as pH, metal ion and biomass concentration, physical or chemical pre-treatment of biomass, presence of various ligands in solution, and to a limited extent on temperature. Fungal biosorption performs well in comparison to sorption on

commercial ion-exchange resins, activated carbon, and metal oxides. Limited data indicate the potential for regenerating the biomass. The cell-wall fraction of biomass plays an important role in the sorption of heavy metals. The mechanisms of biosorption are understood only to a limited extent [7].

In order to establish the effect of pH on the biosorption of cadmium ions, the batch equilibrium studies at different pH values were repeated in the range of approximately 2.0-7.0. The effect of pH is shown on Fig. 1. The optimal pH of cadmium accumulation by fungal mycelia of strains AN1 and AN3 was observed at pH 7.0 and 3.0, respectively.

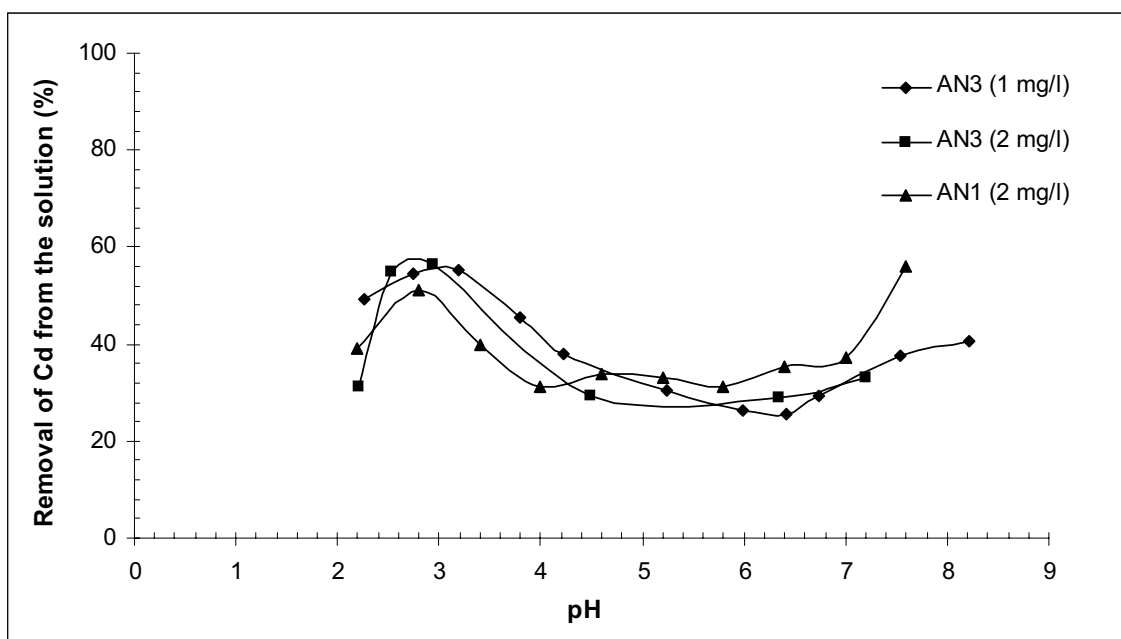


Fig. 1. The study of pH effect on the accumulation of Cd (in %) using the fungus *Aspergillus niger*

The relationship between the initial ion concentrations in the solution and cadmium ions accumulated in the biomass can be seen from Fig. 2.

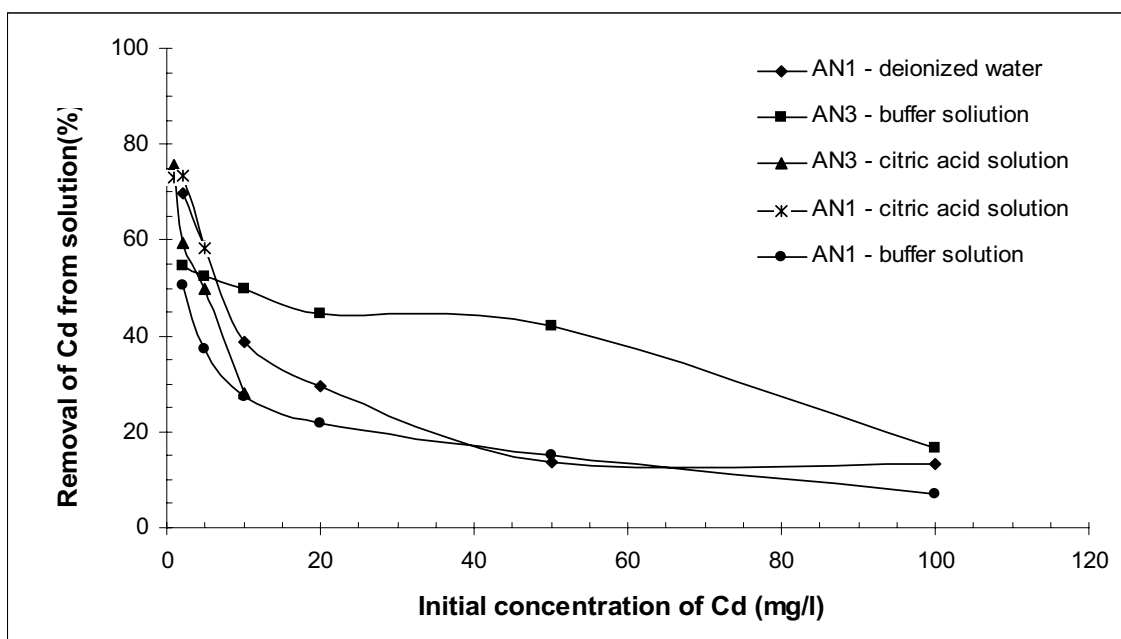


Fig. 2. The study of initial concentration of Cd on the accumulation of Cd using the fungus *Aspergillus Niger*

An attempt was made to use the biosorbent in a batch and dynamic arrangement and to study the effect of the time to reach the equilibrium Fig. 3. The time 24 hours was used for all further experiments.

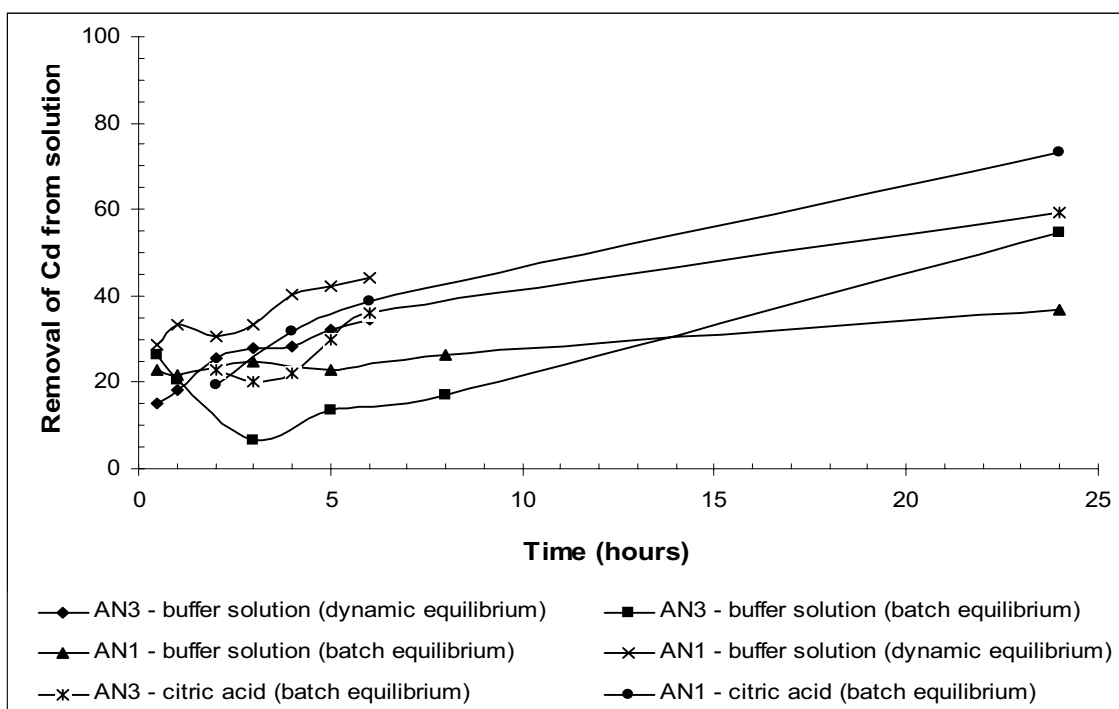


Fig. 3. The study of the time effect on the accumulation of Cd

Both strains of *Aspergillus niger*, AN1 and AN3 are capable to accumulate cadmium from water solutions. The selected strains of *Aspergillus niger*, isolated from two various types of environment, not contaminated AN1 and contaminated AN3, were studied in model water solutions from the point of view of the possibility of accumulation and preconcentration of Cd. The digests of dry mycelium samples after microwave decomposition were used for determination of cadmium preconcentrated in the biomass. The flame atomic absorption technique was used for the determination of cadmium concentration to study cadmium bio-accumulation. The results are given in Table 1.

Table 1. The results of Cd after preconcentration using two Strains of *Aspergillus niger* AN1 and AN3

Strain of <i>Aspergillus niger</i>	Preconcentration factor	Theoretical concentration of cadmium (mg/l)	Determined cadmium concentration					
			Dynamic procedure			Batch procedure		
			Cal. curve method (mg/l)	s (mg/l)	Recovery (%)	Cal. curve method (mg/l)	s (mg/l)	Recovery (%)
AN1	10	2	1.36	0.305	58.8	0.622	0.026	31.1
	20	2	0.735	0.060	36.7	0.395	0.013	19.8
	50	1	0.325	0.018	32.5	0.184	0.018	18.4
AN3	10	2	0.915	0.034	45.8	0.574	0.057	28.7
	20	2	0.729	0.078	36.5	0.374	0.025	18.7
	50	1	0.477	0.015	47.7	0.302	0.024	30.2

Conclusions

The removal of Cd from aqueous solution was approximately to 60 %. With higher cadmium concentrations, the removal efficiency was lower. The potential of fungal biomass as sorbents is indicated by the obtained data, and more research and development of the fungal biosorption technology is recommended.

Acknowledgement

Financial support from the Scientific Grant Agency of the Ministry of Education of the Slovak Republic VEGA 1/0430/08 and VEGA 1/0159/08 is highly acknowledged.

References

- [1] Volesky B.: Bioadsorption of heavy metals. CRC Press, Boca Raton, Florida, 1990
- [2] Richard F.U., Shuttleworth K.L.: Microbial mobilization and immobilization of heavy metals, *Curr. Opin. Biotechnol.*, 1996, 7, 307-310
- [3] Volesky B., Holan Z.R.: Biosorptions of heavy metals, *Biotechnol. Prog.*, 1995, 11, 235-250
- [4] Jianlong W., Xinmin Z., Decai D., Ding Z.: Bioadsorption of lead(II) from aqueous solution by fungal biomass of *Aspergillus niger*, *J. of Biotechnol.*, 2001, 87, 273-277
- [5] Pereira M.G., Arruda M.A.Z.: Trends in preconcentration procedures for metal determination using atomic spectrometry techniques, *Microchim. Acta*, 2003, 141, 115-131
- [6] Senthilkumaar S., Bharathi S., Nithyanandhi D., Subburam V.: Biosorption of toxic heavy metals from aqueous solutions, *Bioresource Technol.*, 2000, 75, 163-165
- [7] Kapoor A., Viraraghavan T.: Fungal biosorption — an alternative treatment option for heavy metal bearing wastewaters: a review, *Bioresource Technol.*, 1995, 53, 195-206

Content of Arsenic in the Fish Muscle from Intensive Breeding

¹Blanka Macharáčková, ¹Čelechovská Olga, ²Vítoulová Eva

¹ University of Veterinary and Pharmaceutical Sciences, Faculty of Veterinary Hygiene and Ecology, Department of Biochemistry, Chemistry and Biophysics, Palackého 1-3, 612 42 Brno, Czech Republic

² University of Technology, Faculty of Chemistry, Brno, Department of Food Chemistry and Biotechnologies, Purkyňova 118, 612 00 Brno, Czech Republic

Abstract

The objective of this study was to determine the total arsenic and the species of arsenic in the Rainbow Trout muscle (*Oncorhynchus mykiss*). Samples were mineralized before determination of the total arsenic by the method of AAS by wet way, then burned in a muffle furnace and reduced to As^{III} by addition of KI in the ascorbic acid. For extraction of the arsenic species, the ultrapure deionized water was used. Total arsenic was determined by hydride method of HG-AAS, species of arsenic were determined by method, which includes the combination of the method of highly effective liquid chromatography, hydrides generation and atomic fluorescence spectrometry (HPLC-HG-AFS). Concentrations of arsenic in the fish muscle were very low, they met the limit valid for the Czech Republic, which is stipulated by the Decree 53/2002 of the Code. Arsenobetain was detected by a method of HPLC-HG-AFS.

Key words: arsenic, arsenobetain, rainbow trout, hydride generation, atomic absorption spectrometry

Introduction

An increase in metal concentrations in the environment is due primarily to erosion and anthropogenic activities, and because metals are very persistent pollutants, they get accumulated in the soil, water sediments and in the food chain [1]. In marketed fish, all factors having impact on the total arsenic levels in the tissues of fish are impossible to determine. One of the factors is the action of physical and chemical properties of water on arsenic accumulation or excretion. Furthermore, it is also impossible to determine the volume of feed consumed by the fish in order to prove that arsenic in marketed fish depends only on this given volume. Neither fish growth is linear. It depends on the season of the year. In the winter, fish growth is significantly slowed down, which is determined by the water temperature [2]. Owing to the fact that there is an increased arsenic content arising from the scrap cake in the fish from the intensive breeding, the samples of feed were analysed as well.

Materials a methods

Arsenic was established in a homogenate of the rainbow trout bodies (*Oncorhynchus mykiss*) from the Kružberk area, in fish 2 to 6 months old and in feedstuff samples. The total content of arsenic in the Rainbow trout muscle was determined by hydride method of HG-AAS. Samples were mineralized before determination of the total arsenic by the method of AAS by wet way (nitric acid 1:1 with hydrogen peroxide), then burned in a muffle furnace and reduced to As^{III} by addition of KI in the ascorbic acid. The measurement validity was tested by certified standard material Dorm-2 (dogfish muscle), which consists of $18.0 \pm 1.1 \mu\text{g}\cdot\text{g}^{-1}\text{As}$.

Species of arsenic were determined by method, which includes the combination of the method of highly effective liquid chromatography, hydrides generation and atomic fluorescence spectrometry (HPLC-HG-AFS). As mobile phase, 10 mM phosphate buffer $\text{K}_2\text{HPO}_4/\text{KH}_2\text{PO}_4$, pH 6.1 was used. Oxidising agent was provided for by the solution of a 1 % concentration $\text{K}_2\text{S}_2\text{O}_8$ in 1 % NaOH.

Results a discussion

Standard arsenate solutions in the concentration of $0.25 - 8.0 \mu\text{g}\cdot\text{l}^{-1}$ were used to create the calibration curve. The calibration curve had a detection limit of $0.187 \mu\text{g}\cdot\text{l}^{-1}$ and quantification limit of $0.703 \mu\text{g}\cdot\text{l}^{-1}$. Arsenic levels established by continuous hydride generation method in a quartz cell ranged in fish body homogenate in an interval of from $0.215 \pm 0.0004 \text{ mg}\cdot\text{kg}^{-1}$ to $1.040 \pm 0.0280 \text{ mg}\cdot\text{kg}^{-1}$. Total arsenic levels in sample fish body homogenate in fish of 6 months of age exceeded the applicable limit, which is provided for by the Decree No. 53/2002 Coll. where the highest tolerable arsenic level for freshwater fish is $1 \text{ mg}\cdot\text{kg}^{-1}$.

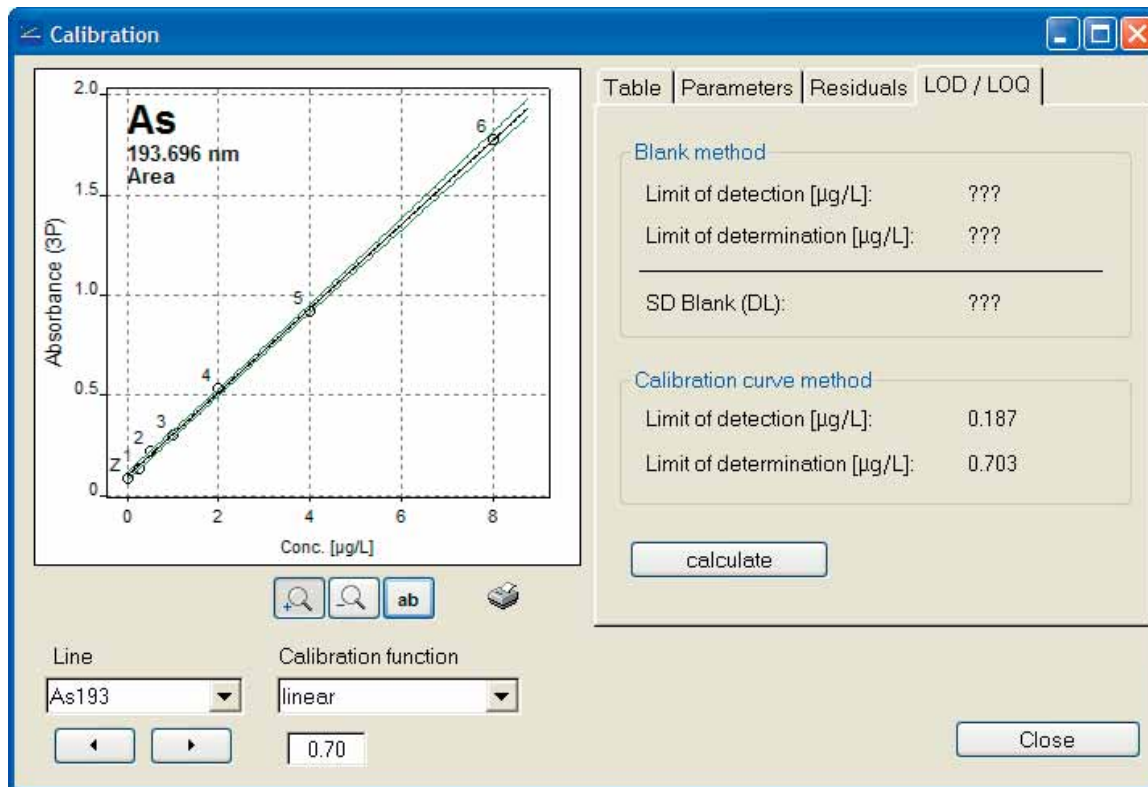


Fig. 1. Calibration curve of the continuous HG-AAS on a graphite cell

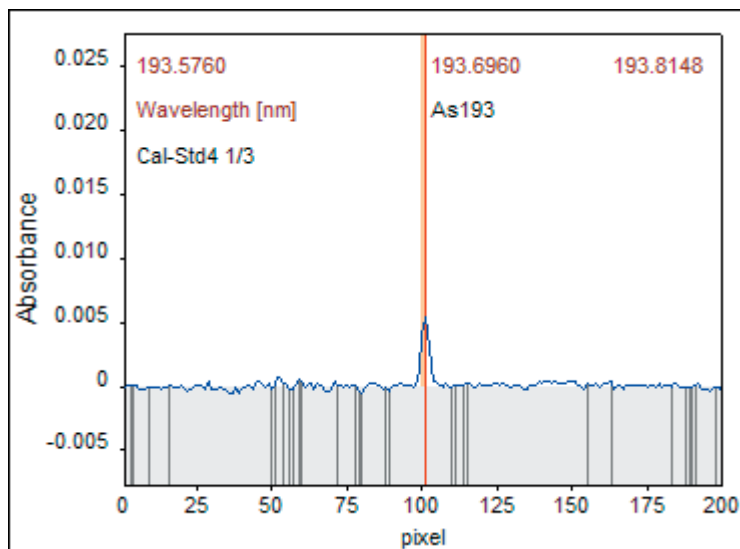


Fig. 2. Calibration standard atomization spectrum data

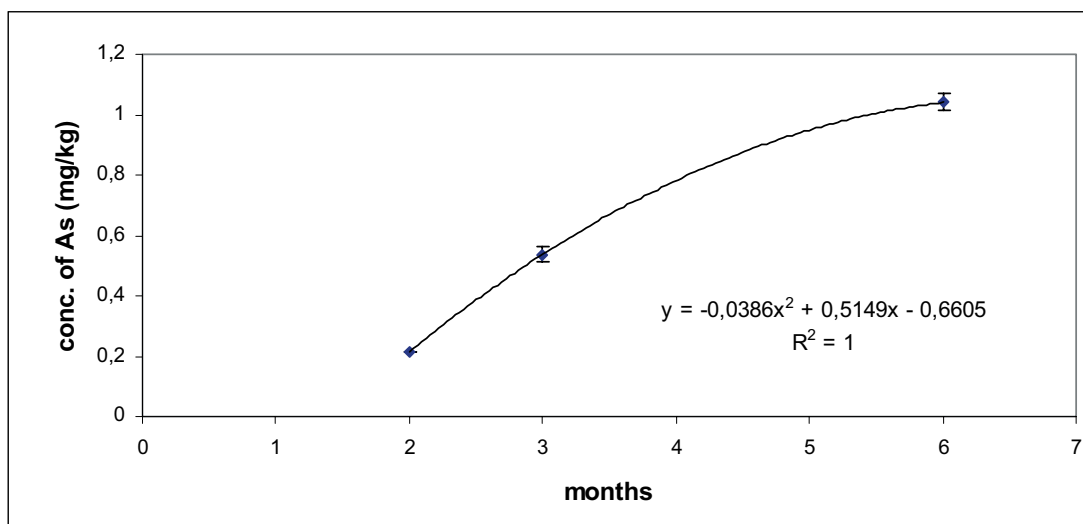


Fig. 3. Arsenic concentration curve in the fish homogenate

Total arsenic levels in the feedstuff used also failed to meet the hygienic feedstuff quality requirements, which are provided by the Decree No. 184/2004 Coll. The applicable limit for arsenic in whole feedstuffs is 2 mg.kg^{-1} . The value of arsenic content was twice as big in the Bio-Optimal START feed from the producer Biomar A/S, namely $4.130 \pm 0.0668 \text{ mg.kg}^{-1}$. With regard to this fact, an assumption can be made that arsenic levels in fish body homogenate depend on the arsenic levels in the feedstuffs.

HPLC-HG-AFS was used to determine the arsenic species. Standard arsenobetaine solution in the concentration of $25\text{-}250 \text{ }\mu\text{g.l}^{-1}$ was used to create a calibration curve. The detection limit of arsenobetaine was established as 3 S/N (signal/noise ratio): $3.393 \text{ }\mu\text{g.l}^{-1}$. The quantification limit (10 S/N) was $11.309 \text{ }\mu\text{g.l}^{-1}$.

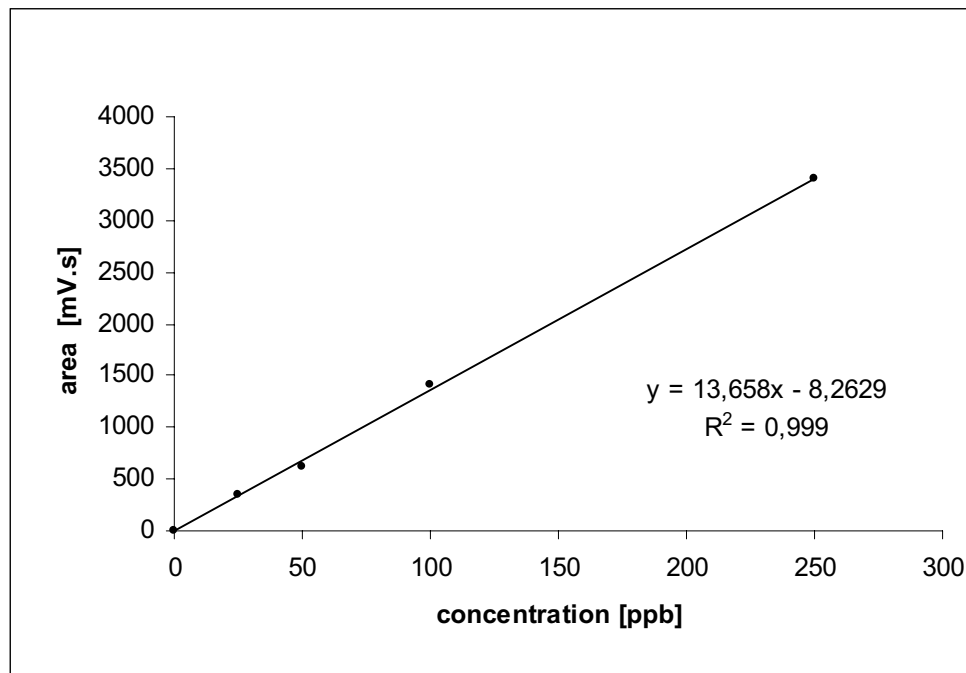


Fig. 4. HPLC-HG-AFS Calibration curve

Arsenobetaine levels ranged in the intervals of 0.096 ± 0.0031 to 0.292 ± 0.0243 mg.kg^{-1} . Arsenobetaine share in total arsenic was 35.16 % in rainbow trout homogenate of the age of 2 months, at 22.24 % in 3 months old homogenate and at 25.84 % in homogenate of 6 months of age. It can be assumed that fish up to the ages of 6 months need not have a well developed arsenic metabolism to be able to transform the inorganic form of arsenic onto a non-toxic organic form.

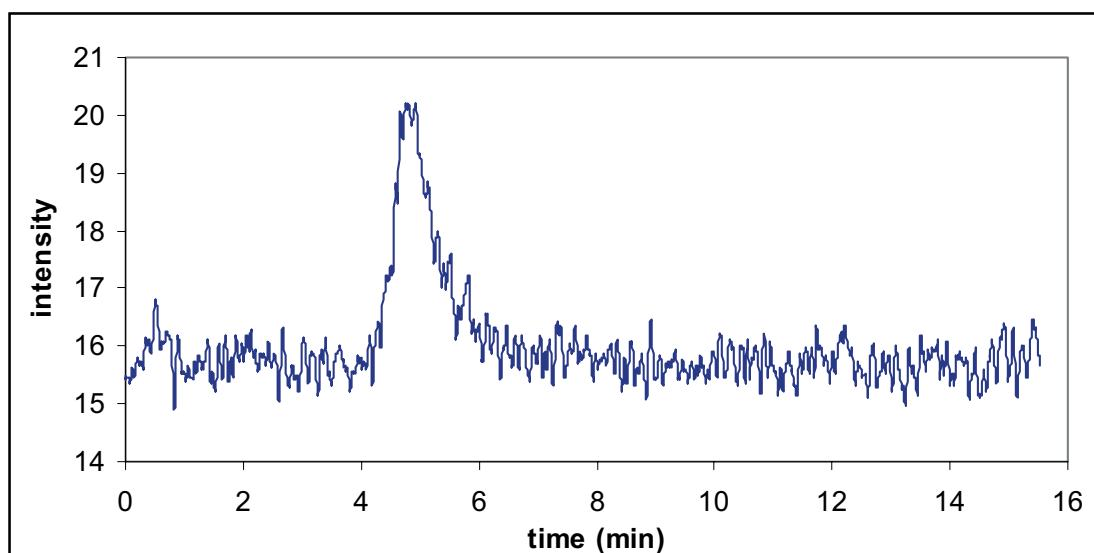


Fig. 5. Arsenobetaine chromatogram data – body homogenate sample

Conclusions

Arsenic was established in rainbow trout body homogenate and in feedstuff samples. Total arsenic levels in the feedstuffs used also failed to meet the requirements for hygienic feedstuff quality. In samples of rainbow trout body homogenate aged 6 months, the limit for total arsenic levels, provided for by the Decree No. 53/2002 Coll., was exceeded. Because the samples contained arsenobetaine, which is considered to be a non-toxic organic form, we cannot consider slight excess in the limit of total arsenic levels as a serious hygienic risk.

References

- [1] Cornelis R., Caruso J., Crews H., Heumann K.: Handbook of Elemental Speciation II. Species in the environment, food, medicine and occupational health. Wiley, Chichester, England, 2005
- [2] Svobodová, Z., Čelechovská, O., Máchová, J., Randák, T.: Content of arsenic in market-ready rainbow trout (*Oncorhynchus mykiss*). Acta Vet Brno, 2002b, 71, 361-367

The project was financed from the research plan No. MSM 6215712402.

FT Raman and Infrared Spectra of Coniferous Needles: What Effects can be Elucidated?

**Pavel Matějka,²Libor Mrnka, Stanislava Procházková, Martin Člupek,
Helena Tokárová, Karel Volka**

*Institute of Chemical Technology, Dept. of Analytical Chemistry, Technická 5, 166 28 Prague 6 – Dejvice, Czech Republic;
e-mail: pavel.matejka@gmail.com*

²*Institute of Botany ASCZ, Dept. of Mycorrhizal Symbioses, Zámek 1, Průhonice, 252 43, Czech Republic*

Abstract

FT Raman spectroscopy is a method that makes possible analyses of coniferous needles performed both *in vitro* and *in vivo*. Infrared spectrometry using ATR technique allows analysis of a surface layer of needles. In the past few years thousands of vibrational spectra of coniferous needles collected in specifically designed series of experiments were evaluated using various chemometric methods to elucidate the variability of several spectral features, e.g. the shape of the background, bands of waxes, water and carotenoids. Some mathematical pre-processing procedures were tested. The relation of spectral changes to various natural (model) factors was studied. Generally, the spectral information can be related to the state of health of needles. Various natural and anthropogenic effects can be discriminated in real conditions based on results of many model experiments.

Key words: *conifer, Raman spectroscopy, infrared spectrometry, solar simulation, soil fungi, principal component analysis, cluster analysis*

Introduction

Norway spruce (*Picea abies* (L.) Karst.) and silver fir (*Abies alba* Mill.) trees dominate European forest ecosystems from Pyrenees to Carpathians, and from north of Greece to the Arctic in Norway. Both survival and performance of coniferous trees strongly depend on many natural and anthropogenic factors of the ecosystems. Plant needles can be used as a bioindicator of environmental pollution. They serve not only as natural samplers of air pollutants but the changes of their surface micromorphology and of their chemical composition can be correlated with an environmental stress of the vegetation. The main problem of bioindicator analysis is to distinguish the natural factors, the anthropogenic influences and the effects of the analysis itself [1]. Hence, well-designed laboratory model experiments are essential to explain reliably data obtained from natural samples. Various analytical methods can be applied to analyze samples of needles; spectral analysis represents a possibility to obtain information relatively fast and without tedious laboratory work.

Fourier transform (FT) Raman spectroscopy is a method that allows possible non-destructive analysis of Norway spruce needles carried out both *in vitro* and *in vivo* [1]. Two near-to-surface layers of needles, i.e. epidermis with cuticular waxes and mesophyll with chloroplasts can be analyzed. A study of Norway spruce needles by attenuated total reflection (ATR) technique in mid-infrared range [4] has already been reported; chemical composition of the surface waxy layer can be described based

on the Fourier transform infrared (FT IR) spectra obtained. Several series of spectroscopic experiments were performed on needles taken from trees of various forest areas of the Czech Republic. Two types of pot experiments modelling natural factors are briefly described in this study.

Firstly, the effects of several ecologically relevant groups of soil fungi on FT Raman spectral variation are demonstrated. Soil fungi are the primary decomposers of the organic matter in forests, and are uniquely able to break down and release nutrients. Nutrition is one of the key factors affecting health of trees. Various types of soil fungi are essential for nutrient recycling in the ecosystem. Root colonisation by mycorrhizal fungi can considerably affect the growth and health of host plants that benefit e.g. from improved nutrient uptake, higher resistance to drought, heavy metals or pathogens. Saprotrophic fungi convert dead organic material into fungal biomass and small molecules. These fungi release the locked-up nutrients that can then be used by other living organisms, making the fungi vital to the health of terrestrial ecosystems. Nevertheless, the interaction of soil filamentous fungi can substantially affect belowground processes, e.g. the competition of the mycelia of mycorrhizal and saprotrophic fungi for nutrition sources influences the physiology of the mycorrhizal tree hosts. The nutrition conditions of the host tree should be related to the status of needles monitored by means of vibrational spectroscopy.

Secondly, the influences of simulated solar irradiation on both Raman and infrared spectral changes are shown. Solar radiation is an important environmental factor that significantly affects growth and development of green plants. Photosynthetic pigments present in chloroplast capture the light energy necessary for photosynthesis. Two main groups of photosynthetic pigments of green plants are chlorophylls and carotenoids. In photosynthetic organisms, carotenoids play two vital roles in the chloroplasts; they either participate in the energy-transfer process, or protect the photosynthetic reaction centre from auto-oxidation. The bands of carotenoids are better pronounced in FT Raman spectra of needles than the spectral features of chlorophylls.

Finally, an overview of key results of both studies is given and some general consequences are drawn. Chemical information on three key components of needles, i.e. cuticular waxes, chloroplast pigments and water, can be obtained from vibrational spectra. The physiological role of these needle components in photosynthesis, transpiration and protection against external attacks, is crucial for the whole trees. Thus we demonstrate that the health state of trees can be estimated from the analysis of vibrational spectra of corresponding needles.

Materials, sample preparation a experiment setup

Ex vitro cultivated Norway spruce (*Picea abies* (L.) Karst.) seedlings inoculated by soil filamentous fungi were used to obtain vibrational spectral data on the effect of soil fungi. Uncontaminated, aseptically on agar media germinated spruce seedlings of similar size were transferred into two-compartment pot cultivation systems. The pot systems consisted of root and needle compartments separated by nylon membrane (pore size 42 µm). The membrane was used to prevent growth of spruce roots into needle compartment but to allow growth of fungal hyphae between compartments. Root compartment was filled with the mixture of perlite, peat and sterilized fallen spruce needles, while needle compartment consisted of sterilized fallen spruce needles. Representatives of three ecological groups of fungi (saprotrophic, mycorrhizal and endophytic) were used for inoculation either individually or in combination of two fungal strains from different groups (details including variant codes are given in Table 1). Each of ten variants consisted of twelve seedlings in six pots (2 seedlings per pot). Systems were cultivated under uniform conditions in a growing chamber (18/6h light/dark cycle at 21/15 °C and 80 % relative humidity) for ca. six months. At the harvest two fresh needles were cut from each of the seedlings and FT Raman spectra were recorded as described below. Totally, 240 spectra (24 spectra per variant) were recorded and evaluated together for the pot experiment. Finally, a set of 24 spectra of needles taken from natural seedlings sampled at Šumava Mountains was co-added to perform comparative spectral and chemometric analyses.

Table 1. Description of the experimental variants with inoculated fungi

Variant code	Inoculated fungi		Fungal ecological group
	Root compartment	Needle compartment	
K	None	None	None
S	None	<i>Setulipes androsaceus</i>	Saprotrophic
M1	<i>Serpula himantoides</i>	None	Saprotrophic
M1S	<i>Serpula himantoides</i>	<i>Setulipes androsaceus</i>	Saprotrophic
M2	<i>Hebeloma bryogenes</i>	None	Ectomycorrhizal
M2S	<i>Hebeloma bryogenes</i>	<i>Setulipes androsaceus</i>	Ectomycorrhizal and saprotrophic
E2	<i>Cadophora finlandica</i>	None	Ectomycorrhizal/ericoid
E2S	<i>Cadophora finlandica</i>	<i>Setulipes androsaceus</i>	Ectomycorrhizal/ericoid and saprotrophic
E1	<i>Phialocephala fortinii</i>	None	Endophytic
E1S	<i>Phialocephala fortinii</i>	<i>Setulipes androsaceus</i>	Endophytic and saprotrophic

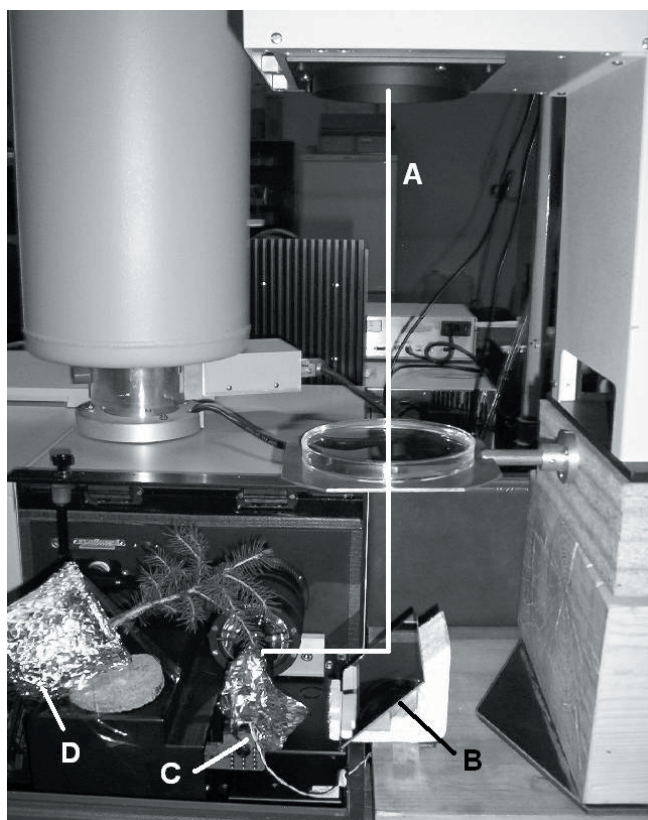


Fig. 1: Irradiation setup - fixation of a coniferous seedling into the sample compartment of the FT Raman spectrometer under conditions of solar simulation experiment

- A – path of solar beam
- B – planar mirror
- C – connection of a contact temperature sensor
- D – protection of trees rootage in a pot against desiccation and overheating

Small three-year-old seedlings of Norway spruce tree and fir tree cultivated in pots under laboratory conditions were used for study of spectral changes caused by simulated solar radiation. Living seedlings were irradiated by output beam of solar simulator 91193 (Oriël) fitted with 300 W xenon arc lamp and two optical filters Air Mass 0 (AM0) and Air Mass 1D (AM1D). The irradiation power at the seedling position was equivalent to ~1 sun. The irradiation sequence was adjusted using digital timer 68945 (Oriël). Surrounding conditions in laboratory during an experiment were monitored using a set of sensors and devices (Greisinger electronic) to measure values of laboratory

temperature (TFS0100E), air humidity (TFS0100E), absolute pressure (GMH3180-12) and air oxygen content (GOO369, GMH3691). Temperature values in the course of irradiation and spectral data accumulation were acquired directly on the spectrally-analyzed needle using a contact temperature sensor (GTF300) connected to the device GMH3350 (Greisinger electronic). Data from the sensors were recorded on-line on a PC using the software EBS9M (Greisinger electronic). Every individual experiment was performed in four days. A living seedling in a pot (spruce or fir tree) was fastened in Raman sample compartment all the experiment time. Tree rootage in the pot was protected against desiccation and heating using polyethylene wrapping and aluminium foil. Single needle (examined needle) of a lateral branch of the sample tree was fixed into transparent holder (made of acrylic glass) in front of the Raman optics. The simulated solar beam was redirected from vertical direction to lateral side of the fixed needle using reflection on the planar mirror placed under the 45° angle (Fig. 1). The needle (and at-least the whole corresponding branch) was irradiated by simulated solar radiation every day three times for 30 min with 60 min relaxation pause between two consecutive irradiation periods (i.e., the total irradiation time was 90 min per day). Prior every irradiation period and after the last one, Raman/infrared spectra of the needle were recorded (as described below).

Experimental

FT Raman spectra were collected using a Fourier transform near-infrared (FT-NIR) spectrometer Equinox 55/S with FT-Raman module FRA 106/S (Bruker). The selected needle was irradiated by the focused laser beam with a laser power 50 mW of Nd:YAG laser (1064 nm, Coherent). The scattered light was collected in the backscattering geometry. A quartz beamsplitter and Ge detector (liquid N₂ cooled) were used to obtain interferograms. 1024 scans were accumulated for every individual spectrum of a needle from its opposite sides as previously described [2]. Thus two spectra per needle were recorded. A standard 4 cm⁻¹ spectral resolution, 'zero filling' 8 and Blackmann-Harris cosine apodization function were used for all data accumulation and Fourier transform processing. The spectra acquired using software package OPUS (Bruker, Germany) were exported to JCAMP-DX format for chemometric evaluation.

FT IR spectra were recorded using a Fourier transform infrared spectrometer Nicolet Nexus 670 (Thermo Scientific). A horizontal single bounce ATR accessory with ZnSe crystal (MIRACLE™) was used for the measurement of a selected needle as previously described [4]. A perfect optical contact of the needle surface was ensured gently by using a pressure device controlled via a micrometry screw. 64 interferograms were taken for every spectrum with a resolution of 4 cm⁻¹ using OMNIC (Thermo Scientific) software. FTIR spectra were exported to JCAMP-DX format. Repeated measurements were carried out at the tip and the base of every needle both on the top and bottom side. Hence, four spectra were obtained per needle.

Micro-images of needle surface were recorded with objectives 10x and 20x (Nikon) using optical microscope Optiphot 2 (Nikon). The microscope was equipped with a color CCD camera (Sony). The camera was connected directly to PCI TV card (TV Capturer) inserted in standard personal computer. The software TVIEW98 was used to obtain and to save micro-images.

The Uncrambler 9.2 (Camo, Norway) software was used for statistical and chemometric data evaluation including principal component analysis (PCA). OPUS (Bruker) was used to perform cluster analysis. OMNIC and Macros Basic (Thermo Scientific) were used for peak area calculation. A previously described filter setup for background correction [5] was tested.

Results and discussion

Apparent variations of intensities of many bands were observed among the FT Raman spectra of different variants of inoculation (Fig. 2). The strongest bands of carotenoids were observed for both

mycorrhizal variants (M2, E2). The combination of mycorrhizal and saprotrophic fungi causes an apparent decrease of the carotenoid bands. Relatively intense bands of waxes were characteristic for endophytic variant and for inoculation of saprotrophic fungi in outer needle compartment (S).

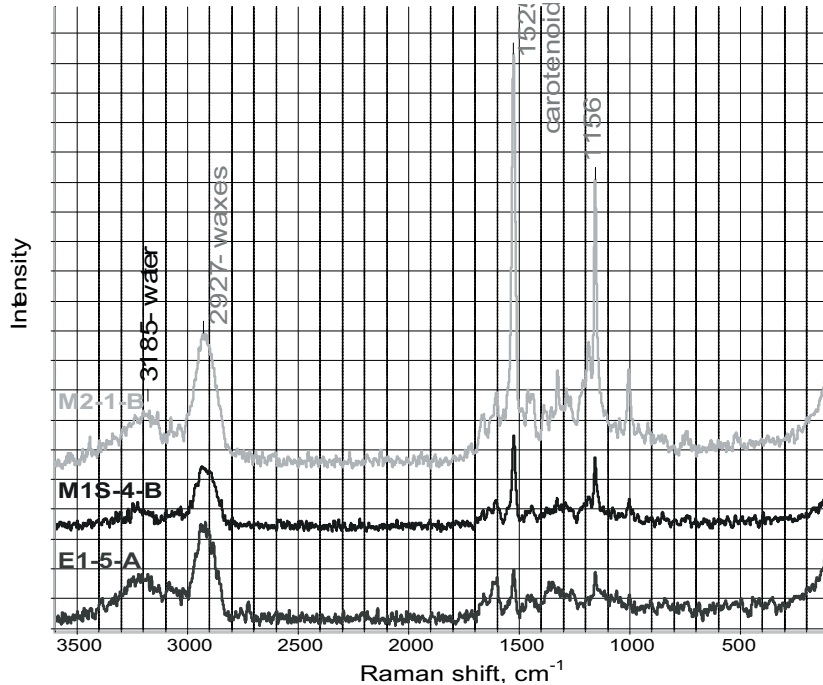


Fig. 2: Examples of individual FT Raman spectra

E1 for endophytic variant

M1S for combination of two saprotrophic fungi

M2 for mycorrhizal variant

Characteristic bands of water, waxes and carotenoids are marked

The importance of variation of bands of waxes and carotenoids is evident from the results of PCA analysis. The X-loading graphs for principal component PC1 and PC2 (Fig. 3) demonstrate the importance of variation of “waxy” bands along PC1, while the “carotenoid” bands are contributing to the data structure mainly along PC2.

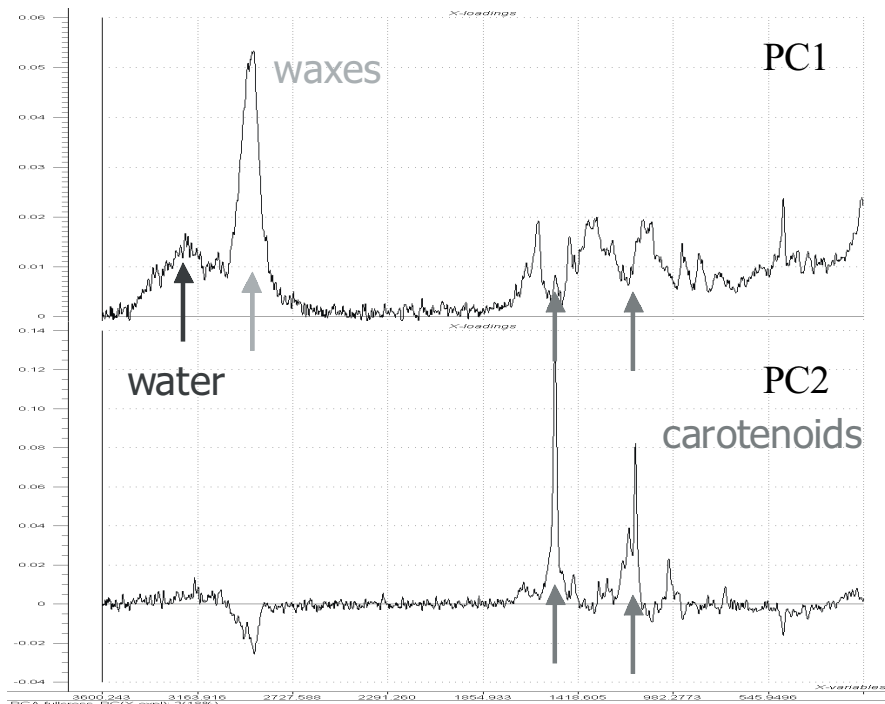


Fig. 3: X-loadings graph

PCA analysis of Raman spectral data obtained for various variants of fungi inoculated

Characteristic bands of water, waxes and carotenoids are marked

The models of individual variants are well differentiated in the plane given by PC1 and PC2 (Fig. 4). Both mycorrhizal variants (E2, M2) are located in the quadrant of positive values of both PC1 and PC2. The combinations of mycorrhizal and saprotrophic fungi (E2S, M2S) are observed in the quadrant of negative values of PC1, while the values of PC2 are positive. All the other variants are characterized by negative values of PC2. Hence, the “carotenoid” bands play the key role for describing a substantial effect of mycorrhizal fungi on the seedlings.

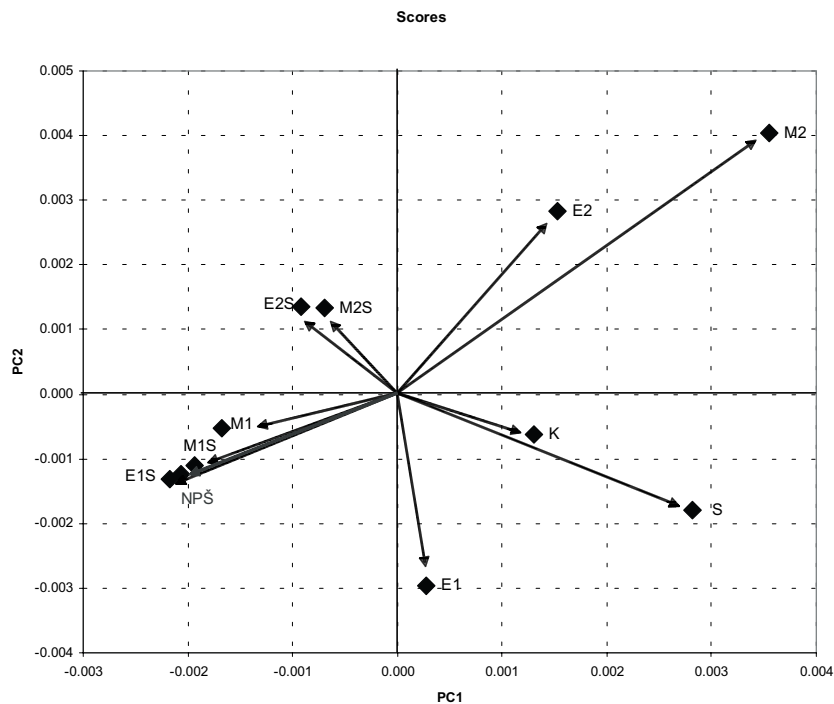


Fig. 4: Scores graph

PCA analysis of Raman spectral data obtained for various variants of fungi inoculated

FT Raman spectra of needles from natural forest area (NPŠ) were co-added

Centers of models of individual variants are marked

The study was supplemented by optical microscopy of needles. The micrographs show evident dissimilarities in the appearance of stomatal waxes for variants (Fig. 5) differing in the results of PCA of Raman spectra (Fig. 4).

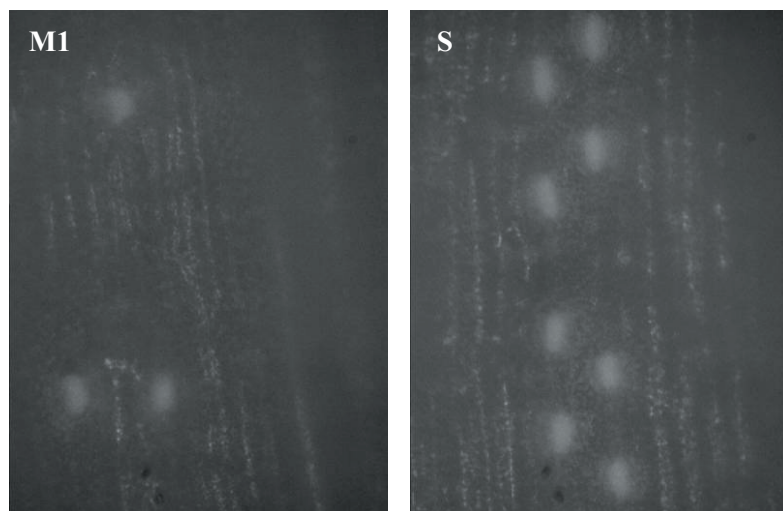


Fig. 5: Micrographs of needle surface

Examples for variants M1 and S are given.

Stomatal waxes are represented by white spots

Calculation of PCA is also very valuable in the case of model experiments using simulated solar radiation (Fig. 6). In the case of Raman spectra, the irradiation periods cause a positive shift of values of PC1 both for spruce and fir seedlings; a backward shift is observed after night. All the early morning measurements (before daily irradiation) are characterized by negative values of PC1 (see points F-X0, where X = 1, 2, 3, 4 – Fig. 6). The key contribution to variation along PC1 is given by bands of carotenoids. An evident shift of data along PC2 is related to an increasing duration of the experiment. Nevertheless, the periodicity of irradiation and night relaxation is apparent. It should be noted that only small systematic shift of data without any periodicity was observed in the case of completely dark experiment.

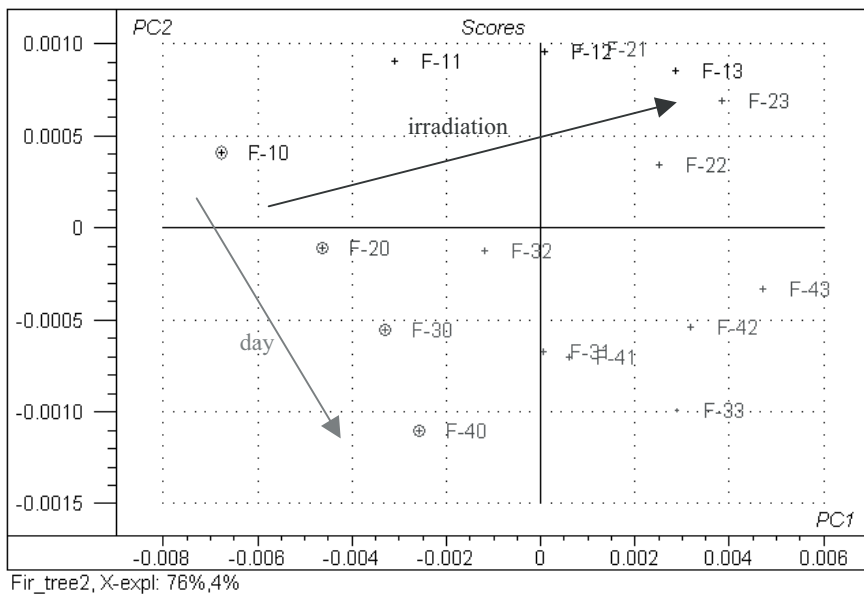


Fig. 6: Scores graph

PCA analysis of Raman spectral data obtained during four-day irradiation experiment for fir tree

F-XY represents individual measurement, where X = 1, 2, 3, 4 is a day numbering, Y = 0, 1, 2, 3 is a number of irradiation period applied during a day

The variation of infrared spectra during an irradiation experiment can be visualized using a matrix plot (Fig. 7). Some changes in intensity are observed for bands attributed to water, while the effect on “waxy” bands is minimal.

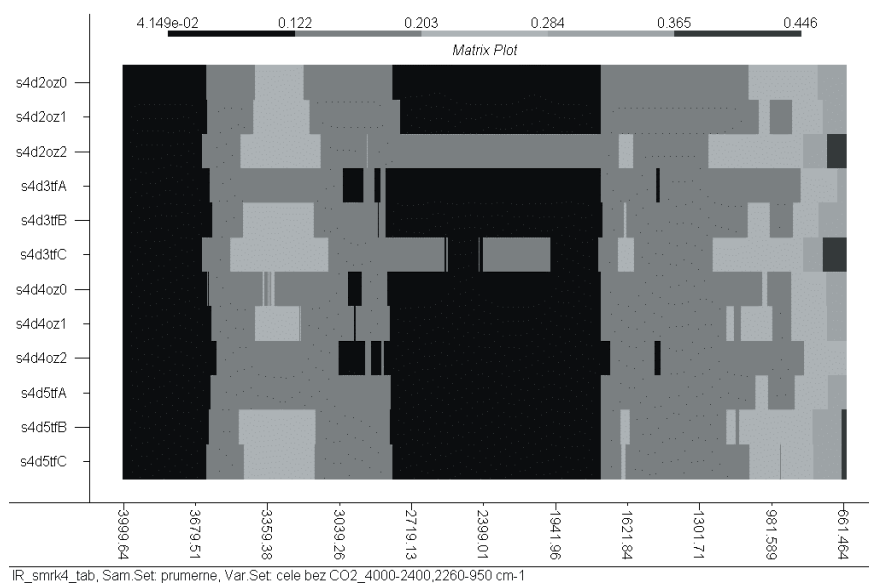


Fig. 7: Matrix plot of infrared spectra during an irradiation experiment

Spectra of a Norway spruce are shown

Individual rows represent the corresponding spectra

Conclusion

Both the effects of various soil fungi and the influences of solar radiation on conifers can be monitored using the methods of vibrational spectroscopy.

Effects of various types of fungi on host trees can be differentiated from each other. Both types of mycorrhizal fungi cause increased content of carotenoids compared to reference variant. The high content of carotenoids is related to the best nutrition conditions of the mycorrhizal variants. The interaction of mycorrhizal fungi with saprotrophic strains and corresponding competition for nutrition sources causes significant decrease of carotenoid content in spruce needles and some changes of waxes. The endophytic and saprotrophic fungi affect the needles in a substantially different way compared to mycorrhizal. The carotenoid content is relatively low; the content of waxes depends on the variant of fungi and on their mutual interaction.

The periodic irradiation of living seedlings causes periodic changes of vibrational spectral data. No periodicity is observed both for living trees under dark conditions and separated twigs under periodic irradiation. FT Raman spectroscopy enables to monitor changes of carotenoids, while infrared spectroscopy reveals the subtle changes of water content. The effects of irradiation are much smaller than the effects caused by different soil fungi.

Generally, the state of health of conifers can be estimated by spectral and chemometric analysis of vibrational spectra of needles. Strong bands of carotenoids, medium band of waxes, evident broad band of water and straight low-level baseline are typical characteristics of healthy needles. A decrease of “water” bands and an increase of spectral background is typical for drying, a decrease of “carotenoid” bands is characteristic for nutrient deficiency. The “waxy” band intensity depends on conflicting factors; therefore, a straightforward tendency cannot be described.

References

- [1] Matějka P., Tokarová H., Pekárek T., Volka K.: Measurement and evaluation of FT-Raman spectra of Norway spruce needles: How the background variability can be explained. *Journal of Molecular Structure*, 2003, 661/662, 333-345
- [2] Matějka P., Plešerová L., Budínová G., Havířová K., Mulet X., Skácel F., Volka K.: Vibrational biospectroscopy: What can we say about the surface wax layer of Norway spruce needles? *Journal of Molecular Structure*, 2001, 565/566, 305-310
- [3] Křížová J., Matějka P., Budínová G., Volka K.: Fourier-transform Raman spectroscopic study of surface of Norway spruce needles. *Journal of Molecular Structure*, 1999, 480/481, 547-550
- [4] Plešerová L., Budínová G., Havířová K., Matějka P., Skácel F., Volka K.: Multivariate analysis of attenuated total reflection spectra of Norway spruce needles. *Journal of Molecular Structure*, 2001, 565/566, 311-315
- [5] Člupek M., Matějka P., Volka K.: Noise reduction in Raman spectra: Finite impulse response filtration versus Savitzky–Golay smoothing. *Journal of Raman Spectroscopy*, 2007; 38, 1174–1179

Acknowledgement

Financial support from the Ministry of Education, Youth and Sports of the Czech Republic (MSM 6046137307) and from Czech Science Foundation (GA CR 203/05/0697) is gratefully acknowledged.

Atmospheric Dustiness of Residential Agglomeration and its Element Analysis

Mikuláš Matherny, Katarína Uhrinová, Silvia Ružičková

*Technical University of Košice, Faculty of Metallurgy, Department of Chemistry, Letná 9, 042 00 Košice, Slovak Republic,
e-mail: mikulas.matherny@tuke.sk*

Abstract

The atmospheric dustiness is a complicated state of the atmosphere. It is created by the direct emission sources of relevant region as well as by transported imissions from distant regions. The dust particles are partially washed out with atmospheric rainfall. The ratio of the gravitation dust sediments and flying particles is the fundamental of the studied phenomena. Beside the total gravitation dust sediments and the flying dust particles the eventual toxicity or essentiality is conditioned also by their element composition. But it is necessary to determine this element composition using optimized analytical method.

Keywords: *gravitation dust sediments, flying dust particles, element determination, statistical evaluation*

1. Introduction

The atmospheric dustiness is characterized by two forms of occurrence. They are the gravitation dust sediments (particles) and the flying dust particles. The gravitation dust sediment is characterized by spontaneous sedimentation. The diameter of these particles is mainly higher than 10 μm . These particles are intensively wash out from the atmosphere by atmospheric precipitations (rain, fog and snow). On the other hand, the flying dust particles do not deposit spontaneously and they are washed out from the atmosphere only trivial. The diameter of these particles is less than 1 μm . The particles between 10 μm and 1 μm do not still sediment, but generally they are washed out by the atmospheric precipitations. Then they appear in the gravitation dust sediments of the wet seasons [1].

2. Experimental

The sampling of the gravitation dust particles was realized in the monthly intervals with the standardized Berghoffer method during 2-years period [2,3]. The amount of sampled dust particles m_{gds} was transformed in the unit's $t\text{ km}^{-2}\text{ month}^{-1}$. Precision of this sampling moved between the ranges from $\pm 4\%$ to $\pm 7\%$. The sampling of flaying dust particles was realized in the accordance with the standard of Ministry of health of the Slovak Republic [4]. There were determined following elements: Cr, Cu, Fe, Mn, Pb, Sn, Ti, and Zn. For the trace element determination of the gravitation dust sediment samples, the emission spectrochemical method [5,6], was used. For the flaying dust samples,

the X-ray spectrometric method [7-9] was applied. The efficiency of emission spectrochemical method was following: limit of detection (LOD) value moved between 0.05 ppm to 10.0 ppm, relative standard deviation (RSD) values was between $\pm 1.0\%$ to $\pm 13.0\%$, and the coefficient of determination (R^2) moved between 90.0 % to 99.6 %. On the other hand, the X-ray spectrometric method for the samples of flying dust particles gave more efficient results: LOD 1.40 ppm to 6.0 ppm, RSD $\pm 1.0\%$ to $\pm 4.8\%$, and the value of coefficient of determination moved between 90.0 to 99.6 %.

3. Results and discussion

Both analytical methods were tested using exploratory analysis [10,11] of unvariant values. These procedures confirmed the repeatability, homogeneity and normal distribution of the input data. These results confirm the applicability of convenient calibration process.

The relation between the gravitation dust sediment and flying dust particles was studied using correlation analysis, concrete coupled comparison of corresponding dustiness values. This comparison is plotted by confidence ellipses [10,11]. The confidence ellipse for the total amount of twenty-four month sampling of gravitation dust and flying dust was nearly round-like (Fig. 1) and therefore no requested correlation was found. Correlation coefficient was $r = -0.02$, the orthogonal regression coefficient was equal zero.

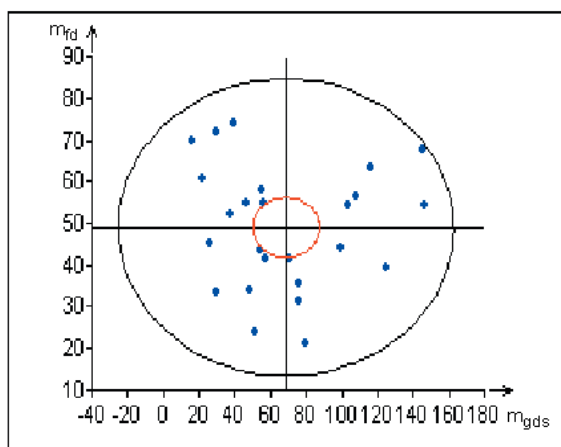


Fig. 1. Confidence ellipse of the relationship of the amount of gravitation dust sediment m_{gds} and flying dust m_{fd} for annual period

If the confidence ellipse is calculated only for the values of “summer” months (May, June, July, August) then the atmospheric washing-out is lower than in “winter” months. In this case is obtained elongated ellipse (Fig. 2). The value of correlation coefficient was $r = 0.94$, and the coefficient of determination $R^2 = 88.4\%$. The values of gravitation dust sediments ranged between 40 to 140 $t\ km^{-2}\ month^{-1}$, and for the flying dust between 20 to 70 $t\ km^{-2}\ month^{-1}$.

Finally, the confidence ellipse (Fig. 3) for the “winter” months (November, December, January, February), when the atmospheric washing-out is more intensive, was calculated. In this case was obtained elongated ellipse with correlation coefficient of $r = 0.99$, and the determination coefficient of $R^2 = 98.0\%$. In this last case, amount of gravitation dust sediments moved in the range from 25 to 55 $t\ km^{-2}\ month^{-1}$. The values of flying dust were in this case marked higher and they were in the interval from 45 to 50 $t\ km^{-2}\ month^{-1}$. This claim is in a good agreement with the categorization performed on the base of the differential factor analysis of the dustiness [12].

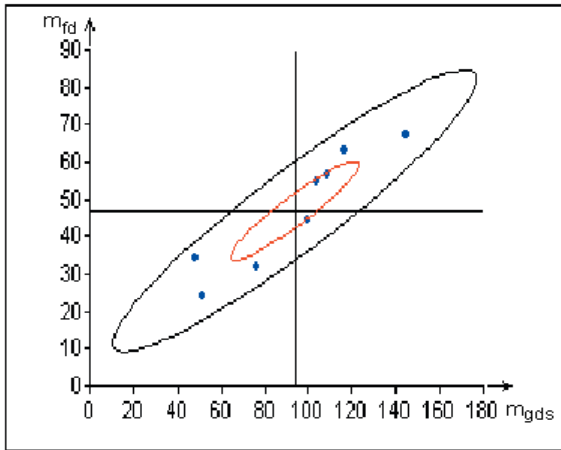


Fig. 2. Confidence ellipse of the relationship of the abundance of gravitation dust sediment m_{gds} and the flying dust m_{fd} in the “summer” months

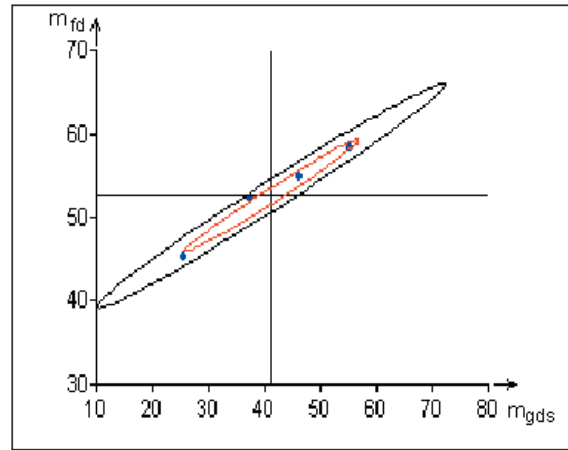


Fig. 3. Confidence ellipse of the relationship of gravitation dust sediment m_{gds} and the flying dust m_{fd} in the “winter” months

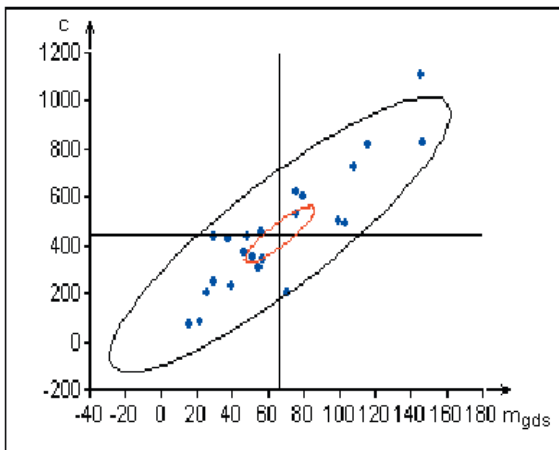


Fig. 4. Confidence ellipse demonstrates the correlation between Fe concentration and gravitation dust sediment amount

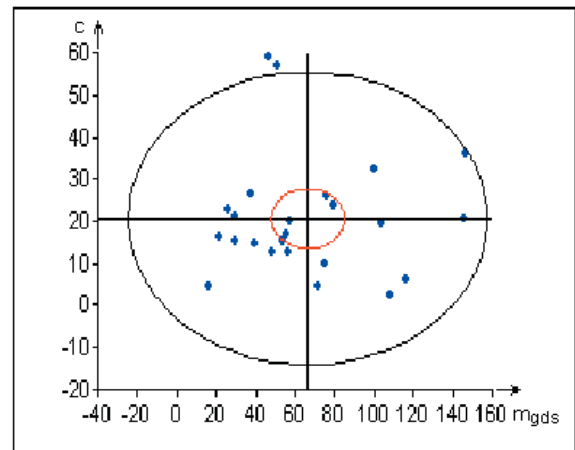


Fig. 5. Confidence ellipse demonstrates the correlation between Pb concentration and gravitation dust sediment amount

The dustiness of gravitation sediments changed in the range $\in \langle 20, 180 \rangle \text{ t km}^{-2} \text{ month}^{-1}$, while the dustiness of flying dust only in the range $\in \langle 20, 80 \rangle \text{ t km}^{-2} \text{ month}^{-1}$. Generally, the correlation between the amount of the gravitation dust sediments and the solo element concentration was higher than correlation of the amount of flying dust particles. The highest values of correlation as well as the highest value of coefficient of determination ($r = 0.88$, $R^2 = 77\%$) were achieved for the combination of amount gravitation dust sediment and the concentration of Fe (Fig. 4). Similar but lower values were achieved for the further transient elements Cr, Mn, Ti, V, and Zn.

The relation between two types of dustiness and the trace elements (Cr, Cu, Fe, Mn, Ni, Ti, V, and Zn) amount was also studied using correlation analysis (coupled comparison) of corresponding trace elements concentration and two dustiness types (Table 1, 2).

Table 1. The correlation coefficient r and coefficient of determination R^2 for the combination of the amount of gravitation dust sediments and concentration of trace elements

Parameter	Element							
	Fe	Ti	Zn	Cr	Mn	Ni	Cu	Pb
r	0.88	0.75	0.67	0.54	0.54	0.19	0.04	0.008
R^2	77.4	56.3	44.9	29.1	29.1	3.4	0.14	0.006

Table 2. The correlation coefficient r and coefficient of determination R^2 for the combination of the amount of flying dust and concentration of trace elements

Parameter	Element							
	Ni	Fe	Mn	Zn	Ti	Cr	Pb	Cu
r	0.54	0.50	0.47	0.47	0.41	0.36	0.35	0.29
R^2	29.1	25.0	22.1	22.1	16.8	13.0	12.3	8.4

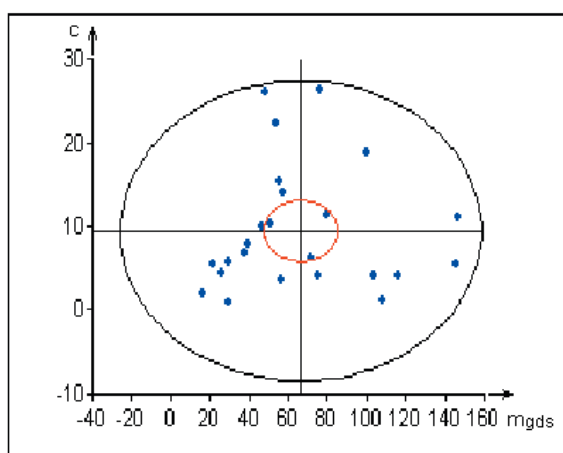


Fig. 6. Confidence ellipse demonstrates the correlation between Cu concentration and gravitation dust sediment amount

While the elements as Cu, Ni, and Pb (Fig. 5) practically show no correlation, and so they show no determination as well. Confidence ellipses for the flying dust particles and solo element concentration show lower correlation as the combination of gravitation sediment and solo element concentration. But the correlation $r \in \langle 0.29, 0.54 \rangle$, and also the determination $R^2 \in \langle 0.8, 0.29 \rangle$ is more balanced. Lowest correlation achieved the combination of flying dust and concentration of Cu (Fig. 6).

5. Conclusion

The total amount of the atmospheric gravitation dust sediment and the flying dust in the yearly average do not show any correlation. Opposite, both dustiness in the typical “summer” and “winter” months achieved very high correlation. This phenomenon is most probably caused by the different influence of atmospheric precipitations. The element composition and the both dustiness forms correlated very differently, and the correlation is lower than the correlation between the both dustiness forms.

Acknowledgement

The authors are obliged to express their gratitude for financial support to the grant projects VEGA 1/7437/20, 1/7418/20, 1/0214/03, 1/0459/08.

References

- [1] Malissa H., Robinson J. W.: Analysis of Airborne Particles by Physical Methods. CRC Press Inc. New York, 1979
- [2] VDI/DIN Handbuch. Reinhaltung der Luft. Beuth Verlag, Berlin 1991
- [3] Lux L., Pliešovská N., Flórián K., Uhrinová K.: Chem. Listy, 2002, **96**, 501
- [4] Ministerstvo zdravotníctva SR: Zisťovanie obsahu škodlivín v ovzduší. Vestník MZ SR, XXX. Ministerstvo zdravotníctva SR, Bratislava 1982
- [5] Flórián K., Gálová M., Koller L., Krakovská E., Lux L., Matherny M., Nickel H., Uhrinová K.: Acta Chim Hung – Models in Chemistry, 1992, **125**, 611
- [6] Flórián K.: Private communication
- [7] Tertian R. Glaisse F.: Principles of Quantitative X-Ray Fluorescence Analysis. Heyden and Sons, London 1982
- [8] Szilágyi K., Hartyáni Zs.: 44. Magyar Spektro. Vándorgyűlés-Baja 117. Magyar Kémikusok Egyesülete, Budapest 2001
- [9] Uhrinová K., Pliešovská N., Matherny M.: Chem. Pap., 2003, **57**, 185
- [10] Kupka J.: QC.ExpertTM Statistical software [computer software]. TriloByte, Pardubice, 2002
- [11] Meloun M., Militký J., Forina M.: Chemometrics for Analytical Chemistry. Ellis Horwood, Chichester 1992
- [12] Einax J., Danzer K., Matherny M.: Intern. J. Environ. Anal. Chem., 1991, **44**, 185

Comparison of Five Different Methods for the Separation and Determination of Aluminium Phytoavailable and (Phytotoxic) Fractions

¹Peter Matúš, ¹Marek Bujdoš, ¹Jana Kubová, ¹Ingrid Hagarová, ¹Ján Medved',
²Pavel Diviš, ²Zuzana Mládková

¹Comenius University in Bratislava, Faculty of Natural Sciences, Mlynská dolina 1, 842 15 Bratislava 4, Slovakia, e-mail: matus@fns.uniba.sk

²Brno University of Technology, Faculty of Chemistry, Purkyňova 118, 61200 Brno, Czech Republic

Abstract

The suggested investigation deals with the separation of phytoavailable and (phytotoxic) Al fractions in soil and soil sediment samples by five different procedures (single and sequential extractions, membrane filtration, chelating solid phase extraction and kinetic strength discrimination method). The concentrations of Al in studied fractions and relevant plant materials were measured by F AAS, ICP OES and UV/VIS spectrophotometry. Weakly efficient single extraction procedures by H₂O, dilute acetic acid, NTA, EDTA, DTPA, salicylic acid, ammonium salicylate and 8-hydroxyquinoline, chelating solid phase extraction by resins Iontosorb Oxin and Salicyl and kinetic strength discrimination method using 8-hydroxyquinoline release from the samples only small amounts of phytoavailable and phytotoxic Al by ion-exchange or complexation processes. The more efficient extractions with KCl, NH₄Cl, CaCl₂, BaCl₂, CuCl₂, LaCl₃, NH₄F and (NH₄)₂C₂O₄ leach approximately the same amounts of phytoavailable Al as the total Al concentrations in plant material (grass *Festuca rubra*) growing on analysed soils and soil sediments. The most aggressive leaching with Na₄P₂O₇, dilute HCl, NH₂OH·HCl in HNO₃ and H₂O₂/ammonium acetate in HNO₃ releases the highest amounts of Al from solid samples, approximately double to fourfold as the total Al concentrations in relevant plant material and it is unsuitable for purpose of this study.

Key words: aluminium, fractionation, phytoavailability, phytotoxicity, *Festuca rubra*, soil, sediment, F AAS, ICP OES, UV/VIS spectrophotometry

Introduction

Although aluminium is the most abundant metal in the Earth's crust, it is non essential for plants. Because of its low solubility in a solution under neutral conditions, aluminium was regarded as a non-toxic element and its environmental and biological effects were not investigated until recently. During the last two decades it has been found that the acid deposition leads to the considerable increases of the dissolved Al concentrations in the acidified soils and surface waters. The continuing acidification of soils with the low buffering capacity leads to an increase of the aluminium mobilization in the environment and may be potentially hazardous to the all terrestrial and aquatic systems. Aluminium is a strongly hydrolysing metal and it is relatively insoluble in the neutral pH

range (from 6.0 to 8.0). Under the acidic ($\text{pH} < 6.0$) or alkaline ($\text{pH} > 8.0$) conditions, and/or in the presence of the complexing ligands, the solubility of Al is enhanced, making it more available for the biogeochemical transformations.

The phytoavailability and phytotoxicity of aluminium is dependent on its distribution among the various forms or species coexisting in the environment. So the form of soil Al is a key factor of its potential risk impact to living organisms. It can be stated that the certain soil Al species represent a limiting factor for the plant growth under the acidic conditions. Aluminium occurs in the various chemical species, of which the free Al^{3+} , AlOH^{2+} , and $\text{Al}(\text{OH})_2^+$ species were found to be the most crucial to evaluate its toxicity and to predict the impact of the proton inputs in the soils and surface waters. The toxicity of AlSO_4^+ is not always accepted and even though polymer Al_{13} (not in a form of phosphates or silicates) seems to be the most toxic Al species, its actual risk in the soil environment is probably smaller.

The concentration of such Al species may be difficult to determine directly [1-12]. For that reason these species are determined in one or more fractions. Generally, these fractions are defined operationally or functionally, respectively, and they are termed according to the used separation method, e.g. the reactive species fraction, or the function of the isolated analyte, e.g. bioavailable species fraction.

In presented paper the five separation procedures (single and sequential extractions, membrane filtration, chelating solid phase extraction and kinetic strength discrimination method) connected with three detection techniques (flame atomic absorption spectrometry, inductively coupled plasma optical emission spectrometry and UV/VIS spectrophotometry) are investigated and evaluated for the separation and determination of phytoavailable and/or phytotoxic Al species fractions. The separation efficiency, selectivity and sensitivity of these procedures are also discussed.

Experimental

Description of the sampling areas

In Záhajnica, Nálepkovo region, Slovenské rudohorie Mts (Eastern Slovakia) the mass dying-tree of forest communities and forest ecosystems decomposition were observed. The forest soil ecosystem in Záhajnica occurs in Al buffered area ($\text{pH} \sim 4$) and the solubility of soil Al is limited by complexing reactions with organic compounds only in low extent. This locality is influenced by the deficit of some nutriment (Ca, Mg, K, P), toxic effects of Al and inhibition of organic matter mineralisation processes. The increased mobility of Al due to soil acidification seems to be the main cause of the decline in quality of spruce forest present in this locality.

The serious negative environmental effects connected with the open quartzite mine were observed in Šobov, Banská Štiavnica region (Central Slovakia). Pyrite oxidation in the mine dump Šobov and subsequent acid mine drainage (AMD) attack on other mineral phases are the main negative environmental factors. Created sulphuric acid attacks other minerals and causes the high migration rate of different toxic elements including Al fixed before in mineral structure. Dissolved primary clay minerals (the most abundant are aluminosilicates, illite and pyrophyllite) release high amount of Al to surrounding environment by the neutralization reaction with H^+ protons from the pyrite oxidation. The pollution of surface and ground water as well as the degradation of soil and vegetation are distributed in the region mainly by extremely acid water.

On the localities Záhajnica and Šobov the changes in dominancy and diversity of plant species were observed. Grass *Poaceae* is the most resistant to extreme soil properties. Along the whole sampling site the percentage of *Poaceae* in total number of plant species increases. Original grassland dominant *Poacea – Arrhenatherum elatius* and *Dactylis glomerata* and other vegetation was almost completely decimated or replaced by more resistant *Poacea* species *Festuca rubra* and *Deschampsia flexuosa*. Furthermore, the aluminium toxicity indexes (ATI), defined as the ratio of the nutrient cations (Ca, Mg, K, Na) concentration sum to the Al concentration in mmol kg^{-1} , were calculated for

some soil and sediment samples, their BaCl₂ and acetic acid extracts and plant material samples investigated in this study, and these ATI values were used for the assessment of the Al phytotoxicity. From the low ATI data results the high toxic impact to the plants (ATI values < 1 mean the high phytotoxicity risk of Al) and vice versa. The ATI values were almost invariable for all original soils and sediments without regard to the sample pH, but the calculation of the ATI values for both extracts and grass samples was more useful. For the majority of studied acid samples the calculated ATI values were lower than 1.

Sampling

The sampling of one acid forest soil marked with the letter Z (type Cambic Podzol) from six different horizons was performed in the area of Záhajnica (Nálepkovo, Slovenské rudohorie Mts, Eastern Slovakia). The sampling of eight acid soils (type Eutric Cambisol) and two acid soil sediments marked with the letter Š from top horizon was performed in the area of Šobov (Banská Štiavnica, Central Slovakia). The characteristics of soil and soil sediment samples are listed in Table 1.

Eleven samples of plant material (the stems of grass *Poacea – Festuca rubra*) growing on the all studied soils and soil sediments were sampled at the same time like. Before the chemical analysis the grass stems were rinsed with doubly distilled water, air-dried and cutted on the small pieces.

Table 1. Characteristics of studied soil and soil sediment samples (NM, not measured; * g l⁻¹; ** mg l⁻¹)

Sample / Horizon (cm)	pH H ₂ O	EC H ₂ O (μS cm ⁻¹)	TOC (%)	S (g kg ⁻¹)	Al H ₂ O (mg kg ⁻¹)
<i>Soils</i>					
Z (5+0)	3.80	NM	41.3	NM	113
Z (0-5)	3.67	NM	11.0	NM	159
Z (5-11)	4.10	NM	4.85	NM	41.1
Z (11-55)	4.43	NM	2.99	NM	13.2
Z (55-65)	4.33	NM	1.27	NM	13.9
Z (65-90)	4.35	NM	1.75	NM	15.0
Š1 (0-15)	1.84	3350	NM	33.0	196
Š2 (0-15)	1.95	2380	NM	10.1	145
Š3 (0-15)	2.45	1149	0.411	4.07	274
Š4 (0-15)	2.36	1718	0.131	3.34	80.5
Š5 (0-15)	2.97	571	1.51	2.10	83.0
Š6 (0-15)	2.83	830	4.67	7.71	238
Š7 (0-15)	2.89	760	7.88	7.38	71.5
Š8 (0-15)	2.95	548	5.14	1.85	49.8
<i>Soil sediments</i>					
Š9 (0-15)	3.10	671	NM	0.694	53.3
Š10 (0-15)	3.60	240	NM	0.163	12.5

Procedures

The total concentrations of Al in soil, sediment and plant material samples and reference materials (RM) were determined after their wet decomposition by a hot mixture of 15HF+5HNO₃+2HClO₄+1H₂O₂ in open system (for soil and sediment samples) and by 2HF+5HNO₃ hot mixture in the autoclave at 160 °C (for plant material samples). Both decomposition procedures were satisfactory validated using suitable RMs.

The single extraction procedures (SEP) were applied to soil and sediment samples using eighteen agents. In all cases the sample-extracting agent suspensions were shaken (100 rpm) and centrifuged (2500 g) for 20 min. The SEP conditions and appropriate references are listed in Table 2.

The sequential extraction procedure was applied to soil and sediment samples using the optimised BCR three-step sequential extraction protocol (BCR SEP; first acid extractable step: 40 ml

0.11 M acetic acid solution (AA), second reducible step: 0.5 M $\text{NH}_2\text{OH}\cdot\text{HCl}$ in 0.05 M HNO_3 solution (2), third oxidizable step: H_2O_2 followed by 1 M ammonium acetate solution adjusted to pH 2.0 by HNO_3 (3), the residue was decomposed by $15\text{HF}+5\text{HNO}_3+2\text{HClO}_4+1\text{H}_2\text{O}_2$ hot mixture in open system). The BCR SEP was satisfactory validated using suitable RMs.

The membrane filtration was applied to water samples and H_2O , 8-hydroxyquinoline, salicylic acid and ammonium salicylate extracts of soil and sediment samples. These solutions were filtered through 0.40 μm cellulose nitrate membrane filters under low vacuum in a polysulphone filtration apparatus.

The kinetic strength discrimination method, so-called 8-hydroxyquinoline method (HQNM), was applied to filtered water samples and H_2O extracts of soil samples by flash reaction of 1 % 8-hydroxyquinoline with sample Al followed by extraction of analyte product to organic phase (MIBK, methyl isobutyl ketone): 500 μl redistilled H_2O and 400 μl of 1 % 8-hydroxyquinoline in 2 % acetic acid solution buffered with 1 M sodium acetate at pH 5 were mixed in 20 ml glass or plastic tube and then 5 ml of filtered sample was injected with sufficient turbulences. The reaction was stopped by immediately injection of 4.5 ml of MIBK (the injection must be terminated 5 s after the beginning of sample injection). It was shaken vigorously up to 15 s (counted from the beginning of sample injection). While two phases were separated, absorption of MIBK phase was readed.

The chelating solid phase extraction (CSPE) with utilization of ion-exchangers Iontosorb Oxin and Iontosorb Salicyl (IO and IS; cellulose resins containing covalently bound 8-hydroxyquinoline and salicylic acid functional groups, respectively) was applied to filtered water samples and H_2O extracts of solid samples using the batch technique with 1 min extraction time (25 ml of sample solution was stirred with magnetic stirrer in the presence of 10 g damp resin, after 1 min the stirring was stopped and after flash centrifugation the aliquot of supernatant was removed and analysed for Al).

Table 2. Single extraction procedure conditions and appropriate references (AA, acetic acid; HQN, 8-hydroxyquinoline; SA, salicylic acid; AS, ammonium salicylate)

Extracting agent	Concentration (mol l^{-1})	Ratio volume/weight	Extraction time (h)
doubly distilled H_2O		5/1	24
KCl	1	10/1	1
NH_4Cl	1	10/1	1
NH_4F	0.5	10/1	1
CaCl_2	0.1	10/1	1
BaCl_2	0.1	10/1	1
CuCl_2	0.5	10/1	1
LaCl_3	0.3	10/1	1
$(\text{NH}_4)_2\text{C}_2\text{O}_4$	0.2	20/1	1
$\text{Na}_4\text{P}_2\text{O}_7$	0.1	10/1	1
NTA	0.005	10/1	1
EDTA	0.005	10/1	1
DTPA	0.005	10/1	1
HCl	0.5	20/1	1
AA	0.11	40/1	16
HQN in 2 % AA	1 %	10/1	1
SA	0.2 %	10/1	1
AS	0.31 %	10/1	1

Instrumentation

The concentration of Al was measured in all cases (except 8-hydroxyquinoline method) by FAAS using a Perkin–Elmer Model 5000 atomic absorption spectrometer (wavelength of 309.3 nm, nitrous oxide-acetylene flame, limit of quantification (LOQ) $\sim 0.5 \text{ mg l}^{-1}$) or by ICP OES using a Kontron Plasmakon Model S 35 sequential optical emission spectrometer (wavelength of 396.152 nm, LOQ $\sim 0.03 \text{ mg l}^{-1}$). UV/VIS spectrophotometers Hach Model DR 3000 and Carl Zeiss Model Spekol

11 (wavelengths of 390 and 600 nm, LOQ $\sim 0.02 \text{ mg l}^{-1}$) were used for Al quantification in 8-hydroxyquinoline method (HQNM).

Results and discussion

The selectivity of used fractionation methods was investigated with the relation to Al phytoavailability and phytotoxicity, respectively. The relationship between Al concentrations in separated individual soil and soil sediment fractions and total Al concentrations in grass stems with the given correlation coefficients was observed (Fig. 1. and Table 3.). The determined concentrations of Al in grass stem samples ranged from 244 to 1177 mg kg^{-1} with the median 612 mg kg^{-1} and the mean \pm standard deviation (SD) $634 \pm 295 \text{ mg kg}^{-1}$.

The slopes of these dependences decrease with increased separation efficiency of used methods (from 8-hydroxyquinoline method (HQNM) and chelating solid phase extraction (CSPE) by Iontosorb Oxin and Salicyl to $\text{Na}_4\text{P}_2\text{O}_7$, dilute HCl single and optimised BCR three-step sequential extraction protocol (BCR SEP) extraction procedures, respectively). Likewise, the selectivity of used methods decreases in the same order.

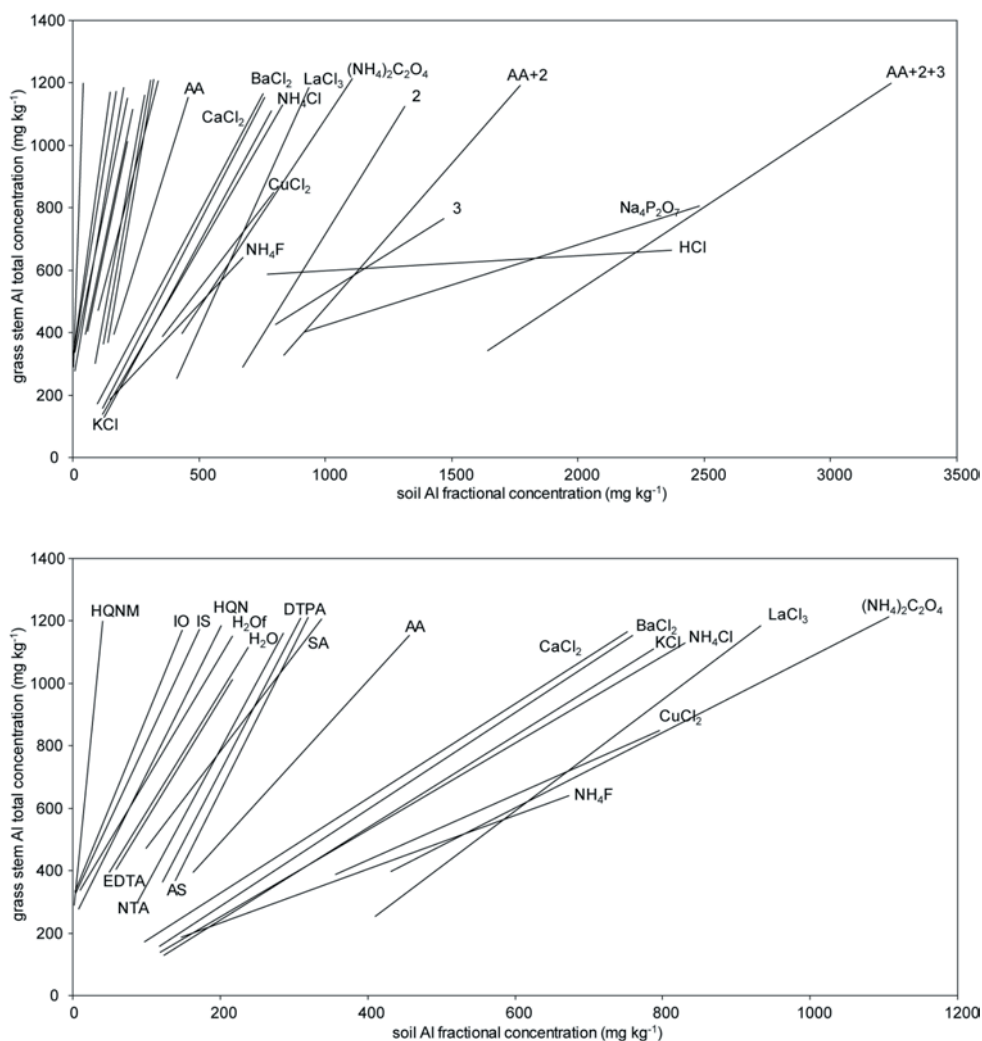


Fig. 1. The relationship between Al concentrations in individual soil and sediment fractions and Al concentrations in grass stems presented on two concentration scales (HQNM, 8-hydroxyquinoline method; IO, chelating solid phase extraction by Iontosorb Oxin; IS, chelating solid phase extraction by Iontosorb Salicyl; HQN, 8-hydroxyquinoline; H₂Of, H₂O SEP followed by the filtration step; SA, salicylic acid; AS, ammonium salicylate; AA, dilute acetic acid; 2, second step of BCR SEP and 3, third step of BCR SEP)

The used fractionation procedures can be divided into three groups in accordance with their selectivity and separation efficiency. The first group is consisting of weakly efficient single extraction procedures (SEP) by H₂O, dilute acetic acid (AA), NTA, EDTA, DTPA, 8-hydroxyquinoline (HQN), salicylic acid (SA) and ammonium salicylate (AS), the chelating solid phase extraction by resins Iontosorb Oxin (IO) and Iontosorb Salicyl (IS) and 8-hydroxyquinoline method (HQNM) which release only small amounts of Al. These methods are most suitable for the separation of phytoavailable Al species. They have the ability to selectively separate the phytoavailable species of Al by ion-exchange or complexation processes.

The extraction by H₂O simulates the Al release to soil solution under normal conditions. The Al released by H₂O from studied soil and sediment samples corresponded to 0.01-0.3 % of total Al. Dilute acetic acid dissolves the sample carbonate phase and water and acid soluble, exchangeable or adsorbed fraction of Al (0.3-3.6 % of total Al). The complexing agents NTA, EDTA and DTPA are used usually as the extractants in functionally defined fractionation. These extractants show the similar extraction efficiency like previous agents. The sample Al amounts released by NTA, EDTA and DTPA solutions are very similar (0.06-1.6 % of total Al).

Table 3. Correlation coefficient values for the relationship between Al concentrations in individual soil and sediment fractions and Al concentrations in grass stems
(H₂O_f, H₂O SEP followed by the filtration step; AA, acetic acid; HQN, 8-hydroxyquinoline; SA, salicylic acid; AS, ammonium salicylate; 2, second step of BCR SEP; 3, third step of BCR SEP; IO, chelating solid phase extraction by Iontosorb Oxin; IS, chelating solid phase extraction by Iontosorb Salicyl; HQNM, 8-hydroxyquinoline method)

Separation method	Correlation coefficient
H ₂ O	0.7122
H ₂ O _f	0.7699
KCl	0.6888
NH ₄ Cl	0.6569
NH ₄ F	0.6233
CaCl ₂	0.5800
BaCl ₂	0.5021
CuCl ₂	0.3899
LaCl ₃	0.4150
(NH ₄) ₂ C ₂ O ₄	0.4688
Na ₄ P ₂ O ₇	0.2124
NTA	0.6111
EDTA	0.6458
DTPA	0.6145
HCl	0.1154
AA	0.5963
HQN	0.8011
SA	0.7411
AS	0.5115
2	0.3674
3	0.2469
AA+2	0.4585
AA+2+3	0.2984
IO	0.8552
IS	0.8705
HQNM	0.8895

The functional groups of 8-hydroxyquinoline and salicylate were used in different fractionation protocols (single extraction, chelating solid phase extraction and 8-hydroxyquinoline method) with the best correlation coefficients (R=0.7411-0.8895, except ammonium salicylate), see Table 3. They separate the operationally defined fraction of labile Al species (i.e. mainly inorganic aqua, hydroxy

and sulphato Al cationic monomers), which are mostly responsible for aluminium phytotoxicity. In small extent also the species of Al bound in weak organic and some fluoride complexes may be presented in this fraction. The fraction of nonlabile Al species is represented mainly by organic complexes of Al. The main problem with using of this method is that it groups together the toxic hydroxycomplexes and some nontoxic fluoride complexes and other low molecular weight (LMW) species of Al in the same separated fraction.

The fractionation of aluminium by single extraction procedure (SEP) with 8-hydroxyquinoline (HQN), salicylic acid (SA) and ammonium salicylate (AS) allows the direct separation of labile Al species. The separation efficiency of 8-hydroxyquinoline (0.02-0.2 % of total sample Al) decreases and the selectivity of obtained results increases with increased concentration of 8-hydroxyquinoline in the extractant. Reversely, in the case of salicylic acid and ammonium salicylate the extraction efficiency (0.03-1 % of total Al) increases and the selectivity decreases with increased concentration of salicylate functional groups in the extractant. It seems (Fig. 1.) that the use of 8-hydroxyquinoline extractant offers the more selective results. The membrane filtration (0.40 μm) of 8-hydroxyquinoline, salicylic acid and ammonium salicylate extracts has not evident effect on extracted Al amount.

The fractionation of aluminium by chelating solid phase extraction (CSPE) using resins Iontosorb Oxin (IO) and Iontosorb Salicyl (IS) includes the sample membrane filtration (0.40 μm) step. For the analysis of soil and soil sediment samples the sequential procedure with preliminary included H_2O single extraction step is needed. The concentration of labile Al ranged from 78 to 98 % of soluble Al for Záhajnica soil samples and from 46 to 82 % of soluble Al for Šobov soil and soil sediment samples. In average, the distribution of H_2O extracted Al in investigated soil and sediment samples is followed: Al concentrations decrease in the order $\text{Al}_l > \text{Al}_{nl} > \text{Al}_{\text{part}}$ (Al_l , labile; Al_{nl} , nonlabile; Al_{part} , particulate Al species). Fraction of Al_{part} represents nonsoluble Al bound in particulate matter (e.g. organic compounds of Al with high molecular weight or inorganic polymerized Al compounds).

The 8-hydroxyquinoline method (HQNM) based on kinetic strength discrimination utilizes the reaction of labile Al species with 8-hydroxyquinoline solution with pH 5 and their consecutive extraction to methyl isobutyl ketone (MIBK). The separated labile species of Al are similar as in the previous CSPE method. They are represented mostly by phytotoxic aqua, hydroxy and sulphato Al cationic monomeric species. This procedure in sequential arrangement with H_2O single extraction and membrane filtration (0.40 μm) allows the sufficient selectivity with respect to aluminium phytoavailability and phytotoxicity. The obtained concentration of labile Al species in soil samples ranged from 4 to 59 % of soluble Al. The selectivity of this method is given at first and foremost by the very short reaction time of 5 s, analogically with the extraction time of 1 min for chelating solid phase extraction (CSPE) by IO and IS and extraction time of 1 h for single extraction procedure (SEP) with 8-hydroxyquinoline (HQN), salicylic acid (SA) and ammonium salicylate (AS). From the used time intervals and obtained results it is obvious that 8-hydroxyquinoline method reaches the best selectivity which is given by the sequential coupling of three different analytical techniques and high reactivity of 8-hydroxyquinoline in H_2O phase. Chelating solid phase extraction (CSPE) using 8-hydroxyquinoline or salicylic acid fixed on the resins and single extraction procedures (SEPs) with 8-hydroxyquinoline, salicylic acid or ammonium salicylate solutions are probably less selective because of the slower kinetics of reaction between labile Al species and agent functional ligands. However, the rate of these reactions between liquid and solid phases can be influenced by many different sorption and diffusion effects.

The concentrations of soil and soil sediment labile Al (Al_l) species obtained by using of CSPE and HQNM were also studied with the relation to sample pH and aluminium toxicity index (ATI) values among others for BaCl_2 and acetic acid extracts of some soil and sediment samples and plant material samples used in this study. The given ATI values very well correspond to sample pH values, total Al concentrations in grass stems and plant species diversity. The highest concentrations of Al_l are related to the lowest sample pH values, the lowest number of plant species on sampling site, the highest total Al concentrations in grass stems and the lowest ATI values (< 1). On the contrary, the

lowest concentrations of Al_i are related to the highest sample pH values, the highest number of plant species on sampling site, the lowest total Al concentrations in grass stems and the highest ATI values.

Under the certain conditions of aluminium fractionation in solid samples (soil, sediment and weathered rock) the single extraction procedure (SEP) with 8-hydroxyquinoline (HQN) solution without the need of extract filtration can supersede both chelating solid phase extraction (CSPE) and 8-hydroxyquinoline method (HQN) which require the consecutive application of extraction and filtration steps for the obtaining of soluble Al fraction. But in the case of filtered liquid samples (soil solution, solid sample extract and other liquid samples) it is favourable to use the chelating solid phase extraction (CSPE) by Iontosorb Oxin and Iontosorb Salicyl or the 8-hydroxyquinoline method (HQN) based on kinetic strength discrimination (Fig. 2.). This scheme can be useful for the routine monitoring of mobility, phytoavailability and phytotoxicity of aluminium in the environment. The proposed procedures can be the useful tools in Al environmental risk assessment. The described separation procedures can be applied also in the field with utilization of given extractant (HQN) or resin (IO or IS) filled plastic syringe with the possibility of sample membrane filtration (0.40 μm). The results from the application of these methods were in the best agreement with local phytodiversity changes in Záhajnica and Šobov sampling areas.

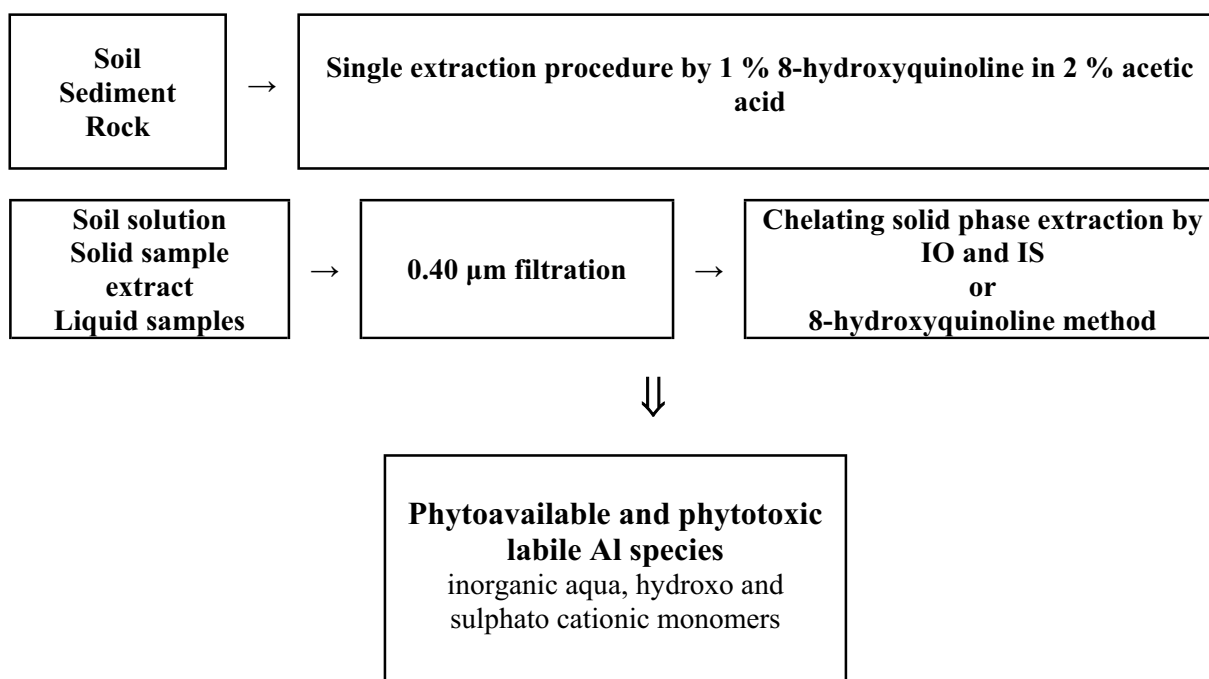


Fig. 2. Scheme of the proposed procedures

The more efficient single extraction procedures (SEP) with KCl , NH_4Cl , NH_4F , $CaCl_2$, $BaCl_2$, $CuCl_2$, $LaCl_3$ and $(NH_4)_2C_2O_4$ leach from the samples approximately the same amounts of Al as the total Al concentrations in plant material samples (grass *Festuca rubra*) growing on analysed soils and sediments (Fig. 1.). These methods can better describe a potential threat for the case of strong disturbance in the natural system conditions. They can be also useful in the routine environmental risk assessment. The third group of separation procedures contains the most aggressive leaching with $Na_4P_2O_7$, dilute HCl and second ($NH_2OH \cdot HCl$ in HNO_3) and third (H_2O_2 /ammonium acetate in HNO_3) step from the optimised BCR three-step sequential extraction protocol (BCR SEP). These extractants release the highest amounts of Al, approximately double to fourfold as the total Al concentrations in relevant plant materials (Fig. 1.) and they are not suitable for the separation of phytoavailable nor phytotoxic Al species.

The above-mentioned simple salt (KCl , NH_4Cl , NH_4F , CaCl_2 , BaCl_2) solutions with low concentrations release the soluble and exchangeable forms of Al from soil and sediment samples (0.2-1.5 % of total Al). Fluorides with their complexing power are suitable for the release of polymerized Al compounds. The single extractions with CuCl_2 , LaCl_3 and $\text{Na}_4\text{P}_2\text{O}_7$ do not allow the effective separation of Al organic species in studied samples with low pH values. CuCl_2 and LaCl_3 extractants released about 0.2-1.4 % of total Al from investigated soil and sediment samples. The high concentrations of Al in $\text{Na}_4\text{P}_2\text{O}_7$ extracts (up to 4 % of sample total Al) are probably connected with the complexation ability of this agent and the damage of the clay minerals or the weathered secondary minerals presence.

The reducible agent $(\text{NH}_4)_2\text{C}_2\text{O}_4$ extracts mainly Al species bound to oxocompounds, e.g. the crystalline oxides and the most of organic complexes. But the reducible Al fractions separated by $\text{NH}_2\text{OH}\cdot\text{HCl}$ in second step of the optimised BCR three-step sequential extraction protocol (BCR SEP) contain the higher Al amounts. The sample Al amounts released by $(\text{NH}_4)_2\text{C}_2\text{O}_4$ (0.2-2.2 % of total Al) were lower than in the $\text{NH}_2\text{OH}\cdot\text{HCl}$ fraction (0.2-3.7 % of total Al). It seems that $\text{NH}_2\text{OH}\cdot\text{HCl}$ agent has the more reducible effect than $(\text{NH}_4)_2\text{C}_2\text{O}_4$.

The direct oxidation of organic matter by H_2O_2 used in third step of BCR SEP is the better approach for the estimation of organically bound Al than the using of single extraction procedures with CuCl_2 , LaCl_3 or $\text{Na}_4\text{P}_2\text{O}_7$. H_2O_2 destroys the oxidizable sample matter and acidic ammonium acetate with weak complexing ability leaches the released Al. But this procedure can separate also Al species bound to present sulphides. For studied soil and sediment samples the concentration of Al in this fraction ranged from 0.2 to 2.3 % of total Al.

The mobile and mobilizable (sum of fractions from first two (AA+2) or three steps (AA+2+3) of the optimised BCR three-step sequential extraction protocol) Al fractions (Fig. 1) are highly related to Al amounts extracted by dilute HCl (0.3-3.6 % of total Al) and in less extent also by $\text{Na}_4\text{P}_2\text{O}_7$ agent. The dilute HCl extracts mainly Al species connected with anthropogenic contamination of the environment. Thus, the single extraction procedures with HCl and $\text{Na}_4\text{P}_2\text{O}_7$ can supersede the optimised BCR three-step sequential extraction protocol (BCR SEP) for the separation of mobile or mobilizable Al fraction. The nonmobilizable Al fraction (more than 93 % of total Al) obtained as insoluble residue after three steps of BCR SEP contains mostly the primary and secondary aluminosilicate minerals. This residue can be decomposed only by using of strong acids hot mixture (HF , HNO_3 , HClO_4) and H_2O_2 . As aluminium is strongly bound in the alumino-silicate lattice, neither the aqua regia extraction protocol according to the ISO Norm 11466 ($3\text{HCl} + \text{HNO}_3$ reflux) nor the EPA Method 3050 (treatment with HNO_3 and H_2O_2 reflux) are suitable for the determination of BCR SEP residual or total Al concentrations in soil, sediment and rock samples because of the used reagents (HCl, HNO_3 and H_2O_2) do not completely destroy the alumino-silicate lattice. It can be concluded that Al concentrations in the all sample fractions obtained by optimised BCR three-step sequential extraction protocol (BCR SEP) decrease in the order residual > oxidizable = reducible > acid extractable.

The scheme for classifying of all Al species (according to their degree of the lability) and all used analytical procedures (according to their efficiency and selectivity) is showed in Fig. 3. Three methods (8-hydroxyquinoline method, chelating solid phase extraction by Iontosorb Oxin or Salicyl and single extraction procedure with 8-hydroxyquinoline) were taken from other procedures in first group because they are most selective for the separation of very labile Al species, which are considered to be the most phytoavailable and phytotoxic chemical forms of aluminium. Also the analytical sensitivity of these three methods is highest from all used fractionation techniques (see the slopes of dependence lines for used fractionation methods in Fig. 1.).

- [2] P. Matúš, J. Kubová, V. Streško: Utilization of Chelating Ion-Exchange for Aluminium Speciation, *Chem. Pap.* 57 (2003) 176-178
- [3] J. Polakovič, J. Polakovičová, J. Kubová: Application of thermodynamics in a specific force field to the adsorption of Al^{3+} ions on the chelating resins Ostsorb Oxin, Ostsorb Salicyl, Spheron Oxin, and Spheron Salicyl - Mathematical analysis of sorption isotherms using nonlinear mean square software, *Anal. Chim. Acta* 488 (2003) 123-132
- [4] P. Matúš, J. Kubová, M. Bujdoš, V. Streško, J. Medved': Chemical partitioning of aluminium in rocks, soils, and sediments acidified by mining activity, *Anal. Bioanal. Chem.* 379 (2004) 96-103
- [5] P. Matúš, J. Kubová, M. Bujdoš, J. Medved': Determination of operationally defined fractions of aluminium in reference materials and acid attacked environmental samples, *Anal. Chim. Acta* 540 (2005) 33-43
- [6] J. Kubová, P. Matúš, M. Bujdoš, J. Medved': Influence of acid mining activity on release of aluminium to the environment, *Anal. Chim. Acta* 547 (2005) 119-125
- [7] P. Matúš, J. Kubová: Complexation of labile aluminium species by chelating resins Iontosorb - a new method for Al environmental risk assessment, *J. Inorg. Biochem* 99 (2005) 1769-1778
- [8] P. Matúš, J. Kubová: Complexation efficiency of differently fixed 8-hydroxyquinoline and salicylic acid ligand groups for labile aluminium species determination in soils – comparison of two methods, *Anal. Chim. Acta* 573-574 (2006) 474-481
- [9] P. Matúš, J. Kubová, M. Bujdoš, J. Medved': Leaching of aluminium from various reference materials and acid soils with relation to plant availability, *Talanta* 70 (2006) 996-1005
- [10] P. Matúš: Evaluation of separation and determination of phytoavailable and phytotoxic aluminium species fractions in soil, sediment and water samples by five different methods, *J. Inorg. Biochem.* 101 (2007) 1214-1223
- [11] P. Matúš, J. Kubová: Recent developments in the determination, fractionation and speciation analysis of aluminium by spectrochemical analytical methods and computer modelling, v: A.N. Dubois (Ed.), *Soil Contamination: New Research*, Nova Science Publishers, Hauppauge, New York, 2008
- [12] M. Bujdoš, P. Diviš, H. Dočekalová, M. Fišera, I. Hagarová, J. Kubová, J. Machát, P. Matúš, J. Medved', D. Remeteiová, E. Vitoulová: *Špeciácia, špeciálna analýza a frakcionácia chemických prvkov v životnom prostredí*, Univerzita Komenského v Bratislave, Bratislava, 2008

Quantification of Biosorption, Bioaccumulation and Biovolatilization of Labile Aluminium and Thallium Species by Fungal Biomass Using the Atomic Spectrometry Techniques

¹Peter Matúš, ¹Slavomír Čerňanský, ¹Martin Urík, ¹Ján Medved', ¹Marek Bujdoš, ¹Zuzana Kramarová, ¹Milan Kališ, ¹Ingrid Hagarová, ¹Jana Kubová, ¹Jaroslav Ševc, ²Pavel Diviš, ²Lukáš Brulík

¹Comenius University in Bratislava, Faculty of Natural Sciences, Mlynská dolina 1, 842 15 Bratislava 4, Slovakia, e-mail: matus@fns.uniba.sk

²Brno University of Technology, Faculty of Chemistry, Purkyňova 118, 61200 Brno, Czech Republic

Abstract

Paper deals with the investigating of biosorption, bioaccumulation and biovolatilization of labile aluminium and thallium species by biomass of three strains of microscopic filamentous fungi (*Neosartorya fischeri*, *Aspergillus niger*, *Aspergillus clavatus*). The recoveries of studied processes were quantified by the techniques of atomic spectrometry (flame and graphite furnace atomic absorption spectrometry, inductively coupled plasma optical emission spectrometry). Results showed that the highest amounts of labile Al were biosorbed and bioaccumulated by *Aspergillus clavatus*. The amounts of biosorbed, bioaccumulated and biovolatilized of labile Tl by *Neosartorya fischeri* were described also. It is assumed that dimethylthallium (Me_2Tl^+) is the main biovolatilized Tl chemical form.

Key words: aluminium, thallium, fungi, biosorption, bioaccumulation, biovolatilization, F AAS, GF AAS, ICP OES

Introduction

The separation and determination of metal species is the important problem in the environmental analysis in present, since the total concentrations of chemical elements don't represent sufficiently their physiological or clinical impacts [1]. The complexity of laboratory speciation of aluminium and thallium relates to the using of different methods for separation and determination of individual metal species or their operationally/functionally defined fraction [1-6].

Bioaccumulation and biosorption of labile aluminium and thallium species by different kinds of microbial fungi (*Neosartorya fischeri*, *Aspergillus niger*, *Aspergillus clavatus*) were used as the bioseparator-based tools for operationally/functionally defined fractionation of both metals in synthetic solutions. The speciation of both metals was investigated also. The concentrations of Al and Tl were measured by F AAS, GF AAS and ICP OES [7-9].

Experimental

Biosorption of Al and Tl

Compact fungal biomass of *Neosartorya fischeri*, *Aspergillus clavatus* and *Aspergillus niger* was prepared in 100 ml Erlenmeyer flask by the inoculation of 45 ml sterile SAB medium solution with 5 ml spore suspension. After 30-day cultivation the compact fungal biomass was separated from SAB medium solution, moved to the prepared metal nitrate solution and shaken for given time interval. The dead *Neosartorya fischeri* fungal biomass (autoclaved at 120 °C) was used for the evaluation of bioaccumulation effects during the 1-hour biosorption of Al.

Pelletized fungal biomass of *Neosartorya fischeri* was prepared by 3-day cultivation of 10 ml spore suspension in 100 ml SAB medium solution on the shaker. The pelletized fungal biomass (the pellets had a spherical shape with a maximal radius of 0.5 cm) was separated from SAB medium solution, moved to the prepared metal solution and shaken for given time interval. The compact/pelletized fungal biomass and SAB medium were then analysed for total Al and Tl concentration.

Bioaccumulation and biovolatilization of Al and Tl

40 ml sterile Sabouraud (SAB) medium solution in 100 ml Erlenmeyer flask were inoculated with a 5 ml spore suspension of *Neosartorya fischeri*, *Aspergillus clavatus* and *Aspergillus niger*. The inoculated SAB medium was then enriched with 5 ml metal nitrate solution. After 30-day cultivation the compact fungal biomass was separated from SAB medium solution. The compact fungal biomass and SAB medium were then analysed for total Al and Tl concentration.

Decomposition procedure

The fungal biomass samples were decomposed after their drying at 40 °C to a constant weight. High-pressure digestion in closed vessels with 5 ml of concentrated HNO₃ at 160 °C for 5 hours was used.

Validation of analytical procedures

Accuracy of the entire analytical procedures was tested by the analysis of total Al and Tl in certified reference materials (CRM) of water, plant (lucerne) and yeast biomass. All results were consistent with certified values. Further, the analyte addition technique was applied to real samples of fungal biomass digest and SAB medium solutions with the acceptable results.

Measurement conditions

Table 1. Optimal instrumental and working parameters

Spectrometry	F AAS	GF AAS	ICP OES	
Spectrometer	Perkin-Elmer 5000	Perkin-Elmer 3030/HGA 600	Jobin-Yvon 70 Plus	
Metal	Al	Tl	Al	Tl
LOD ($\mu\text{g l}^{-1}$)	150	0.8	10	100
LOQ ($\mu\text{g l}^{-1}$)	500	2.7	33	330
Linearity (mg l^{-1})	100	0.1	800	1000
Wavelength (nm)	309.3	276.8	396.152	351.924
Slit	0.7 nm	0.7 nm	20/25 μm	20/25 μm
Lamp	Perkin-Elmer HCL	Perkin-Elmer EDL	-	-
Platform	-	L'vov pyrocoated	-	-
Gas	Acetylene/Nitrous oxide	Argon	Argon	Argon
Background correction	-	Zeeman	+	+
Signal mode	-	Peak height	Gaussian	Gaussian
Read time (s)	3	5	3	3
Sample volume (μl)	-	20	-	-
Modifier I (1000 mg l^{-1} Pd)				
Volume (μl)	-	8	-	-
Mass (μg)	-	8	-	-

Modifier II (1 % ascorbic acid)				
Volume (μl)	-	5	-	-
Mass (μg)	-	50	-	-

Table 2. Optimal operating program of Perkin-Elmer HGA 600 for the determination of Tl by GF AAS

Step	Temperature ($^{\circ}\text{C}$)	Ramp time (s)	Hold time (s)	Ar flow rate (ml min^{-1})	Read
Drying I	90	10	20	250	
Drying II	120	10	20	250	
Pyrolysis	900	20	10	250	
Atomisation	2000	0	5	0	On
Cleaning	2400	1	3	250	

Speciation of Al and Tl

The speciation of Al(III) and Tl(I) in synthetic solutions was obtained by computer modelling (MINEQL⁺ V 2.2 chemical equilibrium program).

Results

Optimisation of Perkin-Elmer HGA 600 operating program and selection of optimal matrix modifier for the determination of Tl by GF AAS

The sensitivity of thallium determination by GF AAS is strongly dependent to experimental conditions. The pyrolysis and atomisation temperatures were optimiaed in the absence and presence of a Pd-Mg(NO₃)₂ (8 μg Pd + 3 μg Mg(NO₃)₂) and Pd-ascorbic acid (8 μg Pd + 50 μg ascorbic acid) matrix modifiers in SAB medium and fungal biomass digest solutions. Both SAB medium and fungal biomass digest solutions were spiked with 50 $\mu\text{g l}^{-1}$ Tl.

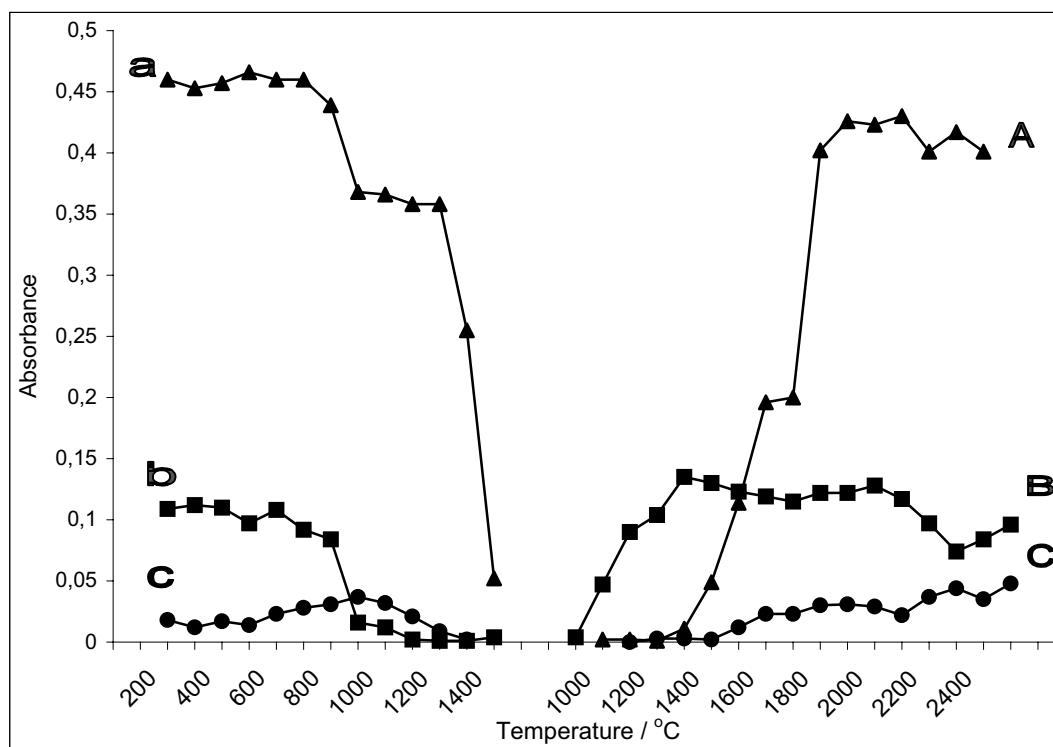


Fig. 1. Pyrolysis (a, b, c) and atomization (A, B, C) curves for Tl in spiked SAB medium solution containing 0 $\mu\text{g l}^{-1}$ Tl: a, A – with modifier Pd-ascorbic acid; b, B – without modifier; c, C – with modifier Pd-Mg(NO₃)₂

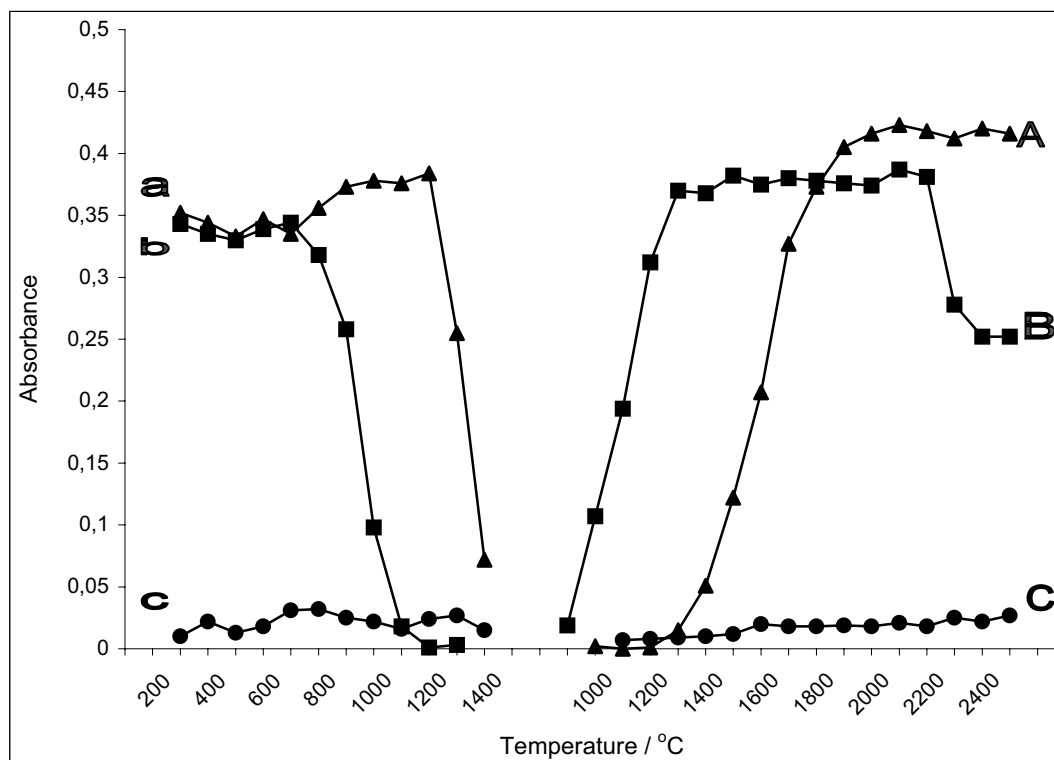


Fig. 2. Pyrolysis (a, b, c) and atomization (A, B, C) curves for Tl in spiked fungal biomass digest solution containing $50 \mu\text{g l}^{-1}$ Tl: a, A – with modifier Pd-ascorbic acid; b, B – without modifier; c, C – with modifier Pd-Mg(NO₃)₂

Integrated absorbance was used for the signal measurement. The pyrolysis and atomization curves for Tl are presented in Fig. 1. (in SAB medium solution) and Fig. 2. (in fungal biomass digest solution). The experimental results show that thallium absorbance decreased in the presence of Pd-Mg(NO₃)₂ matrix modifier for both SAB medium and fungal biomass digest solutions. The optimal pyrolysis and atomisation temperatures and suitable matrix modifier (Pd-ascorbic acid) were selected for Tl determination by GF AAS.

Biosorption of Al and Tl

The sorption equilibrium for both metals and both forms of fungal biomass was stabilized after cca 1 hour, see Fig. 3. and 4. The Al sorption capacity of *Neosartorya fischeri* pelletized biomass seems cca two times higher than Al sorption capacity of *Neosartorya fischeri* compact form. On the contrary in case of Tl the pelletized biomass of *Neosartorya fischeri* has cca two times lower sorption capacity than its compact form. The pH value increased during the biosorption by cca two tenths for Al meanwhile pH value of Tl biosorption decreased by cca two tenths. The time interval 1 hour was selected for the study of biosorption by another fungi, see Table 3. and Fig. 5.

The recovery of 1 h biosorption reached 13-31 % for Al and all three fungi and 12-13 % for Tl and *Neosartorya fischeri*, see Table 3. and Fig. 5. *Aspergillus clavatus* has the highest sorption capacity for Al. The Tl biosorption recovery values are very similar for all three initial amount of Tl (25 μg , 50 μg , 250 μg). The pH values during the biosorption of Al increased (especially for the system Al/*Aspergillus niger*) while in the case of Tl biosorption the pH values slightly decreased for all studied fungi. For the comparison of results also *Neosartorya fischeri* biomass was autoclaved at 120 °C before the Al biosorption but the similar recoveries were obtained. Probably the biological metabolism of *Neosartorya fischeri* has not the most important influence on the biosorption of Al.

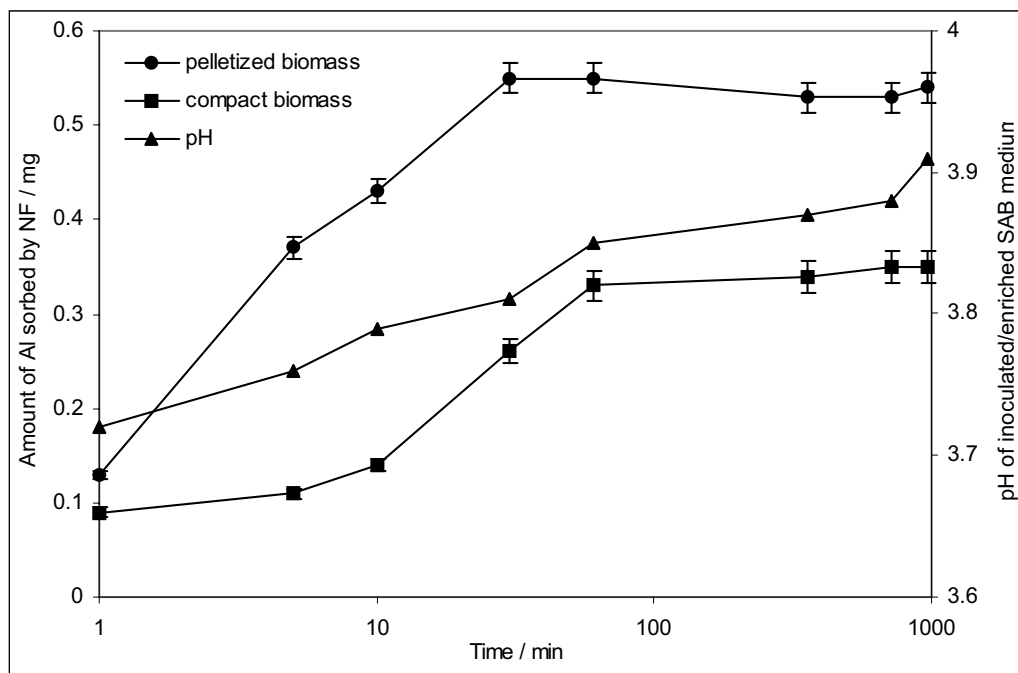


Fig. 3. Results from 16-hour biosorption of Al by compact and pelletized fungal biomass of *Neosartorya fischeri* in $Al(NO_3)_3$ solution with initial amount of 2.5 mg Al (n=3)

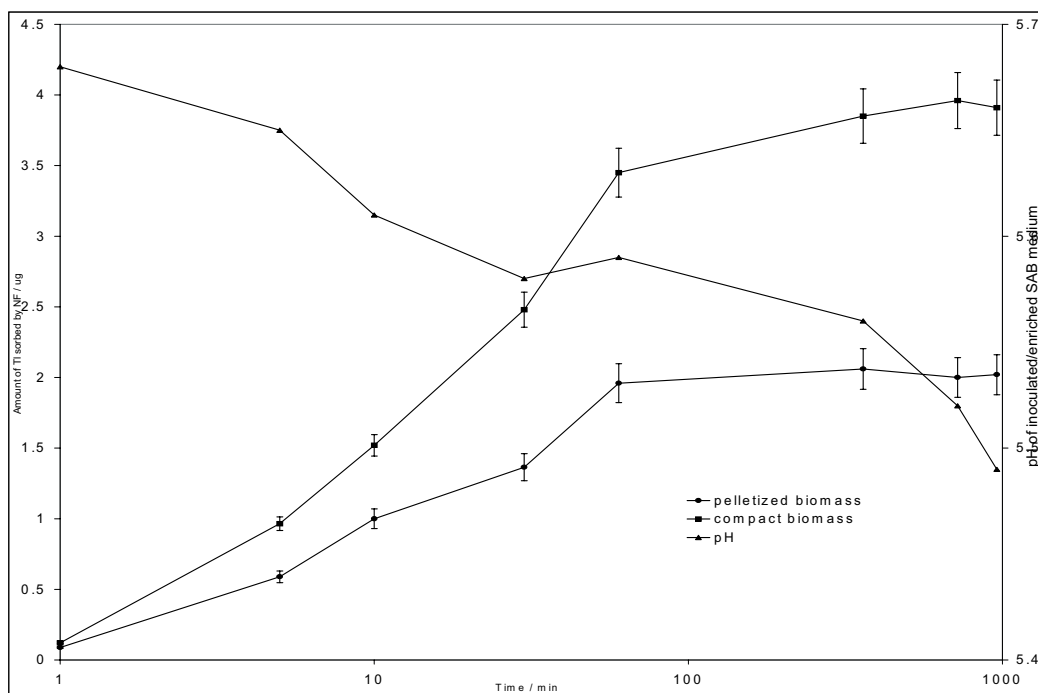


Fig. 4. Results from 16-hour biosorption of Tl by compact and pelletized fungal biomass of *Neosartorya fischeri* in $TlNO_3$ solution with initial amount of 25 µg Tl (n=3)

Table 3. Results from 1-hour biosorption of Al and Tl by compact biomass of selected fungi (n=3); NF, *Neosartorya fischeri*; AC, *Aspergillus clavatus*; AN, *Aspergillus niger*; * NF biomass was autoclaved at 120 °C before the Al biosorption

Metal / Fungi	Initial amount of metal in enriched SAB medium (mg)	Initial / Final pH of enriched SAB medium	Amount of metal non-biosorbed by fungi (mg)	Amount of metal biosorbed by fungi (mg)
Al/NF	2.50	3.70/3.85	2.16±0.09	0.33±0.04
Al/NF*	2.50	3.91/3.93	2.19±0.11	0.34±0.01
Al/AC	2.50	3.95/4.11	1.69±0.12	0.77±0.03
Al/AN	2.50	3.86/4.56	2.01±0.08	0.56±0.03
Tl/NF	25.0 µg	5.61/5.59	26.6±1.6 µg	3.45±0.10 µg
Tl/NF	50.0 µg	5.55/5.50	38.8±3.1 µg	6.04±0.65 µg
Tl/NF	250 µg	5.24/5.02	198±8 µg	31.8±1.8 µg

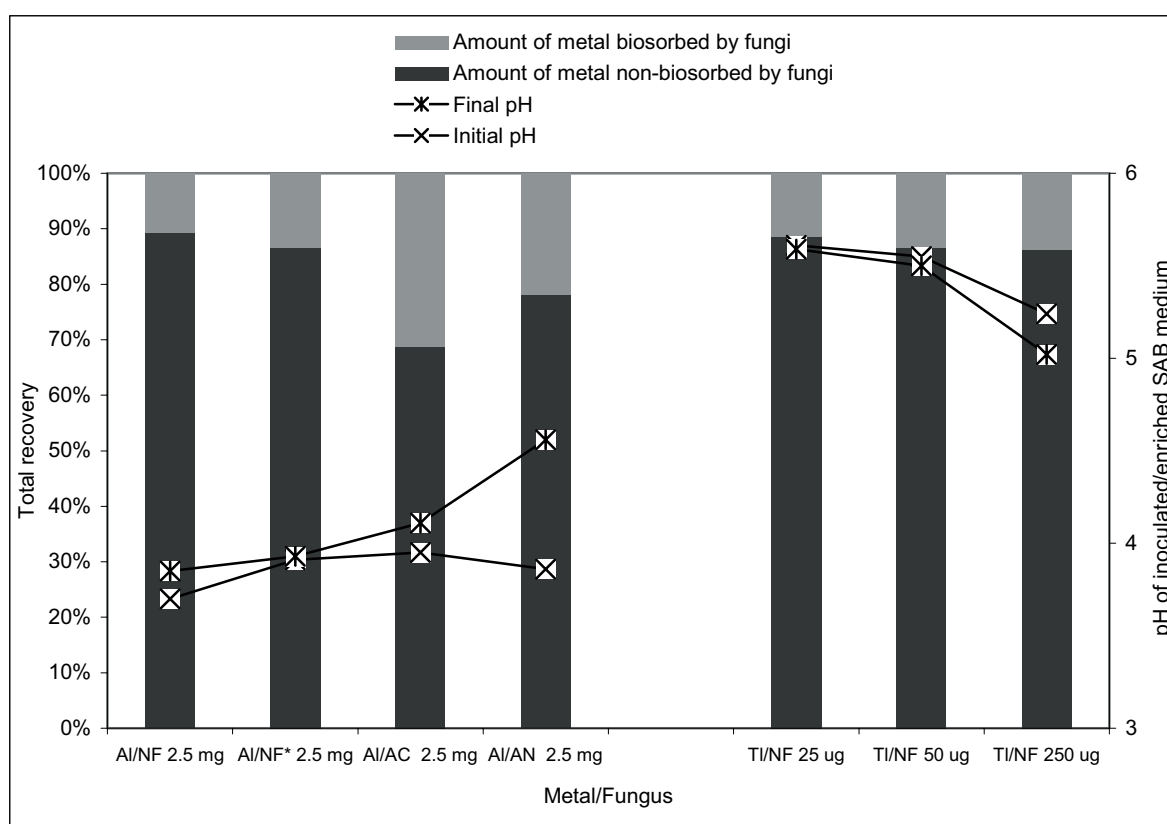


Fig. 5. Results from 1-hour biosorption of Al and Tl by compact biomass of selected fungi (n=3); NF, *Neosartorya fischeri*; AC, *Aspergillus clavatus*; AN, *Aspergillus niger*; * NF biomass was autoclaved at 120 °C before the Al biosorption

Bioaccumulation and biovolatilization of Al and Tl

The results from 30 day bioaccumulation and biovolatilization of Al and Tl are showed in Table 4. and Fig. 6. The obtained data refer to 44-75 % bioaccumulation of Al for all studied fungi, 32-57 % bioaccumulation of Tl and 22-31 % biovolatilization of Tl for *Neosartorya fischeri* after 30 day experiment. The highest amount of Al was bioaccumulated by *Aspergillus clavatus*. The different initial amounts of Tl (50 µg and 250 µg) caused different Tl bioaccumulation and biovolatilization recovery values. The biggest change in pH values was observed for the system Al/*Aspergillus niger*, similarly like in the case of Al biosorption. Likewise the trends of pH changes are the same like in the

case of Al and Tl biosorption, i.e. the pH values during the bioaccumulation of Al increased while in the case of Tl bioaccumulation and biovolatilization the pH values decreased.

Table 4. Results from 30-day bioaccumulation of Al and Tl by compact biomass of selected fungi (n=5); NF, *Neosartorya fischeri*; AC, *Aspergillus clavatus*; AN, *Aspergillus niger*; ND, not detected

Metal / Fungi	Initial amount of metal in enriched SAB medium (mg)	Initial / Final pH of enriched SAB medium	Amount of metal non-bioaccumulated by fungi (mg)	Amount of metal bioaccumulated by fungi (mg)	Amount of metal biovolatilized by fungi (μg)
Al/NF	2.50	3.74/4.02	1.46 \pm 0.11	1.11 \pm 0.06	ND
Al/AC	2.50	3.89/4.29	0.63 \pm 0.03	1.88 \pm 0.08	ND
Al/AN	2.50	3.91/7.56	0.89 \pm 0.06	1.65 \pm 0.05	ND
Tl/NF	50.0 μg	5.43/3.86	23.1 \pm 0.8 μg	15.8 \pm 0.7 μg	11.8 \pm 0.7
Tl/NF	250 μg	5.18/3.62	27.8 \pm 1.1 μg	143 \pm 5 μg	72.8 \pm 2.3

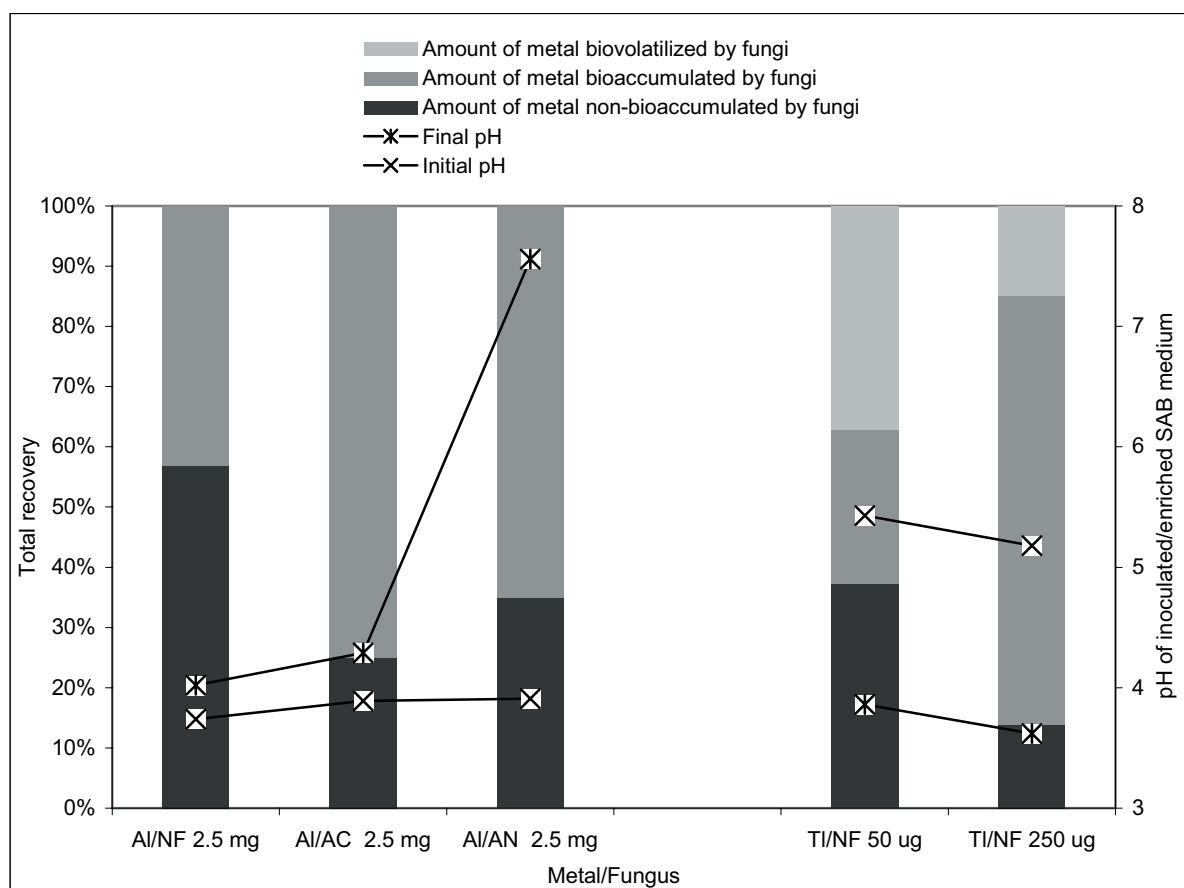


Fig. 6. Results from 30-day bioaccumulation of Al and Tl by compact biomass of selected fungi (n=5); NF, *Neosartorya fischeri*; AC, *Aspergillus clavatus*; AN, *Aspergillus niger*

Speciation of Al and Tl

The results obtained from computer modeling show that only soluble inorganic momomers of Al(III) and Tl(I) are presented in the prepared water synthetic solutions at given pH values. These species are considered to be the most toxic for both metals.

The labile aqua cations Al^{3+} , $\text{Al}(\text{OH})^{2+}$ and $\text{Al}(\text{OH})_2^+$ are the prevailing species below pH 5.0. In the pH range between 5.0 and 6.2, there is a mixture of these cations and colloidal $\text{Al}(\text{OH})_3$ species. At pH higher than 6.2, the dominant species is $\text{Al}(\text{OH})_4^-$.

The labile cations Tl^+ and relatively weak neutral complexes (TlNO_3 , TlOH) are the prevailing species at given conditions. It is assumed that dimethylthallium (Me_2Tl^+) is the main Tl chemical form biovolatilized by fungal biomass of *Neosartorya fischeri*.

Conclusion

In certain conditions the studied fungi can be also used as the bioanalytical tools for operationally and/or functionally defined fractionation of both metals. This approach can be used for in-situ separation of toxic Al and Tl species directly in the ecosystem, e.g. in the analysis of polluted waters. The biotechnological application of the remediation techniques by long-term bioaccumulation of both metals by studied fungi presented in contaminated areas affected e.g. by acidification processes from mine activity can markedly help in the revitalization of given ecosystem.

Acknowledgements

The work was supported by Science and Technology Assistance Agency under the contracts No. APVT-20-010204, LPP-0038-06, LPP-0188-06 and SK-CZ-0044-07, by Scientific Grant Agency of Ministry of Education of Slovak Republic and the Slovak Academy of Sciences under the contracts No. VEGA 1/3555/06, VEGA 1/3561/06, VEGA 1/4463/07, VEGA 1/4464/07 and VEGA 1/0272/08 and by Ministry of Education, Youth and Sports of Czech Republic under the contract No. MEB 080813.

References

- [1] M. Bujdoš, P. Diviš, H. Dočekalová, M. Fišera, I. Hagarová, J. Kubová, J. Machát, P. Matúš, J. Medved', D. Remeteiová, E. Vitoulová: Špeciácia, špeciálna analýza a frakcionácia chemických prvkov v životnom prostredí, Univerzita Komenského v Bratislave, Bratislava, 2008
- [2] P. Matúš, J. Kubová, Speciation of aluminium in waters and soil solutions, Chem. Listy 96 (2002) 174-181
- [3] J. Kubová, V. Streško, P. Matúš, Analytical methodologies for aluminium speciation in environmental samples – a review, Slovak Geol. Mag. 9 (2003) 125-127
- [4] P. Matúš, State of the art in determination, fractionation and speciation analysis of aluminium in environmental samples by spectrochemical analytical methods, Trans. Univ. Košice 2-3 (2006) 80-91
- [5] P. Matúš, J. Kubová, Recent developments in the determination, fractionation and speciation analysis of aluminium by spectrochemical analytical methods and computer modelling, v: A.N. Dubois (Ed.), Soil Contamination: New Research, Nova Science Publishers, Hauppauge, New York, 2008
- [6] M. Kališ, P. Matúš, M. Bujdoš, J. Medved': Fractionation, speciation analysis and determination of the thallium in the environmental samples, Chem. Listy 101 (2007) 782-789
- [7] P. Matúš, S. Čerňanský, M. Urík, J. Medved', M. Bujdoš, I. Hagarová, J. Kubová, M. Kališ: Biosorption and Bioaccumulation of Labile Aluminium and Thallium Species by Fungal Biomass, XXXV Colloquium Spectroscopicum Internationale, Xiamen, 23-27 September 2007, Abstract Book, 405

- [8] P. Matúš, M. Urík, S. Čerňanský, J. Medved', M. Bujdoš, I. Hagarová, J. Kubová, M. Kališ: Bioaccumulation and Biosorption of Labile Aluminium and Thallium Species by Microscopic Filamentous Fungi – Suitable Bioseparator-Based Tools for Metal Fractionation Analysis, 22nd International Symposium on MicroScale Bioseparations and Methods for Systems Biology, Berlin, March 9-13, 2008, Book of Abstracts, 331
- [9] L. Brulík, M. Bujdoš, S. Čerňanský, P. Diviš, Z. Kramarová, P. Matúš, J. Medved', J. Ševc, M. Urík: Fractionation and speciation analysis of aluminium and thallium after bioaccumulation and biosorption their labile species by microscopic filamentous fungi and computer modelling, 35th International Symposium on Environmental Analytical Chemistry, Gdansk, June 22-26, 2008, Book of Abstracts, 187

Solid-Phase Extraction and ETAAS Determination of Thallium Species in Water Samples

Ján Medved', Milan Kališ, Ingrid Hagarová, Marek Bujdoš, Peter Matúš, Jana Kubová
Comenius University in Bratislava, Faculty of Natural Sciences, Geological Institute, Mlynská dolina G, 842 15 Bratislava 4, Slovak Republic, e-mail: medvedj@fns.uniba.sk

Abstract

Thallium species in natural water samples was determined by electrothermal atomic absorption after solid –phase extraction from 1000 mL sample solution. In this method, Tl(III) was stabilized by formation of a cationic Tl(III)-DTPA complex. Tl(I) remained in its original form. The two species were separated by using a strong acid, gel-type cation exchange resin Amberlite IR120 and nitric acid as the eluent. The calibration curve for thallium was linear from 4 to 100 $\mu\text{g L}^{-1}$. The limit of detection (LOD) and the limit of determination (LOQ) were about 1.0 $\mu\text{g L}^{-1}$ and 3.6 $\mu\text{g L}^{-1}$. The accuracy of the analytical results for Tl was checked by the analysis of the known concentrations of the Tl species in the water samples. Precision expressed by a RSD varied in the range from 3 – 19 %. The optimized conditions for separation/preconcentration technique and ETAAS determination were used for the determination of thallium species in acid attacked waters (acid mine drainage which is mainly a product of pyrite oxidation) from open quartzite mine in the Banska Stiavnica – Sobov region (Slovakia).

Key words: *thallium, Water, speciation, solid phase extraction, preconcentration, ETAAS*

1. Introduction

Thallium is a very toxic metallic element, which occurs in earth's crust in an estimated abundance from 0.1 to 0.8 mg.kg^{-1} . In the environment, it is mainly combined with other elements (primarily oxygen, sulfur, halogens, K and Rb) in inorganic compounds. During the weathering processes it can be mobilized by aqueous media and accumulated in sediments and soils. The main sources of pollution nowadays come from anthropogenic emissions from refineries, coal-fired power stations, mining activities, metal smelters and the cement industry [1]. In natural waters, it can exist as either Tl(I) or Tl(III). Its oxidation state affects its complexation and subsequent bioavailability and toxicity. Thallium content in surface waters is within the range 1.2 - 82 ng L^{-1} [2]. Humans may be toxically exposed to thallium by ingestion, inhalation or dermal absorption. Due to the low contents of thallium species Tl(I) and Tl(III) in water samples, it is necessary to combine laboratory instrumentation with preconcentration and separation techniques [3,4]. Electrothermal atomic absorption spectrometry (ETAAS) is widely used for the determination of Tl, due to its high sensitivity [5]. The scope of the presented work was to use an ion-exchange separation/preconcentration technique for thallium species in waters followed by ETAAS determination. In this method, Tl(III) was stabilized by formation of a cationic Tl(III)-DTPA complex. Tl(I) remained in its original

form. The two species were separated by using a strong acid, gel-type cation exchange resin Amberlite IR120 and nitric acid as the eluent.

2. Experimental

2.1 Apparatus

The experiments were performed using a Perkin–Elmer atomic absorption spectrophotometer (Zeeman/3030) with a graphite furnace atomizer (HGA 600), and an autosampler (AS-60). Pyrocoated graphite tubes with pre-inserted L'vov platforms (Id. No.: BO112660) were purchased from Perkin-Elmer. The instrumental parameters and temperature programme for the thallium measurements are gathered in Table 1.

Table 1. Instrumental parameters and thermal programme for thallium determination by ETAAS

Wavelength	276.8 nm				
Spectral width slit	0.7 nm				
Lamp	Perkin-Elmer EDL system				
Lamp power	7 W				
Background correction	Zeeman-effect BC				
Sample volume	20 μL				
Modifier volume I. (Pd solution – 1000 mg L^{-1} Pd)	8 μL (8 μg mass of Pd)				
Modifier volume II. (Ascorbic acid – 1 % solution)	5 μL (50 μg mass of ascorbic acid)				
Calibration mode	Peak height				
Step	Temperature ($^{\circ}\text{C}$)	Ramp (s)	Hold (s)	Ar flow rate (mL min^{-1})	Read
Drying	90	10	20	250	On
	120	10	20	250	
Pyrolysis	900	20	10	250	
Atomization	2100	0	5	0	
Cleaning	2400	1	4	250	

2.2 Reagents

Analytical-grade reagents and doubly distilled water were used.

Standard Tl solutions: A stock solution of Tl(I) was prepared by dissolving a commercial standard solution (Titrisol, Merck) containing 1 g of Tl(I) in the form of TlNO_3 in 1 L of water. A 1 000 mg L^{-1} Tl(III) stock solution was prepared by dissolving an appropriate amount of $\text{Tl}(\text{NO}_3)_3 \cdot 3\text{H}_2\text{O}$ (Sigma Aldrich) in 1 L of water.

Stabilizer of Tl(III): A 10 mmol L^{-1} HNO_3 and 5 mmol L^{-1} DTPA (diethylenetriamine-pentaacetic acid, Merck) was used for standard solution containing Tl(III) [5].

Chemical modifier solutions: A $\text{Pd}(\text{NO}_3)_2$ in 1 % (v/v) HNO_3 (1000 mg L^{-1} of Pd), and ascorbic acid in H_2O (10.0 g L^{-1} of ascorbic acid) were obtained from Analytika (Prague, Czech Republic).

Cation exchange resin: AMBERLITE[®] IR-120 strongly acidic cation exchange resin, sodium form (Rohm and Haas Company, Philadelphia, USA).

2.3 Preparation of water samples

Water samples from the defined sampling points were collected in PE bottles and filtered through a Whatman 0.45 μm filter to remove the suspended solids. The filtrates were then acidified to the pH about 2-3 with distilled HNO_3 and stabilized with 5 mmol/L DTPA, and stored in a refrigerator (4 $^{\circ}\text{C}$) until analysis. After stabilisation of Tl(III) two species exist in aqueous media as Tl(I) and

[Tl(DTPA)]²⁻ [5]. Aliquots (1 L) of water samples were subjected to the separation and preconcentration methodology as described below.

2.4 Separation and preconcentration procedure

0.2 g of AMBERLITE® IR-120 strongly acidic cation exchange resin, sodium form was added to aliquot of 1000 mL of water sample (pH 2-3; stabilized with DTPA). The suspension was stirred (400 rpm) for 15 min at 60 °C. A cation exchange resin AMBERLITE® IR-120 with bound Tl(I) was filtered and eluted with 5 mL of HNO₃. The solution was transferred to 25 mL volumetric flask and filled up to the mark with the doubly distilled water. The total Tl could be analyzed after the rapid reduction of Tl(III) by hydrazine into Tl(I) and by the replication of preconcentration procedure. 40-fold enrichment was thus attained within a few min.

3. Results and discussion

3.1 Optimisation of the furnace conditions

Optimisation of the furnace conditions for the determination of thallium species in water samples was focused mainly on the study of pyrolysis and atomisation temperatures with and without using of the Pd-ascorbic acid (8 µg of Pd + 50 µg of ascorbic acid) chemical modifiers. Thallium solutions (containing a 25 µg L⁻¹ Tl(I) and 25 µg L⁻¹ Tl(III)) in a water matrix solution and aqueous standards were used for the pyrolysis and atomization curves measurement. In order to check for matrix effects on thallium species atomized from real samples, the water sample No. 5 was used. No matrix effects were observed for determination of thallium in the aqueous standard and water sample by using the modifiers. On the contrary, a depressive effect was observed when thallium was atomized from aqueous standard without modifiers. With no modifiers, thallium was lost at relatively low pyrolysis temperature (600 °C). The chemical modifiers containing Pd + ascorbic acid efficiently stabilised thallium; losses were observed from 900 °C. The optimal atomisation temperature of 2100 °C can be used in all the cases. Comparing sensitivity and accuracy in the presence of the chemical modifiers and in the absence of any modifier, higher sensitivity and satisfactory accuracy was observed in the presence of the Pd-ascorbic acid modifiers. The pyrolysis and atomization curves obtained in the presence of the studied modifiers and in the absence of any modifier are shown in Fig. 1.

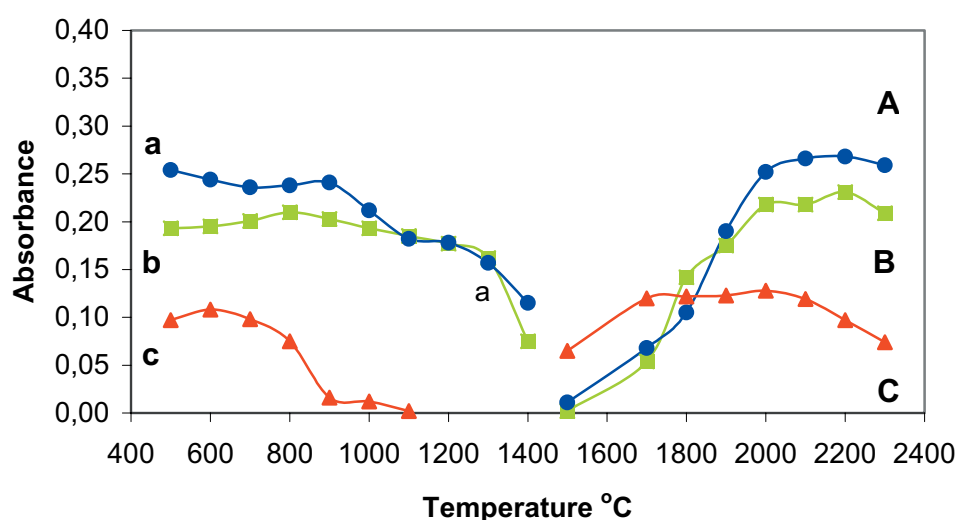


Fig. 1. Pyrolysis (a, b, c) and atomization (A, B, C) curves for Tl (containing a 25 µg L⁻¹ Tl(I) and 25 µg l⁻¹ Tl(III)). a, A – in a water matrix solution (sample 5) with Pd + ascorbic acid chemical modifiers; b, B – in a aqueous standard solution with Pd + ascorbic acid chemical modifiers and c, C – in an aqueous standard solution without chemical modifiers

3.2 Effect of pH

The optimum pH values for the separation/preconcentration of Tl(I) by using a cation exchange resin AMBERLITE® IR-120 were pursued. Fig. 2 shows the effect of pH on the sorption of Tl(I). It was found that the optimum pH value for sorption of Tl(I) was in the pH range 2-3.

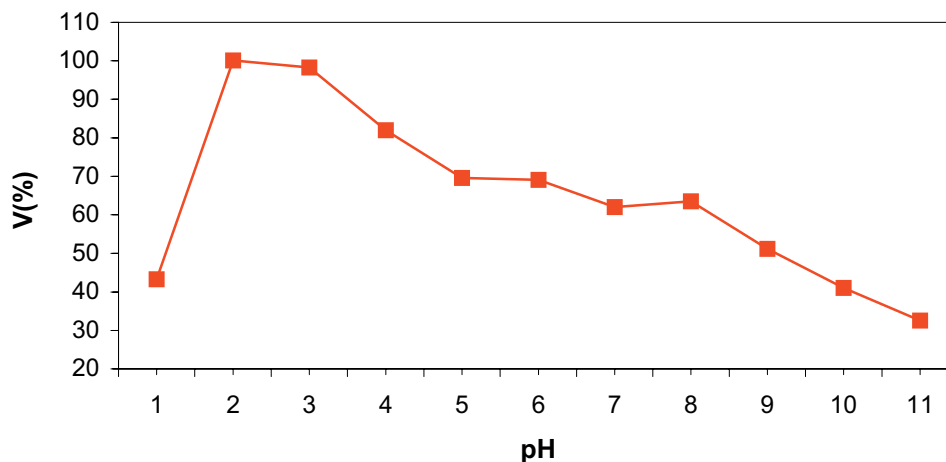


Fig. 2. The sorption yield (V) dependence of Tl(I) on the pH. $V=c_s/c_o \cdot 100$ [%], c_s – determined concentration, c_o – added concentration; Applied condition is 50 mL of $50 \mu\text{g L}^{-1}$ Tl(I), 0.2 g resin AMBERLITE® IR-120 and 5 mL HNO_3 as eluent; $\theta = 70^\circ\text{C}$, incubation time = 15 min

3.3 Effect of incubation time and temperature

The incubation time and temperature of the Tl(I) sorption on the cation exchange resin AMBERLITE® IR-120 were also optimized. The dependence of sorption efficiency upon incubation time was studied in the range 5-120 min (Fig. 3). An incubation time of 15 min was sufficient for quantitative sorption of the Tl(I) on the resin. The sorption temperature was studied in the range from 30 to 90°C . The optimum temperature for the efficiency of thallium sorption was at 60°C .

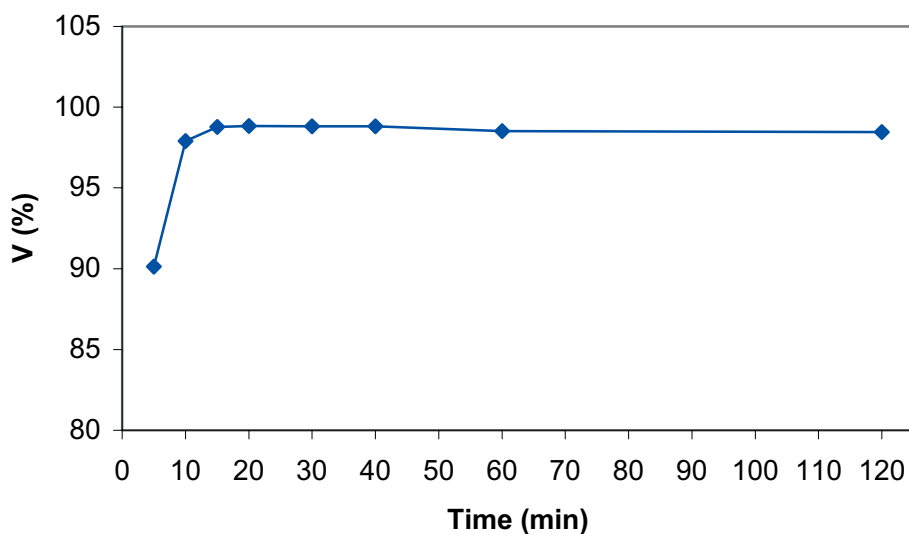


Fig. 3. The sorption yield (V) dependence of Tl on the time. $V=c_s/c_o \cdot 100$ [%]; c_s – determined concentration; c_o – added concentration. Applied condition is 50 mL of $50 \mu\text{g L}^{-1}$ Tl(I), 0.2 g resin AMBERLITE® IR-120 and 5 mL HNO_3 as eluent; $\theta = 70^\circ\text{C}$, incubation time = 15 min

3.4 Interferences

The ETAAS method is sensitive to interferences by other elements e.g. halides and Fe, which can considerably reduce the signal [6]. The interference effects from various inorganic constituents of natural waters was studied. It was observed that the anions SO_4^{2-} and HPO_4^{2-} (excepting Cl^- , which is leading in studied water samples), show no interference for the determination of Tl. The cations Fe(III) and Al(III) can form complexes with DTPA and may elute with Tl(III)-DTPA. Ca(II) and Mg(II), which are abundant in natural waters pose as no treat to the analytical procedure since they show no affinity for the selected cation exchange resin. Other metal species were not found to affect the analytical results.

3.5 Characteristics of the method

A calibration curve was constructed by using 20 μL of the 5, 10, 30, 50 and 100 $\mu\text{g L}^{-1}$ Tl(I) standard solutions with 8 μL Pd solution (1 000 mg L^{-1} Pd) and 5 μL ascorbic acid (1% solution) as chemical modifiers. Under the optimum experimental conditions, the calibration curve for thallium was linear from 3 to 100 $\mu\text{g L}^{-1}$ (Fig. 4).

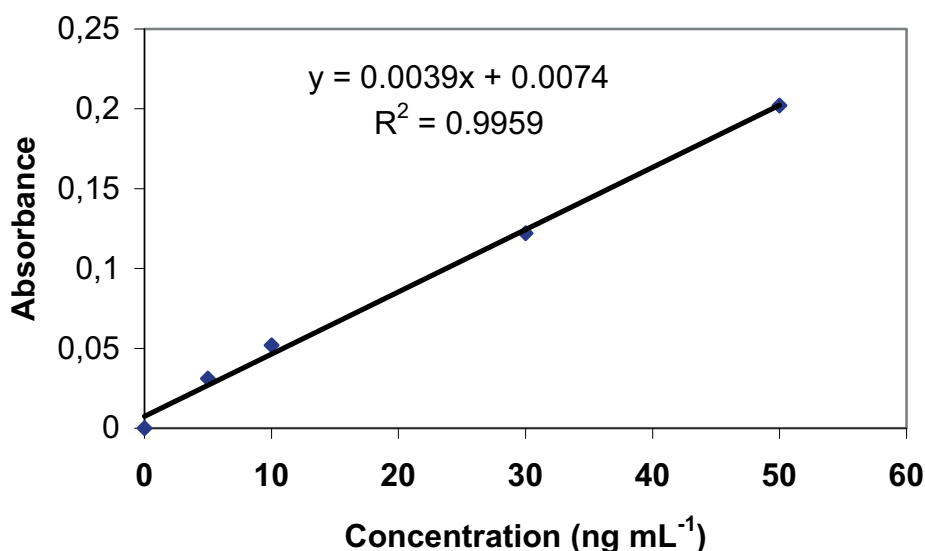


Fig. 4. Calibration curve for Tl(I) using peak height as response function

The enhancement factor of about 40 was obtained by preconcentration 1 000 mL of sample. The limit of detection (LOD) and the limit of determination (LOQ) in $\mu\text{g L}^{-1}$ were calculated as follows: $\text{LOD} = x_{b1} + 3s_{b1}$; $\text{LOQ} = x_{b1} + 10s_{b1}$; where x_{b1} is the mean of the blank measurements and s_{b1} is the standard deviation of the blank measurements. The LOD and LOQ values for Tl was about 1.0 $\mu\text{g L}^{-1}$ and LOQ was 3.6 $\mu\text{g L}^{-1}$. The accuracy of the analytical results for Tl was checked by the analysis of the known concentrations of the Tl species in the water samples. The measured concentrations and recoveries are summarised in Table 2. The F-test ($\alpha = 0.05$) showed non-significant differences between the obtained content of Tl species and the known values. Precision expressed by a RSD varied in the range from 3 – 19 %.

3.6 Application of Zeeman – ETAAS for Tl speciation

In order to validate the method for accuracy and precision water samples with known concentrations of the Tl species were analysed. The measured concentrations and recoveries are summarised in Table 2. The known values are in good agreement with obtained values and very good recoveries were obtained (from 96 to 102 %). These results showed no matrix interferences.

Table 2. Determination of various Tl(I) and Tl(III) concentrations in water samples (n = 5)

Water sample	Known ($\mu\text{g L}^{-1}$)	Tl(I) determined ($\mu\text{g L}^{-1}$)	RSD (%)	Recovery (%)	Known ($\mu\text{g L}^{-1}$)	Tl(III) determined ($\mu\text{g L}^{-1}$)	RSD (%)	Recovery (%)
1	90	90.2 \pm 4,9	5.4	100.2	10	9.7 \pm 1.8	18.5	97.0
2	80	78.3 \pm 3.6	4.5	97.9	20	19.8 \pm 2.1	10.8	99.0
3	70	70.3 \pm 3	4.3	100.4	30	29.2 \pm 2.2	7.5	97.3
4	50	48.0 \pm 4.3	8.9	96.0	50	49.8 \pm 3.6	7,2	99.6
5	30	30.5 \pm 2.4	8.0	101.7	70	68.5 \pm 2.2	3.2	97.8
6	10	9.7 \pm 1.6	16.9	97.0	90	89.3 \pm 3.2	3.6	99.2

4. Conclusion

An analytical Zeeman–ETAAS method enabling the separation/preconcentration and determination of Tl species in an experimental procedure was presented. The methodology offers simple, fast, rapid, sensitive, good extraction efficiency, accurate, interference-free and gives a low limit of detection and good RSD. The proposed method will be applied for separation/preconcentration and ETAAS determination of thallium species in acid attacked waters (acid mine drainage which is mainly a product of pyrite oxidation) from open quartzite mine in the Banska Stiavnica – Sobov region (Slovakia).

Acknowledgements

This work was financially supported by Scientific Grant Agency of the Ministry of Education of the Slovak Republic and the Slovak Academy of Sciences under the contracts No. VEGA 1/3555/06, VEGA 1/3561/06, VEGA 1/4464/07 and VEGA 1/0272/08 and by Slovak Research and Development Agency under the contracts No. LPP-0038-06 and SK-CZ-044-07 and by Ministry of Education, Youth and Sports of Czech Republic under the contract No. MEB 080813.

References

- [1] Adriano, D.C.: Trace Elements in Terrestrial Environments - Biogeochemistry, Bioavailability, and Risks of Metals (Sec. Ed.) Springer – New York: 2001
- [2] Lin, T.J., Nriagu, J.: Thallium speciation in river waters with Chelex-100 resin. *Analytica Chimica Acta*, 1999, 395, 301-307
- [3] Stafilov, T., Čundeva, K.: Determination of total thallium in fresh water by electrothermal atomic absorption spectrometry after colloid precipitate flotation. *Talanta*, 1998, 46 (6), 1321-1328
- [4] Meng, Ya.J., Zhang, Z.R., Zheng, B. Hu, J.T.: Determination of trace thallium by platform-GFAAS after preconcentration with polyurethane foam. *Journal of Sichuan University (Medical Ed.)*, 2006, 37, 305-308
- [5] Coetzee, P.P., Fischer, J.L., Hu, M.: Simultaneous separation and determination of Tl(I) and Tl(III) by IC-ICP-OES and IC-ICP-MS. *Water SA*, 2003, 29, 17-22
- [6] Griepink, B., Sager, M., Tölg, G.: Determination of traces of thallium in various matrices. *Pure & Applied Chemistry*, 1988, 60 (9), 1425-1436

Simultaneous Determination of Trace Amounts of Mercury and Copper by Derivative Spectrophotometric H-Point Standard Addition Method after their Separation and Preconcentration on Modified Natural Clinoptilolite Zeolite

¹Alireza Mohadesi, ²Rasool Roohparvar, ²Mohammad Ali Taher

¹ Department of Chemistry, Payame Noor University (PNU), P.O. Box 76175-559, Kerman, Iran,
e-mail: mohadesi_a@yahoo.com

² Department of Chemistry, Shahid Bahonar University, P.O. Box 76175-133, Kerman, Iran

Abstract

As a part of removal of toxic heavy metals from hazardous fruits and vegetables, solid phase extraction of mercury(II) and copper(II) at trace and ultra trace levels were studied using 2-nitroso-1-naphthol-4-sulfonic acid (Nitroso-S) modified natural clinoptilolite zeolite. This method has been developed for the simultaneous preconcentration and determination of mercury and copper based on the adsorption of their Nitroso-S complexes on a natural clinoptilolite zeolite. The adsorbed complexes could be eluted using dimethylformamid and the concentration of mercury and copper were determined by derivative spectrophotometry at appropriate ($dA/d\lambda$)s in order to work on the basis of H-point standard addition method. In optimum conditions, detection limits in original solution are obtained 0.1 ng/mL for mercury and 0.5 ng/mL for copper. The preconcentration factor attainable for quantitative recovery (> 95 %) of mercury(II) and copper(II) were 95 and 110, respectively. Five times replicating determination a mixture of mercury and copper in 5.0 mL final solution gave a relative standard deviation of 3.6 % for Hg(II) and 2.8 % for Cu(II). The suggestive method is applied to determine of mercury and copper ions in plant and biological samples successfully.

Key words: mercury(II), copper(II), solid phase extraction, H point standard addition method, derivative spectrophotometry

Introduction

Mercury is widely distributed in nature, circulating among several media and occurring in different chemical forms, which shows various degrees of toxicity, especially its organospecies [1-3]. Mercury and its compounds are included in all lists of priority pollutants. Different regulations and guidelines have been developed to limit their levels in water and sediments [4]. From health and biological viewpoints, some attention has been focused on the toxicology of mercury in low concentration. For example, mercury can cause allergic reactions and also certain mercury compounds would be carcinogenic [5-6]. Toxicity of copper is also distinguished when organisms are excessively

exposed, homeostatic control mechanisms become overwhelmed, and toxicity arises owing to copper adverse effects on the structure and function of macromolecules such as DNA and proteins [7-8]. In total, to estimate effectively the hazards involved; the variation in toxicity, transport and bioavailability, which are dependent on the chemical species of mercury and copper must be taken into account. Copper and mercury can be together or alone in many real samples. Simultaneous preconcentration of copper and mercury is required to meet the detection limits as well as to determine the lower concentration levels of the favorite analyte [5].

The H-point standard addition method (HPSAM) is one of the mathematical treatment data procedures utilized for the analysis of multicomponent systems. The principles of HPSAM were presented by Campins-Falco [9]. The main advantages of the HPSAM are that it can eliminate and evaluate the errors resulting from an interfering and blank reagent. Principle component analysis for selection of variable in the application of HPSAM was developed [10]. The use of HPSAM with derivative analytical methods has seldom been investigated. HPSAM as well as derivative spectrophotometry was used for glafenine and glafenic [11], cephalosporins and ninhydrin [12], ninhydrin and cefoxitin [13], cobalt and nickel [14] and copper and nickel [15].

In this work, Combining of first-order derivative spectrophotometry (FDS) with H-point standard addition method (HPSAM) has been satisfactorily applied for the determination of mercury(II) in fruits and vegetables in the presence of copper(II). This has been done after separation and preconcentration of these metals from a large aqueous solution on surfactant modified clinoptilolite that is loaded with 2-nitroso-1-naphthol-4-sulfonic acid (Nitroso-S) as a new sorbent. One of the important points of this work is the possibility to use a cheap natural adsorbent for preconcentration of trace amounts of mercury and copper ions in the regime of solid phase extraction (SPE).

Experimental

Apparatus and reagents

UV-Visible absorbance spectra were recorded on a Varian scanning spectrophotometer (model CARY 50 Conc) using quartz cells. Metrohm pH-meter (model 713) with a combined glass electrode (Metrohm) was used for pH measurements. A mechanical shaker with speed control was used for the preparation of the zeolite. A glass column (500×10 mm) equipped with Teflon tap was used as column for preconcentration steps. The all glass apparatus were soaked in 4 mol/l HNO₃ overnight and cleaned with double distilled water before use.

1000 µg/mL stock solution of mercury(II) was prepared by dissolving 0.4045 g of the mercury nitrate (Merck, analytical grade) in 250.0 mL of distilled water. Standard solutions of this metal ion were prepared daily by stepwise dilution of 1000 µg/mL stock solution with 0.1% (v/v) nitric acid. The stock copper(II) solution (1000 µg/mL) was prepared by dissolving 0.2500 g of copper powder 99.9995 % (Aldrich) in a minimum volume of 1:1 nitric acid [0.1 % (v/v)] and heating. The solution was boiled to expel brown fumes, cooled and diluted with distilled water to 250.0 mL. The standard working solutions were diluted prior to use. A 0.1 % Nitroso-S solution and 0.5 % benzyldimethyl-tetradecylammonium chloride (BDTA) (Merck, analytical grade) in water were prepared. Solution of alkali metal salts and various metal salts were used for studying of anionic and cationic interferences, respectively. Buffer solution of pH 8.5 was prepared from 0.5 mol/l ammonia and 0.5 mol/l ammonium chloride. Natural clinoptilolite zeolite was collected from Semnan, Iran.

Zeolite modification

The structure of clinoptilolite zeolite was determined by wet chemical method and XRD. The chemical composition of zeolite was reported to be 67.6 % SiO₂, 13.9 % Al₂O₃, 0.7 % Fe₂O₃, 3.1 % CaCO₃, 1 % MgO, 0.3 % Na₂O, 2.6 % K₂O, 10.8 % H₂O. After purification of zeolite [16], clinoptilolite zeolite was milled and sieved to fraction grain size 110-125 µm. 10 g of powdered clinoptilolite was shaken with 100 mL of 1.0 mol/l ammonium nitrate for three days to decreasing of

calcite impurities. After that clinoptilolite was dried in an oven at 100 °C. Ammonium ions have high affinity to clinoptilolite, so they can replace other cations. For preparation of H-form of clinoptilolite, it was put in furnace at 380 °C for 2 h. Clinoptilolite was saturated with cadmium to ensure a uniform substrate and prevent to entire of copper and mercury ions in the porous of clinoptilolite by shaking 10 g of clinoptilolite for 2 h with 100 mL of 100 $\mu\text{g l}^{-1}$ cadmium solution. This was followed by 2 rinses nitric acid 4 mol/l and 3 rinses with distilled water, then air drying. The cadmium-saturated clinoptilolite was modified with BDTA. The BDTA reagent was added to zeolite for increase the adsorption of ligand on to zeolite [17]. Surfactant modification consisted of 10 g of clinoptilolite with 250 mL of the BDTA solution (0.5 %) for 24 h at 25 °C. This amount of time was shown to be sufficient for complete reaction of BDTA on clinoptilolite. The BDTA-modified clinoptilolite was placed on a paper filter in a buchner funnel, rinsed with 30 to 50 mL of distilled water and air-dried.

1 g of the BDTA modified clinoptilolite was added to a glass column (500 mm height \times 10 mm internal diameter) equipped with Teflon tap. Then 5 mL of Nitroso-S solution (0.1%) passed through it at flow rate of 1 mL/min. After sample loading the column was preconditioned by passing a buffer solution.

Procedure for the sorption of copper and mercury ions on the column

An appropriate amount of sample solution containing mercury and copper, and various standard solutions of mercury or copper in appropriate volumes were poured into a 100 mL beaker and it was added to it 5.0 mL of buffer solution with pH 8.5, then diluted to 50 mL with distilled water. This solution was passed through the column at flow rate 3 mL/min. After passing this solution, the column was washed with 2 mL of distilled water. The adsorbed copper and mercury ions on the column were eluted with 5.0 mL DMF, at flow rate 1 mL/min. The eluent was collected in a 5.0 mL volumetric flask. The first derivative spectra of the working solutions were recorded against reagent blank solution in the range of 400 – 650 nm. Simultaneous determination of Hg(II) and Cu(II) with FDS-HPSAM was performed by measuring the first derivative spectra at 556 and 623 nm with wavelength interval ($\Delta\lambda$) = 5 nm.

Result and discussion

Spectral characteristics

The chromogenic reagent Nitroso-S is a very versatile reagent for the determination of trace amounts of numerous metals. The absorption spectra of Cu-(Nitroso-S) and Hg-(Nitroso-S) complex in DMF versus that of a blank prepared under the similar conditions were recorded and shown in Fig. 1A. As revealed by the absorbance spectra, HPSAM cannot be applied for the simultaneous determination Hg(II) and Cu(II), due to the high overlap between their two spectra and absence two sufficient wavelengths for Cu-(Nitroso-S) and Hg-(Nitroso-S) complexes. By FDS (Fig. 1B), minor spectral characteristics are obtainable with better resolutions against the zero-order spectra. When mercury is selected as the analyte, one pair of wavelengths showing the same $dA/d\lambda$ for the copper complex will be 556 and 623 nm. Therefore these two wavelengths can apply for simultaneous determination of Hg(II) and Cu(II) by FDS-HPSAM.

Applying FDS-HPSAM for the simultaneous determination of copper(II) and mercury(II)

The HPSAM is able to simultaneously determine species X and Y in a mixture even if their spectra overlap and their maxima are coincident. The determination of X concentration by the HPSAM requires working at two wavelengths, λ_1 and λ_2 , where the analytical signal due to the interferent, Y , remains the same during successive additions of X with known standard concentrations to the mixture of X and Y . In derivative spectrophotometry the resulting derivative signals are measured at the signals of X are considerably different [18-19].

The simultaneous determination of copper(II) and mercury(II) has been evaluated by adding standard solutions of mercury using the selected wavelengths of 556 and 623 nm. Amount of mercury

can be obtained directly by value of H-point $-C_H$. The concentration of interfering component Cu(II) can be calculated indirectly by calibration method using standard solutions of Cu(II) and the ordinate value of H-point $(dA/d\lambda)_H$. Fig. 2A and B clearly show the effect of change in the concentration of copper and mercury on the position of H-point, respectively. As shown in the figures, the value of $(dA/d\lambda)_H$ is independent of the amounts of mercury in the samples. This analytical signal enables calculation of the concentration of copper from a calibration curve constructed from the ordinate of several HPSA plots with various concentrations of copper.

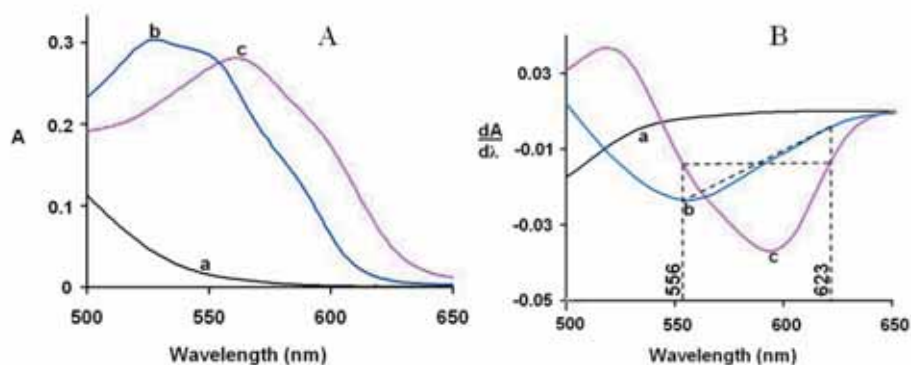


Fig. 1. (A) Zero derivative spectra of: (a) Nitroso-S against DMF, (b) Hg-(Nitroso-S) against blank, (c) Cu-(Nitroso-S) against blank. (B) First derivative spectra of: (a) Nitroso-S against DMF, (b) Hg-(Nitroso-S) against blank, (c) Cu-(Nitroso-S) against blank. Conditions: 15.0 μg Mercury or 10.0 μg copper; 5 mL of 0.1 % Nitroso-S solution; ammonia buffer, 5 mL (pH=8.5); flow rate of sample = 3 mL/min; eluent, 5.0 mL DMF; flow rate eluent = 1 mL/min, wavelength interval ($\Delta\lambda$) = 5 nm

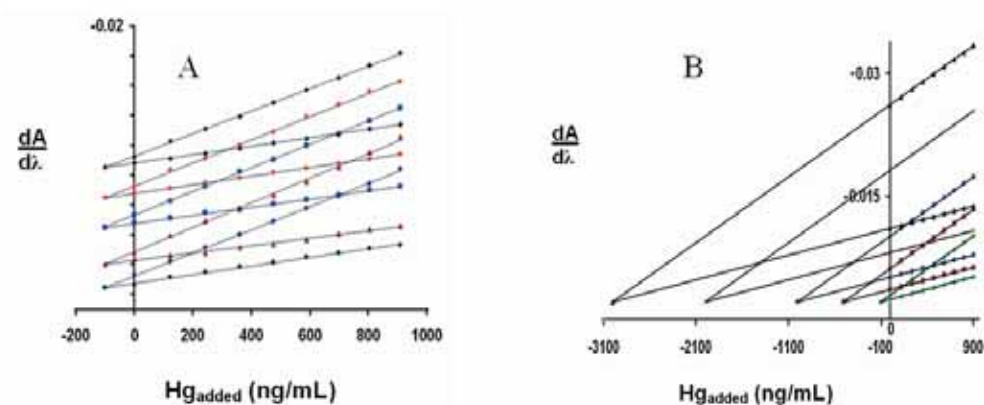


Fig. 2. Plot of H-point standard addition method for simultaneous determination of a fixed amount of (A) mercury (0.5 μg in original solution) and different amounts of copper (0.5, 2.5, 5, 7.5 and 10 μg in original solution), when different standard mercury solutions are added, (B) copper (0.5 μg in original solution) and different amounts of mercury (0.5, 2.5, 5, 10 and 15 μg in original solution), when different standard mercury solutions are added. Other conditions were the same as Fig. 1

Optimization of SPE conditions

In order to find the optimum conditions, the effect of pH on the spectrum of a constant concentration of each complex was investigated. The sorption of copper(II) and mercury(II) on the column was found to be maximum in the pH range of 4.0 – 10 and 5 – 10, respectively. In the pH < 4, concentration of hydronium ion is high then protonated Nitroso-S cannot complex with mercury and

copper ions very well. Therefore in the $\text{pH} < 4$ adsorption of Hg(II) and/or Cu(II) on the adsorbent will be decreased. The pH of the solutions was adjusted at 8.5 with ammonia buffer.

The flow rate of sample solution was varied from 0.5 – 8.0 mL/min did not affect adsorption. A flow rate of 3 mL/min was recommended in all experiments. Under optimum conditions, the volume of the aqueous phase was varied in the range up to 600 mL for Hg(II) and Cu(II). It was observed that the absorption was almost constant up to 500 mL for Hg(II) and 550 mL for Cu(II), however for convenience, all the experiments were carried out with 50 mL of aqueous phase. Preliminary observation indicated that copper and mercury were desorbed completely with 5 mL DMF by flow rate of 1 mL/min. Therefore, 5.0 mL of DMF was used in the present work.

Analysis of mercury–copper binary mixtures

Known amounts of mercury and copper were determined to assess the accuracy of the suggestive method. The accuracy of the FDS-HPSAM has been shown in Table 1. In order to study the precisions of the suggestive method, five times replicating determination of 0.100 μg Hg(II) and 0.100 μg Cu(II) taken in initial solution gave a relative standard deviation (RSD) of 3.6 % for mercury and 2.8 % for copper. In view of the accuracy and precision obtained, the applicability of the method for simultaneous determination of mercury and copper in their different binary mixtures is apparent. According to the procedure under the optimum conditions detection limit in original solution was obtained 0.1 ng/mL for mercury and 0.5 ng/mL for copper.

Table 1. Determination of mercury and copper in the different binary mixtures

(dA/d λ) - c equation	r	Taken in original solution (μg) ^a		Found in final solution (μg) ^b		Recovery (%)	
		Hg(II)	Cu(II)	Hg(II) ^c	Cu(II) ^c	Hg(II)	Cu(II)
(dA/d λ) ₅₅₆ = $-5.116 \times 10^{-6} c - 3.388 \times 10^{-3}$	0.999	0.10	0.10	0.09 \pm 0.03	0.09 \pm 0.02	104.5	99.6
(dA/d λ) ₆₂₃ = $-1.045 \times 10^{-6} c - 2.859 \times 10^{-3}$	0.996						
(dA/d λ) ₅₅₆ = $-8.946 \times 10^{-6} c - 1.749 \times 10^{-2}$	0.998	2.00	0.10	2.00 \pm 0.25	0.09 \pm 0.02	100.3	99.9
(dA/d λ) ₆₂₃ = $-4.961 \times 10^{-6} c - 6.485 \times 10^{-3}$	0.997						
(dA/d λ) ₅₅₆ = $-6.976 \times 10^{-6} c - 1.081 \times 10^{-2}$	0.999	0.10	2.00	0.09 \pm 0.03	1.98 \pm 0.30	99.3	99.0
(dA/d λ) ₆₂₃ = $-2.979 \times 10^{-6} c - 2.031 \times 10^{-2}$	0.996						
(dA/d λ) ₅₅₆ = $-7.917 \times 10^{-6} c - 1.925 \times 10^{-2}$	0.997	2.00	0.50	2.09 \pm 0.15	0.48 \pm 0.08	100.9	96.3
(dA/d λ) ₆₂₃ = $-2.961 \times 10^{-6} c - 3.238 \times 10^{-3}$	0.999						
(dA/d λ) ₅₅₆ = $-6.947 \times 10^{-6} c - 2.725 \times 10^{-2}$	0.998	3.00	0.50	3.04 \pm 0.29	0.49 \pm 0.07	100.3	99.2
(dA/d λ) ₆₂₃ = $-2.962 \times 10^{-6} c - 9.224 \times 10^{-2}$	0.995						
(dA/d λ) ₅₅₆ = $-6.975 \times 10^{-6} c - 2.984 \times 10^{-2}$	0.998	3.00	2.00	3.03 \pm 0.40	1.95 \pm 0.29	100.2	97.4
(dA/d λ) ₆₂₃ = $-2.980 \times 10^{-6} c - 2.182 \times 10^{-2}$	0.995						
Mean recovery						100.8	98.7

^a Amounts of Hg(II) and Cu(II) added to original solution

^b Amounts of Hg(II) and Cu(II) found in final solution using of HPSAM plots and total volume of eluent (5 mL)

^c mean of five determinations, \pm standard deviation

Interference study

The effects of different ions on the simultaneous determination of 5.0 μg each Hg(II) and Cu(II) by proposed method was studied. An ion was considered as interferent, when it caused a variation in the absorbance of the sample (at constant wavelength) greater than $\pm 3\%$. Tolerance limits were less than 50 mg for Al(III), Zn(II), Pb(II), Bi(III), Ce(III), Ca(II), La(I), Fe(II), Na(I), K(I), iodide, bromide, chloride, acetate, thiocyanate, oxalate and carbonate; 23 mg for Cr(III), U(VI), sulfate and thiourea; 18 mg for Te(IV); 11 mg for Ag(I); 9 mg for Rh(III); 6 mg for Ga(III), Co(II) and Cd(II); 3 mg for Ti(VI) and Mn(II); 1 mg for Ni(II), V(V), Os(VIII) and Ru(III); 0.5 mg for Se(VI) and

Mo(VI); 0.3 mg for Cs(I) and 0.1 mg for Fe(III) and Tl(III). Results indicate that most of the cations and anions do not interfere.

Determination of copper and mercury in biological standard samples, fruits and vegetables

The accuracy and applicability of the proposed method was evaluated to the determination of copper and mercury in National Institute for Environment Studies NIES No. 1 pepperbush, NIES No. 5 human hair and NIES No. 6 mussels. A 0.5 g each one of samples was added to a beaker and dissolved in concentrated nitric acid (~5 mL) with heating. The solution was cooled, diluted and filtered. The filtrate was increased to 100 mL with distilled water in a calibrated flask. An aliquot of the sample solution was taken individually and Hg(II) and Cu(II) were determined by the general procedure. The results were in good agreement with the certified value (don't show).

Finally, the proposed method was applied for determination of Hg(II) and Cu(II) in some fruits and vegetables. First various fruits and vegetables were dried in 80 °C for 72 h. A 0.1 g of the fruits and vegetables (date, tomato, cucumber, apple and white radish) was taken separately in a beaker and dissolved in concentrated nitric acid and perchloric acid (3:1) by heating on a hot plate. The solution was cooled, diluted and filtered if needed. The filtered solution was made to 100.0 mL with distilled water in a calibration flask. A 50 mL of the pretreated sample solution was taken and analyzed by the general procedure. In order to compare the proposed method, the actual fruits and vegetables were analyzed by direct flame atomic absorption spectroscopy (FAAS) method. The results were given in Table 2.

Table 2. Analysis of fruits and vegetables for Mercury and Copper Ions

Product Type	Found by FAAS Method ($\mu\text{g}/\text{kg}$) ^a		Found by Present Method ($\mu\text{g}/\text{kg}$) ^a	
	Mercury	Copper	Mercury	Copper
Date	1.39±0.03	14.81±0.30	1.35±0.04	14.78±0.36
Tomato	7.73±0.19	35.13±0.70	7.74±0.23	35.14±0.88
Cucumber	1.17±0.03	16.33±0.33	1.19±0.02	16.29±0.40
Apple	4.51±0.11	29.85±0.59	4.51±0.10	29.86±0.75
White radish	18.88±0.47	38.63±0.76	18.86±0.49	38.67±0.97

^a mean of five determinations, ± standard deviation

Conclusion

This manuscript explains simultaneous separation and preconcentration of trace amounts of mercury(II) and copper(II) using modified natural clinoptilolite zeolite (cadmium-saturated clinoptilolite modified with BDTA and then loaded with Nitroso-S). The result of this process is to use a very cheap and abundant natural absorbent for the recovery of Hg and Cu ions from plant and biological samples. Simultaneous determination of Hg(II) and Cu(II) by derivative spectrophotometric H-point standard addition method was performed by measuring the first derivative spectra at 556 and 623 nm with wavelength interval ($\Delta\lambda$) = 5 nm. By the time being, H-point standard addition method has been used to measure simultaneously two cations, which have overlapping normal spectra in UV-Vis spectrophotometry. As derivative spectrophotometry peaks are fairly sharper than normal spectrophotometry peaks, the selectivity is increased. Also by amplifying the signal and lowering the noise, derivative spectra improve the sensitivity.

References

- [1] Hempel, M., Chau, Y.K., Dutka, B.J., McInnis, R., Kwan, K.K., Liu, D.: *Analyst* 1995, 120, 721-724
- [2] Bloom, N.S., Gill, G.A., Cappellino, S., Dobbs, C., McShea, L., Driscoll, C., Mason, R., Rudd, J.: *Environ. Sci. Technol.* 1999, 33, 7-13
- [3] Horvat, M.: *Anal. Bioanal. Chem.* 2002, 374, 981-982
- [4] Koppe, P., Stozek, A.: *Kommunales Abwasser, Germany, Vulkan*, 1999
- [5] Mahmoud, M.E., Osman, M.M., Amer, M.E.: *Anal. Chim. Acta* 2000, 415, 33-40
- [6] Yang, M.L., Colombini, V., Maxwell, P., Mester, Z., Sturgeon, R.E.: *J. Chromatogr. A* 2003, 1011, 135-142
- [7] Zahir, F., Rizwi, S.J., Haq, S.K., Khan, R.H.: *Environ. Toxicol. Pharmacol.* 2005, 20, 351-360
- [8] Reig, F.B., Falco, P.C.: *Analyst* 1998, 113, 1011-1016
- [9] Rigin, V.: *Anal. Chim. Acta* 1993, 283, 895-901
- [10] El-Sayed, A.Y., El-Salem, N.A.: *Anal. Sci.* 2005, 21, 595-614
- [11] Sabry, S.M., Khamis, E.F.: *Talanta* 2000, 51, 1219-1231
- [12] Martinez, L.G., Falco, P.C., Cabeza, A.S.: *J. Pharm. Biomed. Anal.* 2002, 29, 405-423
- [13] Falco, P.C., Cabeza, A.S., Martinez, L.G., Reig, F.B.: *Anal. Chim. Acta* 1996, 334, 199-208
- [14] Afkhami, A., Bahram, M.: *Spectrochim. Acta, Part A* 2004, 60, 181-186
- [15] Roohparvar, R., Taher, M.A., Mohadesi, A.: *J. AOAC Int.* 2008, 91, 637-645
- [16] Taher, M.A., Mostafavi, A., Afzali, D., Rezaeipour, E.: *Bull. Korean Chem. Soc.* 2004, 25, 1125-1129
- [17] Afzali, D., Mostafavi, A., Taher, M.A., Moradian, A.: *Talanta* 2007, 71, 971-975
- [18] Safavi, A.; Abdollahi, H.: *Talanta* 2001, 54, 727-734
- [19] Eskandari, H.: *Spectrochim. Acta Part A* 2006, 63, 391-397

Some of our Contributions to the Statistical Valuation of Spectrochemical Results

Eduard Plško

Donská 97, 841 06 Bratislava, Slovakia

Abstract

The paper deals with two authors till now not published contributions to the statistical evaluation of spectrochemical results contained in his numerous publications on this item. After a short historical review dedicated to the development of statistical treatment in analytical chemistry, the first part deals with the precision of spectral lines wavelengths measurement, as well as with the sense of its optimization. It was shown that the optimization of this comparatively complicated, but in any spectrochemical laboratory performable procedure, does not bring any significant improvement of the gained results. In the second part of the paper the existence and causes of an asymmetric, expressively left skewed distribution of spectral lines repeatedly measured intensity values is described. This phenomenon was found earlier at photographically recorded spectral lines but as shown, it occurs also in results of modern computer controlled spectrometers. Its effect leading to possible systematic errors of quantitative analyses is discussed and the necessity of its correction in corresponding softwares stated.

Key words: *spectrochemical analysis, chemometrics, wavelength measurement, optimization, asymmetric distribution of intensities*

Introduction

Whereas some basic principles of mathematical statistics were known already in 19th century (1821, normal distribution, F.Gauss) but they were applied namely for the calculation of win probabilities in games of chance. A serious use of mathematical statistics in analytical chemistry for quality valuation of obtained results started first in the middle of the 20th century by the statistical approach to the limit of detection [1] and its fast development has been observed namely not only thanks to the development of efficient computers, but also thanks to the merits of numerous scientists working in this field.

During my whole university studies (1949-1953) in our country there was in chemical courses fully nothing told about statistics, even the expression “*standard deviation*” was not mentioned at all and there did not exist practically any available textbooks of this science written in Slovak or Czech language. Some books written on this item in Russian were too theoretical and German or English books were practically not accessible. So I was forced to find my own way how to master the necessary knowledge. I found the solution in a polish book on spectrochemical analysis edited in 1957 by J. Swętosławska [2] containing 100 pages on statistical methods. I acquired the book in 1959 and started my private studies in mathematical statistics.

My first work dedicated to mathematical treatment of spectrophotometrical results for the determination of product stability, presented already 50 years ago on the Colloquium spectroscopicum internationale in Liège (Belgique) [3-5] has been followed by a lot of my works having statistical character, presented on different home and abroad scientific conferences and published in scientific journals. They deal with following original, today called chemometrical items as listed for short in the next review: Conditions for the use of basic distributions: normal, logarithmic normal and by me introduced pragmatic distribution, a new by me discovered and explained left-skewed distribution caused by the narrow shape of spectral lines, distribution of spectroanalytical results, optimization (The word optimization was used and performed by me already in 1963) of spectrochemical methods: Calibration, Extrapolation in the case of non linear analytical calibration function, Choice of reference spectral lines – scatter diagrams, Calculation of distribution parameters if one part of results is below determination limit, Measurement of wavelengths, Resolution as the basic parameter for the quality of results, Photographic photometry and some others. A list of appropriate citations was presented in more details in my oral lecture in this conference and is prepared for publication in an other place. In the present work I would like to inform you at least on some till now not published results representing my contribution to the optimization of spectrochemical results, especially to the measurement of wavelengths and to the left skewed distribution of measured spectral line intensities.

Thanks to several existing reliable wavelength tables the wavelengths of the majority of common spectral lines has already been recorded, so that the wavelength measurement can occur only exceptionally. In spite of that, some new, till now not described spectral lines, like e.g. 7 new Ca lines, were identified [6].

According to the well known procedure for the wavelength determination of an unknown spectral line or an edge of a molecular spectrum in a routine spectroscopic laboratory, interpolation of photoelectrically or photographically recorded position readings (for photoelectric recording: reading on a wavelength drum or in modern devices by digital presentation and for practically obsolete photographic recording: position on the photographic plate in mm which has till now given the most precise results) of the spectral line in question and at least two spectral lines of known wavelengths, usually spectral lines of iron from the vicinity of the unknown line can be used. For this procedure a grating spectral apparatus having practically constant linear dispersion can be advantageously used. With the use of mathematical statistics I derived the dependence of the error for the determined wavelength upon the error of the determination of the line positions as well as the conditions for its optimization [7].

In the present work experimental proof of these parameters and their importance will be presented. If we are interested not only in the wavelengths of spectral lines but for quantitative applications also in their intensities we have to do with quite other situation. Already at the beginning of sixties of the past century I found, presented on international analytical conference in Budapest in April 1961 and published [8,9] a curious important phenomenon that the distribution of photographically and photoelectrically (with hand controlled setting of wavelengths) determined spectral lines intensity values obtained by repeated measurement did not obey the Gaussian normal distribution and showed an expressive left skewness, i.e. their mode was higher than their arithmetical mean. The same effect occurs also in consequence of radial wandering of the excitation source [10]. In that time I expressed also my opinion that the same skewed distribution would occur also in the case of photoelectric intensity recording with the use of computer controlled spectral devices. This assumption will be studied and confirmed in the present work too.

Theoretical part

The interpolation equation used for the determination of an unknown wavelength (λ_x) using the position readings (a , b) of two known wavelengths (λ_a , λ_b) left and right to the unknown line reads [7]:

$$\lambda_x = (x - a) \cdot (\lambda_b - \lambda_a) / (b - a) + \lambda_a \quad (1)$$

If the standard deviation of the lines position equals s and its estimation is calculated only once, the a value is measured m times and the measurement of the position b is repeated n times, then:

$$s_x = s; \quad s_a = s/\sqrt{m}; \quad s_b = s/\sqrt{n}; \quad (2)$$

The transfer of the measurement errors expressed by the equation (2) in the error of precision of the calculated unknown wavelength s_λ can be expressed by the following equation:

$$s_\lambda = s_x \cdot \{(\delta\lambda_x/\delta x)^2 + (\delta\lambda_x/\delta a)^2/m + (\delta\lambda_x/\delta b)^2/n\}^{1/2} \quad (3)$$

After having expressed the present partial differential quotients the equation (3) gains the form:

$$s_\lambda = s_x \cdot \{(\lambda_b - \lambda_a)/(b - a)\} \cdot \{1 + [(x - b)/(b - a)]^2/m + [(x - a)/(b - a)]^2/n\}^{1/2} \quad (4)$$

In accordance with the equation (4) the minimization of the error of wavelength determination characterized by s_λ can be achieved by the minimization:

a) The error of spectral lines positions s . At current laboratory conditions the lowest standard deviation for spectral lines positions can be achieved using photographic spectral records and measurement with Abbe's comparator. This, today practically not more used and by younger spectroscopists practically unknown instrument for measuring distances (described e.g. in [4]) enables, thanks to special spiral micrometer, position readings of 0.1 μm and several further, in experimental part described advantages.

b) Of the expression in the first braces. Its reciprocal corresponds to the linear dispersion of the used spectral apparatus. It means, for to achieve the best precision of the wavelength determination spectral apparatus with the highest linear dispersion should be applied.

c) The expression, which square root is in the second braces. Its minimum value can be calculated by putting its first differential quotient equal to zero. The obtained minimization condition is fulfilled at the following condition for the repetition of measured values:

$$(m/n) = (b - x)/(x - a) \quad (5)$$

One of the goals of the presented work consists in the experimental proof of the greatness and consequently the sense of the last mentioned optimization step.

If we are interested apart from the wavelength also in the intensity of a spectral line the measurement technique uses other principles and the obtained intensity distribution will obey quite other laws as I found and described the obtained new skewed distribution already in the beginning of sixties of the XXth century [8,9]. Their causes can be explained as follows: For the intensity measurement of spectral lines we try to bring the middle of the spectral line having the maximum intensity in the optical axis of the measuring device. At this endeavor we, however, make inevitable random errors which distribution can be accepted as Gaussian [8] what, however, corresponds to the distribution of measurement position and not to the distribution of intensities. Caused by the narrow shape of the intensities, the determined intensity values are always lower independently upon the either left or right random deviation from the optical axis. In accordance with this behavior and the endeavor to measure in the middle of the spectral line the obtained intensity distribution shows a left skewness i.e. the occurrence of great intensity values is the highest and it sinks to lower intensity values, i.e. the distribution shows an expressive left skewness as it can be seen in the Fig.1 representing the distribution of microdensitometrically measured intensity of a photographically recorded spectral line as dependent on the intensity value [8]. In the present work the appearance of similar skewed intensity distributions of photoelectrically measured values using computer controlled spectrometer will be presented.

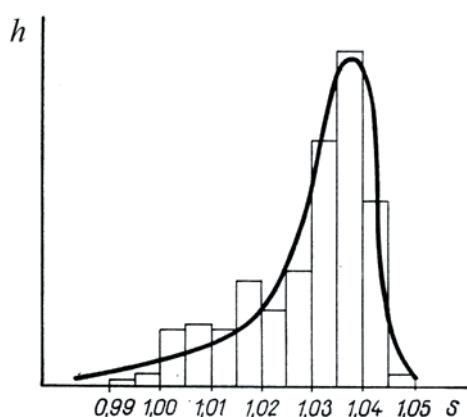


Fig. 1

Experimental part

In order to achieve the most reliable determination of investigated spectral lines positions used for the planned experiments, their values were measured on photographic records of spectra by Abbe's comparator of C. Zeiss Jena ensuring not only the best precision and what is of special importance for the calculations, the obtained results are homoskedastic, i.e. their standard deviation does not depend on the wavelength. The distribution of the intensity values obtained by repeated measurement without any position changes of the photographic plate position only with new settings and readings the corresponding position value was performed with the aim to calculate the precision of position measurement and for comparison with results obtained after a repeated as precise as possible new setting the middle of the spectral line in the axis of the Abbe's comparator indicated by the optical cross. The measurement of spectral lines positions used for the further calculations was performed at the following experimental conditions:

Photographically recorded arc spectra were taken using iron electrodes containing low concentration of Mn and B by the plane grating spectrograph PGS-2, product of Carl Zeiss, Jena, Germany, focal length 2m, grating 652 lines/mm, 1st order, in the wavelength range 220-390 nm having linear dispersion 0.74 nm/mm. The spectral lines intensities were calculated using I – transformation [11] from blackening values measured on microdensitometer G2, Carl Zeiss, Jena.

Photoelectrically recorded intensity of the chosen spectral line of Pb 217.0 nm separated from the radiation of a hollow cathode lamp and intensity of the continuum in its vicinity produced by a deuterium lamp were taken in emission mode using a computer controlled AAS spectrometer AAS 5 EA (Analytik Jena AG) without any atomization medium (flame, or ETA) after a full repetition of finding the programmed position for measurement.

Results and discussion

a) Precision of wavelength determination

The precision of results for spectral lines position was checked by the estimation of standard deviation (s_x) calculated from 50 times repeated measurement performed without any movement of the carriage with the photographic plate, so that only the error of reading of the comparator comes in the calculus. The data for the used spectral lines are presented in Tab. 1 and their positions in the photographic record are presented in Fig. 2 (Numbers correspond to spectral lines in Tab. 1).



Fig. 2

The product of the standard deviation of the position (s_x) with the linear dispersion of the spectrograph (0.74 nm/mm) gives the wavelength standard deviation (s_λ) published in Tab. 1

Table 1

No.	element	λ nm	x mm	s_x mm	s_λ nm
1	boron	B249.77	165.2035	0.00179	0.00132
2	iron	Fe259.94	151.4343	0.00248	0.00183
3	manganese	Mn260.57	150.5845	0.00280	0.00207
4	iron	Fe261.19	149.7481	0.00280	0.00207

The calculated standard deviation of wavelength is in about 2 pm, what is fully satisfactory for our further work. The distribution of the measured values shows symmetry, so that arithmetical mean of multiple results can be correctly used. As example the histogram for the Mn spectral line verifying this statement is presented in Fig. 3.

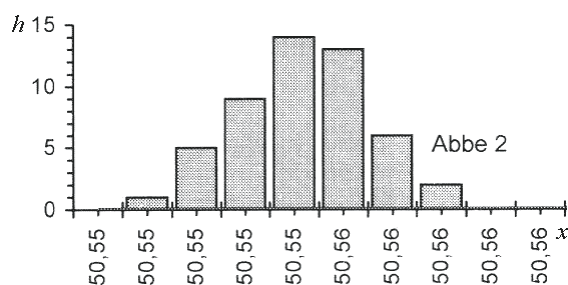


Fig. 3

By the following experiments we want to show the influence on the precision of wavelength calculation results obtained using equation (4) for a model spectral line Mn 260.57 by the optimization performed using the choice of auxiliary spectral lines fulfilling the equation (5) and without any optimization.

The auxiliary spectral lines of iron were chosen so that their distance from the manganese line is practically identical: $(x_3 - x_4) = 0.8364$ mm; $(x_2 - x_3) = 0.8498$ mm. It means that according to the equation (5) the optimal precision of the wavelength determination will be achieved at the same number of repeated measurements of the both auxiliary lines. We performed 8 repeated measurements. The calculated optimal standard deviation for the wavelength is presented as No 1 in the Tab. 2. In the following case the standard deviation for the position of the model Mn spectral line was calculated using the auxiliary wavelength of the iron line 4 (Tab. 1) and boron line 1 (Tab. 1). These lines are of quite different distance to the model Mn line: $(x_3 - x_4) = 0.8364$ mm; $(x_1 - x_3) = 14.619$ mm. In the following case we calculated the standard deviation of the model Mn line using condition given by the equation (5) that we measured the line 4 only once and the line 1 fifteen times, what approximately corresponds to the relation of their distances from the model Mn line and the full number of measurements has not been changed. The resulting standard deviation is presented in Tab. 2 as No 2. The third measurement was performed using lines 1 and 4 without any optimization. Both lines were measured 8 times. The result is in Tab. 2 indicated as No 3.

Table 2 Standard deviation (in mm) of the wavelength calculation performed at different conditions

No 1	No 2	No 3
0.00194	0.00197	0.00207

According to theoretical expectations the best precision is obtained in the case No 1 and the worst in the case No 3. The differences between the results at optimized conditions and results obtained are however so small, that the application of optimization process does not bring any

significant improvement ($F_{exp} \ll F_{tab}$) so that it is possible to leave it out what brings economical advantage. As already mentioned we found and using the presented procedure without any optimization reliably characterized 7 not yet described Ca spectral lines and used the gained information for to explain and to correct the Ca interference on V determination [6].

At the investigation of spectral lines intensity distribution obtained using a computer controlled spectrometer we obtained following results:

b) Distribution of wavelength determination results

The repeated setting of wavelengths for the spectral line Pb 217.0 by the computer controlled spectrometer gives a similar left skewed distribution of spectral line intensities as it was found with the use of photographic or photoelectric detection with hand setting what can be seen on the histogram presented in Fig. 4. In difference the histogram in Fig. 5 presenting the distribution results obtained with continuous deuterium spectrum in the vicinity of the measured Pb line shows a symmetric shape representing in a sufficient extent the shape of the normal distribution. The appearance of the left skewed distribution is so at the measurement on spectral lines caused without doubt by presence of computer random errors in the setting of the correct wavelength leading to lower intensity values independently on higher or lower wavelength setting.

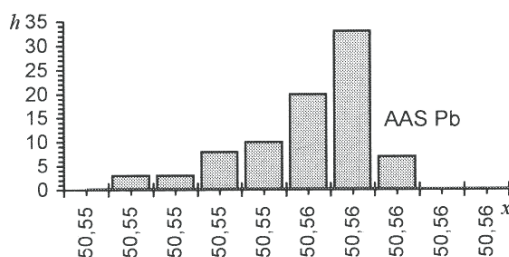


Fig. 4

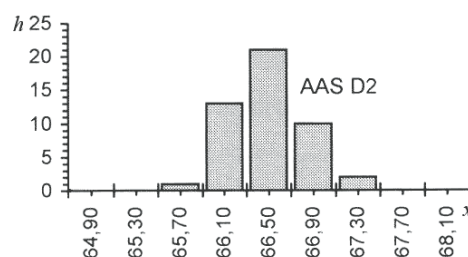


Fig. 5

The measurement of spectral lines intensity using a computer controlled spectrometer enabling automatic finding and setting of chosen wavelengths performed with the aim of comparison their distribution with the non symmetric, left skewed distribution at photographically and hand controlled photoelectrically recorded data brought the expected results confirming the presence of identical behavior also for this modern top technique. It is therefore surprising that the already before almost 50 years described behavior leading to systematic errors of the spectral lines intensities expressed by arithmetical mean which represent the basic input for all spectral quantitative analyses has till now not found application in any corresponding software.

References

- [1] Kaiser, H., Specker, H.: Z.anal.Che., **149**, 46 (1956)
- [2] Śwetosławska, J.: Spektralna analiza emisyjna, Państwowe wydawnictwo naukowe, Warszawa 1957, p.300
- [3] Plško, E.: Revue univ. des mines, serie 9, XV, 520(1959)
- [4] Plško, E.: Praktické základy optických metod v chémii, SVTL, Bratislava 1963, p.317
- [5] Plško, E.: Zajištění kvality analytických výsledků, 2THETA, Český Těšín, 2008, p.38
- [6] Plško, E., Kubová, J.: Spectrochim. Acta, **39B**, 1493 (1984)
- [7] Plško, E.: Ondokuz Mayıs Üniversitesi Fen Dergisi Özel Sayısı, 2, Samsun, Turkey, (1), 27 (1990)
- [8] Plško, E.: Acta Chim.Hung, **32**,419 (1962)
- [9] Plško, E.: Revue Roumaine de Chimie, **10**, 695 (1965)
- [10] Plško, E.: Rozpravy Nar. techn. muzea, Praha, **4**, 23 (1962)
- [11] Török, T., Zimmer, K., Réti, S.: Microchim. Acta, **1962**, 611

Study of Mobility of Chosen Elements in Soils Contaminated by Pollutants of Metallurgical Industry

¹Dagmar Remeteiová, ¹Radoslav Rusnák, ¹Silvia Stolárová, ²Vojtech Dirner

¹Technical University of Košice, Faculty of Metallurgy, Department of Chemistry, Letná 9/A, 042 00 Košice, Slovakia, e-mail: dagmar.remeteiova@tuke.sk; radoslav.rusnak@tuke.sk

²Technical university of Ostrava, Faculty of Mining and Geology, Department of Environmental Engineering, 17. listopadu 15, 708 33 Ostrava-Poruba, Czech Republik

Abstract

This work presents results of investigation of risk elements mobility in the four samples of agricultural soils collected in locality Košice – Veľká Ida, near by U.S.Steel Ltd. (metallurgy plant). The method of the fractionation analysis was used for classification (isolation and quantification) of various forms (fractions) of Cu, Ni, Pb, and Zn, which may be mobile during given soil conditions. The single-step extraction was applied for the isolation of elements forms. Elements content in isolated extracts was detected by flame atomic absorption spectrometry. The obtained results was compared with results of fractionation analysis of the gravitation dust sediment sample collected in the same locality with the aim of determination of possible soil contamination by risk elements from dust. The results of this study referred to increased mobility of chosen elements in the all soils samples during conditions of farming technology application and soil fertilisation, which are typical for agricultural soils. The gravitation dust sediment may contaminate soils by Cu, Pb, and Zn, but it isn't the source of contamination of soils by Ni. However mobility of Ni in the soils is the highest from all chosen elements.

Key words: *fractionation analysis, soils, gravitation dust sediment, single-step extraction*

Introduction

Gravitation dust sediments and soils number among the solid environmental samples. Dust sediments in the industrial sites are predominantly formed by solid pollutants, which are unwelcome product of an industrial production. Various risk elements forms enrich the surface of these dust particles. The gravitation dust sediment after deposition on the soils is getting one of sources of risk elements input to the soil ecosystem.

The soil is one of the components of the environment. The properties of the agricultural soils are affected by various farming activities. With regard to different origin and position of both samples in the environment it is possible to suppose different chemical properties of their matrix (mineralogical composition, content of organic and inorganic carbon) and kind of risk elements binding. The presence of dust particles in soils as extraneous substances may evocate formation of the artificial system with very variable properties [1]. The elements forms released from the dust can be immobilizable, eventually mobilizable in soils. Heavy metals in soils exist in the various chemical forms and determination of

these forms give a lot of information about mobility, toxicity, and bioavailability of elements. For this reason the determination of total elements content in the soils samples isn't suitable for evaluation of the soil contamination.

From the standpoint of mobility and bioavailability of elements in soils, the "mobile" forms or fraction, respectively constitutes the highest danger. This fraction includes non-specific sorbed, easily changeable and water-soluble forms of elements [2]. These elements forms may be mobile during normal soil conditions. The fertilization and utilization of farming techniques are typical for agricultural soils. For these conditions will be mobile in the soil so-called „mobilizable“ fraction of elements. This fraction includes mobile elements forms and potentially mobile forms (bounded on the carbonate and organic matter). During of extreme changes of soil conditions e. g. in the case of an ecological damage may by mobile all potentially releasable forms besides of these, which are fixed with matrix matter. These forms is possible named as "maximum potential mobilizable" forms or "environmental risk" and they include "mobile" forms, "mobilizable" forms and others releasable forms (Mn/Fe oxide bound).

The fractionation analysis is method of analytical chemistry, which enables isolation and quantification of different element forms according to their various physical or chemical properties [3]. The single-step extraction by defined extraction reagent is very often used in the fractionation analysis of soils for isolation of the various elements fractions [2,4-6].

On the base of the extraction effect reagents used for the single-step extractions is possible divided to three groups. Each group of reagents is able extracted these forms of elements, which are mobile under the definite soil conditions. For the isolation of "mobile" forms (fraction) from soil samples are very often used as extraction reagents non-buffered solutions of salts ($0.01 - 0.1 \text{ mol dm}^{-3} \text{ CaCl}_2$, $0.1 \text{ mol dm}^{-3} \text{ NaNO}_3$, $1 \text{ mol dm}^{-3} \text{ NH}_4\text{NO}_3$...) with weakest extraction effect [2,4].

The reagents on the base of organic complexes (1 mol dm^{-3} ammonium acetate, 0.05 mol dm^{-3} EDTA or Na_2EDTA respectively, 0.005 DTPA ...) have the stronger extraction effect [4,7]. These reagents are used for the isolation of "mobilizable" elements forms. The extraction reagent $2 \text{ mol dm}^{-3} \text{ HNO}_3$ is used for isolation of elements content in "maximum potential mobilizable" forms. For evaluation of the hygienic state of the soil, determination of elements content in the HNO_3 -extract is relatively more sensitive than determination of the total elements content [2,7].

Experimental

The four samples of the soils (P1 – P4) and the sample of gravitation dust sediment (GDS) from metallurgical sites have been collected near of U.S.Steel Ltd. (a metallurgy plant). The sampling areas are given in Fig. 1.



Fig. 1. Sampling areas

The gravitation dust sediment sample was collected into glass settling vessels replete by 250 cm³ distilled water. After expiration of exposition time the content of vessels was quantitatively flushed by distilled water into the Pt-vessels and then evaporated to dryness on the water bath. After drying the sample was homogenised by crushing and grinding in the agate mill. The soil samples have been collected by spade to depth approximately 20 – 25 cm. Sampling places were selected so that they represented properties of given area.

For isolation of “mobile” element fraction was used 1 mol dm⁻³ NH₄NO₃, for isolation of “mobilizable” elements fraction was applied 0.05 mol dm⁻³ EDTA (pH = 7, treated by NH₄OH) and for isolation of “maximal potential mobilizable” fraction was used 2 mol dm⁻³ HNO₃. Individual single-step extraction procedures were carried out by mechanical shaking of the samples and the extraction reagent in 100 cm³ polyethylene extraction vessel for the duration of 1 hour (NH₄NO₃, EDTA) and 6 hours for HNO₃ at room temperature. The extractions of soil samples were realized by validated extraction procedures [2,4] and the extractions of the gravitation dust sediment sample by the modifying extraction procedure [8 9].

After finishing of extractions, the content of extraction vessels was immediately filtered through filter paper with narrow pores and diameter = 18.5 cm. Determination of Cu, Pb, and Zn content in filtered extracts was carried out using of the flame atomic absorption spectrometer (Perkin–Elmer 3030 equipped with a deuterium lamp for background correction and air/acetylene flame, Germany). Other analytical conditions of the FAAS method are listed in Table 1.

Table 1. The total elements content and results of conventional extraction

Lamp	Perkin Elmer HCL system			
Carrier gas	Air			
Flow rate	v/dm ³ min ⁻¹	40		
Fuel gas	H ₂ C ₂			
Flow rate	v/dm ³ min ⁻¹	20		
Element	Cu	Pb	Ni	Zn
Wavelength/nm	324.6	216.7	231.9	213.7
Slit-width/nm	0.7	0.7	0.2	0.7
Lamp intensity/mA	15	10	20	15
Concentration of calibration solutions/ $\mu\text{g cm}^{-3}$	0.1; 0.2; 0.5; 1; 2; 5	0.2; 0.5; 1; 2; 5; 10	0.2; 0.5; 1; 2	0.1; 0.5; 1

The mineralogical composition of soil samples was determined on the base of results of XRD analysis (equipment: fully automatic diffractometer URD-6, Rich. Seifert-FPM, Germany, radiation - CoK α /Ni filter, voltage – 40 kV, current intensity - 35 mA, single-step mode with step - 0,05° 2 θ time of step – 3 s) and individual elements generating of obtained minerals was confirmed by SEM-EDS analysis (equipment: electron raster microscope, TESCAN VEGA TS 5130 LM, ČR with energy-dispersive spectrometer OXFORD INCA Energy 350). The content of organic and inorganic carbon was determined by elementary analysis (EOROVECTOR, EuroEA 90001).

Results and discussion

The XRD pattern of the soil sample (P1) and the portion of obtained minerals in the soil are shown in Fig. 2. The XRD analysis results confirmed similarity of mineralogical composition of all soil samples. The matrix of soils is created by quartz and aluminosilicates: albite, muscovite, kaolinite and microcline. The elements, from which consist these minerals (Al, Fe, K, Mg, Na, O, and Si) were confirmed by results of local surface analysis. The results of this analysis of three areas are given in Table 2.

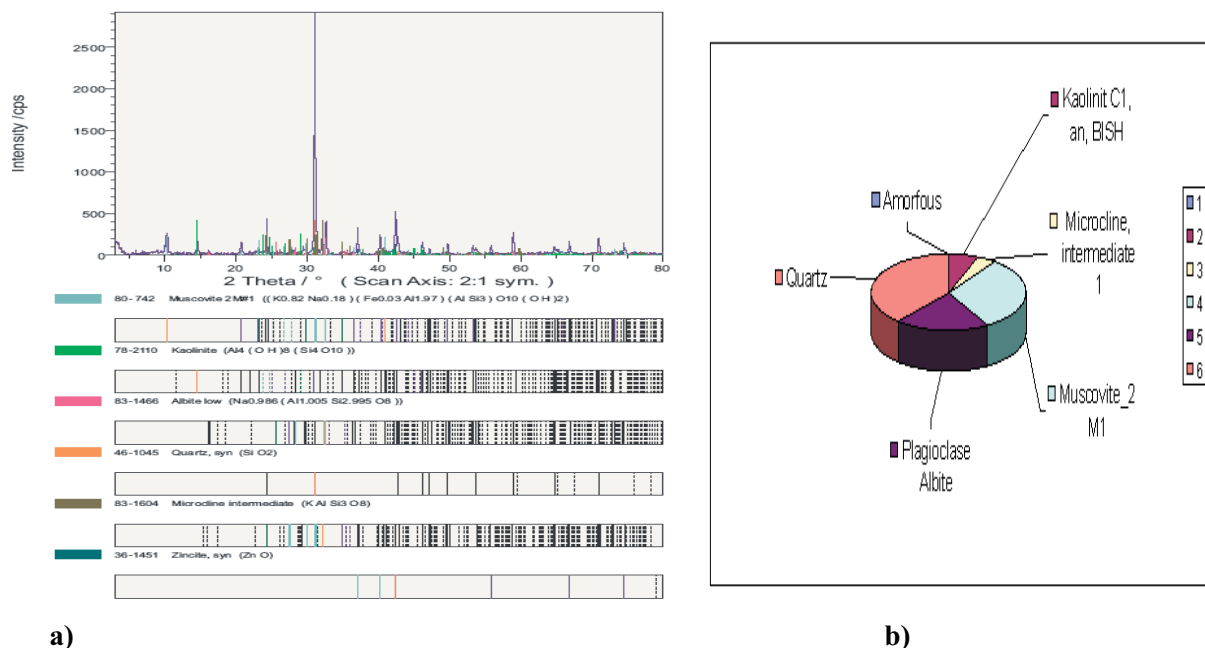


Fig. 2. The results of XRD analysis
a) The XRD pattern of the soil sample (P1); b) The portion of obtained minerals

Table 2. The percentage content of major and minor elements in the soil sample (P1) determined from results of surface local analysis

Element	O	Na	Mg	Al	Si	P	S	K	Ca	Ti	Mn	Fe
Area 1	53.50	1.02	0.63	6.79	30.98	0.36	0.10	2.79	0.38	0.60	0.10	2.76
Area 2	53.59	0.90	0.53	7.53	30.67	0.27	0.26	2.35	0.57	0.39	0.22	2.73
Area 3	52.83	0.93	0.92	7.46	30.06	0.33	0.40	2.79	0.47	0.58	0.10	3.12

From the results of elementary analysis of soil samples (Table 3) is possible to state that content of both carbons (TOC and TIC) is relatively low. The low content of inorganic carbon is in accordance with results of XRD analysis, which not confirmed presence of carbonates. The content of the total organic carbon occurs in the range from 1 % to 1.6 % approximately.

Table 3. The percentage content of total carbon (TC), total organic carbon (TOC), and total inorganic carbon (TIC)

Soil sample	TC / %	TOC / %	TIC / %
P1	1.77	1.59	0.18
P2	1.96	1.37	0.59
P3	1.69	1.28	0.41
P4	1.12	1.07	0.05

The mobility of chosen elements (Cu, Ni, Pb, and Zn) from dust sediment to soils and in soils was evaluated from the results of fractionation analysis. For each extraction reagents and soil sample were realised two parallel extractions and for each extraction reagents two blank experiments. The content of elements in the HNO₃-extracts, which represented their content in all releasable forms was taken as base of calculation of the relative recoveries and presented 100 %. The values of relative recoveries are plotted in Figs. 3 and 4.

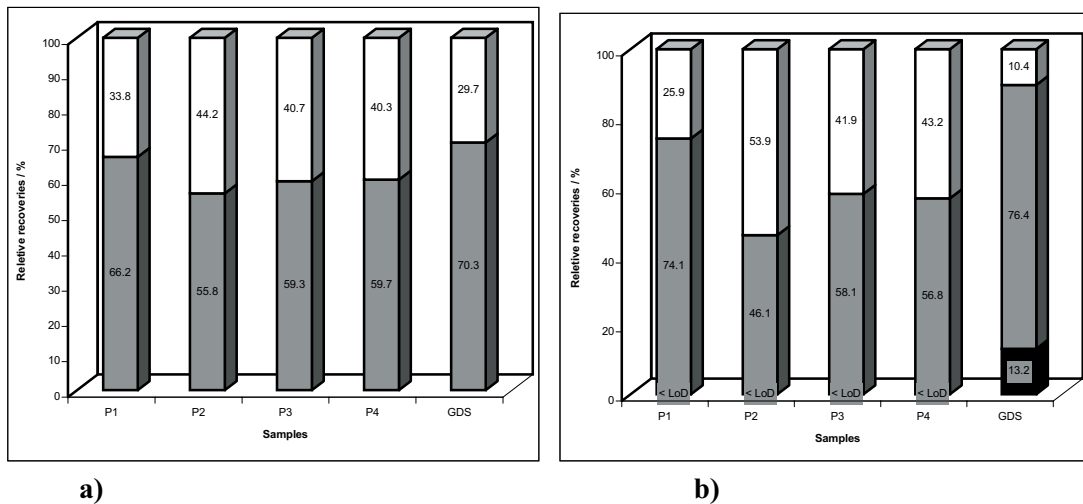


Fig. 3. The relative percentage recoveries of Cu (a) and Pb (b)

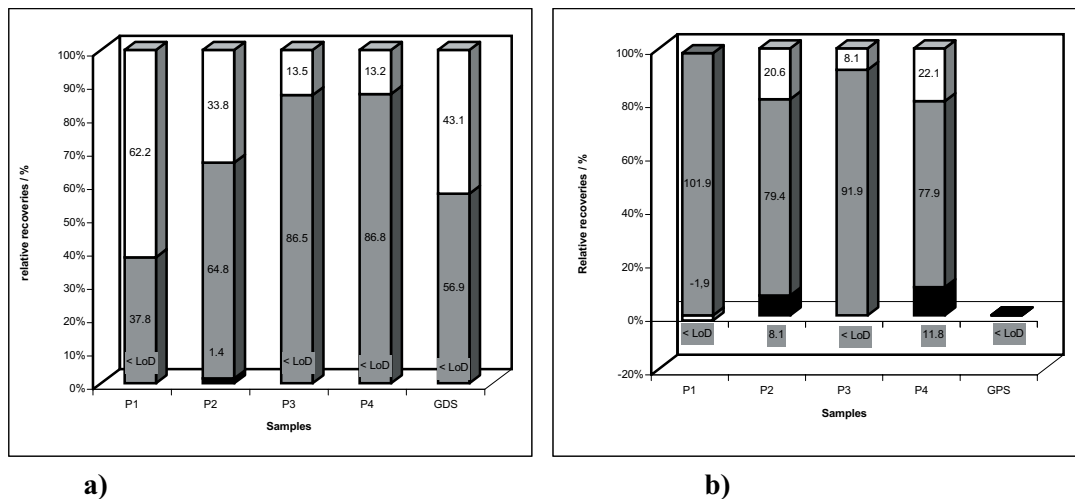


Fig. 4. The relative percentage recoveries of Zn (a) and Ni (b)

The black cells in the column graphs represent percentage portion of the element in “mobile” forms. In the extracts of soil samples were detected in these forms only Ni. In the gravitation dust sediment it was Pb. The sum of black and gray cells represents the percentage portion of elements in “mobilizable” forms. The gray cells respond to portion of elements in the “potential mobile” forms, which will be mobile in soils during application of farming activities. In the extracts of soil samples were detected in these forms all chosen elements and in the dust sample Cu, Pb, and Zn. The white cells respond to forms of elements, which may be mobile during extreme changes of soils conditions.

The results of study of the basic chemical properties (mineralogical composition, content of organic and inorganic carbon, and mobility risk elements) of the gravitation dust sediment sample [10] and the soils samples are given in Table 4. These results respond to different chemical properties of both solid environmental samples as well as different mobility of risk elements. The content of elements in various mobile forms in this table is sequenced according to decreasing order.

Table 4. The results of comparative study of the gravitation dust sediment and soils

Properties	Gravitation dust sediment	Soils
Dominant mineralogical composition	Quartz, calcite	Quartz, aluminosilicates
TOC, TIC	$C_{inorg}(20-30\%) > C_{org}(15-20\%)$	$C_{inorg}(0.05-0.6\%) < C_{org}(1-1.6\%)$
Content in „mobile“ forms	Only Pb	Only Ni
Content in „potential mobile“ forms	Pb, Cu, Zn	Ni, Zn, Cu, Pb
Content in the other releasable forms	Zn, Cu, Pb	Pb, Cu, Zn, Ni

Conclusion

In consideration of obtained results we can state that:

- Both studied samples have different chemical properties.
- The matrix of soil samples was created predominantly by aluminosilicates and quartz. In contrast to dust samples they contain lower amount of both carbon.
- The results of the fractionation analysis refer to higher mobility of all chosen elements in the all soils samples during conditions of farming technology application and soil fertilisation, which are typical for agricultural soils.
- The gravitation dust sediment may contaminate soils by Cu, Pb, and Zn, but it isn't the source of contamination soils by Ni. However mobility of Ni in the soils is the highest from all chosen elements.

Acknowledgements

This research was supported by projects VEGA No. 1/3149/06, 1/0459/08 and 1/0461/08.

References

- [1] Dirner V. et al.: Ochrana životního prostředí, TU-VŠB, Ostrava, 1997
- [2] Makovníková J.: Distribúcia Cd, Pb, Cu, a Zn v pôde a jej hodnotenie so zreteľom na potenciály a bariéry transportu kovov do rastlín. Výskumný ústav pôdozvedectva a ochrany pôdy, Bratislava, 2000
- [3] Templeton D.M., Ariese F., Cornelis R., Danielsson L.G., Muntau H., Leeuwen H.P. van, Łobiński R.: Guidelines for terms related to chemical speciation and fractionation of elements. Definition, structural aspects, and methodological approaches. Pure Appl. Chem., 2000, 8 (72), 1453-1470
- [4] Ure A.M., Davidson C.M., Thomas R.P.: Single and sequential extraction schemes for trace metal speciation in soil and sediment, Quality Assurance for Environmental Analysis, Elsevier Science B. V., 1995
- [5] Kubová J., Matúš P., Bujdoš M., Hagarová I., Medved' J.: Utilization of optimised BCR three-step sequential and dilute HCl single extraction procedures for soil-plant metal transfer predictions in contaminated lands. Talanta 75, 2008, 1110-1122
- [6] Matúš P., Kubová J., Bujdoš M., Medved' J.: Determination of operationally defined fractions of aluminium in reference materials and acid attacked environmental samples. Analytica Chim. Acta 540, 2005, 33-43
- [7] Sabienė N., Brazauskienė D.M., Rimmer D.: Determination of heavy metal mobile forms by different extraction methods. Ekologija 1, 2004, 36-41

- [8] Remeteiová D., Krakovská E., Tomko J., Sminčáková E., Vojteková V.: Extrakcia vzoriek prašných spadov EDTA. Sborník konferencie "Mikroelementy 2002", Slapy, 2002, 124-128
- [9] Tomko J., Krakovská E., Remeteiová D. Sminčáková E.: Stanovenie mobilizovateľného obsahu niektorých kovov v prašnom spade 2M HNO₃. Sborník konferencie "Mikroelementy 2002", Slapy, 2002, 129-338
- [10] Remeteiová D., Sminčáková E., Flórián K.: Study of chemical properties of gravitation dust sediments. *Microchim Acta* 156 2007, 109-113

Comparison of Single-Step and BCR Sequential Extraction Procedures of Gravitation Dust Sediment Samples

Radoslav Rusnák¹, Ilona Fekete², Gábor Halász², and Dagmar Remeteiová¹

¹ Technical university of Košice, Faculty of Metallurgy, Department of Chemistry, Letná 9, 042 00 Košice, Slovakia, e-mail: radoslav.rusnak@tuke.sk

² Szent István University, Department of Chemistry and Biochemistry, Gödöllő, Hungary

Abstract

This work presents results of single-steps extractions by using extraction reagents with different extraction effect: 1 mol dm⁻³ NH₄NO₃ for isolation of mobile forms (water-soluble, exchangeable), 0.05 mol dm⁻³ EDTA for isolation of mobilizable forms (water-soluble, ion-exchangeable, organic, carbonate) and 2 mol dm⁻³ HNO₃ for isolation of all releasable forms. The content of elements in the extracts was determined by FAAS method. These results were compared with results of three-steps BCR sequential extraction procedures. In this method were applied extraction reagents with increasing extraction effect in the sequential extraction steps: 0.11 mol dm⁻³ acetic acid (1th step) for isolation of water-soluble, exchangeable, and carbonate fraction, 0.1 mol dm⁻³ hydroxylamine hydrochloride (2th step) for isolation of reducible (e.g. Fe/Mn oxides, oxihydroxides) fraction, which may be mobile by change of redox potential, 8.8 mol dm⁻³ hydrogen peroxide, acid-stabilized to pH 2-3 followed by 1 mol dm⁻³ ammonium acetate adjusted to pH 2 (3th step) for isolation of oxidizable (organic, sulphides) fraction and the aqua regia for decomposition of rest after the third step.

Key words: *fractionation analysis, chemical forms, single-step extraction, BCR sequential extraction, gravitation dust sediment*

Introduction

The increasing interest in obtaining available information about the toxicity, mobility, and bioavailability of risk elements present in the environmental samples has led to use various types of extraction schemes [1]. One of the isolation methods of fraction based on different solubility forms of elements is extraction by using properly extraction reagent and that in single step (for the obtained information about the bioavailable fraction of metals) or multiple (sequential extraction procedure).

The single-step extraction procedures are often used in the fractionation analysis of soils for isolation of various mobile fractions of elements in dependence on the soil-ecological conditions. These fractions are representing by various chemical forms of elements. The so-called "mobile" fraction includes nonspecific sorbed, water-soluble and ion-exchangeable forms of elements and these forms are mobile under normal soil conditions. The so-called "mobilizable" fraction includes the "mobile" fraction and elements forms bounded on the carbonates and organic matter and these forms

may be mobile under changed normal soil conditions. The so-called “maximal potential mobilizable” fraction of elements represents all releasable forms of elements besides of these, which are strongly bounded on the matrix material. Because the gravitation sediment after sedimentation becomes a soil component, the application of soil extraction can be suitable method for isolation of risk element forms from the dust sediment as well. It is necessary modify and optimise this procedures before their application on the gravitation dust sediment samples so that take into account requirement to operate with lower masses of samples for the extraction.

The BCR sequential extraction scheme was originally developed for fractionation of heavy metals from sediment. The modified BCR sequential extraction methods were applied for fractionation of heavy metals from different type of soils, too [1, 2, 3]. Extension of BCR-fractionation studies to gravitation dust sediment samples is also suitable for evaluation of soil contamination by toxic elements from gravitation dust sediments. In reason of the sequential extraction application is possible to isolate fractions of elements, which include various elements forms too. In the first step of the BCR extraction are isolated ion-exchangeable, water and acid-soluble (e.g. carbonates) elements forms. In the second step are isolated reducible (e.g. Fe/Mn oxides, oxihydroxides) forms and in the third step they are oxidisable (e.g. bound to organic matter or sulphides) forms of elements.

Experimental

The sample of the gravitation dust sediment, in next text referred to as “dust” from Košice residential city agglomeration in East Slovakia has been collected in glass settling vessels replete by 250 cm³ distilled water. After expiration of exposition time the content of vessels was quantitatively flushed by distilled water into the Pt-vessels and then evaporated to dryness on the water bath. After drying the sample was homogenised by crushing and grinding in the agate mill.

For extraction of “mobile” elements fraction was used 1 mol dm⁻³ NH₄NO₃, for isolation “mobilizable” elements fraction was used 0.05 mol dm⁻³ EDTA (pH = 7, treated by NH₄OH) and for isolation of “maximal potential mobilizable” fraction was used 2 mol dm⁻³ HNO₃ (pH = 0.7). The ratio value of the sample mass to volume of extracting solution (w/v) was constant (0.5 g/75 cm³) for all experiments [4,5].

Conventional single-step extraction procedures were carried out by mechanical shaking of the gravitation dust sediment samples in extraction reagent in 100 cm³ polyethylene extraction vessel for the duration of 1 hour for NH₄NO₃ and EDTA, and 6 hours for HNO₃ at room temperature.

After finishing of extractions, the content of extraction vessels was filtered through filter paper with narrow pores and diameter = 18.5 cm. Determination of Cu, Pb, and Zn content in filtered extracts was carried out using of the flame atomic absorption spectrometer (Perkin–Elmer 3030 equipped with a deuterium lamp for background correction and air/acetylene flame). Hollow cathode lamps were used as the radiation source. The resonance lines 324.6 nm for Cu, 216.7 nm for Pb, 231.9 nm for Ni and 213.7 nm for Zn were employed.

The first step of the conventional BCR extraction was carried out by mechanical shaking of the sample and extraction reagent (0.11 mol dm⁻³ acetic acid) in 100 cm³ polyethylene centrifuge tube for the duration of 16 hrs at ambient temperature [6]. The extract was separated from the solid residue by centrifugation at 3800 rpm for 20 min and decanting the supernatant into a glass container. The residue was washed with 20 cm³ of double-deionized water by shaking for 15 min and centrifuging. The residue from the Step 1 was slurred in a 50 cm³ polyethylene centrifuge tube by adding of 0.1 mol dm⁻³ hydroxylamine hydrochloride solution adjusted to pH 2 with HNO₃. After shaking the tube for 16 hrs, the extract was centrifuged for 15 min at 3800 rpm and then decanted slowly into a beaker. The residual solid was washed with some water, shaken, and centrifuged. To the residue from the second step, 10 cm³ of 8.8 mol dm⁻³ H₂O₂ solution was carefully added, in little aliquots, to avoid losses due to violent reaction. The vessel was covered and occasionally shaken by hand at room temperature for 1 h. Then it was placed on a sand bath heated at 85 °C and evaporated to near dryness, and the same procedure repeated by adding 10 cm³ of H₂O₂. Hereafter, 50 cm³ of CH₃COONH₄ was

introduced into the mosit residue. The extraction process was carried out as mentioned above at the first and second stages, then the extract was putted into a beaker. In the Step 4, 5 cm³ of doubly-distilled water and 12 cm³ of aqua regia solutions were added to approximately 0.4 g of the remaining residue and the solution obtained was evaporated near to dryness at 150 °C on a sand bath and the same procedure repeated for 8 cm³ aqua regia solution. After adding 2 mol dm⁻³ HNO₃ in small aliquots to the last residue, the extract was filtered on a filter paper with blue ribbon. All vessels were cleaned by soaking in 4 mol dm⁻³ nitric acid and rinsing with distilled water [7]. The shaking speed has been adapted in order to ensure a continuous suspension of the mixture. The ratio value of the sample mass to volume of extraction solution (w/v) was constant (1 g/40 cm³) for all experiments. In all experiments have been realised three repeated measurements and for each series of experiments were performed also reagent blanks.

Determination of elements content in extracts was carried out using of the flame atomic absorption spectrometer Perkin–Elmer 3030.

Results and discussion

The results of the single-steps extractions of the dust sediment sample are given in Table 1.

Table 1. The percentage recoveries of elements in the extracts of single-steps extractions

Element	Relative recoveries / %		
	1 mol dm ⁻³ NH ₄ NO ₃	0.05 mol dm ⁻³ EDTA	2 mol dm ⁻³ HNO ₃
Cu	17.7	44.2	92.0
Pb	<LoD	27.4	72.9
Zn	20.9	27.1	76.7
Ni	<LoD	1.3	6.2

From these results it is possible to state that Pb and Ni aren't in the gravitation dust sediment sample bounded in the water-soluble and ion-exchangeable forms. Their content in EDTA-extracts corresponds to content in the carbonate or organic forms.

The percentage recoveries of chosen elements in the extracts of the gravitation dust sediment sample from each steps of the BCR sequential extraction procedure are given in Table 2.

Table 2. The percentage recoveries of elements in the BCR extracts

Element	Relative recoveries / %			
	BCR 1	BCR 2	BCR 3	BCR 4
Cu	37.7	21.8	35.1	4.4
Pb	9.4	37.7	42.4	5.8
Zn	26.3	27.1	17.8	18.3
Ni	2.5	0.1	4.2	107.5

On the basis of relative recoveries mentioned in the Table 2 it can be stated, that for every each determinable element was achieved the highest recoveries in the other steps of the BCR sequential extraction. This differences related to the forms of observed elements in the dust particles. The higher recoveries of Ni impressed with error in the measurement.

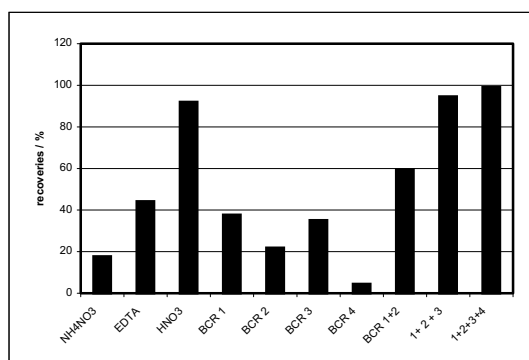
The percentage recoveries of elements in the BCR extracts were compared with recoveries in the extracts of the single-steps extractions.

On the basis of different effect of extraction reagents in compared extraction procedures, the probable content of elements in the some concrete chemical forms is possible to determine. The percentage content of elements in the carbonate fraction is possible to determine from differences of relative recoveries in the 1st step of BCR extraction procedure (BCR 1 = water soluble + exchangeable + carbonate fraction), and of relative recoveries into the NH_4NO_3 (water soluble + exchangeable). The percentage content of elements in the organic fraction is possible to determine from differences of relative recoveries into the EDTA (water soluble + exchangeable + organic bounded + carbonate fraction), and of relative recoveries in the 1st step of BCR extraction. The differences between relative recoveries in the 3rd step of BCR extraction (BCR 3 = organic + sulphides fraction) and dedicated percentage content of elements in the organic fraction may represent the percentage content of elements in the sulphide fraction. The determined percentage contents of elements are listed in Table 3.

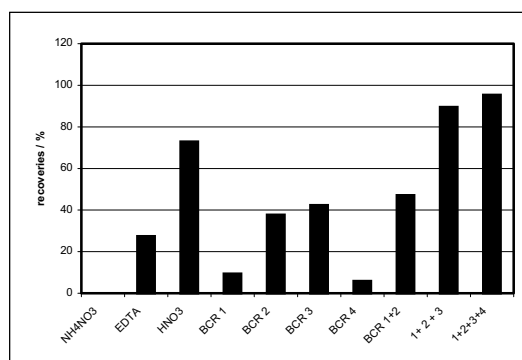
Table 3. The percentage contents of elements in the determine chemical forms

Element	Percentage content / %		
	Chemical form		
	Carbonate	Sulphide	Organic
Cu	20.0	28.6	6.5
Pb	9.4	24.4	18.0
Zn	5.4	17.0	0.8
Ni	2.5	5.4	-

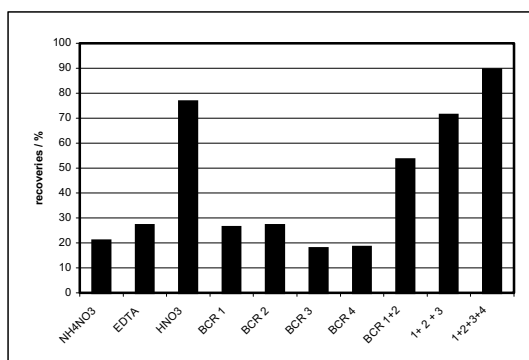
The percentage recoveries of chosen elements in the individual extracts are plotted in Fig. 1a, b, c, d.



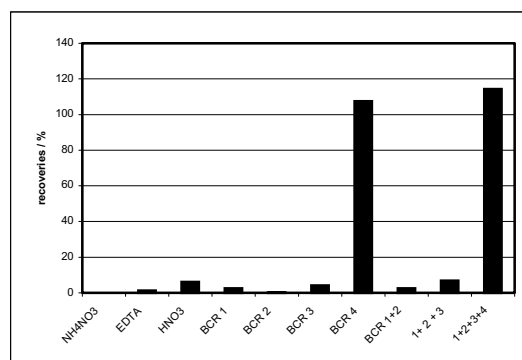
a) The percentage recoveries of Cu



b) The percentage recoveries of Pb



c) The percentage recoveries of Zn



d) The percentage recoveries of Ni

Fig. 1a, b, c, d: The graphic comparison of the relative recoveries of Cu, Pb, Zn, and Ni

Conclusion

Extractions in the fractionation analysis make for isolation of elements fractions, which consists from several chemical forms. By comparison of results of various extraction procedures is possible to determine approximative content of elements in some concrete chemical forms in within individual fractions.

On the basis of obtained results it is possible to state, that:

- Differences between recoveries in the EDTA-extracts and HOAc-extracts (part of elements bounded on the organic matter) decrease in the order: Pb, Cu, Zn, Ni.
- Differences between recoveries in the HOAc-extracts and NH_4NO_3 -extracts (part of elements bounded in the carbonates forms) decrease in the order: Cu, Pb, Zn, Ni.
- The recoveries in the HNO_3 -extracts are approximately equal to sum of recoveries of 1th 2th and 3th step of the BCR extraction.
- The content of elements in the sulphides forms decrease in the order: Cu, Pb, Zn, Ni.

Acknowledgements

This research was supported by projects: Slovak – Hungarian (SK-MAD-02406) and VEGA (1/0459/08, 1/0461/08, 1/3149/06).

References

- [1] Kubová J., Matúš P., Bujdoš M., Hagarová I., Medved' J.: Utilization of optimised BCR three-step sequential and dilute HCl single extraction procedures for soil-plant metal transfer predictions in contaminated lands. *Talanta* 75, 2008, 1110-1122
- [2] Golia E.E., Tsiropoulos N.G., Dimirkou A., Mitsios I.: Distribution of heavy metals of agricultural soils of central Greece using the modified BCR sequential extraction method. *Intern. J. Environ. Anal. Chem.* 87, No. 13-14, 2007, 1053-1063
- [3] Žemberyová M., Barteková J., Hagarová I.: The utilization of modified BCR three-step sequential extraction procedure for fractionation of Cd, Cr, Cu, Ni, Pb and Zn in soil reference materials of different origins. *Talanta* 70, 2006, 973-978
- [4] Remeteiová D., Krakovská E., Tomko J., Sminčáková E., Vojteková V.: Extrakcia vzoriek prašných spadov EDTA. Sborník konferencie "Mikroelementy 2002", Slapy, 2002, 124-128
- [5] Tomko J., Krakovská E., Remeteiová D., Sminčáková E.: Stanovenie mobilizovateľného obsahu niektorých kovov v prašnom spade 2M HNO_3 . Sborník konferencie "Mikroelementy 2002", Slapy, 2002, 129-338
- [6] Quevauviller Ph., Rauret G., López-Sánchez J.F., Rubio R., Ure A., Muntau H.: The certification of the EDTA-extractable contents (mass fractions) of Cd, Cr, Ni, Pb and Zn in sediment following a three-step sequential extraction procedure. CRM 601, 1997 Luxemburg: Office for Official of the European Communities
- [7] Ure A.M., Davidson C.M., Thomas R.P.: Single and sequential extraction schemes for trace metal speciation in soil and sediment, *Quality Assurance for Environmental Analysis*. Elsevier Science B. V., 1995

Effect of Soil Sample Treatment on Evaluation of Trace Element (Cu, Fe, Mn, Zn) Mobility in Soils

Jiřina Száková, Pavel Tlustoš, Zuzana Frková, Jana Najmanová, Jiří Balík

Czech University of Life Sciences Prague, Faculty of Agrobiolgy, Food and Natural Resources, Dept. of Agroenvironmental Chemistry and Plant Nutrition, 165 21 Prague 6 – Suchbátov, Czech Republic, e-mail: szakova@af.czu.cz

Abstract

The extractability of Cu, Fe, Mn, and Zn with various extracting agents as well as the effect of sample pretreatment (drying, freezing of the soil sample) were evaluated at eight soil samples differing in their physicochemical parameters. The extractability of elements decreased in order Zn > Cu > Mn > Fe. In the case of mild extraction procedures (0.01 mol.l⁻¹ CaCl₂, water) the released portions of elements were low and affected significantly by differing physicochemical parameters of individual soils and also in behavior of individual elements. Two methods of soil solution collection were tested: i) centrifugation of saturated soil and ii) the application of suction cups. Slightly higher Fe and Zn concentrations were obtained by centrifugation method whereas Cu and Mn concentrations were lower. However, fairly good correlations between these sampling methods were calculated for Cu (r=0.74), Mn (r=0.94), and Zn (r=0.57).

Key words: soil, extraction, soil solution, sample pretreatment, copper, iron, manganese, zinc

Introduction

Various soil extraction procedures were developed and tested for determination of plant-available, mobile, and potentially mobilizable pools of trace elements in soils without general agreement of authors which extractant is the most suitable to estimate mobility of individual elements. Moreover, the effectiveness of individual extractants to predict the plant-available elements depends on soil physicochemical parameters and contamination levels [1].

Soil solution represents essential electrolytic water solution containing dissolved organic and inorganic compounds (colloids, free salts and ions of these salts), atmospheric gases and exudates of plant roots and microorganisms. The knowledge of soil solution composition is substantial for elucidation of processes of element uptake by plants and plant growth. Leaching, evaporation, and plant transpiration can affect contents of trace metals and metalloids more than the changes in the contents of main ions (Ca, Mg, K, Na, NO₃, PO₄) [2,3]. Various methods were developed for collection of soil solution [4] such as centrifugation, suction cups or lysimeters where *in situ* sampling is considered to better represent solution extracted by plants and the physical structure of sample remains intact.

The sample pre-treatment and/or storage before extraction can affect the composition of soil solution (or extract), which is related to element mobility in soils [5,6]. Wang et al. [7] observed increasing water soluble, exchangeable, and carbonate bound fractions of Cu and Zn in air-dried soils

compared to wet soil sample even by 20-50 %. Similarly, the importance of sample drying was reported by McLaren and Clucas [8] for sewage sludge samples. They also described the increasing water extractable portions of Cu and Zn, which were related to concentrations of the dissolved organic carbon in the samples. They speculated that the oxidation of organic matter during drying process can either release the organically bound elements or can result in greater complexing of metals due to increased concentrations of water soluble organic components.

In our experiment the extractability of selected micronutrients (Cu, Fe, Mn, and Zn) with various extracting agents as well as the effect of sample pretreatment were evaluated at eight soil samples differing in their physicochemical parameters. Moreover, different approaches to soil solution sampling were compared and evaluated.

Experimental

Eight soils selected from specific locations of Czech Republic differing in physical-chemical properties and total element contents (Table 1) were extracted by following extraction procedures: (1) extraction with 2 mol.l⁻¹ solution of HNO₃ in ratio 1:10 (w/v) at 20 °C for 6 hours [9], (2) extraction with 0.43 mol.l⁻¹ solution of CH₃COOH in ratio 1:40 (w/v) for 5 hours [10], (3) extraction with 0.05 mol l⁻¹ EDTA aqueous solution at pH 7 in a ratio of 1:10 (w/v) for 1 hour [10], (4) Mehlich III extraction procedure (0.2 mol.l⁻¹ CH₃COOH + 0.25 mol.l⁻¹ NH₄NO₃ + 0.013 mol.l⁻¹ HNO₃ + 0.015 mol.l⁻¹ NH₄F + 0.001 mol.l⁻¹ EDTA in ratio 1:10 (w/v) for 10 minutes) [11], (5) extraction with 0.01 mol.l⁻¹ aqueous CaCl₂ solution in ratio 1:10 (w/v) for 6 hours [12], and (6) extraction with deionized water in ratio 1:10 (w/v) for 16 hours [13]. Each extraction was provided in three replications, all the chemicals used were of electronic grade purity and were purchased from Analytika Ltd., and Lach-Ner Ltd., Czech Republic. For the centrifugation of the extracts, the Hettich Universal 30 RF (Germany) device was used. The reaction mixture was centrifuged at 3000 rpm (i.e. 460xg) for 10 minutes at the end of each step and supernatants were kept at 6 °C before measurement.

The total contents of elements in the soils were determined in the digests obtained by the following decomposition procedure: Aliquots (0.5 g) of air-dried soil samples were decomposed in a digestion vessel with a mixture of 8 ml concentrated nitric acid, 5 ml of hydrochloric acid, and 2 ml of concentrated hydrofluoric acid. The mixture was heated in an Ethos 1 (MLS GmbH, Germany) microwave assisted wet digestion system for 33 min at 210 °C. After cooling, the digest was quantitatively transferred into a 50 ml Teflon[®] vessel and evaporated to dryness at 160 °C. The digest was then dissolved in a 3 ml nitric and hydrochloric acid mixture (1+3), transferred into a 25 ml glass tube, filled up by deionized water, and kept at laboratory temperature until measurement. A certified reference material RM 7001 Light Sandy Soil was applied for the quality assurance of analytical data.

Soil samples were air-dried at 20 °C ground in a mortar and passed through a 2-mm plastic sieve before extraction and total element content determination. Alternatively, aliquots of the samples were extracted as moist samples (saturated to 100 % of its maximal water holding capacity) immediately after soil sample collection where dry mass of the soils was determined separately. Finally, aliquots of the samples were freeze-dried at -18 °C for 14 days and then air dried, ground, and sieved. In this case, the effect of sample pre-treatment was tested for 0.05 mol l⁻¹ EDTA, 0.01 mol.l⁻¹ CaCl₂, and water extracts.

Element concentrations in soil solution represent the element portion determining directly the plant-availability of these elements. However, there are different approaches of soil solution collection [4]. We tested i) centrifugation of fully saturated soil at 10 000 rpm for 10 minutes and ii) the application of suction cups, where specialized plastic suction cups (DI Gottfried Wieshammer, Wien, Austria) were applied into pots containing cca 350 g of the soil at the beginning of the experiment to get a soil solution. The pots with installed suction cups were watered with deionised water to full water capacity one day before suction and leave 24 h to equilibrate. It was sampled always 10 ml of soil solution from each pot and immediately analyzed for element concentrations.

The contents of Cu, Fe, Mn, and Zn in soil digests and extracts were determined by optical emission spectroscopy with inductively coupled plasma (ICP-OES) with axial plasma configuration, Varian, VistaPro, equipped with autosampler SPS-5 (Australia). Measurement conditions were for all elements: power 1.2 kW, plasma flow 15.0 l.min⁻¹, auxiliary flow 0.75 l.min⁻¹, nebulizer flow 0.9 l.min⁻¹.

Table 1. Basic characteristics of the experimental soils

Soil location	CEC mmol.kg ⁻¹	Cox %	pH	Cu mg.kg ⁻¹	Fe mg.kg ⁻¹	Mn mg.kg ⁻¹	Zn mg.kg ⁻¹
Píšťany	201±4	2.6±0.1	6.8±0.5	60.9±3.9	16400±790	975±13	202±5
Mikulov	99.1±8.2	4.2±0.1	4.2±0.2	37.8±0.5	18330±1662	1185±161	145±5
Pramenáč	157±1	3.9±0.2	3.5±0.1	10.4±1.1	26697±3465	1500±98	83.2±3.6
Příbram meadow	166±20	3.6±0.4	5.2±0.1	31.4±1.7	13123±415	1042±43	200±0
Kbely	299±4	1.9±0.1	7.2±0.4	83.7±6.8	15101±174	440±23	119±6
Příbram arable	151±2	2.1±0.1	6.0±0.2	44.3±0.1	14751±1895	991±146	269±20
Litavka	134±3	1.9±0.2	4.6±0.1	92.0±11.0	21617±2280	3831±546	2187±346
Kutná Hora	295±13	2.9±0.1	7.1±0.2	57.0±7.4	16676±177	434±26	401±8

Results and discussion

As evident from the Table 1, almost all the experimental soils (except the soils Pramenáč and Kbely) belong to the zinc contaminated soils where the rate of contamination significantly differed among the soils. The highest total zinc content was determined in the soil Litavka representing serious anthropogenic contamination. Fluvisol from the alluvium of the Litavka river was heavily polluted by wastes from smelter setting pits. In the case of Cu, total concentrations of this element exceed limit permitted by Czech national legislation slightly in the soils Píšťany, Kbely, and Litavka. Soil concentration limits are 60 and 120 mg kg⁻¹ for Cu and Zn, respectively [14].

Among the strong extractants used the extractability decreased in order 2 mol.l⁻¹ HNO₃ > 0.05 mol.l⁻¹ EDTA > Mehlich III > 0.43 mol.l⁻¹ CH₃COOH whereas the extractability of individual elements in order Zn > Cu > Mn > Fe (Fig. 1). Diluted nitric acid is able to dissolve the element portion comparable to the sum of labile soil element fractions [9] and its efficiency to extract the investigated elements was the highest for all the elements. In the case of Cu, however, the effectivity of 2 mol.l⁻¹ HNO₃ was comparable to 0.05 mol.l⁻¹ EDTA the most probably because of high affinity of this element to soil organic matter [15]. The advantage of the Mehlich III extraction method is that it may offer the possibility of using one test for P and other nutrients across acid, neutral, and high-pH soils [16]. Many authors stated that Mehlich III results showed good correlation with other extractants, *i.e.* EDTA- extractable Cu and Zn [17], and 1 mol.l⁻¹ HCl - extractable Cu and Mn [18]. Low effectivity of Mehlich III extractant for release of soil Fe [19] was confirmed not exceeding 2 % of total content. Concerning 0.43 mol.l⁻¹ CH₃COOH extraction, this agent is recommended to predict the behavior of soil elements under changing soil pH conditions [20]. Menzies et al. [1] documented poor correlations of strong soil extraction procedures with plant-available portion of soil elements and recommended neutral salt extractants such as 0.01 mol.l⁻¹ CaCl₂ and 0.1 mol.l⁻¹ NaNO₃ as more useful extractants for this purpose.

In the case of mild extraction procedures (0.01 mol.l⁻¹ CaCl₂, and water) the released portions of elements were lower, affected significantly by differing physicochemical parameters of individual soils and also in behavior of individual elements (Figure 2 and 3). The extractability of individual elements decreased in order Zn ≈ Cu > Mn >> Fe for 0.01 mol.l⁻¹ CaCl₂, and in order Zn ≈ Cu ≈ Mn > Fe for water extracts. The results suggested higher extractability of Cu, Mn, and Zn from the soils with low pH (Mikulov, Pramenáč), and in the soil affected by anthropogenic contamination. In the

opposite, low mobility of the elements was observed in the soils characterized by high sorption capacity and/or high pH level (Pramenáč, Kbely, Kutná Hora). Significantly higher extractability of Cu from air-dried samples suggested the effect of the oxidation of organic matter during drying of the samples as described by McLaren and Clucas [8]. This effect, however, was not significant for any other investigated element due to stronger affinity of copper to soil organic matter compared to Fe, Mn, and Zn [15].

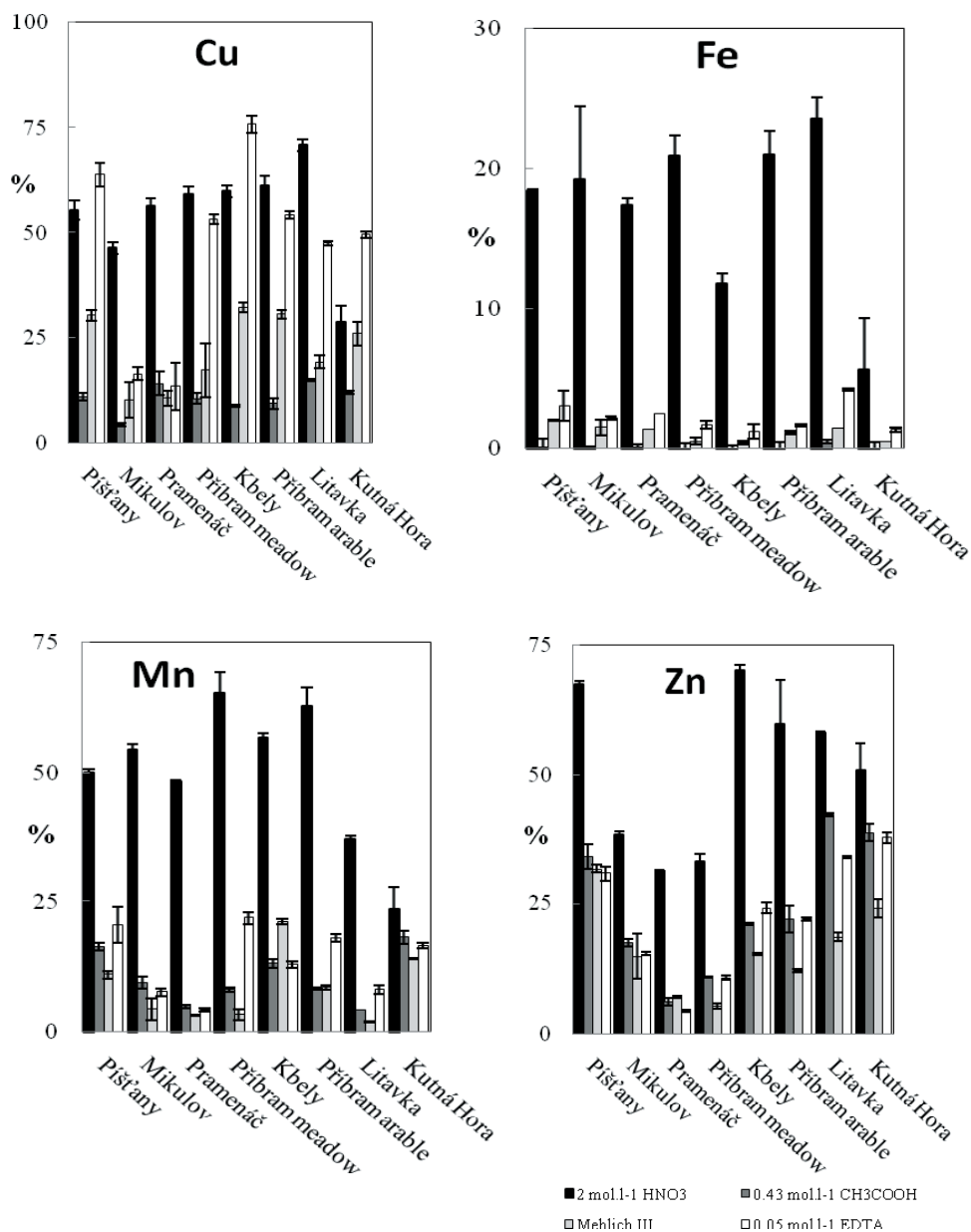


Fig. 1. Comparison of the set of strong extraction procedures (% of total element content in soil)

Three sample pre-treatments before extraction were compared: i) air-dried samples; ii) fresh samples; iii) samples frozen for 14 days and then air-dried. The results showed significant response of elements on individual sample pre-treatments as well as the influence of extraction agent applied. Whereas the water extractable portions of elements decreased in order air-dried soil > frozen+air-dried soil > fresh soil completely opposite behavior of extractable elements were observed in 0.01 mol.l⁻¹ CaCl₂ extracts where the air-dried soils showed the lowest contents, most significantly in the

case of iron. Evidently, the effect of soil pretreatment is manifested in dependence to individual extraction agent and should be evaluated according to different methodological approaches within group of mild soil extraction procedures.

Element concentrations in soil solution should represent the element portion determining directly the plant-availability of these elements. However, there are different approaches of soil solution collection. We tested: i) centrifugation of saturated soil and ii) the application of suction cups (Fig. 4). Nolan et al. [4] reviewed the data of different sample solution collection methods and centrifugation methods tended to perform higher concentrations compared to other methods. Our data showed that slightly higher Fe and Zn concentrations were obtained by centrifugation method whereas Cu and Mn concentrations were lower.

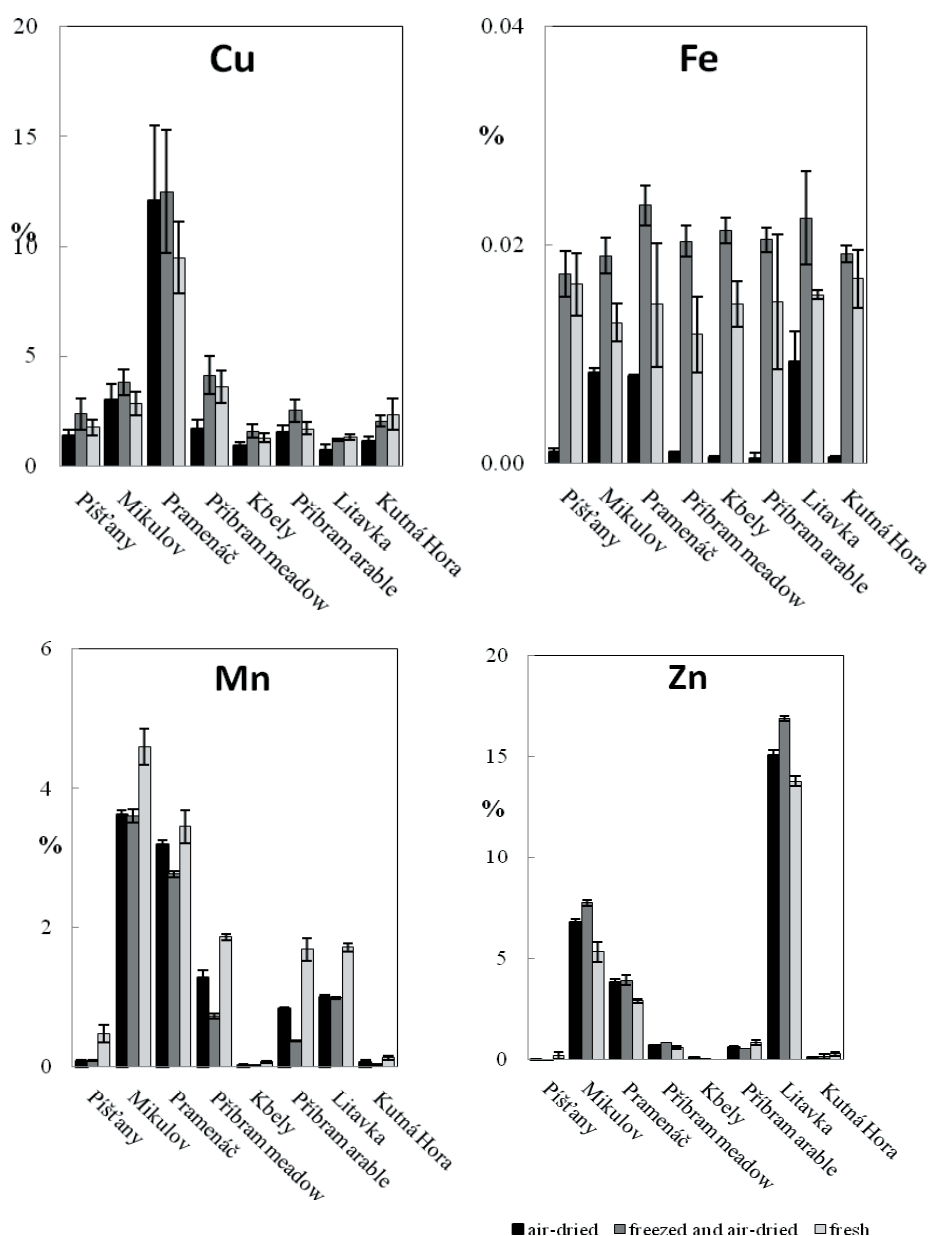


Fig. 2. The effect of sample pre-treatment on $0.01 \text{ mol l}^{-1} \text{ CaCl}_2$ extractable portion of elements in soils (% of total element content in soil)

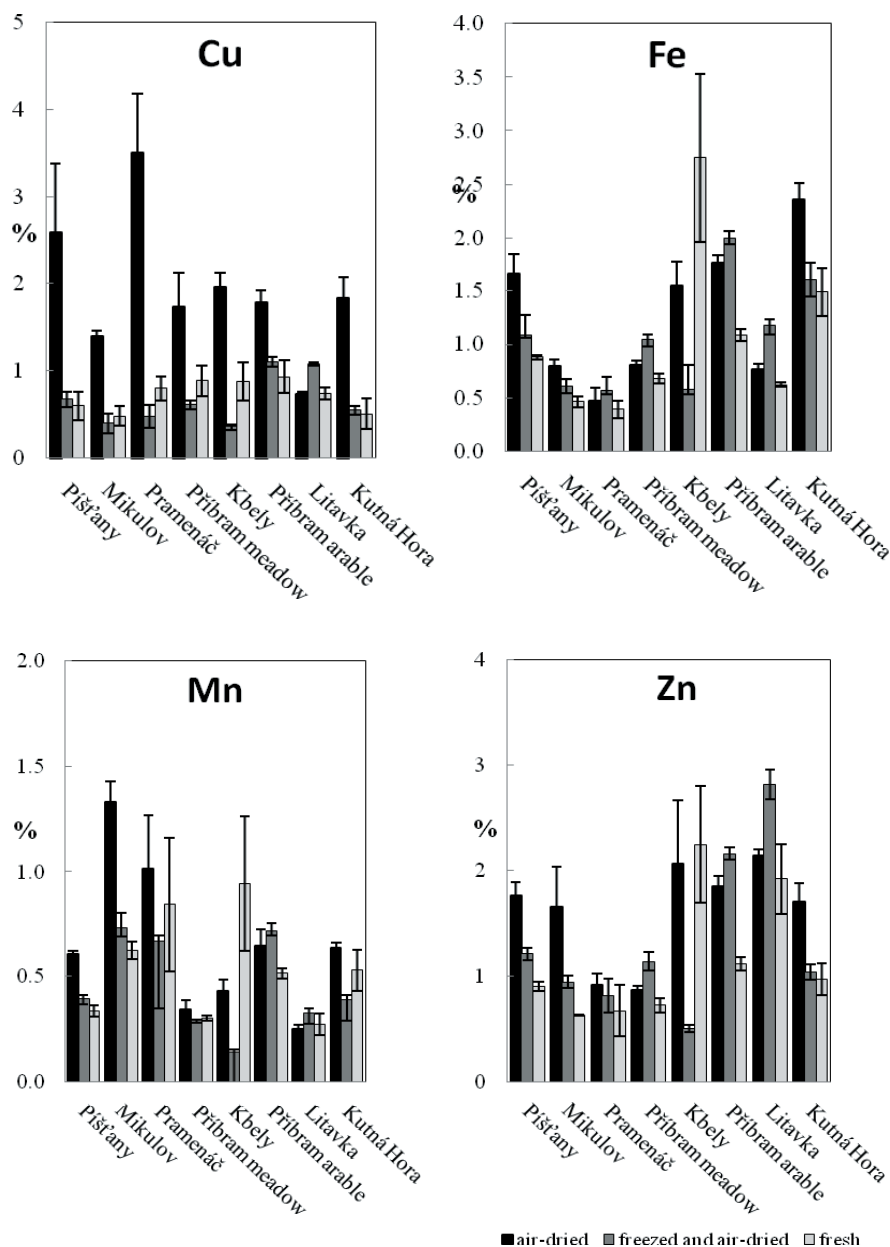


Fig. 3. The effect of sample pre-treatment on water extractable portion of elements in soils (% of total element content in soil)

Wang et al. [7] and Gray and McLaren [6] recommended to apply the extraction and/or soil solution sampling of field-moist soil samples reflecting more intensively *in situ* conditions for better correlations with plant-available element portions. As documented by our results, different sample pretreatment and/or different mild soil extraction procedures can lead to different absolute values of mobile element content in soils. However, the interpretation of the data can lead to similar conclusions comparing the individual soils as apparent from the comparison of the soil solution sampling methods. Fairly good correlations between these sampling methods were calculated for Cu ($r=0.74$), Mn ($r=0.94$), and Zn ($r=0.57$). For Fe high variability of the data due to very low element concentrations limited the statistical evaluations of the analytical data. Substantial portion of elements in the soil solution is present in organic complexes [21] and are not directly available to plants. Therefore, determination of total element concentrations in soil solution is insufficient for exact evaluation of the

plant-availability of individual elements and element speciation should be involved to the schemes of soil solution analyses.

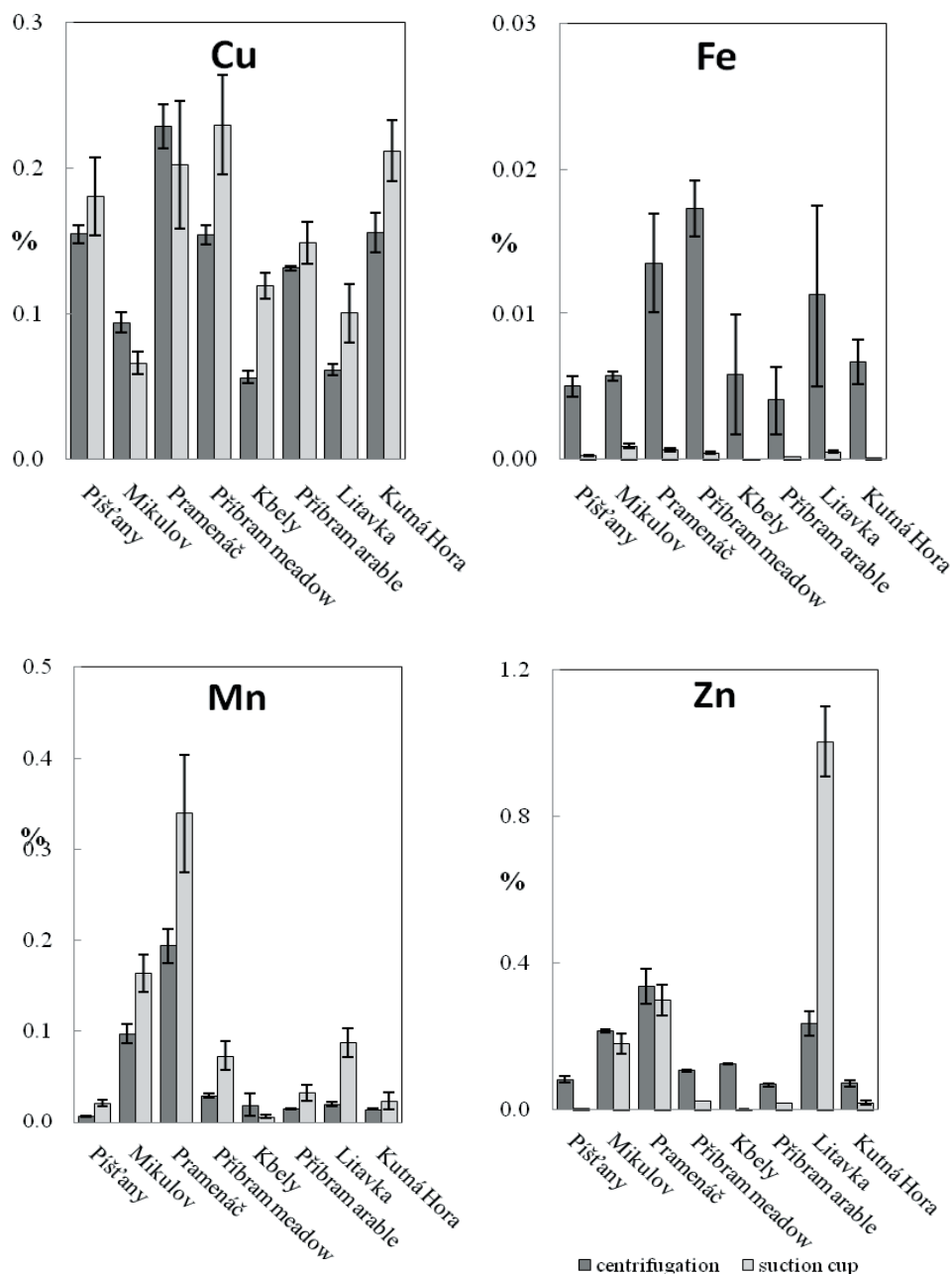


Fig. 4. Comparison of the methods of soil solution sampling (% of total element content in soil)

References

- [1] Menzies N.W., Donn M.J., Kopittke P.M.: Evaluation of extractants for estimation of the phytoavailable trace metals in soils. *Environ Pollut*, 2007, 145, 121-130
- [2] Adriano D.C.: Trace elements in terrestrial environments: Biogeochemistry, bioavailability, and risks of metals. Second edition, Springer-Verlag, New York, 2001
- [3] Kabata-Pendias A., Pendias, H.: Trace Elements in Soils and Plants, Third Edition, CRC Press, Boca Raton, USA, 2001

- [4] Nolan A.L., Lombi E., McLaughlin M.J. (2003): Metal bioaccumulation and toxicity in soils – Why bother with speciation? *Austr. J. Chem.* 56: 77-91
- [5] Pérez D.V., De Campos C., Menequelli N.A.: Effects of soil sample storage treatment on the composition and Fe, Al, and Mn speciation of soil solutions obtained by centrifugation. *Water, Air, Soil Pollut*, 2004, 151, 195-214
- [6] Gray C.W., McLaren R.G.: Effects of air drying or sample storage on soil-solution properties of biosolids-amended soil. *Commun Soil Sci Plant Anal*, 2003, 34, 2327-2338
- [7] Wang Z., Shan X., Zhang S.: Comparison of speciation and bioavailability of rare earth elements between wet rhizosphere soil and air-dried bulk soil. *Anal Chim Acta*, 2001, 441, 147-156
- [8] McLaren R. G., Clucas L. M.: Fractionation of copper, nickel, and zinc in metal-spiked sewage sludge. *J Environ Qual*, 2001, 30, 1968-1975
- [9] Borůvka L., HuanWei C., Kozák J., Křištofková S.: Heavy contamination of soil with cadmium, lead and zinc in the alluvium of the Litavka river. *Rost Vým*, 1996, 42, 543-550
- [10] Quevauviller P., Ure A., Muntau H., Griepink B.: Improvement of analytical measurements within the BCR-program – Single and sequential extraction procedures applied to soil and sediment analysis. *Intern J Environ Anal Chem*, 1993, 51, 129-134
- [11] Mehlich A.: Mehlich 3 Soil Test Extractant: A modification of Mehlich 2 Extractant. *Commun Soil Sci Plant Anal*, 1984, 15, 1409-1416
- [12] Novozamsky J., Lexmond T. M., Houba V.J.G.: A single extraction procedure of soil for evaluation of uptake of some heavy metals in plants. *Int J Environ Anal Chem*, 1993, 51, 47-58
- [13] Kiekens L., Cottenie A.: In: Leschber R. (ed), Chemical methods for assessing bio-available metals in sludges and soils. p 42, Elsevier Applied Science, London, 1985
- [14] Anonymous, 2001. Public notice No. 382/2001 about the application of sewage sludge into the agricultural soils. Czech Ministry of the Environment, Prague, October 17th, 2001
- [15] Bolan N., Adriano D., Mani S., Khan A.: Adsorption, complexation, and phytoavailability of copper as influenced by organic manure. *Environ Toxicol Chem*, 2003, 22, 450-456
- [16] Mallarino A., Sawyer J.E.: Interpreting Mehlich-3 soil test results. In: Integrated Crop Management Newsletter, IC-482(2). Iowa State University, Ames, IA, 1999
- [17] Brennan D., Coulter B., Mullen G., Courtney R.: Evaluation of Mehlich 3 for extraction of copper and zinc from Irish grassland soils and for prediction of herbage content. *Commun Soil Sci Plant Anal*, 2008, 39, 1943 – 1962
- [18] Loide V., Nõges M., Rebane J.: Assessment of the agrochemical properties of the soil using the extraction solution Mehlich 3 in Estonia. *Agron Res*, 2005, 3, 73-80
- [19] Franklin R.E., Duis, L., Smith B.R.: Mehlich extractable and total elemental concentrations in South Carolina soils. *Commun Soil Sci Plant Anal*, 2006, 37, 679-691
- [20] Sastre J., Hernández E., Rodríguez R., Alcobé X., Vidal M., Rauret G.: Use of sorption and extraction tests to predict the dynamics of the interaction of trace elements in agricultural soils contaminated by a mine tailing accident. *Sci Total Environ*, 2004, 329, 261-281
- [21] Ge Y., Murray P., Hendershot W.H., Trace metal speciation and bioavailability in urban soils. *Environ Pollut*, 2000, 107, 137-144

Authors thank for financial support of the GAČR project No. 521/06/0496

Instructions to authors

The manuscript of every single contribution has to be submitted:

1. On a separate DS HD, IBM PC compatible formatted 3.5" 1.44 MB diskette. The text must be written in MS Word 97, MS Word 2000 or some other compatible editors. The article must contain all tables, graphs and pictures in common software formats, arranged to appropriate positions in the article, in the final size and form.
2. Simultaneously, you are requested to enclose two additional physical copies, single side-printed in "camera ready" quality. Printed manuscripts may be in some cases directly copied or scanned for final journal printing. Pictures will be printed in black and white. No changes will be performed in the Editorial Office. The page heads and foots with the page numbers will be added by the Editorial Office during printing, they should not be printed in manuscripts.
3. In any world language, but English is preferred and recommended. When the language is different from English, then abstracts, key words, tables and descriptions of graphs and pictures must be added also in English.
4. Either the first author's name and page number slightly indicated with a pencil on the backside of each single side-printed page.
5. In absolute accordance with the next example page.

Publication of articles is free of charge. Authors are fully responsible for the content, form, wording and grammar correctness of their articles. Articles should not exceed 8 pages (not a condition). The Editorial Office maintains reserved the possibility to make minimal formal and text changes without previous consent of authors. The Editorial Office is not responsible for making any corrections, instructive remarks or other changes in accepted neither in refused articles; authors should follow the instructions printed in every issue of the journal. Omitting any single one detail described in the instructions to authors can cause refusing the manuscript. Articles refused due to format errors only (not those refused due to negative referee's comments) can be published later, after corrections made by authors.

Special requirements (color pictures, extra large articles, monothematic issues etc.) must be previously addressed in written form to the Editorial Board. The Editorial Board will inform you whether your special requirements can be or cannot be accepted at the actual time, and further details will be sent to you.

For further details, contact us:

Editorial Board Secretary

Ing. Helena Fialová

Dept. of Chemistry

Metallurgical Faculty

Technical University, Letná 9

042 01 Košice, SLOVAK REPUBLIC

tel.: ++421 55 602 2318

fax: ++421 55 633 7048

e-mail: Helena.Fialova@tuke.sk

Page margins: top 3 cm; bottom, left and right 2.5 cm.

12 p space (2 x)

12 p space

How to write articles (article title from the left margin; only the 1st capital) **20 p bold**

12 p space (3 x)

12 p space

12 p space

¹Helena Fialová, ²Marek Dudáš (from the left margin, no titles and degrees)

12 p bold

¹Technical University, Metallurgical Faculty, Dept. of Chemistry, Letná 9, 042 00 Košice, Slovak Republic 9 p italic

²P. J. Šafárik University, Dept. of Medical Biology, Trieda SNP 1, 040 01 Košice, Slovak Republic 9 p italic

11 p space (5 x)

11 p space

11 p space

11 p space

11 p space

Abstract (from the left margin, no full stop)

12 p bold

12 p space

English text that briefly shows ideas and conclusions of presented work. The abstract should be structured, but this is not the *condition sine qua non*. English abstract with key words is always the first in non-English articles; the second abstract with key words follows in the same form.

Structured abstracts. If you use structured abstract, every paragraph begins with the use of not bold 11 points high italics. The text always starts from the left margin, no tabulator is used. It is recommended not to use unexplained or uncommon abbreviations and numbered citations [3] in abstracts. Abstracts usually should not exceed approx. 10 lines.

11 p bold

11 p space

Key words: all key words in English (resp. in the other language) -- italic type -- words and expressions are separated with two adjacent short dashes -- usually no more than 4 lines

11 p italic

11 p space (2 x)

11 p space

Headlines (from the left margin, no full stop)

12 p bold

11 p space

Continuous text 11 points high, divided appropriately in paragraphs; tabulator 1 cm. The entire article, starting from the title and ending with references, must be written with the use of the font Times New Roman. Mathematical equations are written in italics, centered and numbered, e.g.:

$$c^2 = a^2 + b^2$$

11 p space

(1)

11 p space

Pictures, graphs and tables must be included in the text at the appropriate places, separated minimally with two 11 p space lines (from the object's text resp. object's top or bottom).

11 p

11 p space

11 p space

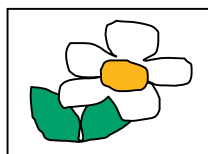


Fig. 1. The 9 to 11 p text should be upon the tables or under the pictures and graphs, separated with one 9 p space line. Or the text may be in the left or right side of a table, graph or picture, like this text. If the article is not in English, the text in the other worldwide language must be situated at the second place, after English version. The picture numbering and description are voluntary, but must be uniform in the entire article.

11 p space (2 x)

11 p space

References or References and notes (full form with article names, alphabetical order) **12 p bold**

11 p space etc.

[1] Author B.A.von, Writer J.K.L.: **Article name.** *Our J Transactions*, 1999, **127**, 122-136

[2] Van Loon J.C.: *Selected methods of trace metals analysis.* J. Wiley, New York, 1991

[3] * **note:** *The citations and notes are numbered in the same fashion and may be mutually mixed. Also you can add all notes collected at the end of the citation list, continuing it's numbering.*